Synthesis of Majucin-Type Sesquiterpenes and Immobilization and Visualization of Quorum Sensing Signaling Molecules

Inauguraldissertation

zur Erlangung der Würde eines Doktors der Philosophie

vorgelegt der
Philosophisch-Naturwissenschaftlichen Fakultät
der Universität Basel

von

José Gomes

aus Zermatt, Wallis

Basel 2014

Genehmigt von der Philosophisch-Naturwissenschaftlichen Fakultät auf Antrag von

Prof. Dr. Karl Gademann

Prof. Dr. Karl-Heinz Altmann

Basel, den 25. März 2014

Prof. Dr. Jörg Schibler
- Dekan -

Für Marina und
meine Familie

Bad times have a scientific value.
These are occasions a good learner would not miss.

Ralph Waldo Emerson (1803-1882)

Table of Content

Abstract

The science of chemical biology is the ability to answer biological questions by analyzing living systems at the chemical level. Two entirely different approaches to reach this goal are presented in this thesis. The work is divided in three experimental chapters and each one highlights the combination of modern synthetic chemistry with biological applications. Experimental data, spectroscopic analysis and appendices can be found at the end of this thesis.

Chapter 1 starts with a general introduction on important natural products that contributed to the progress of drug development in an historical perspective. The second part of this chapter presents the basic principle of combining multiple bioactive natural products to a single hybrid molecule and its potential application field.

Chapter 2 gives a broader introduction into the chemical communication used in the bacterial world. The communication pathways of Gram-positive and Gram–negative bacteria are discussed with a special focus on the latter. The concept of quorum sensing and its importance in pathogenesis and biofilm formation are described in detail. The progress of synthetic signaling molecules that can modulate quorum sensing are discussed in chronological order.

The combination of molecular anchors to quorum sensing modulators is reported in **Chapter 3**. Inspired by the surface adherent properties of catechols, quorum sensing modulators were functionalized on metal oxide surfaces thereby maintaining their activity. The immobilized natural product hybrids were recognized by bacterial reporter strains as quorum sensing modulators. The mode of action was determined to be *via* slow release of the bioactive hybrid compounds.

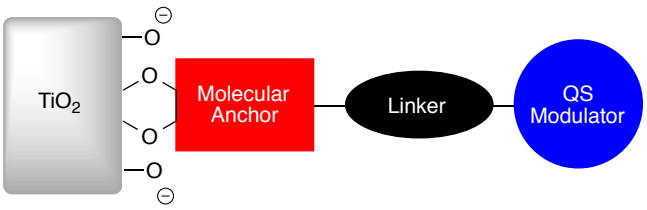

The recognition pattern for quorum sensing receptors was further developed in **Chapter 4** by the attachment of fluorescent dyes. First generation fluorescent labeling agents for quorum sensing (FLAQS) was successfully applied for the selective labeling of the CepR receptor used by *Burkholderia cenocepacia*. Further improvement of the fluorescent moiety allowed the first labeling of quorum sensing receptors in wild-type bacteria.

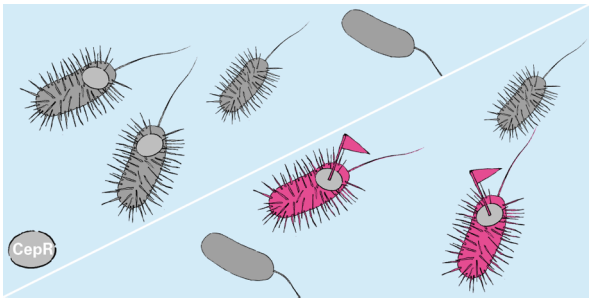

Second generation FLAQS bearing 3-oxo functionality in the acyl side chain were applied for the labeling of LasR, one of the quorum sensing receptors used by *Pseudomonas aeruginosa.*

A variety of natural products from *Illicium* species have been shown to possess exceptional neuritogenic properties. The synthesis of majucin-type sesquiterpenes and the preparation of 10-deoxy-jiadifenolide is the topic of **Chapter 5**. The synthetic key features include a cascade three-component reductive alkylation, a diastereoselective intramolecular Nozaki-Hiyama-Kishi coupling with a ketone, and an unprecedented cyanide addition to an aldehyde with subsequent lactonization under neutral conditions. The synthesis was accomplished in 25 linear steps with an overall yield of 3.7% for the first 24 steps.

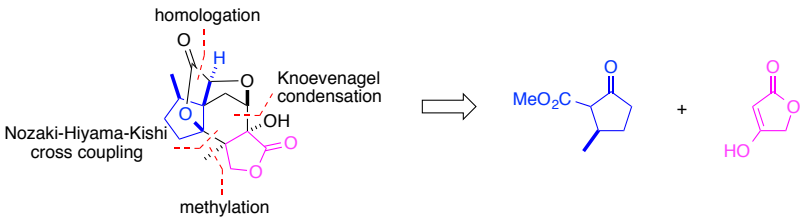

Zusammenfassung

Die Wissenschaft der chemischen Biologie ist die Fähigkeit, biologische Fragestellungen durch die Analyse von lebenden Systemen auf chemischer Ebene zu beantworten. Zwei völlig verschiedene Ansätze um dies zu tun werden in dieser Arbeit präsentiert. Die Arbeit ist in drei experimentelle Kapitel unterteilt und jedes hebt die Kombination von moderner synthetischer Chemie mit biologischen Anwendungen hervor. Experimentelle Daten und spektroskopische Analysen sind am Ende dieser Arbeit zu finden.

Kapitel 1 beginnt mit einer allgemeinen Einführung über bedeutende Naturstoffe, die für den Fortschritt der Arzneimittelentwicklung beigetragen haben. Der zweite Teil dieses Kapitels befasst sich mit dem Grundprinzip der Kombination mehrerer bioaktiver Naturstoffe zu einem einzigen Hybrid-Molekül und seine möglichen Anwendungsfelder.

Kapitel 2 bietet eine breitere Einführung in die chemische Kommunikation der bakteriellen Welt. Die Kommunikationswege von Gram-positiven und Gram-negativen Bakterien werden mit einem speziellen Fokus auf letztere diskutiert. Das Konzept des Quorum Sensing und seine Bedeutung in der Pathogenese und Biofilmbildung sind ausführlich beschrieben. Die Fortschritte der synthetischen Signalmoleküle, die Quorum Sensing modulieren können, sind in chronologischer Reihenfolge besprochen.

Die Kombination von molekularen Ankern und Quorum Sensing Modulatoren wird in **Kapitel 3** beschrieben. Inspiriert von den Hafteigenschaften von Catecholen, wurden Quorum Sensing-Modulatoren auf Metalloberflächen funktionalisiert unter Erhaltung ihrer Aktivität. Die immobilisierten Naturprodukthybride wurden durch bakterielle Reporter Stämme als Quorum Sensing-Modulatoren erkannt. Der Wirkungsmechanismus wurde als langsame Freisetzung der biologisch aktiven Hybrid-Verbindungen festgestellt.

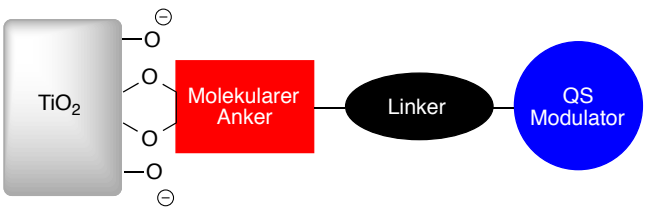

Das Erkennungsmuster für Quorum Sensing-Rezeptoren wurde in **Kapitel 4** durch die Anlage von Fluoreszenzfarbstoffen ausgebaut. Die erste Generation von Fluoreszenzmarkierungsmittel für Quorum Sensing (FLAQS) wurde erfolgreich für die selektive Markierung des von *Burkholderia cenocepacia* verwendeten CepR Rezeptors benutzt. Eine weitere Verbesserung der fluoreszierenden Gruppe ermöglichte die erste Markierung von Quorum Sensing-Rezeptoren in Wildtyp-Bakterien.

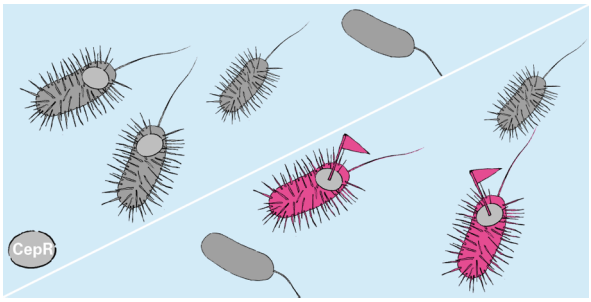

Zweite Generation FLAQS mit 3-Oxo-Funktionalität in der Acyl-Seitenkette wurden für die Kennzeichnung von LasR, einer der Quorum Sensing-Rezeptoren durch *Pseudomonas aeruginosa* verwendet, entwickelt.

Eine Vielzahl von natürlichen Produkten aus *Illicium* Spezies besitzen aussergewöhnliche neuritogene Eigenschaften. Die Synthese von Majucin-Sesquiterpenen und die Fertigstellung von 10-Deoxy-Jiadifenolid ist das Thema von **Kapitel 5**. Die synthetischen Hauptmerkmale sind ein Kaskadendreikomponenten reduktive Alkylierung, eine diastereoselektive intramolekulare Nozaki-Hiyama-Kishi-Kopplung mit einem Keton, eine beispiellose Cyanid Addition an einen Aldehyd und anschliessende Lactonisierung unter neutralen Bedingungen. Die Synthese wurde in 25 linearen Stufen mit einer Gesamtausbeute von 3.7% für die ersten 24 Stufen erreicht.

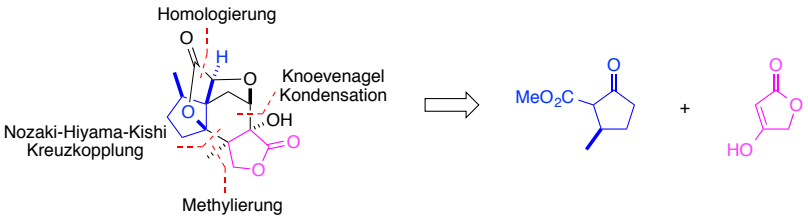

List of Abbreviations, Acronyms and Symbols

Ac	acetyl
AcOH	acetic acid
AD	Alzheimer's disease
AD-mix	asymmetric dihydroxylation-mix
AHL	acylated homoserine lactone
AI	autoinducer
AIP	autoinducing peptide
AIBN	2,2′-azo*bis*(2-methylpropionitrile)
aq.	aqueous
B.	*Burkholderia*
Bcc	*Burkholderia cepacia* complex
brsm	based on recovered starting material
BSA	*N*,*O*-*bis*(trimethylsilyl)acetamide
Boc	*tert*-butyloxycarbonyl
Bu	butyl
°C	degrees centigrade
c	concentration
C.	*Chromobacterium*
calc.	calculated
CAN	ceric ammonium nitrate
CAM	ceric ammonium molybdate
cat.	catalytic
CF	cystic fibrosis
δ	chemical shift
d	doublet
D	deuterium
d.r.	diastereomeric ratio
Da	dalton(s)
DBU	1,8-diazabicyclo[5.4.0]undec-7-en
DCC	*N*,*N*′-dicyclohexylcarbodiimide
DCE	1,2-dichloroethane

DIBAL-H	diisobutylaluminium hydride
DMAP	4-dimethylaminopyridine
DME	dimethoxyethane
DMF	dimethylformamide
DMP	Dess-Martin periodinane
DMPU	1,3-dimethyl-3,4,5,6-tetrahydro-2(1*H*)-pyrimidinone
DMSO	dimethyl sulfoxide
DMS	dimethyl sulfide
DPD	4,5-dihydroxy-2,3-pentanedione
DSF	diffusible signal factor
e.g.	*exempli gratia*
e.e.	enantiomeric excess
EC_{50}	50% effective concentration
EI	electron impact ionization
ESI	electrospray ionization
Et	ethyl
Et_3N	triethylamine
Et_2O	diethyl ether
EtOAc	ethyl acetate
EtOH	ethanol
eq.	equivalent
FC	flash chromatography
FISH	fluorescence *in situ* hybridization
FLAQS	fluorescent labeling agent for QS receptors
FTIR	Fourier transform infrared spectroscopy
g	gram(s)
h	hour(s)
HCD	high-cell-density
HMDS	hexamethyl disilazane
HMPA	hexamethylphosphoramide
HPLC	high-performance liquid chromatography
HRMS	high-resolution mass spectrometry
Hz	hertz (s^{-1})

GFP	green fluorescent protein
IBX	2-iodoxybenzoic acid
IC_{50}	50% inhibition concentration
J	coupling constant
L	liter(s)
L-DOPA	3,4-dihydroxyphenylalanine
LC	liquid chromatography
LCD	low-cell-density
LDA	lithium diisopropylamide
M	molarity (mol./L^{-1})
m	multiplet
m-CPBA	*meta*-chloroperoxybenzoic acid
M.p.	melting point
MAP	mussel adhesive protein
Me	methyl
MeOH	methanol
Mes	mesityl
min	minute(s)
MMC	magnesium methyl carbonate
MOPS	3-(*N*-morpholino)-propanesulfonic acid
MS	molecular sieves or mass spectroscopy
MTA	methylthioadenosine
MTR	methylthioribose
n.d.	not determined
NCS	*N*-chlorosuccinimide
NGF	nerve growth factor
NHK	Nozaki-Hiyama-Kishi
NMO	*N*-methylmorpholine *N*-oxide
NMR	nuclear magnetic resonance spectroscopy
NMP	*N*-methyl-2-pyrrolidone
NOESY	nuclear Overhauser effect spectroscopy
NSC	*bis*-succinimidyl-carbonate
OdDHL	*N*-3-(oxododecanoyl)-L-homoserine lactone

OHHL	*N*-3-(oxo-hexanoyl)homoserine
P.	*Pseudomonas*
PCC	pyridinium chlorochromate
PCR	polymerase chain reaction
PEG	poly(ethylene glycol)
Ph	phenyl
PHL	phenylacetanoyl homoserine lactone
PPh_3	triphenylphosphine
ppm	parts per million
PPTS	pyridinium *p*-toluenesulfonate
PQS	*Pseudomonas* quinolone signal
Pr	propyl
p-TSA	*para*-toluenesulfonic acid
q	quartet
QS	quorum sensing
quant.	quantitative
r.t.	room temperature
R_f	retention factor
RP	reverse phase
R_t	retention time
RNA	ribonucleic acid
s	singlet
SAM	*S*-adenosyl methionine or self-assembled monolayer
SAR	structure-activity relationship
sat.	saturated
t	triplet
TBAB	tetrabutylammonium bromide
TBAC	tetrabutylammonium chloride
TBAF	tetrabutylammonium fluoride
TBS	*tert*-butyldimethylsilyl
TEMPO	2,2,6,6-tetramethylpiperidin-1-yloxy
TES	triethylsilyl
Tf	trifluoromethanesulfonyl

TFA	trifluoroacetic acid
THF	tetrahydrofuran
THMF	2-methyl-2,3,3,4-tetrahydroxytetrahydrofuran
TMS	trimethylsilyl
TLC	thin layer chromatography
Ts	tosyl
UPLC	ultra high-performance liquid chromatography
UV	ultraviolet
ν	wavenumber
V.	*Vibrio*
WT	wild-type

1 INTRODUCTION

1.1 Natural Products in Drug Discovery

Natural products have served as the most successful source of potential drug leads.[1] Due to their unique structural diversity in comparison to standard combinatorial chemistry and the fact that less than 10% of the world's biodiversity has been evaluated for potential biological activity, natural products remain to offer excellent opportunities for discovering novel low molecular weight lead compounds. Thus, pharmaceuticals of natural origin and derivatives contribute to about 50% of all drugs on the market.[2] Natural products can be found everywhere and the major sources of new secondary metabolites are fungi, plants, marine environment, algae, sponges and microorganisms.[3]

The earliest pharmaceutical record, which documents over 700 plant-based drugs, originates from Egypt dated 2900 B.C. and is known as the Ebers Papyrus. Further findings from Mesopotamia (2600 B.C.) documented oils from *Cupressus sempervirens* (cypress) and *Commiphora* species (myrrh), which are still used today to treat inflammation, colds and coughs.[1c] Ever since, the use of natural products as medicines has persisted throughout history in the form of traditional medicines, potions, remedies and oils. Some selected findings are discussed (Figure 1).

The basis of early medicine was the use of traditional therapies followed by subsequent clinical, pharmacological and chemical studies.[1e] The most famous example to date would be the synthesis of the anti-inflammatory agent acetylsalicylic acid (**I**, aspirin). This substance is derived from the natural product salicin, which was isolated from the bark of the willow tree *Salix alba* L. by Edward Stone in 1763.[4] The synthesis of **I** was accomplished more then a century later by the chemist Felix Hoffmann and was commercialized by Bayer.[5] Acetylsalicylic acid (**I**) is still one of

---

1 (a) B. B. Mishra, V. K. Tiwari, *Eur. J. Med. Chem.* **2011**, *46*, 4769; (b) J. Rey-Ladino, A. G. Ross, A. W. Cripps, D. P. McManus, R. Quinn, *Vaccine* **2011**, *29*, 6464; (c) G. M. Cragg, D. J. Newman, *Pure Appl. Chem.* **2005**, *77*, 7; (d) B. Haefner, *Drug Discov. Today* **2003**, *8*, 536; (e) M. S. Butler, *J. Nat. Prod.* **2004**, *67*, 2141; (f) I. Paterson, E. A. Anderson, *Science* **2005**, *310*, 451.

2 D. J. Newman, G. M. Cragg, *J. Nat. Prod.* **2007**, *70*, 461.

3 D. A. Dias, S. Urban, U. Roessner, *Metabolites* **2012**, *2*, 303,

4 A. Der Marderosian, J. A. Beutler, *The Review of Natural Products*, 2nd ed.; Facts and Comparisons; Seattle, WA, USA, **2002**; p. 13.

5 W. Sneader, *BMJ* **2000**, *321*, 1591.

the most widely used drugs worldwide with an estimated 40'000 tones being produced every year.[6]

In 1805, investigations of *Papaver somniferum* L. (opium poppy) led to the isolation of the analgesic drug morphine (**II**), which was the first active ingredient purified from a plant source. The chemical company Merck began its marketing in 1827. Later, in the 1870s, crude **II** was boiled in acetic anhydride to yield diacetylmorphine (heroin), which was found to be readily converted to the painkiller codeine. The first total synthesis of **II** was reported by Gates in 1952.[7] The authors accomplished this masterpiece in 31 steps with an overall yield of 0.06%. Even if more efficient approaches have been published to date, this achievement remains a classic example of total synthesis.

Quinine (**III**), isolated from the bark of *Cinchona succirubra*, had been used for centuries for the treatment of malaria, indigestion, fever, mouth and throat diseases and cancer. The curative properties of **III** were originally discovered by the Quechua in South America and the plant was later brought to Europe by the Jesuits. In the 17th century, chemotherapy using **III** was the first effective treatment for malaria caused by *Plasmodium falciparum*. It was just in the mid 1800s that the British started cultivating the plant worldwide in order to overcome the colonization-associated malaria problem.[4] The first total synthesis of **III** by Woodward and Doering in 1944 can be considered as a milestone in organic chemistry.[8]

Artemisinin (**IV**) was isolated for the first time from the plant *Artemisia annua* and has been approved as another antimalarial drug.[2] This compound allows the most efficient treatment of all current drugs against *Plasmodium falciparum*.[9] Originally, the plant was used in traditional Chinese medicine as a remedy for chills and fevers. The first total synthesis of artemisinin was reported by Schmid and Hofheinz in 1983 from the natural (–)-isopulegol.[10] Derivatives of **IV** are currently in various stages of clinical development as antimalarial drugs.[1c,11]

---

6 T. D. Warner, J. A. Mitchell, *Proc. Natl. Acad. Sci. U.S.A.* **2002**, *99*, 13371.

7 M. Gates, G. Tschudi, *J. Am. Chem. Soc*. **1952**, *74*, 1109.

8 R. B. Woodward, W. E. Doering, *J. Am. Chem. Soc*. **1944**, *66*, 849.

9 N. J. White, *Antimicrob. Agents Chemother*. **1997**, *41*, 1413.

10 G. Schmid, W. Hofheinz, *J. Am. Chem. Soc*. **1983**, *105*, 624.

11 P. M. Dewick, *Medicinal Natural Products: A Biosynthentic Approach*, 2nd ed.; John Wiley and Son: West Sussex, UK, **2002**; p. 520.

Another prominent natural product is penicillin (**V**). A serendipitous discovery by Fleming in 1929[12] and later isolation and characterization from the fungus *Penicillium notatum* by Chain and Florey led to the 1945 Nobel prize in Physiology and Medicine.[13] Their results saved countless lives and revolutionized drug discovery research.[14] Sheehan reported on the first chemical synthesis of penicillin in 1957 after nine years of intensive research.[15] Even if the developed synthesis was not suitable for mass production of **V**, one of the intermediates (6-aminopenicillanic acid) allowed the creation of new forms of penicillin.

Paclitaxel (**VI**, Taxol®) was isolated from the bark of *Taxus brevifolia* in 1967 and is now the most widely used breast cancer drug. Isolation from the bark of the American yew requires three mature 100 year old trees to provide 1 gram of **VI**. However, the current demand for **VI** is about 100-200 kg per year and can therefore hardly be obtained by isolation procedures.[11] Thus, huge efforts have been devoted to in the total synthesis of paclitaxel (**VI**). The synthetic accomplishment of **VI** is called one of the most contested ones with around 30 competing research groups by 1992.[16] The first accepted article for publication was submitted by the Holton group in 1994.[17]

Another important natural product is pilocarpine (**VII**), an L-histidine-derived alkaloid found in *Pilocarpus jaborandi*. This compound has been used as a therapeutic in the treatment of chronic and acute open-angle glaucoma for over 100 years. Interestingly the FDA approved oral formulation of **VII** in 1994 to treat xerostomia (dry mouth), which is a side effect of radiation therapy for head and neck cancer.[18] In addition, oral preparation of **VII** was approved for the management of Sjogren's syndrome, an autoimmune disease that damages the salivary and lacrimal glands in 1998.

---

[12] J. Mann, *Murder, Magic, and Medicine*; Oxford University Press: New York, NY, USA, **1994**; p. 164.

[13] E. P. Abraham, E. Chain, C. M. Fletcher, *Lancet* **1941**, *16*, 177.

[14] (a) A. L. Alder, *The History of Penicillin Production*; American Institute of Chemical Engineers: New York, NY, USA, **1970**.; (b) E. Lax, *The Mold in Dr. Florey's Coat: The Story of the Penicillian Miracle*; John Macrae/Henry Hol: New York, NY, USA, **2004**; p. 308.

[15] J. C. Sheehan, K. R. Henery-Logan, *J. Am. Chem. Soc*. **1957**, *79*, 1262.

[16] N. Hall, *Chem. Commun*. **2003**, 661.

[17] R. A. Holton, C. Somoza, H.-B. Kim, F. Liang, R. J. Biediger, P. D. Boatman, M. Shindo, C. C. Smith, S. Kim, H. Nadizadeh, Y. Susuki, C. Tao, P. Vu, S. Tang, P. Zhang, K. K. Murthi, L. N. Gentile, J. H. Liu, *J. Am. Chem. Soc*. **1994**, *116*, 1597.

[18] T. Aniszewski, Alkaloids - Secrets of Life. In *Alkaloid Chemistry, Biological Significance, Applications and Ecological Role*; Elsevier Science: Amsterdam, The Netherlands, **2007**; p. 334.

In 1953, Edmund Kornfeld isolated a glycopeptide antibiotic produced in cultures of *Amycolatopis orientalis* from soil samples collected from the jungles of Borneo by a missionary in the Eli Lilly Company laboratories and termed it vancomycin (**VIII**). Even though synthetically accessible,[19] industrial production of **VIII** is mostly conducted by fermentation. Activity was shown against Gram-negative bacteria, mycobacteria and fungi and it was used for the treatment of severe infection and against susceptible organisms in patients hypersensitive to penicillin (**V**).[1e]

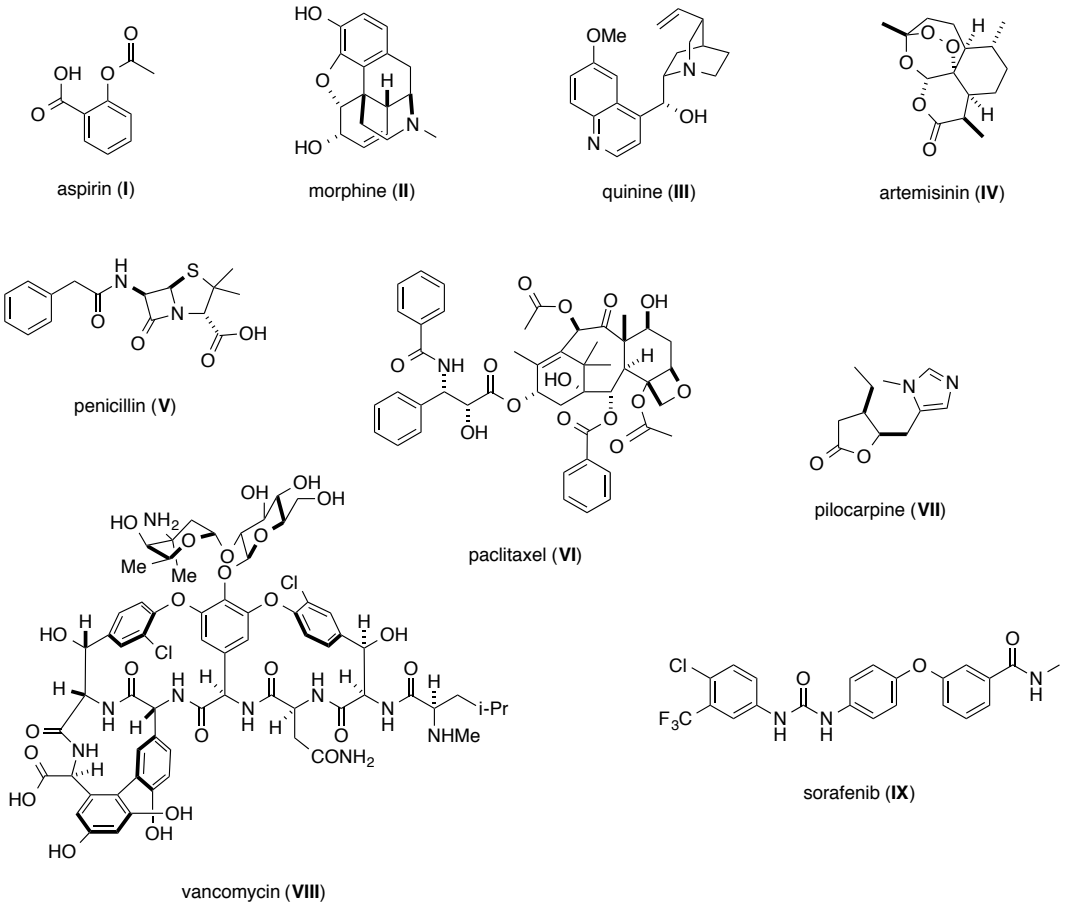

Figure 1: Examples of important bioactive drugs.

Natural product discovery programs driven by pharmaceutical companies provided lead compounds for the treatment of cancer, microbial infections, hypercholesteremia and tissue rejection in organ transplantation.[20] However, major pharmaceutical

[19] (a) D. A. Evans, M. R. Wood, B. W. Trotter, T. I. Richardson, J. C. Barrow, J. L. Katz, *Angew. Chem. Int. Ed*. **1998**, *37*, 2700; (b) K. C. Nicolaou, H. J. Mitchell, N. F. Jain, N. Winssinger, R. Hughes, T. Bando, *Angew. Chem. Int. Ed*. **1999**, *38*, 240.

[20] (a) D. D. Baker, M. Chu, U. Oza, V. Rajgarhia, *Nat. Prod. Rep.* **2007**, *24*, 1225; (b) I. Ojima, *J. Med. Chem.* **2008**, *51*, 2587.

companies decommissioned their programs in the 90s and 2000s due to continuous re-discovery of previously isolated compounds and the structural complexity of natural products. The later requires total synthesis and derivatization, which is both economically and synthetically challenging. Thus, combinatorial chemistry was thought to be the future source of novel drug leads or new chemical entities. However, only one combinatorial new chemical entity has been approved by the FDA to date, namely the kinase inhibitor sorafenib (**IX**).[21] The innate disadvantage of large libraries of compounds produced by combinatorial chemistry is the lack of complexity compared to the intricate natural products synthesized by nature.

Therefore, the development of drug candidates is strictly linked to the progress in total synthesis and structure-activity relationship (SAR) studies of complex natural products. Furthermore, it enables biological investigations towards target understanding, metabolism and mode of action of the selected compounds. The second part of this thesis focuses on the synthesis of complex natural products bearing important biological activities.

1.2 Natural Product Hybrids in Drug Discovery

The combination of two or more natural products to form hybrids has been proposed as the next stage to profit from natural products.[22] This concept is not completely new and some examples can be found in Nature, for example, vitamin E (**X**, Figure 2). The terpenoid phytyl chain interacts with the cell membrane, while the phenol moiety derived from shikimic acid forms a radical trap. Another interesting natural hybrid is the antimicrobial antibiotic thiomarinol (**XI**), isolated from the marine bacterium *Alteromonas rava* sp. nov. SANK 73390.[23] This compound was shown to be a hybrid of a pseudomonic acid C analogue and holothin and shows characteristics of both parent moieties, namely activity against Gram-positive and Gram-negative bacteria. Moreover, the effects of **XI** are more pronounced than those of either parent compound.

---

[21] D. J. Newman, *J. Med. Chem.* **2008**, *51*, 2589.

[22] Reviews: (a) L. F. Tietze, H. P. Bell, S. Chandrasekhar, *Angew. Chem. Int. Ed.* **2003**, *42*, 3996; (b) K. Gademann, *CHIMIA* **2006**, *60*, 841.

[23] H. Shiozawa, T. Kagasaki, T. Kinoshita, H. Haruyama, H. Domon, Y. Utsui, K. Kodama, S. Takahashi, *J. Antibiot.* **1993**, *46*, 1834 .

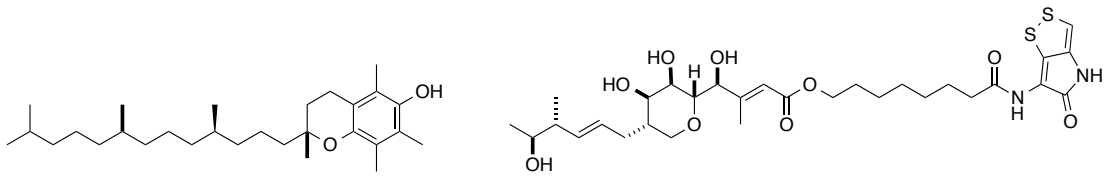

Figure 2: Natural product hybrids found in Nature.

Chemists have adapted this basic principle of combining two bioactive moieties to form a single hybrid bearing both or improved properties. Compound **XII** is an example of a synthetic hybrid molecule tested against expression of different tumor-relevant proteins in MCF7 breast cancer cells (Figure 3).[24] The western part of the molecule is derived from the sex hormone estradiol. The eastern moiety originates from geldanamycin, an antibiotic first isolated from *Streptomyces hygroscopius*. This natural product has been shown to bind to the Hsp90 chaperone protein and causes degradation of several important signaling proteins. The combination of both entities offers the ability to induce a selective degradation of the estrogen receptor. Biological tests showed that **XII** reduces the expression of HER2, ER and Raf-1 in MCF7 breast cancer cells.

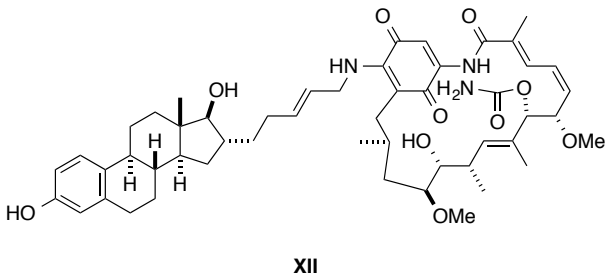

XII

Figure 3: Structure of the anti-cancer natural product hybrid **XII**.

The advantage of this approach over a combinatorial chemistry concept is its high diversity and the inherent biological activity of the hybrids. The hybridization concept was applied to the field of quorum sensing in the first part of this thesis by combining natural agonists to molecular surface anchors and fluorescent moieties.

[24] S. D. Kuduk, F. F. Zheng, L. Sepp-Lorenzino, N. Rosen, S. J. Danishefsky, *Bioorg. Med. Chem. Lett*. **1999**, *9*, 1233.

2 COMMUNICATION IN THE BACTERIAL WORLD

2.1 Introduction

Communication is one of the most precious tools developed by living organisms in order to enable the living together in communities. Humans have evolved a very sophisticated language in order to communicate with each other and therewith enable a fruitful and constructive cohabitation. This basic and fundamental tool has not only been developed by mankind, but is widely spread throughout the living world. Animals use a similar acoustic communication, for instance to warn their conspecifics in case of danger or in need for reproduction. However, such a communication pathway has not only been developed by higher organisms. Also the simplest life forms have evolved a method to improve cohabitation in large communities. This chapter will focus on bacterial communication by exchange of chemical signaling molecules and their biological importance.

Our special interest belongs to the oldest living species on earth, namely bacteria. These unicellular prokaryotic living organisms are broadly distributed in water, soil, air, and on tissue of plants and animals. They play crucial roles in many biological processes, such as nitrogen fixation and decomposition of biomass and dead organisms. For historical reasons, bacterial can be divided into two main classes according to their cell walls's reaction to Gram staining.[25] In 1884, the Danish scientist Hans Christian Gram developed a staining solution and observed that some bacteria turned blue or violet, while others remained red or pink. Gram termed the labeled ones positive and the not labeled ones negative. The difference in staining between these two groups relies in thicker peptidoglycan wall that Gram-negative cells possess, which provides them with an increased protection and robustness and prevents the strain from entering the cell. Gram staining remained an extremely valuable analytical tool in both clinical and research settings. The following section will describe the different modes of communication used by Gram-positive and Gram-negative bacteria.

[25] H. C. Gram *Fortschr. Med.* **1884**, *2*, 185.

2.2 Quorum Sensing – The Bacterial Language

Communication used by bacteria is not only based on direct contact between single cells. In fact, bacteria have developed a complex cell-to-cell communication pathway based on the exchange of chemical signaling molecules. This system is used by a wide variety of bacteria to synchronize their activities in sizeable groups in order to act as multicellular organisms.[26] In this way, bacteria have the ability to coordinate activities, such as swarming motility, surface attachment, sporulation, antibiotic resistance, biofilm maturation or virulence.[27] Such pathogenic traits are seemingly futile if performed by a single bacterium acting alone and therefore, only expressed when the bacterial population density is high enough to overwhelm the host defense mechanism. To control the size of the population bacteria produce and release small signaling molecules, so-called autoinducers (AI), which then accumulate in the direct surroundings. When a certain concentration of AIs is reached, bacteria switch from a low-cell-density (LCD) into a high-cell-density (HCD) mode.[28] Once HCD is reached, a signal transduction cascade is triggered, which culminates in a population-wide alternation in gene expression. This synchronous response of bacterial populations gives multicellular ability to these unicellular organisms and is referred to as quorum sensing (QS).[27] Such QS controlled pathways are only beneficial when carried out by the entire group. If it is induced before a minimal threshold concentration is reached, bacteria are usually not adequate to survive. QS is used by both Gram-negative and Gram-positive bacteria but is not crucial for their viability.

Much attention has been attributed to the phenomenon of QS in the recent years. However, the first report of bacterial communication using chemical signaling molecules goes back to the year 1965. Tomasz published a paper concerning *Pneumococcus* (today known as *Streptococcus pneumoniae*) strains and their growth behavior and genetic competence.[29] In this publication, the author described an extracellular factor produced by *Streptococcus*, which triggered the competence state. This factor was termed "*hormone-like activator*" and enables the synchronization

---

[26] C. M. Waters, B. L. Bassler, *Annu. Rev. Cell Dev. Biol.* **2005**, *21*, 319.

[27] (a) M. B. Miller, B. L. Bassler, *Annu. Rev. Microbiol.* **2001**, *55*, 65; (b) C. D. Nadell, J. B. Xavier, S. A. Levin, K. R. Foster, *PLoS Biol*. **2008**, *6*, 171, (c) M. Boyer, F. Wisniewski-Dyé, *FEMS Microbiol. Ecol*. **2009**, *70*, 1.

[28] W. Ng, B. L. Bassler, *Annu. Rev. Genet.* **2009**, *43*, 197.

[29] A. Tomasz, *Nature* **1965**, *208*, 155.

behavior of bacterial populations.[30] Five years later, Hastings and co-workers reported the control of luminescence in the marine Gram-negative bacterium *Vibrio fischeri* promoted by AIs.[31] Moreover, the authors were able to show that light emission in *Vibrio fischeri* and *Vibrio harveyi* does not correlate with bacterial growth. The *in vivo* bioluminescence emerged at a later stage and much faster than the bacterial population growth and the researchers termed this phenomenon "*autoinduction*".

The combined findings of Tomasz and Hastings suggested that certain bacterial strains use signaling molecules to examine their environment and to control group behavior based on the population density. However, at that time, this cell-to-cell signaling pathway was thought to be anomalous and restricted to only a few specialized bacteria.[30] The discovery of the structure of *N*-3-(oxo-hexanoyl)homoserine lactone (OHHL) of *Vibrio fischeri* as an AI and its capability to diffuse into and out of the cells reported in 1981 was a major breakthrough in this field.[32] The QS system of *Vibrio fischeri* was later found in other bacteria and caused a change to the current view that QS is a common mechanism for cell-to-cell communication in many bacterial species.[33] All these results demonstrate that QS is not a rare phenomenon for specialized bacteria but a rather important tool in the bacterial world.

2.3 Quorum Sensing Pathways

To date, a wide variety of QS pathways have been identified and characterized.[34] The differentiation between the different pathways is based on the chemical structure of the used AIs. However, the fundamental steps involved in detecting and responding to fluctuations in cell density are analogous in all known QS systems. In order to be classified as "*quorum sensing molecules*", a moiety has to match four different criteria as described by Winzer *et al.*:[35]

---

30 B. L. Bassler, R. Losick, *Cell* **2006**, *125*, 237.

31 K. H. Nealson, T.Platt L. W. Hastings, *J. Bacteriol.* **1970**, *104*, 313.

32 A. Eberhard, A. L. Burlingame, C. Eberhard, G. L. Kenyon, K. H. Nealson, N. J. Oppenheimer, *Biochemistry* **1981**, *20*, 2444.

33 E. P. Greenberg, *ASM News* **1997**, *63*, 371.

34 L. Eberl, K. Riedel, *Proteomics* **2011**, *11*, 3070.

35 K. Winzer, K. R. Hardie, P. Williams, *Curr. Opin. Microbiol.* **2002**, *5*, 216.

1. The molecule has to be produced during specific stages of cell growth or in response to a particular environmental change.
2. QS molecules accumulate in the extra-cellular environment and are recognized by a specific receptor.
3. A concerted response has to be stimulated by the accumulation of a threshold concentration of AIs.
4. The cellular response should be greater than the physiological modifications required to detoxify or metabolize the molecule.

The chemical entity of AIs highly depends on the bacterial species. Some representative examples of chemical structures used as QS signaling molecules are shown in Figure 4. The most prevalent QS pathway used by Gram-negative proteobacteria is mediated by acylated homoserine lactones (AHLs, **XIII**) and is composed of a homoserine lactone ring carrying C_4-C_{12} acyl side chains.[36] Gram-positive bacteria, for their part, use a completely different pathway mediated by linear, cyclic, or modified peptides (autoinducing peptides, AIPs, **XIV**) as signaling molecules. Furthermore, a third important pathway uses 4,5-dihydroxy-2,3-pentanedione (DPD, **XV**) derivatives, referred to as autoinducer-2 (AI-2), which is shared by both Gram-positive and Gram-negative bacteria and probably allows them to cross talk. These three major communication pathways will be discussed in more detail in the following sections.

An additional extracellular signaling molecule is called *Pseudomonas* quinolone signal (PQS, **XVI**) and is exclusively produced by the opportunistic pathogen *Pseudomonas aeruginosa*.[37] Together with two well-studied AHL signaling molecules, **XVI** is responsible for the control of a number of genes required for virulence factor expression and biofilm formation. PQS (**XVI**) is rather hydrophobic, obscuring any obvious mechanism for it to act as an extra-cellular signal. However, Whiteley and co-workers demonstrated that a specialized vesicular transport mechanism conveys **XVI** signals packed in vesicles between bacterial cells.[38] These vesicles are believed to be crucial for efficient information transfer between *P. aeruginosa* cells existing in biofilms.[39]

---

[36] A. M. Stevens, Y. Queneau, L. Soulère, S. V. Bodman, A. Doutheau, *Chem. Rev*. **2011**, *111*, 4.

[37] N. Ni, M. Li, J. Wang, B. Wang, *Med. Res. Rev.* **2009**, *29*, 65.

[38] L. M. Mashburn, M. Whiteley, *Nature* **2005**, *437,* 422.

[39] A. Camilli, B. L. Bassler, *Science* **2006**, *311*, 1113.

A further specific QS pathway is used by *Streptomycetes*. These common soil-dwelling Gram-positive bacteria use γ-butyrolactones (**XVII**), which are structural analogues of AHLs (**XIII**), as communication signals. However, no cross recognition between the two pathways has been reported to date.[30]

Last, a signaling molecule termed diffusible signal factor (DSF, **XVIII**) is known to stimulate QS in several bacterial strains, such as *Xanthomonas campestris*, *Xylella fastidosa*, or *Burkholderia cenocepacia*.[38]

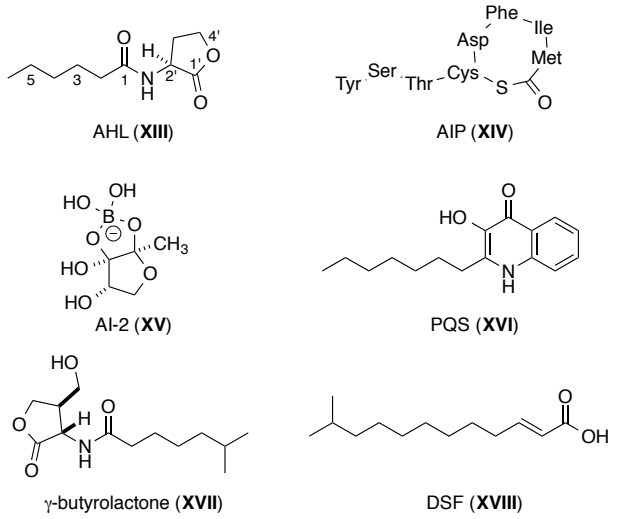

Figure 4: Chemical structures of bacterial communication signals.

Bacteria can use several pathways and balance them to compensate each other and also change their sensitivity towards QS to face evolutionary pressure in order to survive. In the following sections, we will briefly discuss the molecular mechanisms of the three most common cell-to-cell communication systems mediated by AHLs, AI-2, and AIPs.

2.4 Acylated Homoserine Lactone Mediated Quorum Sensing

The AHL mediated QS pathway is the most commonly used by Gram-negative bacteria for intraspecies communication and is also the best-studied example.[40] All AHLs are composed of a homoserine lactone moiety and only differ in the fatty acyl side chains, which can have various lengths from C_4 to C_{18}, generally in increments of two, unsaturated double bonds, and oxidation/reduction state of the third carbon in the acyl chain.[28] Even though the chemical discrepancy between different AHLs might be minimal, they are very specific for certain QS receptors and therewith for individual bacterial species.

The first QS system to be discovered was found in the marine bacterium *Vibrio fischeri* and OHHL (**XIII**) was identified as the natural AI. This species lives in symbiosis with the Hawaiian bobtail squid *Euprymna scolopes* and colonizes its host's light organ as shown in Figure 5. Bacteria produce light at HCD in exchange for a nutritious environment.[41] The produced light can be of high importance for the host. The marine squid *Euprymna japonicas*, for example, uses the emitted light to mask its shadow and therewith remain invisible for predators. Another fascinating biological application can be observed in the pinecone fish *Monocentris japonicus*, which uses the emitted light to attract sexual partners.[42]

---

40 S. Schauder, B. L. Bassler, *Genes Dev*. **2001**, *15*, 1468.

41 K. L. Visick, M. J. McFall-Ngai, *J. Bacteriol*. **2000**, *182*, 1779.

42 (a) E. G. Ruby, *Annu. Rev. Microbiol.* **1996***, 50,* 591; (b) K. J. Boettcher, E. G. Ruby, *J. Bacteriol.* **1990**, *172*, 3701.

Figure 5: Hawaiian bobtail squid, *Euprymna scolopes*.[43]

Additionally, *Vibrio fischeri* has one of the simplest and best understood QS communication pathways. Therefore, it is considered a model for studies of the basic mechanism of QS in Gram-negative proteobacteria (Figure 6). The apparatus of this species is controlled by an AHL synthase and an AHL receptor protein termed LuxI and LuxR, respectively.[44] LuxI produces a basal level of OHHL (**XIII**) at LCD that can then freely diffuse in and out of the cell.[45] As the cell population increases, the intra- and extracellular concentration of AHLs raises proportionally in the growth medium.[27] On reaching a critical threshold concentration, the signaling molecule binds and activates LuxR.[46] The LuxR-AHL complex acts as the transcriptional activator of the luciferase *luxICDABE* operon.[47] LuxR proteins are unstable in the absence of AHL ligands and are rapidly degraded. Upon accumulation, the complex recognizes a consensus binding sequence upstream of the *luxICDABE* operon and

[43] Used with permission from William Ormerod, University of Wisconsin-Madison.

[44] (a) C. Fuqua, M. R. Parsek, E. P. Greenberg, *Annu. Rev. Genet*. **2001**, *35*, 439; (b) S. Swift, J. A. Downie, N. A. Whitehead, A. M. L. Barnard, G. P. C. Salmond, P. Williams, *Adv. Microb. Physiol*. **2001**, *45*, 199.

[45] J. A. Engebrecht, M. Silverman, *Proc. Natl. Acad. Sci. U. S. A*. **1984**, *81*, 4154.

[46] J. A. Engebrecht, K. Nealson, M. Silverman, *Cell* **1983**, *32*, 773.

[47] (a) B. L. Hanzelka, E. P Greenberg, *J. Bacteriol*. **1995**, *177*, 815; (b) A. L. Schaefer, B. L. Hanzelka, A. Eberhard, E. P. Greeberg, *J. Bacteriol*. **1996**, *178*, 2897; (c) A. M. Stevens, K. M. Dolan, E. P. Greenberg, *Proc. Natl. Acad. Sci. U. S. A*. **1994**, *91*, 12619; (d) A. M. Stevens, N. Fujita, A. Ishihama, E. P. Greenberg, *J. Bacteriol*. **1999**, *181*, 4704; (e) A. M. Stevens, E. P. Greenberg, *J. Bacteriol*. **1997**, *179*, 557.

activates its expression. This operon consists of three parts: *luxI*, which is responsible for LuxI production, *luxAB*, which encodes the enzyme luciferase, and *luxCDE*, which activates the proteins required for the biosynthesis of long chain aldehydes necessary for bioluminescence.[42] The expression of *luxI* leads to an exponential increase in AHL biosynthesis and to the flooding of the surrounding environment with signaling molecules. This positive feedback loop is necessary in order to switch the entire population from a LCD into a HCD mode. Once an even higher concentration of AIs is reached, *luxR* is down-regulated as a compensatory measure.[46]

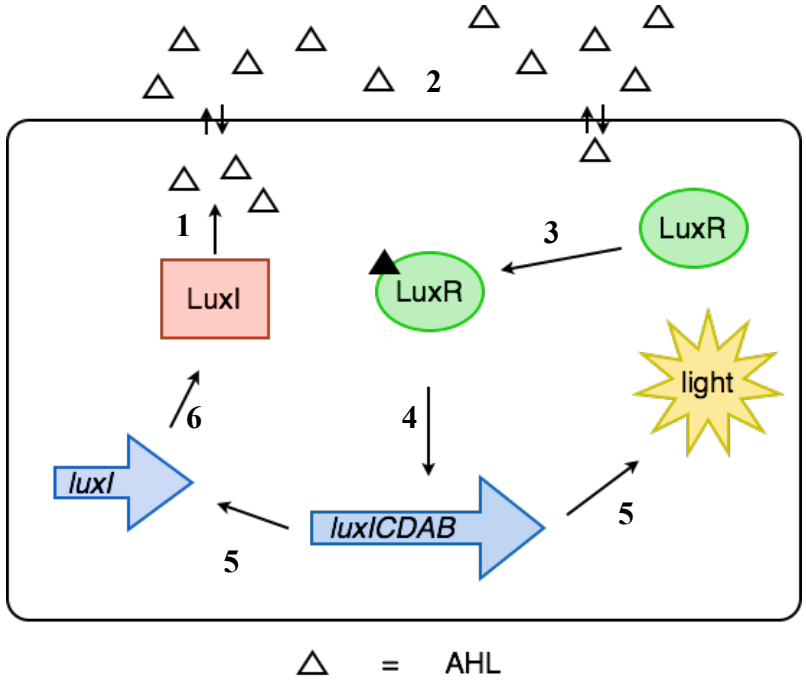

Figure 6: LuxIR QS system of *Vibrio fischeri*. (1) Free diffusible AHLs are produced by LuxI and (2) accumulate in the extra-cellular space. (3) When HCD is reached, AHLs bind their cognate LuxR receptor, (4) thereby inducing the expression of the regulated *luxICDAB* genes, (5) which encode for *luxCDE* (light) and *luxI*. (6) Overexpression of *luxI* leads to an exponential increase of the synthase LuxI.

The QS circuits of Gram-negative bacteria are in most circumstances similar to the ones found in *Vibrio fischeri* and contain at least two homologues of the LuxI and LuxR regulatory proteins. Some examples of different QS systems used by Gram-negative bacteria are shown in Table 1. Several insights can be gained by studying this data. First, some AHL signals are used by different bacteria. For example, *Pseudomonas aeruginosa* and *Seratia liquefaciens* both use C_4-AHL as an AHL signal. The overlap of signals is interesting, because it means that bacteria that live in the same environment may use these signaling molecules for interspecies

communication. Furthermore, one AHL can act as the signaling molecule for more than one receptor within a single species (*e.g.*, OHHL and the ExpR and CalR receptors in *Erwinia carotovora*). This feature could allow the bacteria to conserve valuable resources, or provide a means to carefully modulate the activity of receptors, for example, if one signaling molecule binds to two receptors with different affinities.

Table 1: Representative AHL systems and their corresponding bacteria.

Bacterium	AHL	Nomenclature	LuxI/R
Agrobacterium tumefaciens	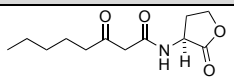	OOHL, 3-oxo-C_8-AHL	TraI/R
Burkholderia cenocepacia	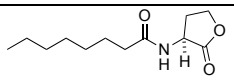	OHL, C_8-AHL	CepI/R
Chromobacterium violaceum	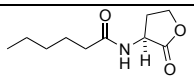	HHL, C_6-AHL	CviI/R
Erwinia carotovora	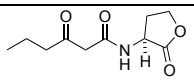	OHHL, 3-oxo-C_6-AHL	ExpI/R; CarI/R
Pseudomonas aeruginosa	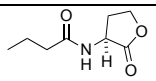	BHL, C_4-AHL	RhlI/R
	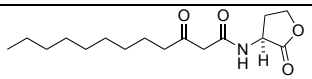	OdDHL, 3-oxo-C_{12}-AHL	LasR/I; QscR
Pseudomonas putida	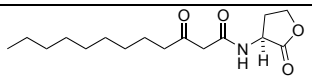	OdDHL, 3-oxo-C_{12}-AHL	PpuI/R
Serratia sp. ATC39006	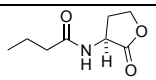	BHL, C_4-AHL	SmaI/R; $CarR_{sma}$
	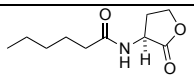	HHL, C_6-AHL	
Seratia liquefaciens MG1	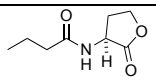	BHL, C_4-AHL	SwrI/R
	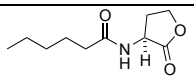	HHL, C_6-AHL	
Serratia marcescens AS-1	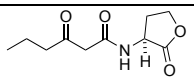	OHHL, 3-oxo-C_6-AHL	SpnI/R
	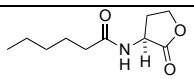	HHL, C_6-AHL	
Vibrio fischeri	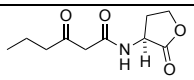	OHHL, 3-oxo-C_6-AHL	LuxI/R
Vibrio harveyi	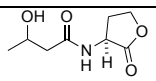	3-hydroxy-C_4-AHL	LuxM/N

Even though the AHL system is predominantly used for bacterial communication, some evidence has been found that also plants and animals are able to recognize AHLs of symbiotic bacterial species.[48]

2.4.1 AHL Biosynthesis

As described in the previous section, AHLs are produced by a LuxI-type synthase and involves *S*-adenosyl methionine (SAM, **XIV**) and particular acyl carrier proteins (ACP) from lipid metabolism as shown in Figure 7.[49] LuxI catalyzes acylation and lactonization reactions between the substrates SAM (**XIV**) and acyl-ACP (**XV**) followed by elimination of methylthioadenosine (MTA, **XVI**) to give AHLs (**XVII**). MTA (**XVI**) is a toxic byproduct, which is then cleaved in a second process by the nucleosidase enzyme Pfs into two nontoxic products, adenine and methylthioribose (MTR).[50] A great diversity of AHLs is made possible due to the fact that acyl-ACPs are common intermediates in the biosynthesis of fatty acids.

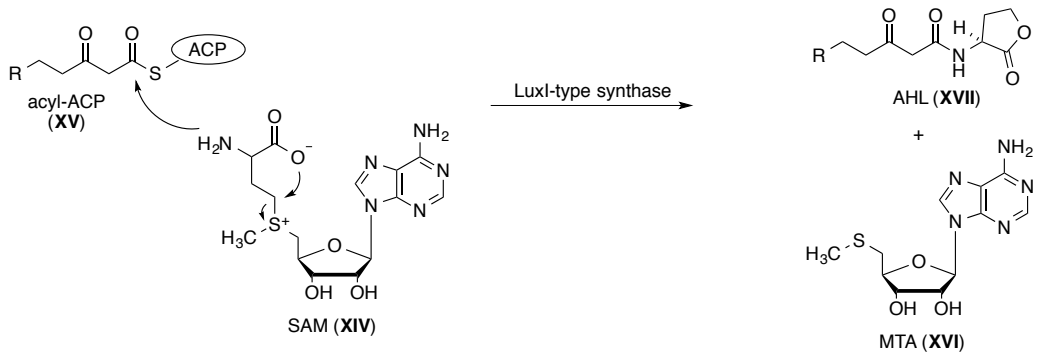

Figure 7: Biosynthesis of AHLs.

---

48 (a) V. V. Kravchenko, G. F. Kaufmann, J. C. Mathison, D. A. Scott, A. Z. Katz, D. C. Grauer, M. Lehmann, M. M. Meijler, K. D. Janda, R. J. Ulevitch, *Science* **2008**, *321*, 259; (b) M. Cooley, S. R. Chhabra, P. Williams, *Chem. Biol*. **2008**, *15*, 1141; (c) A. G. Palmer, H. E. Blackwell, *Nat. Chem. Biol.* **2008**, *4*, 452.

49 (a) Y. Jiang, M. Camara, S. R. Chhabra, K. R. Hardie, B. W. Bycroft, A. Lazdunski, G. P. Salmond, G. S. A. B. Stewart, P. Williams, *Mol. Microbiol*. **1998**, *28*, 193; (b) M. I. Moré, L. D. Finger, J. L. Stryker, C. Fuqua, A. Eberhard, S. C. Winans, *Science* **1996**, *272*, 1655.

50 (a) B. L. Bassler, *Cell* **2002**, *109*, 421; (b) M. R. Parsek, D. L. Val, B. L. Hanzelka, J. E. Cronan Jr., E. P. Greenberg, *Proc. Natl. Acad. Sci. USA* **1999**, *96*, 4360; (c) M. I. Moré, L. D. Finger, J. L. Stewart, P. Williams, *Mol. Microbiol.* **1998**, *28*, 1655.

2.4.2 Synthetic AHLs

The development of new synthetic AHL analogues has obtained large scientific interest in the last three decades due to two main reasons. On the one hand, the fundamental mechanisms involved in QS communication pathways were not known. On other hand, inhibition of QS (quorum quenching) by such synthetic signaling molecules could lead to new therapeutic strategies to inhibit bacterial virulence as an alternative to anti-bacterial approaches. Therefore, various research groups have designed and synthesized a large variety of AHL analogues, thereby modifying the lactone ring, the acyl side chain, or both. These compounds were tested with agonism or antagonism assays using absorbance (β-galactosidase fusion), fluorescence (green fluorescent protein (GFP)) or luminescence (luciferase fusion) to determine the ligand activity in AHL-LuxR-type complexes.[51]

The first report of synthetic AHL analogues goes back to the year 1986 and was published by Eberhard *et al*.[52] The special focus in this study was to investigate and determine the mechanism of action involved in QS pathways. With a small collection of about 20 AHL derivatives (**XVIII** and **XIX**, Figure 8), the researchers tested their compounds for the induction activity and for their ability to inhibit the action of the natural agonists in *Vibrio fischeri* B-61. The used bacteria served as a natural "dim" strain, since more light is produced with the addition of exogenous OHHL (**XIII**). The authors concluded that the γ-lactone and the length of the acyl side chain were crucial for LuxR activation with an optimal length of six carbon atoms. Longer side chains led to a switch from the role of agonist to antagonist. Furthermore, the presence of a carbonyl functionality at C-3 position was determined to be essential for strong agonistic activity. Modifications of this group led to a decrease or even complete vanish of the activity. The natural agonist OHHL (**XIII**) proved to possess the highest agonistic activity compared to the non-natural ones. However, it should be pointed out that all synthetic analogues were prepared as racemic mixtures, which most probably has an impact on the reported results.

---

[51] Review: G. D. Geske, J. C. O`Neil, H. E. Blackwell, *Chem. Soc. Rev.* **2008**, *37*, 1432.

[52] A. Eberhard, C. A. Widrig, P. McBath, J. B. Schineller, *Arch. Microbiol.* **1986**, *146*, 35.

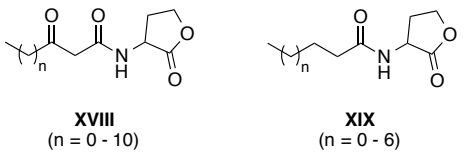

Figure 8: Examples of synthesized racemic AHLs by Eberhard and co-workers.[52]

The next study did not appear until a decade later, when, in 1996, Greenberg and co-workers presented their results on similar synthetic AHL analogues compared to the ones described by Eberhard but in non-racemic form of the γ-lactone ring (**XX-XXVIII**, Figure 9).[53] These analogues were tested using an *E. coli* reporter strain containing *luxR* but lacking functional *luxI*. The results were in agreement with the earlier findings and suggested that the γ-lactone moiety is important for LuxR binding. Most analogues with substitutions in the homoserine lactone ring (**XXII**, **XXIV**, and **XXV**) did not show evidence of binding to LuxR, except for homocysteine thiolactone **XXI**. Also the introduction of double (**XXVI**) and triple bonds (**XXVII**) in the side chain lowered the agonistic activity, suggesting that a flexible side chain is preferred for binding. Interestingly, substrates **XX** and **XXIII** were shown to possess weak agonistic activity.

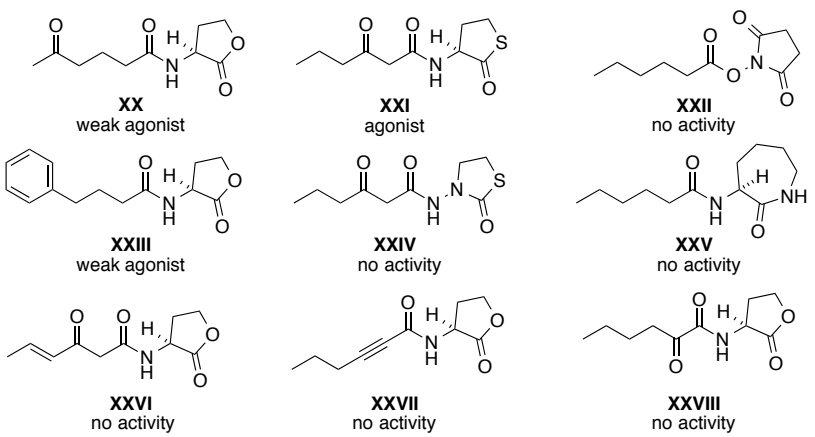

Figure 9: Structures of AHLs investigated by Greenberg and co-workers.[53]

[53] A. L. Schaefer, B. L. Hanzelka, A. Eberhard, E. P. Greenberg, *J. Bacteriol*. **1996**, *178*, 2897.

In 2002, Doutheau and co-workers prepared a series of AHL analogues with bulky substituent at the side chain terminus and retained 3-oxo functionality (**XXIX-XXXVII**, Figure 10).[54] Small substituents at C-5 position, such as cyclopropyl- (**XXIX**) or cyclohexyl-groups (**XXX**), were found to induce luminescence in *Vibrio fischeri*. In contrast, large substituents and aryl groups lead to the loss of agonistic activity or even antagonistic properties.

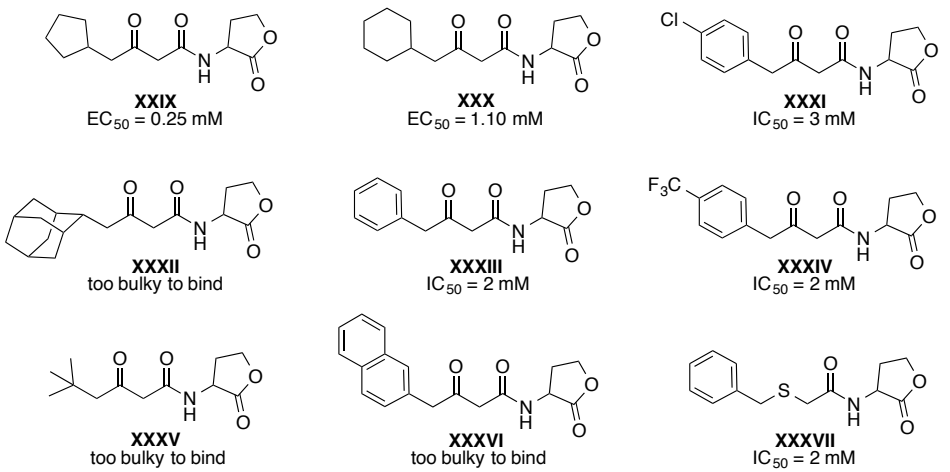

Figure 10: Examples of sterically hindered AHLs studied by Doutheau and co-workers. IC_{50} values given for antagonists and EC_{50} values for agonistic substrates.[54]

In the same year, Nielsen and co-workers expanded the substitution pattern by introducing different groups at C-3' and C-4' position of the lactone ring (**XXXVIII-XLIII**, Figure 11).[55] The synthetic analogues were tested in an *E. coli* JM105 strain, harboring the LuxR-type QS system of *Vibrio fischeri.* Substitution at C-4' position (**XLI**, **XLII** and **XLIII**) led only to weak inhibition of QS. However, C-3'-substituted analogues **XXXVIII** and **XXXIX** showed agonistic activities in the range of the native ligand OHHL (**XIII**) and weak activity when *R*-configured and sterically not too demanding (**XL**).

[54] S. R. Everchon, B. Chantegrel, C. Deshayes, A. Doutheau, N. Cotte-Pattat, *Bioorg. Med. Chem. Lett.* **2002**, *12*, 1153.

[55] J. A. Olsen, R. Severinsen, T. B. Rasmussen, M. Hentzer, M. Givskov, J. Nielsen, *Bioorg. Med. Chem. Lett.* **2002**, *12*, 325.

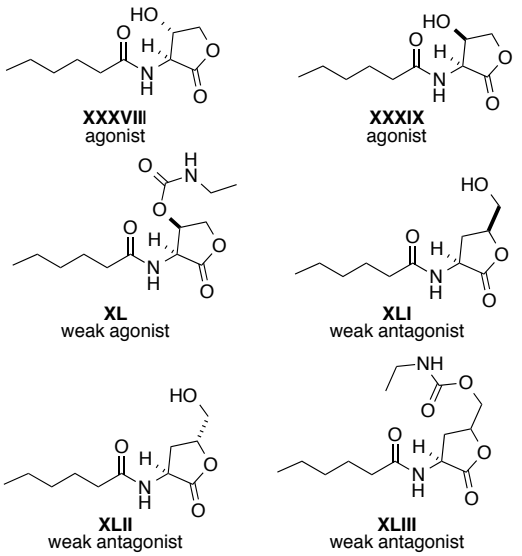

Figure 11: AHL analogues studied by Nielsen and co-workers.[55]

In later studies by the Doutheau group, a different approach was explored by using sulfoneamide (**XLIV-XLVII**, Figure 12) and urea side chains instead of amides (**XLVIII-LI**).[56] The racemic sulfonyl derivatives did not display any agonistic activities but were rather found to be potent LuxR inhibitors. Also the urea derivatives proved to be potent antagonists and the inhibitory effect appeared to be increasing with the hydrophobic character of the ligand.

[56] (a) S. Castang, B. Chantegrel, C. Deshayes, R. Dolmazon, P. Gouet, R. Haser, S. Reverchon, W. Nasser, N. Hugouvieux-Cotte-PAttat, A. Doutheau, *Bioorg. Med. Chem. Lett.* **2004**, *14*, 5145; (b) M. Frezza, S. Castang, J. Estephane, L. Soulère, C. Deshayes, B. Chantegrel, W. Nasser, Y. Queneau, S. Reverchon, A. Doutheau, *Bioorg. Med. Chem.* **2006**, *14*, 4781.

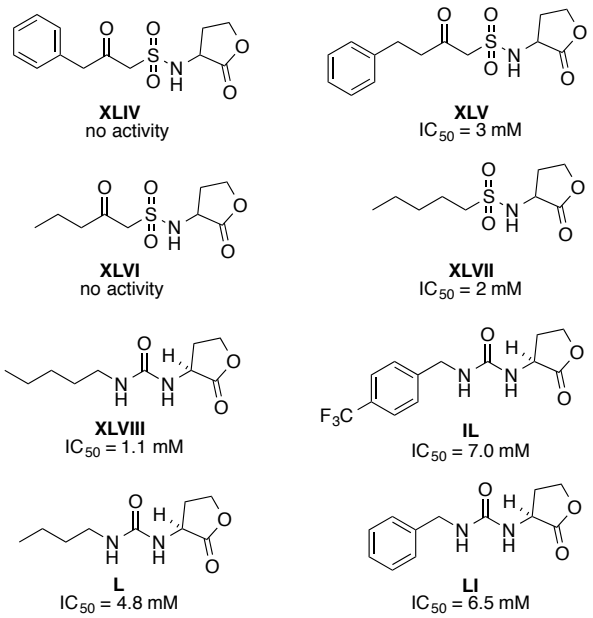

Figure 12: Examples of AHL-analogues prepared by Doutheau and co-workers. IC_{50} values given for antagonistic substrates.[56]

The Blackwell group synthesized a combinatorial library of AHL analogues with the goal of establishing structure-activity-relationships in different bacterial strains.[57] The synthesized AHLs differed in the chain length, absolute configuration of the lactone, and substitution patterns on the acyl side chain (**LII**-**LVI**, Figure 13). Their studies on *V. fischeri* showed that phenylacetyl homoserine lactones (PHLs) are highly potent antagonists when an electron-withdrawing group is placed into the *para* position (**LII, LIII** and **LIV**). However, PHLs can be turned into LuxR agonists by relocating the electron-withdrawing groups from *para* to *meta* position. Thus, a 10-fold higher activity compared to the native ligand OHHL (**XIII**) was observed when a nitro group was installed in *meta* position of the phenyl ring (**LV**). Compounds with opposite absolute configuration at the lactone ring or with indole, furane, and thiophene substituents did not show any activity in the biological assays.

[57] (a) G. D. Geske, R. J. Wezeman, A. P. Siegel, H. E. Blackwell, *J. Am. Chem. Soc.* **2005**, *127*, 12762; (b) G. D. Geske, J. C. O`Neill, D. M. Miller, M. E. Mattmann, H. E. Blackwell, *J. Am. Chem. Soc.* **2007**, *129*, 13613; (c) G. D. Geske, J. C. O`Neill, D. M. Miller, M. E. Mattmann, Q. Lin. R. J. Wezeman, H. E. Blackwell, *ChemBioChem* **2008**, *9*, 389; (d) G. D. Geske, J. C. O`Neil, H. E. Blackwell, *ACS Chem. Biol.* **2007**, *2*, 315.

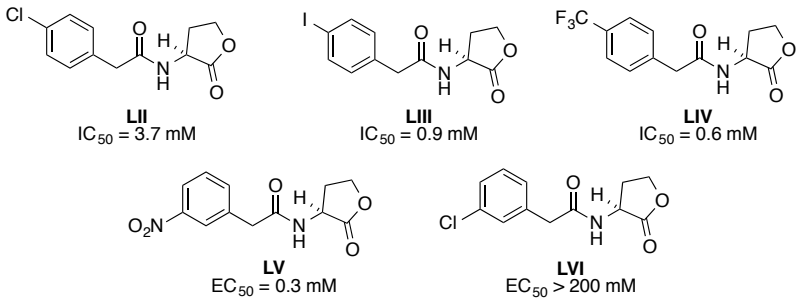

Figure 13: AHL analogues tested for QS activity in *Vibrio fischeri* by Blackwell and co-workers. IC_{50} values given for antagonists and EC_{50} values for agonistic substrates.[57]

Later studies by Iglewski,[58] Kline,[59] Suga,[60] Kato,[61] and Blackwell[57] focused on the QS system of the pathogenically highly relevant strain *P. aeruginosa*. These studies concluded that a certain chain length is important for LasR binding and that the 3-oxo group increases agonistic activity but was not essential for binding. Furthermore, the γ-lactone moiety could be replaced by five- or six-membered rings bearing a similar hydrogen bond acceptor motif for activation. Exchange of the γ-lactone by an aromatic ring with a hydrogen bond acceptor capability resulted in QS inhibition. Last, sterically bulky and structurally diverse acyl groups were tolerated by LasR due to a large ligand-binding site.

More recently, the research groups of Janda[62] and Maison[63] have been focusing on the synthesis of clickable AHL analogues (Figure 14). Both groups reported on the preparation on either azide (**LVII**) or alkynyl functionalized (**LVIII**) AHLs at the terminus of the acyl side chain. Even though *in vitro* binding to the QS receptors could be observed in both cases, it remains to be shown that such analogues have the potential to be applied for *in vivo* studies.

---

58 L. Passador, K. D. Tucker, K. R. Guertin, M. P. Journet, A.S. Kende, B. H. Iglewski, *J. Bacteriol.* **1996**, *178*, 5995.

59 T. Kline, J. Bowman, B.H. Iglewski, T. de Kievit, Y. Kakai, L. Passador, *Bioorg. Med. Chem. Lett.* **1999**, *9*, 3447.

60 (a) K. M. Smith, Y. Bu, H. Suga, *Chem. Biol.* **2003**, *10*, 81. (b) K. M. Smith, Y. Bu, H. Suga, *Chem. Biol.* **2003**, *10*, 563-571. c) G. J. Jog, J. Igarashi, H. Suga, *Chem. Biol.* **2006**, *13*, 123.

61 T. Ishida, T. Ikeda, N. Takiguchi, A. Kuroda, H. Ohtake, J. Kato, *Appl. Environ. Microbiol.* **2007**, *73*, 3183.

62 A. L. Garner, J. Yu, A. K. Struss, C. A. Lowery, J. Zhu, S. K. Kim, J. Park, A. V. Mayorov, G. F. Kaufmann, V. V. Kravchenko, K. D. Janda, *Bioorg. Med. Chem. Lett*. **2011**, *21*, 2702.

63 H. Thomanek, S. T. Schenk, E. Stein, K.-H. Kogel, A. Schikora, W. Maison, *Org. Biomol. Chem*. **2013**, *11*, 6994.

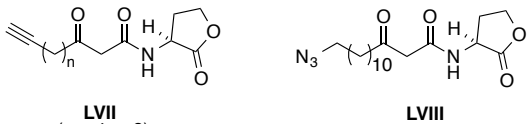

Figure 14: Clickable AHL derivatives.[62,63]

The results obtained in analogue studies by these groups established five activity trends:[51]

1. The length of the acyl side chains is crucial for QS activity. Chains with a similar length as the natural AHL have increased activity.
2. The presence of an oxo-group at C-3 position is important but not essential for activity.
3. The configuration of the lactone ring is critical for recognition.
4. The lactone ring can be replaced by different cyclic groups carrying hydrogen bond acceptors. Modifications of the lactone moiety are accepted but generally lead to decreased activity.
5. Aromatic substituents at the end of the acyl side chains result in antagonistic activity.

2.4.3 AHL Reporter Strains

Synthetic AHLs possess the potential to modulate bacterial behavior by interacting with the QS pathways. A reliable readout from biological assays is however essential in order to discover new modulators. Screening for molecules that inhibit QS (quorum quencher) scan for repressed phenotypes typically induced by QS, such as biofilm formation. However, what is often not studied in detail is the fact that QS activation and quenching highly depends on the added concentration of the substrate. This means that an agonist also possesses antagonistic activity at high concentrations. Unless biological evaluations have not been performed over a wide concentration range, a substrate should not be determined as a quorum quencher.

In order to overcome the problems associated with the biological evaluations of quorum quenchers, we decided to focus our interest on finding new AHL mimics. The induction of QS can be monitored using GFP-tagged biosensors as described by Eberl

and co-workers.[64] The advantage of such a sensor is the simple read-out, which can be realized by measuring the emitted fluorescence. To facilitate our screening efforts, we decided to focus on two sensors containing either pAS-C8 or pKR-C12 plasmids. These sensors are especially interesting for pathogenic reasons as they contain the QS receptors of *Burkholderia cenocepacia* and *Pseudomonas putida*, respectively.

The biosensors consist of *Pseudomonas putida* strains containing either pAS-C8 or pKR-C12 plasmids (Figure 15). The pAS-C8 plasmid was incorporated in a *P. putida* ISO F117 wild-type strain in which the natural QS systems was replaced by a GFP-based system. This QS system is based on the *cep* genes of *B. cenocepacia* and contains a translational *cepI-gfp* fusion and a *cepR* receptor under control of P_{lac}. This means that CepR is expressed in the cells, but not CepI, which was replaced by a GFP-synthase. Therefore, this sensor is able to detect AHLs, but in contrast to natural conditions, it does not produce AHLs by itself. The strain produces GFP upon binding of AHLs to the receptor, which can be measured due to produced fluorescence. This sensor is most sensitive for OHL and DHL as shown in Table 1.

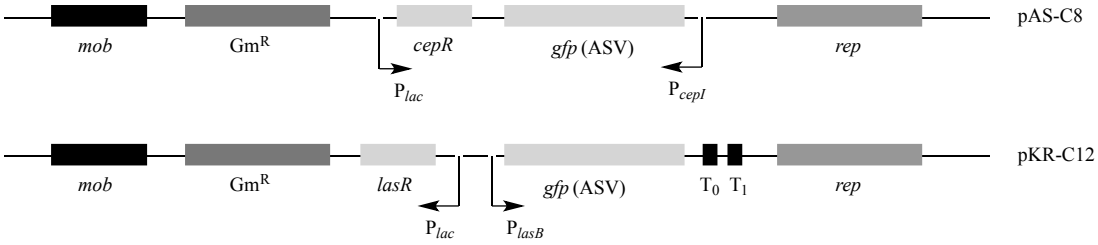

Figure 15: Schematic drawing of the *las*- and *cep*-based AHL sensor plasmids.[64]

The second biosensor is also a *P. putida* ISO F117 wild-type strain that contains a pKR-C12 plasmid. This sensor is based on a translational fusion of *lasB* elastase genes of *P. aeruginosa* to GFP and the *lasR* receptor under control of a *lac*-type promoter. LasR is one out of three QS receptors used by *P. aeruginosa* and is especially sensitive to the natural AHL OdDHL.

The advantage of such biosensors is the lack of AHL production by the bacteria since their synthase genes are knocked out and therefore AHLs need to be added externally for a response. Furthermore, quantitative measurements are feasible since the induced GFP fluorescence correlates to the concentration of the modulators.

---

[64] K. Riedel, M. Hentzer, O. Geisenberger, B. Huber, A. Steidle, H. Wu, N. Høiby, M. Givskov, S. Molin, L. Eberl, *Microbiology* **2001**, *147*, 3249.

2.5 QS in Gram-Positive Bacteria

QS communication is not restricted to Gram-negative bacteria, but is also used by Gram-positive bacteria.[65] However, in the later case, the communication is primarily mediated by chemically modified oligopeptides in a two-component signal-transduction cascade.[30,66] These so called autoinducing peptides (AIPs) range from 5 to 17 amino acids in length and are impermeable to biological membranes. Therefore, AIPs are unable to diffuse into and out of cells. This is carried out by specialized secretion transporters, which are usually connected with signal release. As it is the case for Gram-negative bacteria, the concentration of secreted peptides increases as a function of the cell-population density. One major difference between the AHL mediated and the oligopeptide-based QS systems is the location of the cognate receptors. LuxR-based receptors are cytoplasmic, whereas AIP receptors are membrane-bound. Each species produces a unique sequence for a peptide signal since AIPs are genetically encoded in contrast to Gram-negative bacteria where AHLs can be recognized by multiple species. In *Staphylococcus aureus*, for example, four different AIPs have been found leading to four subtypes of this species. Each AIP must bind to its corresponding receptor to produce signaling interactions. Interactions between AIPs and non-cognate receptors result in quorum quenching due to competitive binding. However, all AIPs belong to the histidine kinase protein family and therefore, they share overall homology.[50]

The signaling pathway (Figure 16) is different from the one used by Gram-negative bacteria. The initially synthesized peptides are posttranslationally modified by the secretion transporter AgrB by incorporation of lactone and thiolactone rings, lanthionines, and isoprenyl groups.[26,28,39] As in AHL QS systems, AIPs accumulate in the extra-cellular space until the minimal concentration is reached. The signaling peptides are then recognized by a membrane-bound two-component histidine kinase receptor AgrA and stimulate its intrinsic autophosphorylation activity. This results in an ATP-driven phosphorylation of a conserved histidine residue in the cytoplasm (H in Figure 16). The phosphoryl group is transferred to an aspartate residue of the cognate response regulator ArgC. The activated receptor regulates gene transcription by inducing the expression of a regulatory RNA. A positive feedback loop is mostly

[65] I. Joint, J. A. Downie, P. Williams, *Phil. Trans. R. Soc. B.* **2007**, *362,* 1115.

[66] C. Fuqua, E. P. Greenberg, *Nature Rev. Mol. Cell Biol.* **2002**, *3*, 685.

accompanied by this event by stimulation of the AIP precursor synthase, similar to the one described in the previous section for Gram-negative bacteria.

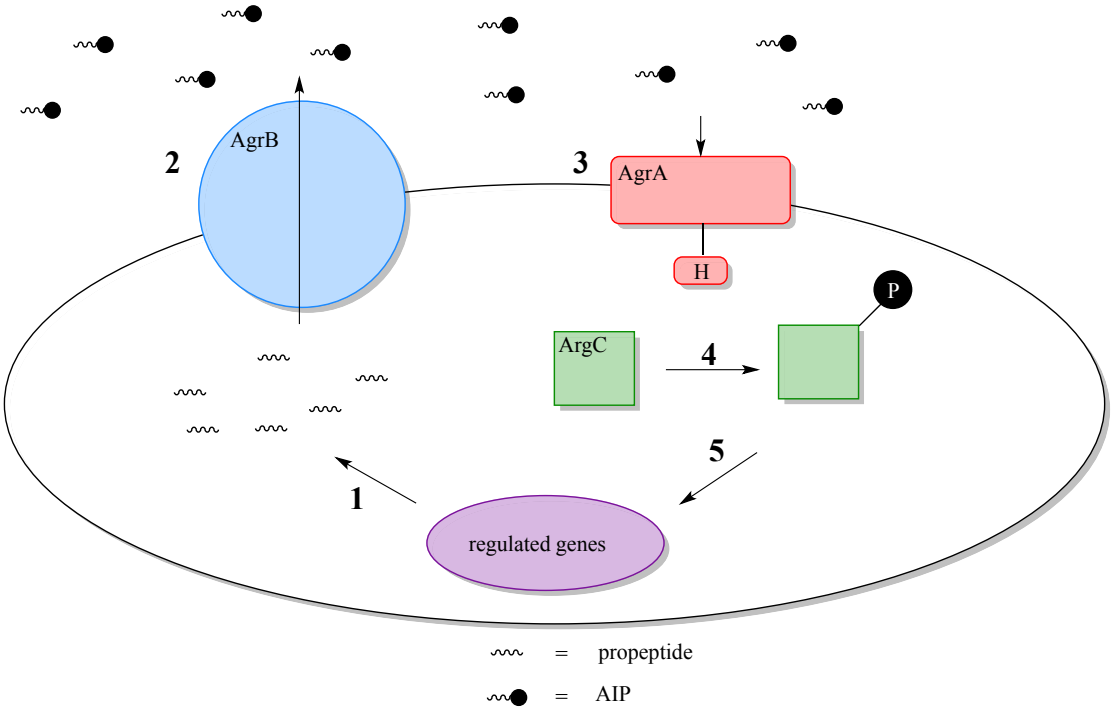

Figure 16: AIP dependent QS pathway. (1) argD (not shown) encodes a propeptide, (2) which is processed and actively exported by AgrB. (3) Mature AIPs interact with the sensor kinase AgrA, (4) leading to the phosphorylation of the response regulator ArgC, (5) which in turn activates the expression of regulated genes.

2.6 AI-2 Mediated Pathway

QS was for a long time thought to be a communication system exclusively used within one bacterial strain. In was only in 1994 when Bassler *et al*. found a different signaling molecule, which could regulate bioluminescence in *Vibrio harveyi*.[67] The identified compound was not structurally related to AHLs and so the authors postulated that a different pathway must be involved, which was termed autoinducer 2 (AI-2). The protein responsible for the synthesis of AI-2 is LuxS, which is encoded by *luxS* and is found in both Gram-positive and Gram-negative bacteria.[68] This finding suggests that AI-2 may connect the two major classes of QS systems by acting as the universal language. AI-2 mediated QS systems have been shown to control

[67] B. L. Bassler, M. Wright, M. R. Silverman, *Mol. Microbiol.* **1994**, *13,* 273.

[68] M. G. Surette, M. B. Miller, B. L. Bassler, *Proc. Natl. Acad. Sci. U. S. A*. **1999**, *96*, 1639.

pathogenicity in *Escherichia coli*, *Salmonella typhimurium* and *Vibrio cholerae* and is also known to influence bacterial fitness.[69]

To date, two different AI-2 ligands have been identified, namely *R*-THMF (**LIX**) and *S*-THMF-borate (**LX**).[70] Interestingly, both signaling molecules are derived from the common intermediate 4,5-dihydroxy-2,3-pentanedione (DPD, **LXI**) as shown in Scheme 1.[71] The small metalloenzyme LuxS is involved in the activated methyl cycle, which is responsible for the production of DPD (**LXI**). The produced **LXI** can undergo spontaneous rearrangements and exists in equilibrium with its two isomers, which depending on the bacterial species can be found in one or the other form. Different species of bacteria recognize distinctly rearranged DPD moieties, thereby allowing them to respond to AI-2 derived from their own DPD and also to that produced by other bacterial species.[39] This phenomenon enables the possibility for interspecies communication in the natural environment. Even though only two AI-2 signaling molecules have been discovered to date (**LX** from *Vibrio harveyi* and **LIX** from *Salmonella enterica* serovar Typhimurium), over 55 types of bacteria are known to possess LuxS homologues.

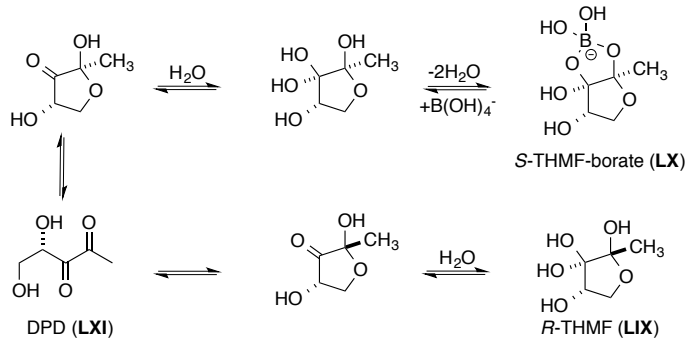

Scheme 1: Isomerization of DPD (**LXI**) to the resulting AI-2 molecules **LX** and **LXI**. DPD (**LXI**) undergoes various rearrangements and additional reactions to form distinct biological active AI-2 signal molecules.

Some species, like *Vibrio harveyi*, took advantage of this feature by being able to monitor their own and the surrounding population density in mixed cultures.[27] AI-2 mediated interactions could occur in natural alcoves, and furthermore, eukaryotes

[69] (a) B. L. Bassler, *Curr. Pin. Microbiol.* **1999**, *2*, 582; (b) A. Vendeville, K. Winzer, K. Heurlier, C. M. Tang, K. R. Hardie, *Nat. Rev. Microbiol.* **2005**, *3*, 383.

[70] X. Chen, S. Schauder, N. Portier, A. Van Dorsselaer, I. Pelezer, B. L. Bassler, F. M. Hughson, *Nature* **2002**, *415*, 545.

[71] K. B. Xavier, B. L. Bassler, *Nature* **2005**, *437*, 750.

could profit from these signaling manipulations by developing particular associations with bacteria that use or interfere with AI-2 mediated communication.

The exact regulation mechanism of *luxS* and LuxS is not yet fully understood and therefore, it is not possible to assign a specific role for AI-2.[72] However, it has been shown that inactivation of *luxS* in several pathogenic strains affected important functions for virulence, such as biofilm production, motility, and toxin production.[73]

[72] S. C. J. De Keersmaecker, K. Sonck, J. Vanderleyden, *Trends Microbiol*. **2006**, *14*, 114.

[73] A. Venderville, K. Winzer, K. Heurlier, C. M. Tang, K. R. Hardie, *Nat. Rev. Microbiol*. **2005**, *3*, 383.

3 Catechol-Based Immobilization of QS Modulators

3.1 Health Care-Associated Infections

Nosocomial infections still remain a major problem for patients worldwide and are rising at an alarming rate.[74] Among those, bacterial infections of implant materials and devices, such as catheters and stents, pose a major threat on the quality of life of those affected.[75] Recent studies showed that almost half of all nosocomial infections are caused by such device-associated infections.[76] The likeliness of an early stage infection has much been ameliorated by improved procedures in sterilization, proper hygiene, and operating techniques.[77] However, infections occurring weeks or months after surgery have barely decreased.

Bacteria possess the ability to attach themselves to biomedical implants and thereby trigger infections in the host organism. Such infections are usually not detected before some damage has occurred to tissue of the host organism. After adherence of the intruders, the microorganisms grow and accumulate in multilayered cell clusters, thereby forming biofilms, which are considered to be the first steps in nosocomial infections.[78] In this state, bacteria defend themselves against the host's innate immune system by forming an exocellular polysaccharide matrix, which also protects them from antibiotics. When bacteria exist as a biofilm, they can become 10-1000 times more resistant to the effects of a direct systemic treatment with antibiotics.[79] The likelihood of a successful treatment is furthermore complicated by

---

74 (a) P. W. Stone, D. Braccia, E. Larson, *Am. J. Infect. Control* **2005**, *33*, 501; (b) D. Cardo, T. Horan, M. Andrus, M. Dembinski, J. Edwards, G. Peavy, J. Tolson, D. Wagner, *Am. J. Infect. Control* **2004**, *32*, 470; (c) L. L. Leape, T. A. Brennan, N. Laird, A. G. Lawthers, A. R. Lacolio, B. A. Barnes, L. Hebert, J. P. Newhouse, P. C. Weiler, H. Hiatt, *N. Engl. J. Med*. **1991**, *324*, 377.

75 (a) J. L. Del Pozo, R. Patel, *N. Engl. J. Med.* **2009**, *361*, 787; (b) W. Zimmerli, A. Trampuz, P. E. Ochsner, *N. Engl. J. Med.* **2004**, *351*, 1645.

76 (a) R. O. Darouiche, *Int. J. Artif. Organ* **2007**, *30*, 820; (b) B. Foxman, *Am. J. Med*. **2002**, 113, 5S; (c) K. L. Garvin, A. D. Hanssen, *J. Bone Jt. Surg. Am. Vol.* **1995**, *77*, 1576; (d) N. Rao, G. L. Soxman, *Op. Techn. Orthop*. **2002**, *12*, 131; (e) S. Saint, C. E. Chenoweth, *Infect. Dis. Clin. North Am.* **2003**, *17*, 411; (f) J. W. Warren, *Med. Clin. North Am*. **1991**, *75*, 481.

77 C. Muto, C. Herbert, E. Harrison, J. R. Edwards, T. Horan, M. Andrus, J. A. Jernigan, P. K. Kutty, *MMWR* **2005**, *54*, 1013.

78 (a) J. M. Higashi, I.-W. Wang, D. M. Shlaes, J. M. Anderson, R. E. Marchant, *J. Biomed. Mater. Res.* **1998**, *39*, 341; (b) K. M. Cunnion, J. C. Lee, M. M. Frank, *Infect. Immun.* **2001**, *69*, 6796.

79 (a) T.-F. C. Mah, G. A. O'Toole, *TRENDS Microbiol.* **2001**, *9*, 34; (b) H. S. Gold, R. C. Moellering, *N. Engl. J. Med.* **1996**, *335*, 1445; (c) J. M. Rodriguez-Martinez, A. Pascual, *Rev. Med. Microbiol*. **2006**, *17*, 65; (d) A. J. J. Wood, H. S. Gold, R. C. Moellering, *N. Engl. J. Med*. **1996**, *335*, 1445.

the rise of resistant bacterial strains.[80] As a result, current treatment usually requires surgical replacement of the infected devices, combined with a prolonged intravenous and oral administration of antibiotics.[81] The outcome of such complications is not only additional costs to the health care system, but most importantly suffering of the patients and occasionally their death. It has been estimated that biofilms are associated with 65% of nosocomial infections.[82] Therefore, about 30% of the hospitals in the US are using antimicrobial catheters to prevent hospital-acquired urinary tract infections.[83] In these cases, the release of silver ions is mostly used to prevent infections. The usage of silver containing medical devices should however be undertaken with caution since recent studies demonstrated that silver exhibits a certain level of toxicity to mammalian cells.[84] Furthermore, the extensive and uncontrolled use of silver-containing products may result in more bacteria evolving resistance,[85] and the clinical efficiency of silver-coated catheters is controversial.[86]

The urgent need for new bioactive surfaces that can prevent infections of implants has driven many research groups to seek for alternatives. Many different techniques have been established in recent years for the coating of biomedical devices. Some of the approaches include biopassive and bioactive surfaces, with either a covalently attached bioactive moiety or one that is released into the surrounding area. Our special interest goes to the use of a biomimetic coating strategy inspired by the strong adhesion of mussels, which will be discussed in more detail in following section.

---

80 (a) J. P. Burke, *N. Engl. J. Med.* **2003**, *348*, 651; (b) J. W. Costerton, *Science* **1999**, *284*, 1318; (c) C. Walsh, *Nature* **2000**, *406*, 775; (d) J. W. Costerton, P. S. Stewart, E. P. Greenberg, *Science* **1999**, *284*, 1318.

81 A. S. Lynch, G. T. Robertson, *Annu. Rev. Med.* **2008**, *59*, 415.

82 L. K. Archibald, R. P. Gaynes, *Infect. Dis. Clin N. Am*. **1997**, *11*, 245.

83 S. Saint, C. P. Kowalski, S. R. Kaufman, T. P. Hofer, C. A. Kauffman, R. N. Olmsted, J. Forman, J. Banaszak-Holl, L. Damschroder, S. L. Krein, *Clin. Infect. Dis.* **2008**, *46*, 243.

84 (a) L. Braydich-Stolle, S. Hussain, J. J. Schlager, M. C. Hofmann, *Toxicol. Sci.* **2005**, *88*, 412; (b) J. M. Schierholz, J. Beuth, G. Pulverer, *Am. J. Med*. **1999**, *107*, 101.

85 S. Silver, *FEMS Microbiol. Rev*. **2003**, *27*, 341.

86 J. M. Schierholz, N. Yucel, A. F. E. Rump, J. Beuth, *G. Int. J. Antimicrob. Agents* **2002**, *19*, 511.

3.2 Bioinspired Adhesion

The adhesion of bioactive molecules to surfaces has been explored by numerous research groups. Especially the preparation of self-assembled monolayers (SAMs) has attracted significant attention in this field since their introduction in 1980.[87] SAMs are formed by the adsorption of compounds from solution or from the gas phase onto a surface. Many different functional groups, such as thiols,[88] silanes,[89] and phosphates,[90] have been established as anchoring moieties for gold and silver surfaces, glass surfaces or various metal surfaces, respectively. However, there has been a limitation that the binding chemistry to be applied is determined by the surface chemistry of the substrate materials. Therefore, surface binding anchoring groups with wide substrate applicability, easy handling, long-term stability and inertness towards environmental conditions are still highly desired.

Recently, catechols have been described as a promising alternative for the use as a mild, rapid, and efficient functionalization of metal and metal oxide surfaces by convenient dip-and-rinse protocols.[91] The development of catechols as molecular anchors has been inspired by the adhesive properties of marine and freshwater mussels to all kind of surfaces (Figure 17).[92] The extremely strong wet adhesion of mussels relies on the production of mussel adhesive proteins (MAPs), which are secreted by the marine organisms.[92b,93] The key constituent for adhesion of MAPs has been shown to be the posttranslationally modified amino acid 3,4-dihydroxyphenyl-L-alanine (DOPA, **LX**), which makes up about 27% of all amino acids.[92a]

---

87 J. Sagiv, *J. Am. Chem. Soc*. **1980**, *102*, 92.

88 (a) J. C. Love, L. A. Estroff, J. K. Kriebel, R. G. Nuzzo, G. M. Whitesides, *Chem. Rev*. **2005**, *105*, 1103; (b) J. Rundqvist, J. H. Hoh, D. B. Haviland, *Langmuir* **2005**, *21*, 2981.

89 (a) Z. Yang, J. A. Galloway, H. Yu, *Langmuir* **1999**, *15*, 8405; A. Papra, N. Gadegaard, N. B. Larsen, *Langmuir* **2001**, *17*, 1457.

90 (a) R. Hofer, M. Textor, N. D. Spencer, *Langmuir* **2001**, *17*, 4014; (b) S. G. P. Tosatti, R. Michel, M. Textor, N. D. Spencer, *Langmuir* **2002**, *18*, 3537; (c) V. Zoulalian, S. Monge, S. Zürcher, M. Textor, J. J. Robin, S. Tosatti, *J. Phys. Chem. B* **2006**, *110*, 25603.

91 (a) J. H. Waite, M. L. Tanzer, *Science* **1981**, *212*, 1038; (b) C. R. Rice, M. D. Ward, M. K. Nazeeruddin, M. Grätzel, *New J. Chem.* **2000**, *24*, 651; (c) J. L. Dalsin, B.-H. Hu, B. P. Lee, P. B. Messersmith, *J. Am. Chem. Soc.* **2003**, *125*, 4253; (d) X. Fan, L. Lin, J. L. Dalsin, P. B. Messersmith, *J. Am. Chem. Soc.* **2005**, *127*, 15843; (e) H. Lee, N. F. Scherer, P. B. Messersmith, *PNAS* **2006**, *103*, 12999; (f) J. L. Dalsin, P. B. Messersmith, *Mater. Today* **2005**, 38.

92 (a) T. J. Deming, *Curr. Opin. Chem. Biol.* **1999**, *3*, 100; (b) H. G. Silverman, F. F. Roberto, *Mar. Biotechnol.* **2007**, *9*, 661.

93 J. H. Waite, *Integr. Comp. Biol*. **2002**, *42*, 1172.

Figure 17: Mussels secrete proteins for adherence to surfaces, such as TiO_2.

The research groups of Waite,[91a] Grätzel,[91b] Messersmith/Textor,[91c-f] Wilker,[94] and Xu [95] demonstrated the benefits of catechols as anchoring moieties for the functionalization of surfaces. Their findings lead to the establishment of many different bioactive applications.[96] Catechol derivatives have been studied and compared for their binding capacities (**LX-LXV**, Figure 18). Dopamine (**LXI**) and L-DOPA (**LX**) exhibit strong binding capacity, but these moieties can easily be oxidized and polymerize, rendering their handling and storage problematic.[97] More stable catechol moieties can be found in nature, such as, for example, the anachelin chromophore (**LXII**), a cyanobacterial siderophore.[98] These bacteria use anachelin to bind and sequester iron, since iron can become a growth-limiting nutrient in marine environment due to its very low bioavailability.[99] The chromophore contains a quaternary ammonium substituent that renders this compound oxidatively more stable than dopamine (**LXI**). Additionally, the positive charge increases the affinity of this anchor towards negatively charged surfaces. Even superior binding properties to

94 M. J. Sever, J. T. Weisser, J. Monahan, S. Srinivasan, J. J. Wilker, *Angew. Chem. Int. Ed*. **2004**, *43*, 448.

95 C. Xu, K. Xu, H. Gu, Z. Guo, B. Xu, R. Zheng, H. Liu, X. Zhang, *J. Am. Chem. Soc*. **2004**, *126*, 9938.

96 Reviews: (a) J. Sedó, J. Saiz-Poseu, F. Busqué, D. Ruiz-Molina, *Adv. Mater.* **2013**, *25*, 653; (b) Q. Ye, F. Zhou, W. Liu, *Chem. Soc. Rev.* **2011**, *40*, 4244.

97 (a) B. Malisova, S. Tosatti, M. Textor, K. Gademann, S. Zürcher, *Langmuir* **2010**, *26*, 4018; (b) S. Zürcher, D. Wäckerlin, Y. Bethuel, B. Malisova, M. Textor, S. Tosatti, K. Gademann, *J. Am. Chem. Soc*. **2006**, *128*, 1064.

98 (a) A. E. Walsby, *Br. Phycol. J.* **1974**, *9*, 371; (b) A. E. Walsby, *Br. Phycol. J*. **1974**, *9*, 383; (c) Y. Ito, K. Ishida, S. Okada, M. Murakami, *Tetrahedron* **2004**, *60*, 9075.

99 Review: K. N. Raymond, E. A. Dertz, S. S. Kim, *PNAS* **2003**, *100*, 3584.

metal oxides are exhibited by this anchoring moiety.[100] Nonsubstituted catechols possess the disadvantage of being easily oxidized and polymerized, which is not beneficial for the stability of adsorbed monolayers. These limitations can be overcome by introducing a substituent in the aromatic ring. The purely chemical derivative nitro-catechol (**LXIV**) demonstrated excellent binding properties, which could be derived from the significantly lower pK_a of its catechol hydroxyl group as a consequence of the strong electron withdrawing NO_2 group.[97a] Although this anchor possesses slightly weaker binding properties than the anachelin chromophore, it is synthetically readily accessible as it can be prepared in a single step from the commercially available and inexpensive dopamine, whereas **LXII** requires multiple synthetic steps, involving heavy-metal-based[101] or enzymatic[102] conversions.

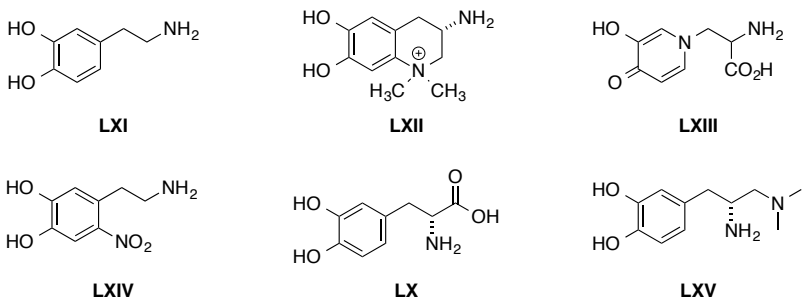

Figure 18: Catechol-based molecular anchors.

Although catechols have been known to be the only functional element required for adhesion and cross-linking, the exact adhesion mechanism is not yet fully understood. Two different coordination schemes were recently proposed for dopamine binding to metal cations of metal oxide surfaces (Figure 19).[97a,103] One possible coordination comprises monodentate binding, in which one of the two catechol hydroxyl groups dissociates and binds to a metal cation and the second one forms hydrogen bond to the next catechol neighbor or hydroxyl group on the metal oxide surface. The second coordination mode is the mixed monodentate-bidentate, where

[100] K. Gademann, J. Kobylinska, J.-Y. Wach, *BioMetals* **2009**, *22*, 595.

[101] (a) K. Gademann, Y. Bethuel, *Org. Lett.* **2004**, *6*, 4707; (b) K. Gademann, Y. Bethuel, *Angew. Chem. Int. Ed.* **2004**, *43*, 3327.

[102] (a) K. Gademann, Y. Bethuel, H. H. Locher, C. Hubschwerlen, *J. Org. Chem.* **2007**, *72*, 8361; (b) K. Gademann, *ChemBioChem* **2005**, *6*, 913.

[103] M. Rodenstein, S. Zürcher, S. G. P. Tosatti, N. D. Spencer, *Langmuir* **2010**, *26*, 16211.

both hydroxyl groups dissociate and become coordinated to two adjacent metal cations.

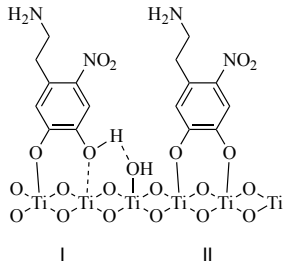

Figure 19: Two possible coordination modes of nitro-dopamine (**LXIV**) adsorbed on TiO_2: (I) monodentate binding with a hydrogen bridge to a neighboring surface hydroxide and (II) bidentate binding.[103]

Dopamine and its derivatives could be used for the coating of most metal oxide surfaces. Nevertheless, we were particularly interested in the functionalization of titanium dioxide (TiO_2) since this metal oxide has been shown to be biocompatible and is also frequently applied in the field of medical devices.[104]

3.3 Catechol-Based Coating Strategies

Much effort has been devoted to the creation of surfaces that can prevent bacterial infections, especially in the preparation of either antifouling or antibacterial surfaces. The following sections will present the latest achievements in this field based on catechol-derived adsorption on TiO_2 surfaces.

3.3.1 Antifouling Coating

Biofouling has been defined as the nonspecific attachment of proteins, carbohydrates, and microorganisms onto surfaces upon their immersion in biological fluids.[105] Once a surface has been covered with proteins, it can easily be colonialized by bacterial populations.[78] Therefore, antifouling materials have been the subject of much interest and extensive research in recent years.[106] Much effort has been made for the development of thin polymer coatings by a number of techniques *e.g.* plasma

[104] (a) P. Tengvall, I. Lunstrom, *Clin. Mater*. **1992**, *9*, 115; (b) X. Liu, P. K. Chu, C. Ding, *Mater. Sci. Eng. Res*. **2004**, *47*, 49.

[105] K. Gademann, *CHIMIA* **2007**, *61*, 373.

[106] (a) I. Banerjee, R. C. Pangule, R. S. Kane, *Adv. Mater.* **2011**, *23*, 690; (b) P. Kingshott, H. J. Griesser, *Curr. Opin. Solid State Mater. Sci*. **1999**, *4*, 403; (c) D. M. Yebra, S. Kiil, K. Dam-Johansen, *Prog. Org. Coat*. **2004**, *50*, 75.

polymerization.[107] The efficiency of such a coating strategy strongly depends on various parameters, such as substrate and polymer type, adsorption time, pH, temperature, solvent choice, and polymer concentration, thereby hampering a facile design of the polymer. Molecular self-assembly systems can overcome these problems by forming well controlled, structurally defined interfaces.

The prevention of bacterial adhesion can be achieved by the formation of biopassive surfaces that decrease the direct contact between the microorganisms and the surface. Polyethylene glycol (PEG) has been shown to possess antifouling properties on the surface of various materials.[108] Various techniques have been adapted for this purpose. All these approaches using PEG-coated biomaterials were shown to drastically decrease the amount of adsorbed proteins due to the formation of an interfacial layer without directly interfering with the bacteria.

Catechols can offer the perfect anchoring properties as already described in the previous section. The key advantage of such a system is the facile functionalization of the surface, which can be achieved by a simple dip-and-rinse procedure in aqueous solutions.[97, 109] The combination of the binding properties of catechols and the antifouling properties of PEG was previously realized in the Gademann research group. Various catechol-based anchors were conjugated to a PEG unit to provide coating agents **LXVI-LXIX** as shown in Figure 20.[97a, 110] These hybrids were adsorbed onto TiO_2 plates and tested for their antifouling properties. A remarkable reduction of the protein adlayer thickness of over 95% was observed upon exposure to full human serum in comparison to untreated control surfaces. This strategy enabled the formation of a stable, protein-resistant adlayer. The best results were obtained with anachelin and the nitro-dopamine derivatives **LXVI** and **LXVII**, respectively. These two entities proved to be particularly useful due to the excellent binding strength of the anchor moiety and the oxidative stability when compared to other dopamine derivatives.

---

[107] (a) K. Vasilev, S. S. Griesser, H. J. Griesser, *Plasma Processes Polym*. **2011**, *8*, 1010; (b) M. Charnley, M. Textor, C. Acikgoz, *React. Funct. Polym*. **2011**, *71*, 329; (c) K. G. Neoh, E. T. Kang, *Appl. Mater. Interfaces* **2011**, *3*, 2808.

[108] (a) R. L. C. Wang, H. J. Kreuzer, M. Grunze, *J. Phys. Chem. B* **1997**, *101*, 9767; (b) K. Yoshimoto, M. Nishio, H. Sugasawa, Y. Nagasaki, *J. Am. Chem. Soc.* **2010**, *132*, 7982; (c) H. J. Kreuzer, M. Grunze, *Europhys. Lett*. **2001**, *55*, 640.

[109] R. Wehlauch, J. Hoecker, K. Gademann, *ChemPlusChem* **2012**, *77*, 1071.

[110] J.-Y. Wach, B. Malisova, S. Bonazzi, S. Tosatti, M. Textor, S. Zürcher, K. Gademann, *Chem. Eur. J.* **2008**, *14*, 10579.

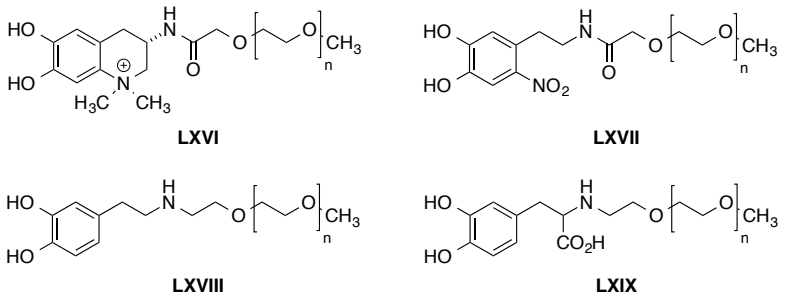

Figure 20: PEG-catechol derivatives as antifouling agents.[97a,111]

Antifouling surfaces have an enormous potential for industrial applications and especially for marine transportation techniques.[111] However, in terms of preventing bacterial infections, an approach that exhibits bactericidal properties would be advantageous. Therefore, alternative strategies that can actively alter bacterial behavior have been explored.

3.3.2 Antibacterial Coating

An appealing strategy to actively interact with bacteria is the incorporation of active biocides into the implant material or their adsorption onto the surface.[104b,112] Such antibiotic surfaces possess the ability to actively combat bacteria upon exposure, in contrast to antifouling surfaces. The mode of action can either be by slow release of the active compound into the local tissue or by killing upon contact with the bacteria.[113] The major advantage of this approach is the high local concentrations of antibiotics at the surface interface, therewith maximizing impact and minimizing undesired side effects.[114] Customary antimicrobials that have been incorporated into such materials include antibiotics,[115] antibodies,[116] and nitric oxide.[117] Default procedures for the immobilization of antibiotics usually requires multiple chemical

[111] M. Callow, *Chem. Ind*. **1990**, *5*, 123.

[112] M. Lucke, *Chem. Biol*. **2005**, *12*, 958.

[113] Reviews: (a) J. C. Tiller, *Adv. Polym. Sci.* **2011**, *240*, 193; (b) L. Ferreira, A. Zumbuehl, *J. Mater. Chem*. **2009**, *19*, 7796.

[114] (a) J. M. Schierholz, J. Beuth, *Hospital Infect*. **2001**, *49*, 87; (b) H. van der Belt, D. Neut, W. Schenk, J. R. van Horn, H. C. vand der Mei, H. J. Buscher, *Acta Orthop. Scand*. **2001**, *72*, 557.

[115] (a) W. S. Anthony, *Adv. Drug Delivery Rev*. **2005**, *57*, 1539; (b) P. Wu, D. W. Grainger, *Biomaterials* **2006**, *27*, 2450.

[116] D. W. Grainger, *Expert Opin. Biol. Ther*. **2004**, *4*, 1029.

[117] (a) P. N. Coneski, K. S. Rao, M. H. Schoenfisch, *Biomacromolecules* **2010**, *11*, 3208; (b) P. N. Coneski, M. H. Schoenfisch, *Polym. Chem*. **2011**, *2*, 906.

steps on the solid surface and scale-up of these processes can be challenging.[118] These disadvantages could be circumvented by the preparation of coated implant surfaces *via* simple dip-and-rinse procedures. This was achieved by linking vancomycin, a well-studied antibiotic agent frequently used against bacterial infections, to the anachelin chromophore *via* a PEG chain (Figure 21).[119] This natural product hybrid **LXX** possesses three important features: strong binding capacity to metal oxide surfaces due to the anachelin chromophore moiety, antifouling character of the PEG linker in order to prevent bacterial adhesion onto the surface, and antiseptic properties against Gram-positive bacteria due to the antibiotic vancomycin.

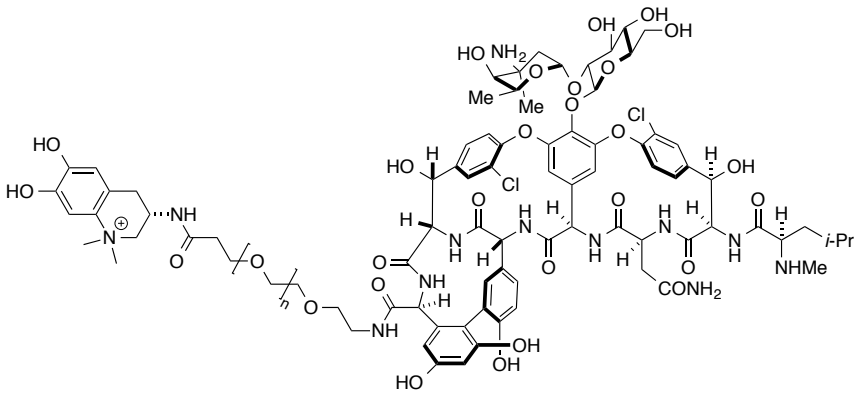

LXX

Figure 21: Antibacterial coating agent.[120]

Biological evaluation of the treated surfaces against *Bacillus subtilis* showed that the desired antibacterial properties could be retained on the surface. In addition, recycling of the used surfaces proved to be successful, as they could be rinsed with water and reused without loss in antimicrobial activity.

The application field for such antibiotic surfaces might even be expanded by combining different antibiotics on biomedical surfaces. Even though it could be shown that bacterial populations can be reduced by exposure to such surfaces, further investigations are required in order to test if resistances of bacteria are developed upon exposure and if accumulation of bacterial biomass on the coated surface will lead to reduction of its antimicrobial activity over a long period of time. The major

[118] B. Jose, V. Antoci, A. R. Zeiger, E. Wickstrom, N. J. Hickok, *Chem. Biol*. **2005**, *12*, 1041.
[119] J.-Y. Wach, S. Bonazzi, K. Gademann, *Angew. Chem. Int. Ed.* **2008**, *47*, 7123.

concern with this approach is the rise of resistant bacterial strains, which might even be accelerated by misuse of antibiotics.

3.4 QS Modulating Coating

The previously described approaches are characterized by specific drawbacks that hamper the application as effective inhibitors of bacterial infections on surface implants. The scope of the present thesis consists of a completely different approach to prevent biofilm formation, namely by inhibition of QS.[120] Extracellular polymer production, surface attachment, sporulation, and the secretion of virulence factors are only few examples of functions that are controlled by QS in various bacterial populations. This means that interfering with the QS system represents an alternative approach to inhibit biofilm development.

Many organisms have found and developed ways to protect themselves from bacterial infections. It is therefore no surprise that some examples of antibiofilm strategies based on the inhibition of QS communication pathways can be found in nature. One of the most fascinating examples can be found in *Delisea pulchra*, a native red algae of southeastern Australia.[121] This microorganism has the ability to store anti-QS substances in vesicles situated on the outside of the algae to inhibit bacterial colonization. The active compounds secreted by the algae are composed of a range of halogenated furanones named fimbrolides. Based on these findings, several research groups have investigated various synthetic methods to immobilize furanones on polymer materials to inhibit biofilm formation.[122] The drawback of these approaches is the cytotoxic and mutagenic properties expressed by such furanones, which limits their practical applications.[123]

---

[120] R. Mittal, S. Sharma, S. Chhibber, S. Aggarwal, V. Gupta, K. Harjai, *FEMS Immun. Med. Microbiol.* **2010**, *58*, 237; M. Juhas, L. Eberl, B. Tummler, *Environ. Microbiol.* **2005**, *7*, 459; S. P. Diggle, S. A. Crusz, M. Cámara, *Curr. Biol.* **2007**, *17*, R907.

[121] M. Manefield, R. de Nys, N. Kumar, R. Read, M. Givskov, P. Steinberg, S. Kjelleberg, *Microbiology* **1999**, *145*, 283.

[122] (a) E. B. H. Hume, J. Baveja, B. Muir, T. L. Schubert, N. Kumar, S. Kjelleberg, H. J. Griesser, H. Thissen, R. Read, L. A. Poole-Warren, K. Schindhelme, M. D. P. Willcox, *Biomaterials* **2004**, *25*, 5023; (b) S. A. Al-Bataineh, L. G. Britcher, H. J. Griesser, *Surf. Interface Anal.* **2006**, *38*, 1512.

[123] (a) R. T. LaLonde, L. Bu, A. Henwood, J. Fiumano, L. Zhang, *Chem. Res. Toxicol.* **1997**, *10*, 1427; (b) T. Janecki, E. Błaszczyk, K. Studzian, M. Różalski, U. Krajewska, A. Janecka, *J. Med. Chem.* **2002**, *45*, 1142.

More recent immobilization strategies are based on the molecular interference with QS pathways for the prevention and eradication of bacterial biofilms.[124] Blackwell and co-workers demonstrated a first approach by achieving controlled release of non-native QS modulators from thin PLG films.[125] However, we focused on preparing coated TiO_2 surfaces bearing covalently bound QS modulators. Based on the previous results obtained in our research group, we envisaged attachment of a QS modulator to a dopamine-based molecular anchor. A large variety of different AHL analogues with different chain lengths and substituents at the terminus of the acyl side chain were prepared in the Gademann research group (Figure 22).[126] Preliminary screening with the AHL biosensor strain *C. violaceum* CV026[127] showed that hybrids bearing a C_{12} linker were able to induce QS. Especially two out of these hybrids caught our attention, namely the dopamine and the anachelin chromophore hybrids **LXXI** and **LXXII**. Compounds with shorter alkyl linker (**LXXIII**) did not show any QS modulating properties. Interestingly, hybrid **LXXIV** bearing biotin at the alkyl chain terminus revealed no agonistic properties in contrast to its dopamine counterparts. This observation might arise from steric hindrance induced by the biotin moiety.

[124] V. Lazar, *Anaerobe* **2011**, *17*, 280.

[125] A. S. Breitbach, A. H. Broderick, C. M. Jewell, S. Gunasekaran, Q. Lin, D. M. Lynn, H. E. Blackwell, *Chem. Comm.* 2011, **47**, 370.

[126] Adrien Lawrence, PhD Thesis, Lausanne, **2010**.

[127] K. H. McClean, M. K. Winson, L. Fish, A. Taylor, S. R. Chhabra, M. Cámara, M. Daykin, J. H. Lamb, S. Swift, B. W. Bycroft, G. S. A. B. Stewart, P. Williams, *Microbiology* **1997**, *143*, 3703.

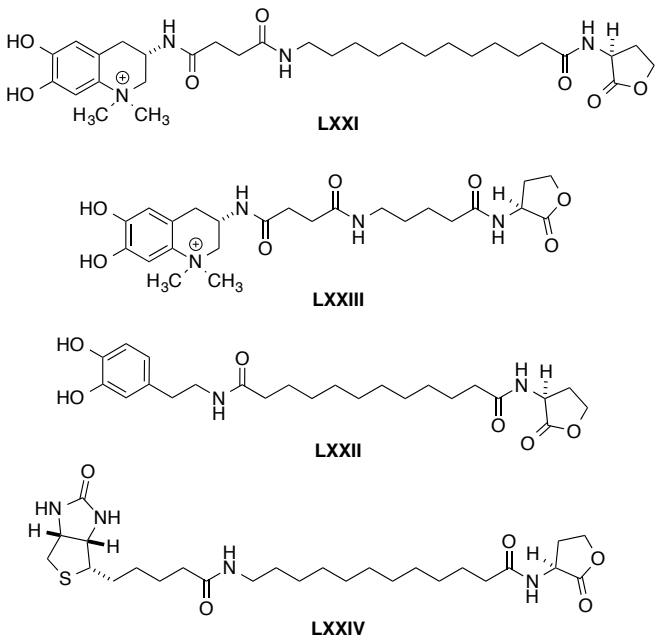

Figure 22: AHL analogues previously prepared.[127]

These initial findings suggested that AHLs bearing a catecholic moiety at the terminus and a chain of twelve carbon units may be used for the coating of TiO_2 surfaces, providing that the molecular anchor is sterically not too bulky. The synthetic and biological results obtained in our further studies will be discussed in the following section.

3.5 Results and Discussion[128]

3.5.1 Synthesis of the Nitro-Dopamine Containing QS Modulator

A first challenge consisted in finding a more suitable surface anchor moiety that remains to be recognized by the bacteria as QS modulator. The previously shown hybrids were either not stable to oxidative conditions or require multiple synthetic steps. Therefore, we envisaged using nitro-dopamine as the binding group since this moiety has been shown to bind strongly to several metal oxides. Furthermore, it can be used for the generation of SAMs using a simple dip-and-rinse procedure.

The bioactive moiety was chosen to be the native AHL as used by Gram-negative bacteria. The length of the linker had been shown to be crucial. Hybrids bearing other linker sizes did not lead to QS induction, even at high concentrations. The synthesis of

[128] J. Gomes, A. Grunau, A. K. Lawrence, L. Eberl, K. Gademann, *Chem. Commun.* **2013**, *49*, 155.

the target molecule **1** is shown in Scheme 2 and could be achieved in only three chemical steps from commercial dodecandioic acid (**2**) in an overall yield of 72%. The purification proved to be cumbersome, since no separation of the desired product could be achieved by using flash chromatography on silica gel. A high purity was obtained by using size exclusion chromatography on Sephadex LH-20 with methanol as the mobile phase.

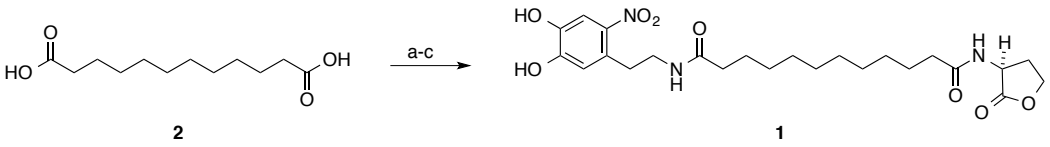

2 1

Scheme 2: a) NSC, pyridine, MeCN, r.t., 7 h, quant.; b) nitro-dopamine, Et_3N, THF/DMSO, r.t., 20 h; c) (*S*)-α-amino-γ-butyrolactone hydrobromide, Et_3N, THF/DMSO, r.t., 20 h, 72% over two steps.

The purified hybrid was then incubated with the two GFP-based biosensors *P. putida* Iso F117 pAS-C8 and pKR-C12. We were pleased to see that fluorescence could only be observed in the pAS-C8 strain, as we were hoping to get selectivity for this sensor. The activation levels were similar to the ones achieved by using *N*-octanoyl-L-homoserine lactone (C_8-AHL), for which it is most sensitive. After having established that compound **1** was able to interfere with QS in a liquid based assay, we wanted to evaluate its activity after immobilization on surfaces.

3.5.2 Immobilization on TiO_2 Beads

TiO_2 served as the perfect surface material for our purposes as this metal oxide is widely used for orthopedic and dental implants due to its biocompatibility.[104] As we were uncertain about the possible mode of action, we decided to use small TiO_2 beads with a diameter of either 1 or 44 μm. The use of beads allowed for the monitoring of the exact position of the QS-active bacteria. The immobilization was performed with a modified procedure, since dipping and rinsing is not practicable with such small particles. Thus, the beads were incubated in a dilute solution of **1** in high salt buffer (0.1 M MOPS/0.6 M NaCl/0.6 M K_2SO_4) for 4 hours at 50 °C and subsequently centrifuged. The obtained beads were then washed with water to remove the remaining salts and unattached hybrids. Next, the resulting beads were incubated with the biosensor *P. putida* F117 (pAS-C8) and again GFP fluorescence could be induced.

These results demonstrate that the bioactive properties of the hybrids can be transferred to the metal oxide surface.

We then wondered if the immobilized hybrids could be removed from the beads by sequential washing operations. Therefore, the beads were washed up to ten times with water and evaluated again as shown in Figure 23. Remarkably, no discrepancy in the biological activity could be observed upon repeated rinsing by measuring the GFP levels in the pAS-C8 reporter strain. The retained activity can be attributed to the strong binding capacity of nitro-dopamine and demonstrates its potential for biological applications.

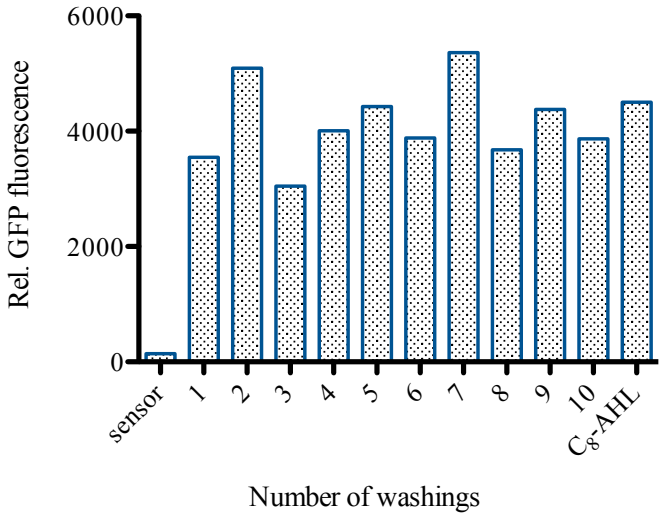

Figure 23: Induced GFP fluorescence after repeated washing of the beads (0.6 mg mL^{-1}) compared to the sensor as the negative and C_8-AHL as the positive control (0.3 µM).

The next point we needed to address was the mode of action of the functionalized beads. The advantage of using beads instead of larger surfaces is the possibility to determine if QS is induced exclusively at the surface or in the entire bacterial population by fluorescence microscopy. Therefore, the functionalized beads were again incubated for two hours with the pAS-C8 biosensor strain along with a positive and a negative control. The negative control experiment was performed without addition of an inducer and no fluorescence could be detected as expected (Figure 24 A and B). Incubation with hybrid **1** served as the positive control for this experiment and the reporter strain produced GFP (C and D). The incubated functionalized beads showed to induce QS in the entire bacterial population similarly to the free

modulators (E and F). These findings showed that the microorganism do not adhere to the activated surfaces, thereby suggesting a different mechanisms of action. One possibility is that QS is induced upon contact of a bacterium with the surface by concomitant capture, implying that QS receptors are present at the cell-surface. Another possibility is that the active compounds are slowly released from the surface and subsequently induce QS in the reporter strain.

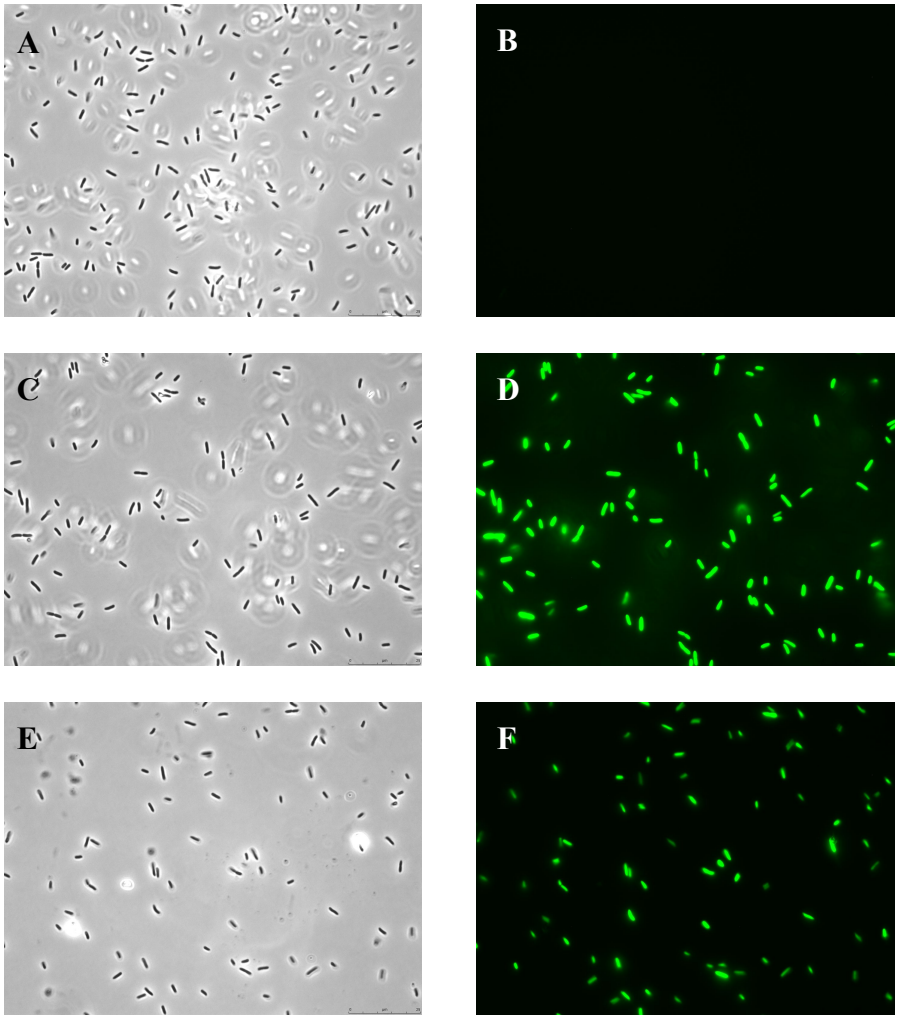

Figure 24: Phase contrast (A) and GFP fluorescence (B) of the sensor as a negative control. Phase contrast (C) and GFP fluorescence (D) of the sensor incubated with hybrid **1** as a positive control. Phase contrast (E) and GFP fluorescence (F) of the sensor incubated with the functionalized beads.

3.5.3 Dialysis Experiments

In order to provide more data to establish a mechanism, we performed dialysis assays using cellulose ester membranes with a 3.5-5 kDa molecular weight cut off. In these assays, the beads were placed inside dialysis bags before incubating with the medium. The membrane does not permit diffusion of the beads, whereas released AHL mimics can simply diffuse into the surrounding medium and induce the biosensor. Dialysis was performed overnight in buffer solution, and the supernatant was then incubated with the sensor for 3 hours at 30 °C. The supernatant was capable of inducing QS in the reporter strain, which supports the mechanism that AHL mimics are released from the beads.

To investigate the release rate, aliquots were taken after different dialysis times and compared the induced GFP fluorescence to known C_8-AHL concentrations. The results are shown in Figure 25 and demonstrate that the positive control using dialyzed compound C_8-AHL reaches its maximum activity after a short induction period as expected. AHLs are known to be slowly hydrolyzed non-enzymatically under physiological condition, explaining the activity decreased after overnight incubation.[129] The release of the hybrids from the beads is, in contrast, much slower and an increasing activity is observed even in the overnight incubation experiment. The precise mechanism of release is not yet fully understood, but the measurements of QS activity follow a linear increase in time. Hydrolysis of the released hybrids could falsify the obtained results, as only the non-hydrolyzed AHLs are capable of inducing QS in biosensor strain. Thus, compound **1** was heated at 50 °C and pH 6 for 4 hours in an aqueous buffer solution, however, no traces of the hydrolyzed product could be observed by UPLC-MS analysis.

[129] (a) F. G. Glansdorp, G. L. Thomas, J. K. Lee, J. M. Dutton, G. P. C. Salmond, M. Welch, D. R. Spring, *Org. Biomol. Chem*. 2004, **2**, 3329; (b) J. T. Byers, C. Lucas, G. P. C. Salmond, M. Welch, *J. Bacteriol.* 2002, **184**, 1163.

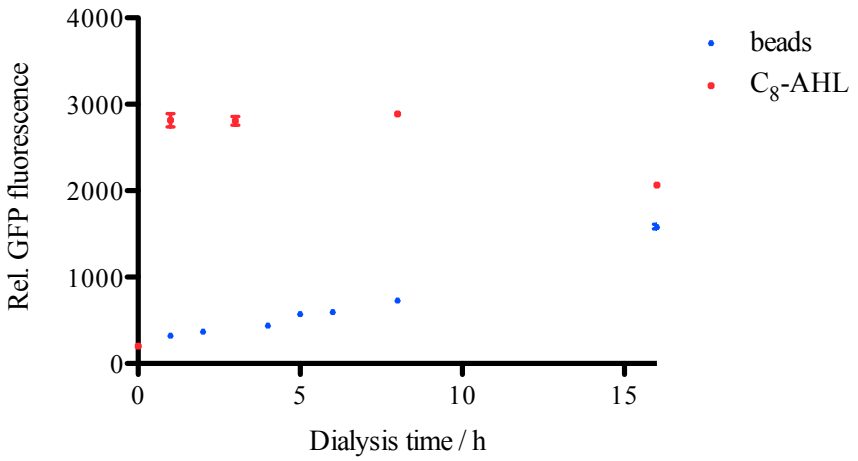

Figure 25: Comparison of activity of coated beads (0.6 mg mL^{-1}) and the positive control C_8-AHL (0.3 µM) in a dialysis experiment (data is reported as mean ± SEM, $N = 9$).

The measured GFP fluorescence was quantified by comparison to the measured induction for C_8-AHL concentrations (Figure 26). The measured concentration was calculated to increase from 4 to 270 nM after 1 hour and 16 hours incubation time, respectively. However, it is difficult to measure the exact concentration of hybrids per mg of TiO_2 beads. Quantification of the washout proved to be unsuccessful as well as other performed techniques, such as IR measurements. These problems arise from the large distribution of particles sizes and the fact that larger beads break apart during centrifugation.

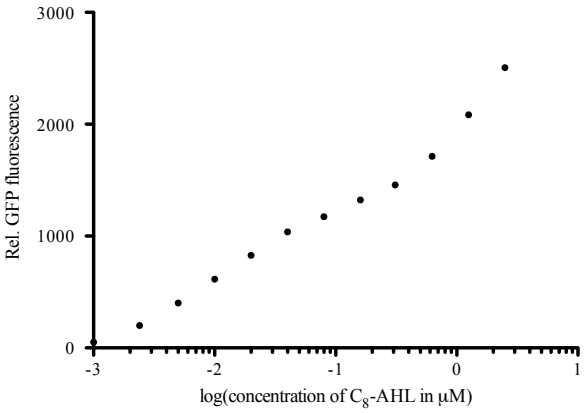

Figure 26: Correlation between GFP-activity and concentration of C_8-AHL (logarithmic scale).

3.5.4 Surface Labeling

Even though we were able to induce a biological response with the coated surfaces, there was still no strong evidence that the hybrids were immobilized on the TiO_2 surface. In order to address this, we designed and synthesized hybrid **3** bearing the nitro-catechol moiety as a molecular anchor, which was combined with a fluorescent dye as shown in Figure 27. Boc-protected lysine (blue in Figure 27 left) served as the linker for this purpose. The synthesis could be achieved with two simple amide coupling reactions with rhodamine B and nitro-dopamine to yield the labeled anchor in 25% overall yield.

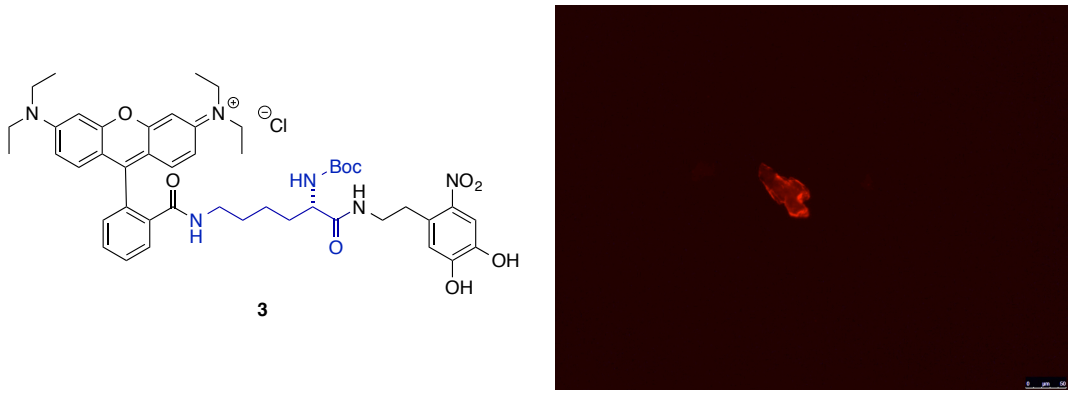

Figure 27: Left: Fluorescently labeled molecular anchor **3**. Right: Coated TiO_2 bead with **3**.

Compound **3** was coated on TiO_2 particles using our established immobilization procedure. The functionalized beads were subsequently analyzed by fluorescence microscopy to verify the presence of **3** on the surface. Figure 27 (right) shows a typical TiO_2 bead visualized by a fluorescent microscopy and it is clearly visible that the hybrids are located on the surface, as expected. However, quantification of the loading remains difficult due to unknown amount of hybrids washed out and surface area.

3.6 Conclusion

In summary, we could achieve the preparation of a natural product hybrid bearing a nitro-dopamine anchor and a bioactive acylated homoserine lactone moiety. Not only are these derivatives still recognized by the AHL biosensor *P. putida* F117 (pAS-C8) as QS modulators, but also coating of TiO_2 beads was achieved by a simple dip-and-rinse procedure. The beads retain the activity of the free compounds even after extensive washing with water. The mechanism of action was determined to be by slow release of the active compounds from the beads' surface as suggested by dialysis assays. Furthermore, we could demonstrate by using fluorescently labeled molecular anchors that the active compounds are effectively attached to the TiO_2 surface. This method might be a highly attractive approach for the preparation of coated surfaces in medical devices capable to interrupt the QS signaling pathway in a wide range of different bacterial strains. Numerous applications for this approach are feasible, such as medical implants, agriculture and material sciences.

4 Labeling OF QS PATHWAYS

4.1 Burkholderia Cenocepacia

Burkholderia cenocepacia are Gram-negative bacteria and of a bacterial group collectively referred to as the *Burkholderia cepacia* complex (Bcc).[130] These organisms are prevalently found in soil, water, and agricultural environments and belong to the genus *Burkholderia*.[131] Various species from this genus cannot only be found throughout the environment, but are also part of universal contaminants in cosmetics and other pharmaceutical solutions. The Bcc is composed of 17 genetically distinct but phenotypically similar *Burkholderia*.[132] Some of these species have shown to be capable of degrading organic compounds, such as herbicides,[133] pesticides,[134] and trichloroethylene,[135] thus, bearing a great potential for them as bioremediation agents.

The scope of interactions between *Burkholderia* species and their environment or hosts is complex, and often contradictory. Some species of *Burkholderia* exist as free-living cells while others occur in endosymbiotic relationships with fungi or plants,[136] such as *B. kirkii*, which is living inside plant leaf galls.[137] However, the exact mechanism by which the bacteria survive and persist within the hosts in not yet fully understood.

Originally identified as plant pathogens,[138] Bcc strains have emerged as a significant opportunistic pathogen, which can cause nosocomial infections as well as severe illnesses in neonates, patients with cystic fibrosis (CF) or cancer, transplant

[130] S. C. Miller, J. J. LiPuma, J. L. Parke, *Appl. Environ. Microbiol*. **2002**, *68*, 3750.

[131] (a) T. Coenye, P. Vandamme, *Environ. Microbiol*. **2003**, *5*, 719; (b) E. Mahenthiralingam, T. A. Urban, J. B. Goldberg, *Nat. Rev. Microbiol*. **2005**, *3*, 144.

[132] E. Vanlaere, A. Baldwin, D. Gevers, D. Henry, E. De Brandt, J. J. LiPuma, E. Mahenthiralingam, D. P. Speert, C. Dowson, P. Vandamme, *Int. J. Syst. Evol. Microbiol*. **2009**, *59*, 102.

[133] R. Y. Stanier, N. J. Palleroni, M. Doudoroff, *J. Gen. Microbiol*. **1966**, *43*, 159.

[134] A. Holmes, J. Govan, R. Goldstein, *Emerg. Infect. Dis*. **1998**, *4*, 221.

[135] B. R. Folsom, P. J. Chapman, P. H. Pritchard, *Appl. Environ. Microbiol*. **1990**, *56*, 1279.

[136] T. Coenye, P. Vandamme, *Burkholderia: Molecular Microbiology and Genomics*. Horizon Bioscience, **2007**.

[137] S. R. van Oevelen, P. de Wachter, P. Vandamme, E. Robbrecht, E. Prinsen, *Int. J. Syst. Evol. Microbiol.* **2002**, *52*, 2023.

[138] W. H. Burkholder, *Phytopathology* **1950**, *40*, 115.

recipients, and other immunocompromized patients.[139] The infection rates caused by Bcc strains have noticeably increased in the past two decades and pose a dramatic threat to the health-care system. Among those, *B. cenocepacia* is considered the most problematic pathogen and can cause life-threatening lung infections and has the ability to spread epidemically between CF patients with prevalence rates in some CF centers of up to 40%.[140] Furthermore, it is responsible for several recent nosocomial outbreaks.[131b,141] CF patients often acquire *B. cenocepacia* in the late course of the disease after precedent chronicle colonization with *Pseudomonas aeruginosa*.[142] The formed mixed biofilms are often associated with reduced survival and the risk of developing a fulminated and fatal pneumonia, the so-called cepacia syndrome.[143] To date, only very little is known about the pathogenic mechanism and virulence determinants of *B. cenocepacia*.

The formation of biofilms on the epithelial cell surface of the lung is believed to be the critical step in the infection progress. Once a biofilm is formed, bacteria can withstand host immune responses and exhibit an increased resistance towards antibiotics. The expression of the responsible pathogenic traits has been shown to be regulated by two QS pathways in *B. cenocepacia*. The first described system is the *cep* system, which is widely distributed among the Bcc strains.[144] There, an AHL synthase termed CepI is responsible for the production of *N*-octanoyl homoserine lactone (C_8-AHL) and minor amounts of *N*-hexanoyl homoserine lactone (C_6-AHL)[145] and the activation or repression of the transcription of genes is regulated by CepR.[146] Epidemic strains of *B. cenocepacia* also possess the *cci* QS system that produces the same AHLs as CepI. These two systems form a global gene regulatory system. The *cep* system was shown to positively regulate biofilm formation, swarming motility, and production of extracellular proteolytic and chitinolytic activity.[147] Interestingly,

[139] (a) P. Drevinek, E. Mahenthiralingam, *Clin. Microbiol. Infect.* **2010**, *16*, 821; (b) E. Mahenthiralingam, A. Baldwin, C. G. Dowson, *J. Appl. Microbiol.* **2008**, *104*, 1539.

[140] T. Coenye, P. Vandamme, J. R. W. Govan, J. J. LiPuma, *J. Clin. Microbiol.* **2001**, *39*, 3427.

[141] D. P. Speert, *Infect. Med*. **2001**, *18*, 49.

[142] L. Saiman, G. Cacalano, A. Prince, *Infect. Immun.* **1990**, *58*, 2578.

[143] (a) A. M. Jones, *Thorax* **2004**, *59*, 948; (b) O. C. Tablan, W. J. Martone, C. F. Doershuk, R. C. Stern, M. J. Thomassen, J. D. Klinger, J. W. White, C. L. A, W. R. Jarvis, *Chest* **1987**, *91*, 527.

[144] Review: L. Eberl, *Int. J. Med. Microbiol*. **2006**, 296, 103.

[145] S. Lewanza, P. A. Sokol, *J. Bacteriol*. **2001**, *183*, 2212.

[146] (a) S. Lewenza, B. Conway, E. P. Greenberg, P. A. Sokol, *J. Bacteriol.* **1999**, *181*, 748; (b) S. Inhülsen, C. Aguilar, N. Schmid, A. Suppiger, K. Riedel, L. Eberl, *Microbiologyopen* **2012**, *1*, 225.

[147] P. A. Sokol, R. J. Malott, K. Riedel, L. Eberl, *Future Microbiol.* **2007**, *2*, 555.

this is the QS system targeted in the previous chapter. Thus, we wondered if we could use the same recognition pattern as already successfully applied for the surface functionalization and add a fluorescent marker to be able to label the QS receptor. Such a labeling technique could not only serve for sample analysis, but moreover, for the monitoring of QS pathways.

4.2 Selective QS Receptor Labeling

The labeling of QS pathways is a very interesting and challenging problem addressed by many different research groups. Several methods for the identification of *Burkholderia* have been developed and their most prominent examples include fluorescence *in situ* hybridization (FISH)[148] and rRNA gene-based PCR assays.[149] Nevertheless, in spite of the importance of QS for virulence and biofilm development, knowledge of the temporal and spatial production of AHL signaling molecules within biofilms or within the infection host is scarce. The lack of techniques to visualize AHL-mediated communication at the single cell level needs to be overcome in order to furnish better knowledge about this communication system. Even though GFP-based biosensors have been used for this purpose,[64] they are limited to genetically engineered experimental model settings.

Recently, there were two examples reported in the literature in order to overcome this problem. The first one was described by Meijler and co-workers in 2011 (Figure 28).[150] These studies are based on previous findings that the isothiocyanate functionalized AHL ITC-12 (**LXXV**) is able to covalently bind to a cysteine residue of LasR (**LXXVI**), which is one of the QS receptors used by *Pseudomonas aeruginosa*. Upon binding to the protein, the AHL analogue can be labeled by the fluorescent marker aminooxy-BODIPY (**LXXVII**) through an aniline-catalyzed bio-orthogonal ligation giving **LXXVIII**. This two-step labeling strategy was successfully applied to live cells and a high labeling quality could be achieved. However, the drawback of this approach is that it is restricted to the absence of native AHLs. That is why the experimental settings were performed with the double mutant strain *P. aeruginosa* JP2 (*lasI*/*rhlI*-deleted), which does not produce competitive

[148] A. R. Brown, J. R. W. Govan, *J. Clin. Microbiol.* **2007**, *45*, 1920.
[149] K. Stoecker, C. Dorninger, H. Daims, M. Wagner, *Appl. Environ. Microbiol.* **2010**, *76*, 922.
[150] J. Rayo, N. Amara, P. Krief, M. Meijler, *J. Am. Chem. Soc.* **2011**, *133*, 7469.

AHLs by itself. This disadvantage hampers its application as a possible tool for the investigation of bacteria-host communication pathways.

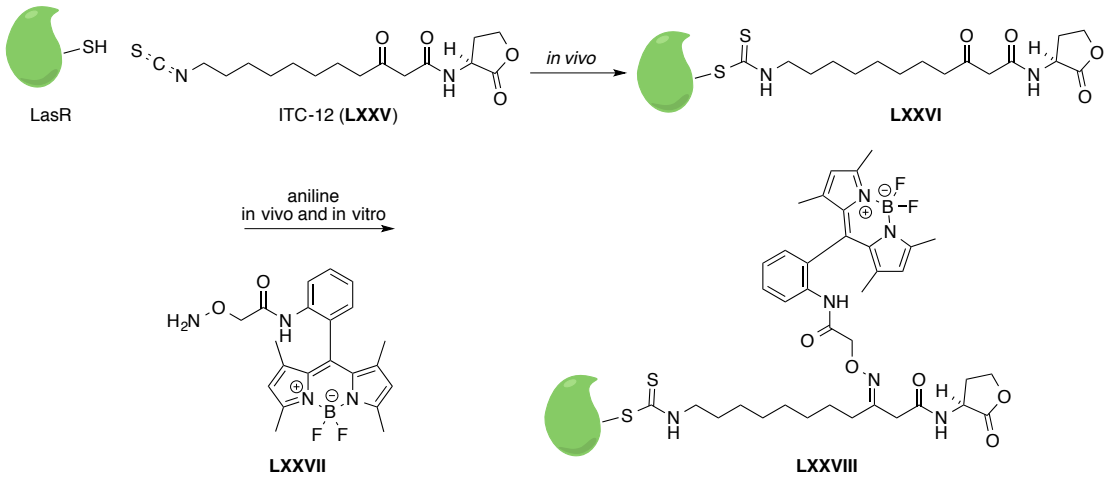

Figure 28: Selective *in vivo* and *in vitro* labeling of ITC-12 (**LXXV**) covalently bound to LasR by aminooxy-BODIPY (**LXXVII**).[151]

The second report was published by Janda and co-workers.[151] The authors focused on a fluorescently labeled multivalent scaffold for bacterial species utilizing Lsr-type AI-2 receptors, used by both Gram-negative and Gram-positive bacteria (see chapter 2). This approach is limited to membrane bound receptors and only very moderate labeling of *Salmonella typhimurium* could be achieved. Even though this represents the first trial towards selective AI-2 fluorescent labeling, the results are far from practical utility.

We wondered if a more general approach using a labeled ligand with a fluorescent tag could be achieved using our recognition pattern. The general drawbacks for such methods are the usually observed decrease in affinity of the modified ligand for its target protein and the competition with native AHLs.[152]

[151] A. L. Garner, J. Park, J. S. Zakhari, C. A. Lowery, A. K. Struss, D. Sawada, G. F. Kaurmann, K. D. Janda, *J. Am. Chem. Soc*. **2011**, *133*, 15934.

[152] A. E. Speers, G. C. Adam, B. F. Cravatt, *J. Am. Chem. Soc*. **2003**, *125*, 4686.

4.3 Results and Discussion[153]

4.3.1 First Generation FLAQS[154]

The design of a fluorescent labeling agent for QS receptors (FLAQS) was the first challenge to be accomplished. We envisaged using the GFP-based *P. putida* F117 pAS-C8 biosensor to monitor the correlation between QS activity and labeling. This reported strain was chosen for preliminary results due to its lack of the AHL synthase gene *ppuI* to prevent competition with native AHLs. Furthermore, this strain had been shown to be sensitive for our biomimetic moiety and better labeling should be expected compared to wild-type (WT) bacteria since *cepR* is overexpressed. The reporter strain produces GFP upon activation. In order to compare activity and labeling, the fluorescent properties of GFP and the fluorescent dye should not interfere. For this reason, we decided to use the rhodamine B fluorophore due to its high luminescence quantum yield and the red fluorescence, which can be clearly separated from the green fluorescence of the biosensor.

The designed fluorescently marked AHL **4** was synthesized in three steps from commercially available rhodamine B (**5**) via intermediate **6** using peptide coupling chemistry in 49% overall yield as shown in Scheme 3.

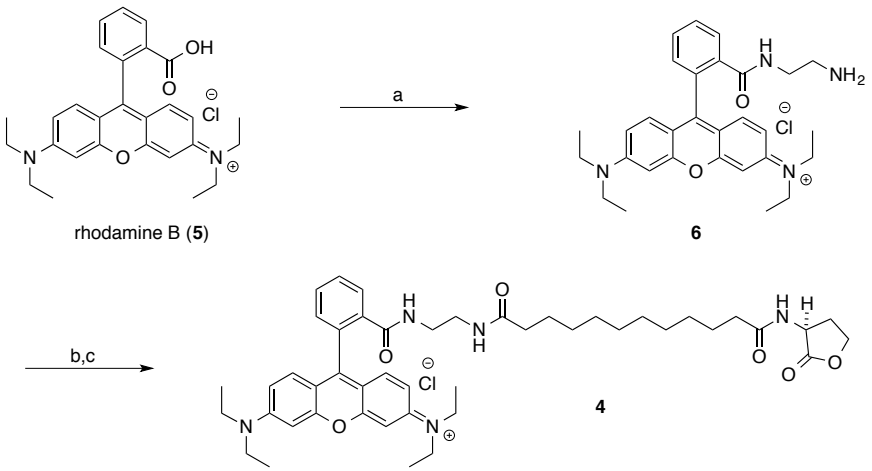

Scheme 3: a) *N*-hydroxysuccinimid, EDC, r.t., 15 h; 1,2-diaminoethane, Et_3N, MeCN, r.t., 6 h, 56%. b) **EP2**, Et_3N, MeCN, r.t., 4 h; c) (*S*)-α-amino-γ-butyrolactone hydrobromide, MeCN, r.t., 19 h, 88% over two steps.

[153] Parts of this chapter were published in: J. Gomes, N. Huber, A. Grunau, L. Eberl, and K. Gademann, *Chem. Eur. J.* **2013**, *19*, 9766.

[154] N. Huber, Master Thesis, Basel, **2012**.

We then continued our studies by incubating FLAQS **4** with the two biosensors *P. putida* F117 pAS-C8 and pKR-C12 for 3 hours. The resulting GFP fluorescence was measured and only the pAS-C8 biosensor was found to induce QS. These observations are in agreement with our previous finding that AHL hybrids bearing a C_{12} linker exhibit the desired selectivity towards CepR.

Next, labeling of the activated bacteria was monitored by fluorescence microscopy. Therefore, a 1.3 mM concentration of FLAQS **4** was incubated with the *P. putida* F117 pAS-C8 sensor for 3 hours and the bacteria were subsequently washed before monitoring. The results are presented in Figure 29. The appearance of green fluorescent cells (A) indicated that QS was induced in the entire population and FLAQS **4** acts as a CepR agonist. The red fluorescence labeling (C) is in good correlation with the GFP fluorescence as shown in the overlay picture (D). These results indicate that FLAQS **4** not only activates the receptors, but also accumulates within the bacteria.

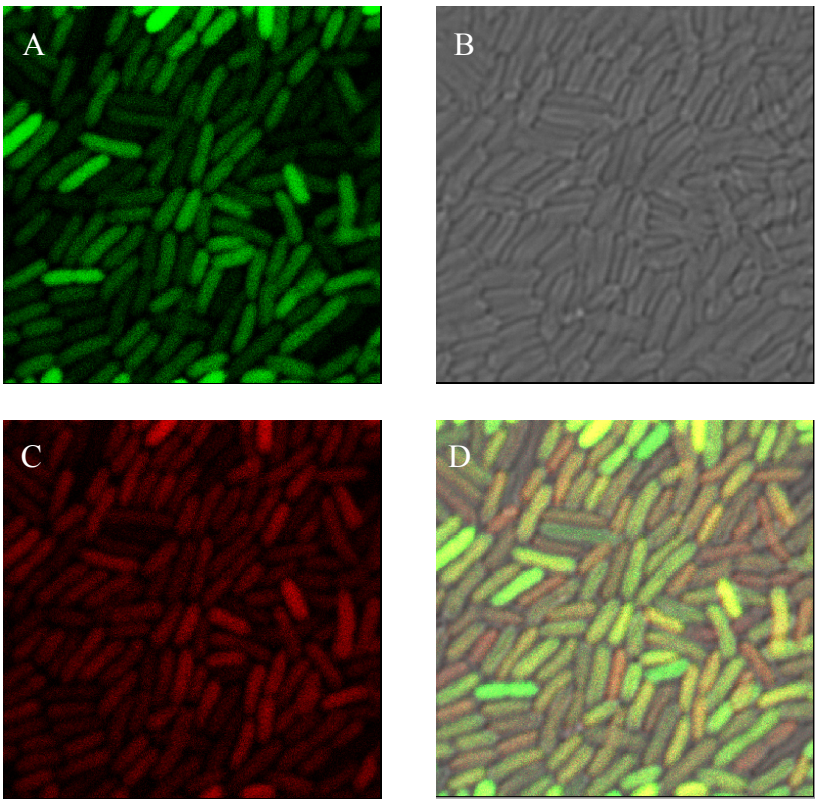

Figure 29: GFP fluorescence (A), phase contrast (B), red fluorescence (C) and overlay of A, B and C (D) of *P. putida* pAS-C8 sensor incubated with first generation FLAQS **4** with a concentration of 1.3 mM.

The labeling of the biosensors was facilitated by the fact that no competition with the native AHL had to be considered and that the target receptor was overexpressed in the reporter strains. Encouraged by the obtained results, we next tested labeling of CepR in the wild-type strain *B. cenocepacia* H111, a strain isolated from a CF patient in Hannover.[155] Its CepIR QS system was shown to be responsible for biofilm formation and swarming motility.[156] This strain was used for rather practical reasons, as it does not belong to an epidemic lineage in contrast to other *B. cenocepacia* pathogens. Furthermore, it is advantageous due to its lack of the CciR/I QS system that is present in some *B. cenocepacia* strains.[157] The labeling of the wild-type is a challenging problem compared to the reporter strain because on one hand, the receptor is not overexpressed, and on the other hand, competition between the natural agonist and the synthetic FLAQS is expected. *B. cenocepacia* H111 was incubated with hybrid **4** using similar conditions as in the standard protocol. However, only few labeled cells could be observed. Increasing the concentration of this poorly water-soluble compound was not feasible since higher solvent (DMSO) concentrations led to cell lysis. Furthermore, FLAQS **4** crystals were not fluorescent in solution due to the formation of the rhodamine base. However, this state could be changed by addition of trifluoracetic acid (TFA) due to reopening of the ring and instauration of the delocalized π-system (Scheme 4).

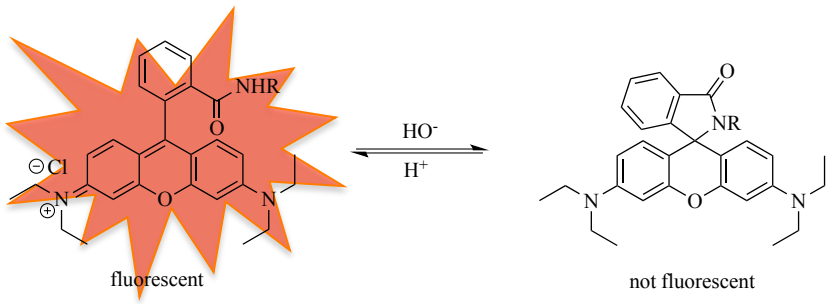

Scheme 4: Formation of the non-fluorescent rhodamine form.

Solvatochromic fluorophores offer various advantageous properties for the monitoring of several biological systems.[158] However, in our case, such a dependency

[155] O. Geisenberger, M. Givskov, K. Riedel, N. Hoiby, B. Tummler, L. Eberl, *FEMS Microbiol. Lett.* **2000**, *184*, 273.

[156] B. Huber, K. Riedel, M. Hentzer, A. Heydorn, A. Gotschlich, M. Givskov, S. Molin, L. Eberl, *Microbiology* **2001**, *147*, 2517.

[157] A. Baldwin, P. A. Sokol, J. Parkhill, E. Mahenthiralingam, *Infect. Immun.* **2004**, *72*, 1537.

[158] G. S. Loving, M. Sainlos, B. Imperiali, *Trends Microbiol.* **2009**, *28*, 73.

is not desired as we wished to be able to observe the labeled hybrids throughout the entire process. Consequently, FLAQS **4** proved unsuitable for an efficient labeling of *B. cenocepacia* H111, hence other rhodamine-based dyes had to be considered.

4.3.2 Second Generation FLAQS[154]

In search for appropriated fluorophores, we intended to investigate lissamine rhodamine B sulfonyl chloride (Figure 30, **7**), rhodamine isothiocyanate (**8**), and two rhodamine B derivatives (**9** and **10**[159]) from which we expected to achieve better solubility and pH independence.

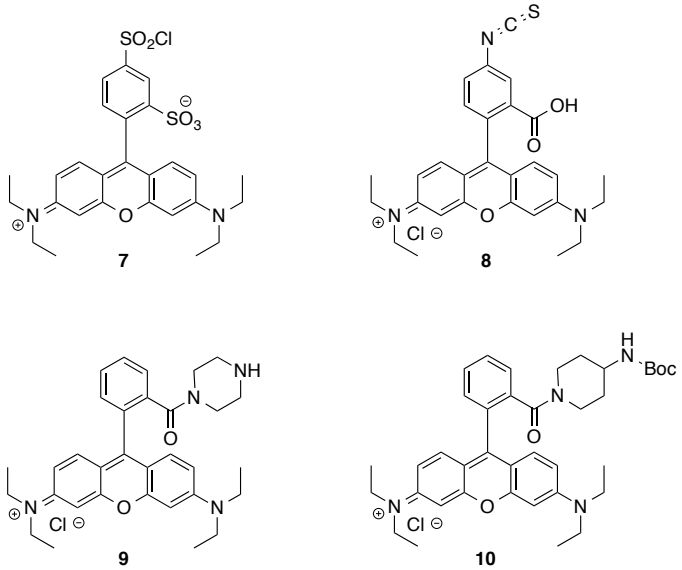

Figure 30: Various red fluorescent dyes.

In order to change only one parameter, we coupled these dyes to our C_{12}-AHL recognition pattern. Most synthesized fluorescent hybrids proved to be difficult to purify and decomposition was observed during silica gel and size exclusion chromatography, but also during reverse phase HPLC. The only exception was hybrid **11**, which could be obtained in pure form after preparative reverse phase HPLC purification. This fluorophore had recently been prepared and used by Caddick and co-workers. The synthesis of this fluorescently labeled AHL analogue was achieved in five synthetic steps from commercially available rhodamine B and dodecandioic

[159] P. Moody, M. E. B. Smith, C. P. Ryan, V. Chudasama, J. R. Baker, J. Molloy, S. Caddick, *ChemBioChem* **2012**, *13*, 39.

acid as shown in Scheme 5. The advantage of this rhodamine moiety compared to rhodamine B is the fact that it cannot build the non-fluorescent spirolactone form due to the presence of the non-nucleophilic tertiary amide making it pH independent and water-soluble.

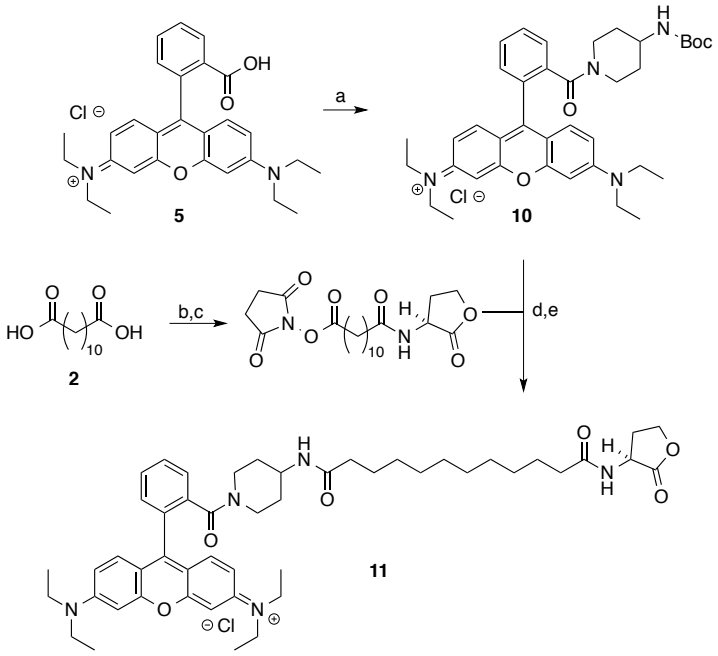

Scheme 5: a) Ref [158]; b) *N*,*N*'-disuccinimidyl carbonate, pyridine, MeCN, 6 h, r.t.; c) (*S*)-α-amino-γ-butyrolactone hydrobromide, Et_3N, MeCN, 7 h, r.t.; d) CH_2Cl_2, TFA, 5 h, r.t.; (e) MeCN, 15 h, r.t., 71 % over four steps.

With the stable hybrid in hand, we wanted to evaluate the fluorescence properties of FLAQS **11** in aqueous medium. The measured fluorescence spectrum (Figure 31) shows almost no overlap of both bands providing improved fluorescence properties compared to rhodamine B (**5**). Furthermore, the absorption maximum is located at 560 nm with almost no absorption occurring at 510 nm, which accords to the maximum GFP emission wavelength. It is crucial for the experimental settings that no interaction between the two fluorophores can occur in order to prevent fluorescence quenching, which otherwise could negatively influence the activity assays. The emitted maximum wavelength is located in the red spectral area at 600 nm.

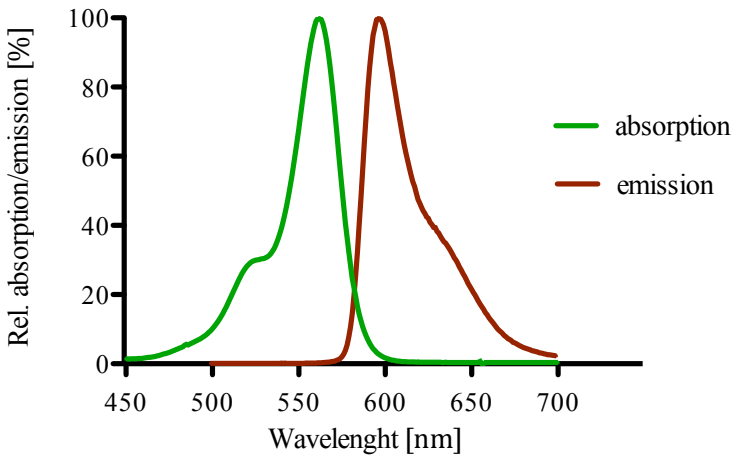

Figure 31: Fluorescence spectrum of **11**.

Appropriate fluorescence properties are essential for the success of the experimental set-up, but even more important is the induced activity of the synthesized AHL analogue **11**. Therefore, we proceeded to compare the QS activities of the synthetic and the natural agonists with respect to binding to the receptor proteins. As we wanted to obtain a labeled signaling molecule with similar properties as the natural agonist, we decided to compare the induced GFP fluorescence of the *P. putida* F117 (pAS-C8) biosensor over a large concentration range from 58 pM to 488 µM. The natural agonist C_8-AHL showed the expected QS induction with a maximum activity at a concentration of 15 µM (blue in Figure 32). Low concentrations do not activate the QS pathways until the quorum is reached. It is also worth mentioning that high concentrations of agonist lead to quorum quenching. This means, that AHLs can act as both agonist and antagonist, depending on the concentration. The synthetic AHL **11** shows a very similar activity profile compared to the native C_8-AHL. The activity maximum was observed at 4 µM as shown in red in Figure 32. Many different synthetic AHL analogues have been reported in literature over the last decades (see section 2.4.2), but our results show the first AHL analogue that mimics the activity of the natural ligand over such a large concentration range. A negative control was performed using the fluorophore **10** under identical conditions and no QS activity was found at any concentration (purple in Figure 32).

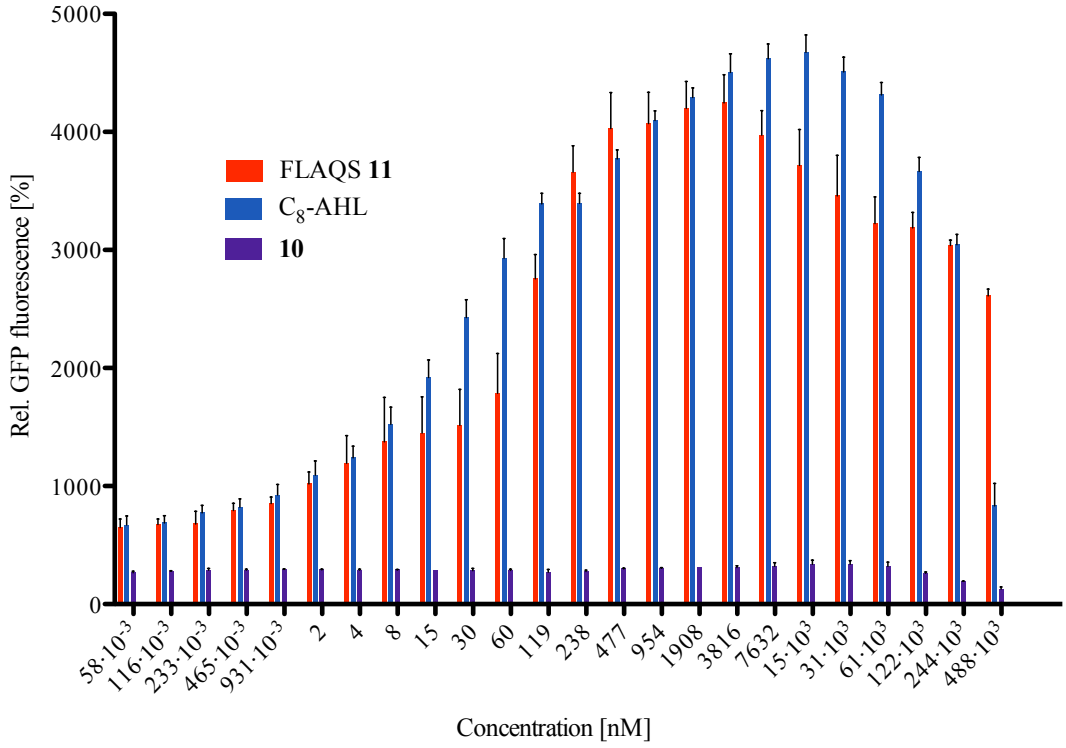

Figure 32: Activity tests with the *P. putida* F117 (pAS-C8) biosensor comparing FLAQS **11**, fluorescent dye **10**, and the natural C_8-AHL (data is reported as mean ± SEM, $N = 3$).

The obtained results were fascinating and we continued our studies with the labeling of WT bacteria. We therefore first investigated the labeling of the wild-type strain *B. cenocepacia* H111 with the new FLAQS. The used reporter strain has the advantages that CepR is overexpressed and no competition between the natural agonist and the synthetic FLAQS is possible in contrast to the wild-type. The first labeling experiments were performed with the *B. cenocepacia* H111 strain by incubation with a 244 µM concentration of FLAQS **11** for 3 hours. Upon washing, the bacteria were evaluated by confocal microscopy. We were pleased to find that labeling of the entire bacterial population could be achieved with the new red FLAQS as shown in Figure 33 A. The distribution of red fluorescence was found to be equal over the bacteria, suggesting that the binding CepR receptor is a soluble cytoplasmic protein.

We subsequently studied the minimal concentration of FLAQS to still achieve sufficient labeling. Therefore, *B. cenocepacia* H111 cells were incubated with different concentrations of hybrid **11** and the captured fluorescent pictures were compared. An excellent yield of red fluorescence labeling could be observed with a

concentration of 31 µM (B), however, only minor or no fluorescence was achieved at lower concentrations as shown with 8 and 2 µM concentrations (C and D, respectively) due to competition with the natural agonists. A required concentration of about 30 µM is highly satisfying for practical uses since no cytotoxicity could be observed in this range.

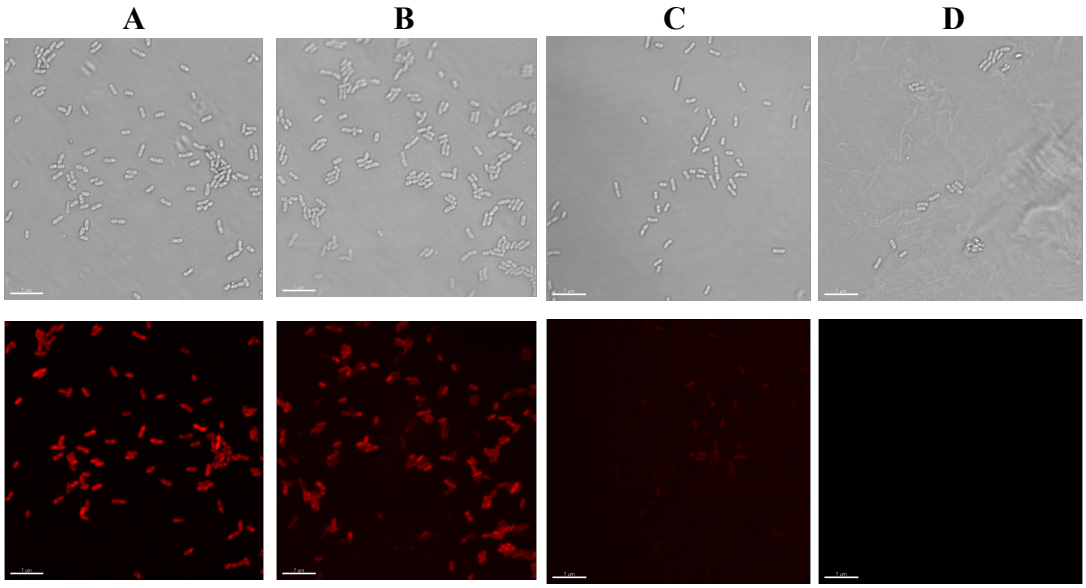

Figure 33: *Burkholderia cenocepacia* H111 incubated in the presence of (A) 244 µM, (B) 31 µM, (C) 8 µM, and (D) 2 µM FLAQS **11**. Phase contrast images are shown at the top, red fluorescence images at the bottom.

To exclude possible random binding of FLAQS **11** to the bacterial population we decided to incubate the marker with the double knockout mutant *B. cenocepacia* H111 Δ*cepRI*. In this strain, where the *cepR and cepI* genes were knocked out, no labeling should occur due to the lack of the QS receptor. Incubation was performed under the same conditions used for the wild-type. No fluorescent labeling was detected, which showed that no unspecific binding could occur in the absence of the QS receptor (Figure 34, A). Two further negative control experiments were performed to ensure our results. The first one was done by using an *E. coli* XL1-Blue strain. This strain does not encode an AHL-dependent QS system, and as expected, no fluorescence labeling was observed under the same incubation conditions (B). For the last control experiment, *B. cenocepacia* H111 was incubated with the fluorophore **10** alone to confirm that the labeling properties do not originate from fluorophore moiety alone, but that the bioactive moiety is indeed responsible for the selective binding towards CepR. Again, no labeling of the bacteria could be monitored (C). This indicates that

the rhodamine derivative is not incorporated into the cells or accumulated in the bacterial cell walls.

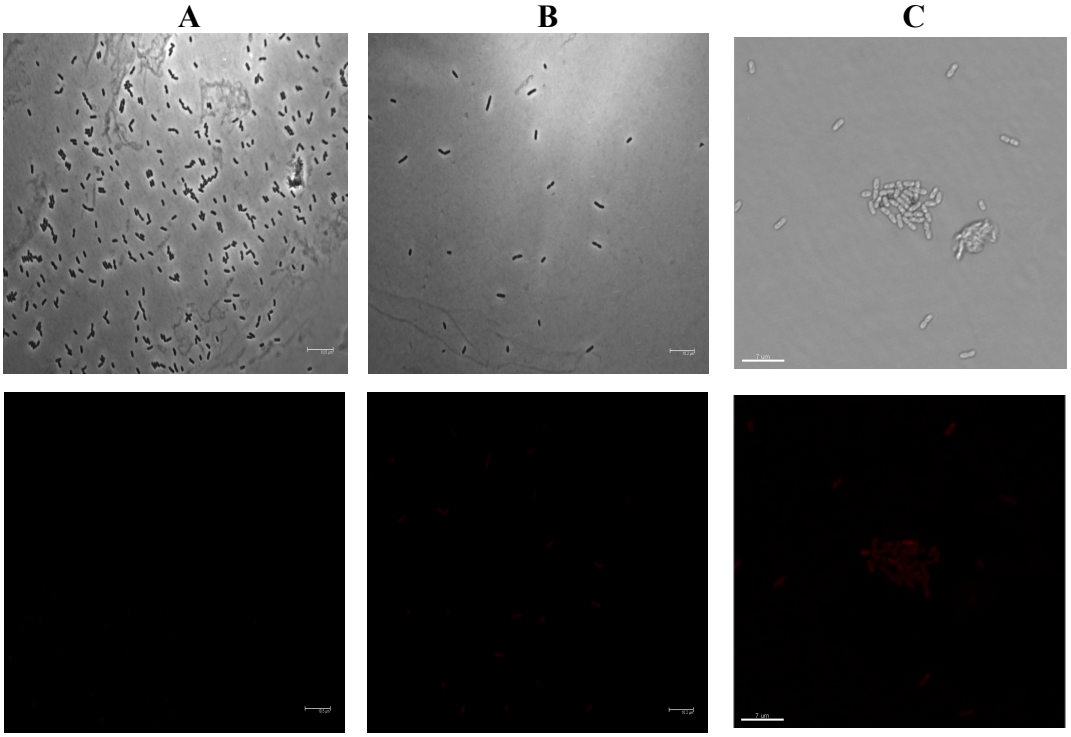

Figure 34: *Burkholderia cenocepacia* mutant Δ*cepR*/*I* incubated in the presence of (A) 244 µM FLAQS **11**. *Escherichia coli* XL1-Blue incubated in the presence of (B) 244 µM FLAQS **11**. *Burkholderia cenocepacia* H111 incubated in the presence of (C) 244 µM **10**. Phase contrast images are shown at the top, red fluorescence images at the bottom.

The site of action was the next target to be investigated. We assumed that the synthetic FLAQS bind to the same target site as the natural AHL molecule. However, in order to verify this hypothesis, we performed competition assays between the synthetic and the natural ligands as shown in Table 2. Therefore, the wild-type strain *B. cenocepacia* H111 was treated and incubated with a certain concentration of FLAQS **11** (244 µM) and different concentrations of C_8-AHL (1 µM and 100 µM entry 1 and 2, respectively). The results reveal that higher concentrations of the natural agonist lead to a decrease in labeling. Furthermore, more fluorescent labeling could be obtained by using the sensor overexpressing CepR (entry 3). Thus, we can conclude that both compounds compete for the same binding pocket of the CepR receptor in *B. cenocepacia*.

Table 2: Competition assays between FLAQS **11** (244 µM) and C_8-AHL.

Entry	Strain	C_8-AHL concentration	Overlay red fluorescence and phase contrast	Red fluorescence
1	H111	100 µM	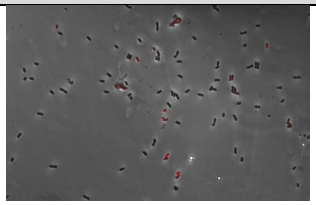	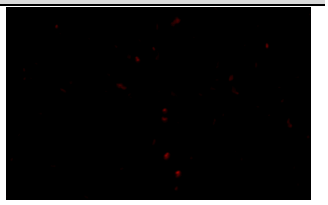
2	H111	1 µM	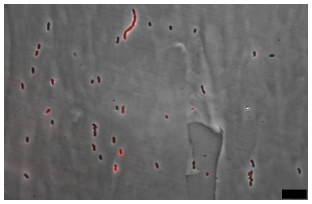	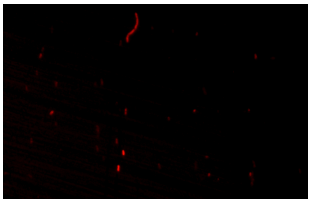
3	*cepR*$^+$	1 µM	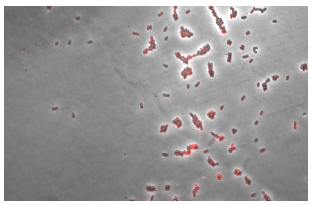	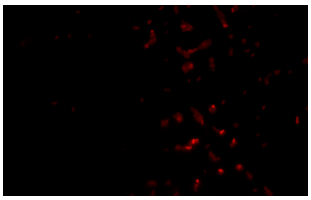

One possible application for this tool could be the analysis of sputa in order to identify the presence of *B. cenocepacia*. Therefore, the labeling of a pathogenic *B. cenocepacia* strain should work in the presence of other bacteria present in the lung, such as *P. aeruginosa*. That is why we decided to use a mixed bacterial culture of the *cepR* overexpression strain H111 (*cepR*$^+$) and the GFP-tagged *cepR* knockout mutant H111Δ*cepR*:GFP. These two strains are only differentiated by the presence of the CepR, our target receptor. Thus, the mixed strains were incubated with FLAQS **11** for 3 hours and visualization was performed by fluorescence microscopy. The pictures shown in Figure 35 clearly demonstrate that the GFP-tagged knockout mutant (green) could not be labeled with FLAQS **11** in contrast to the strain overexpressing CepR (red). These results enable the selective labeling of bacteria based on their unique requirements for AHL signaling with FLAQS.

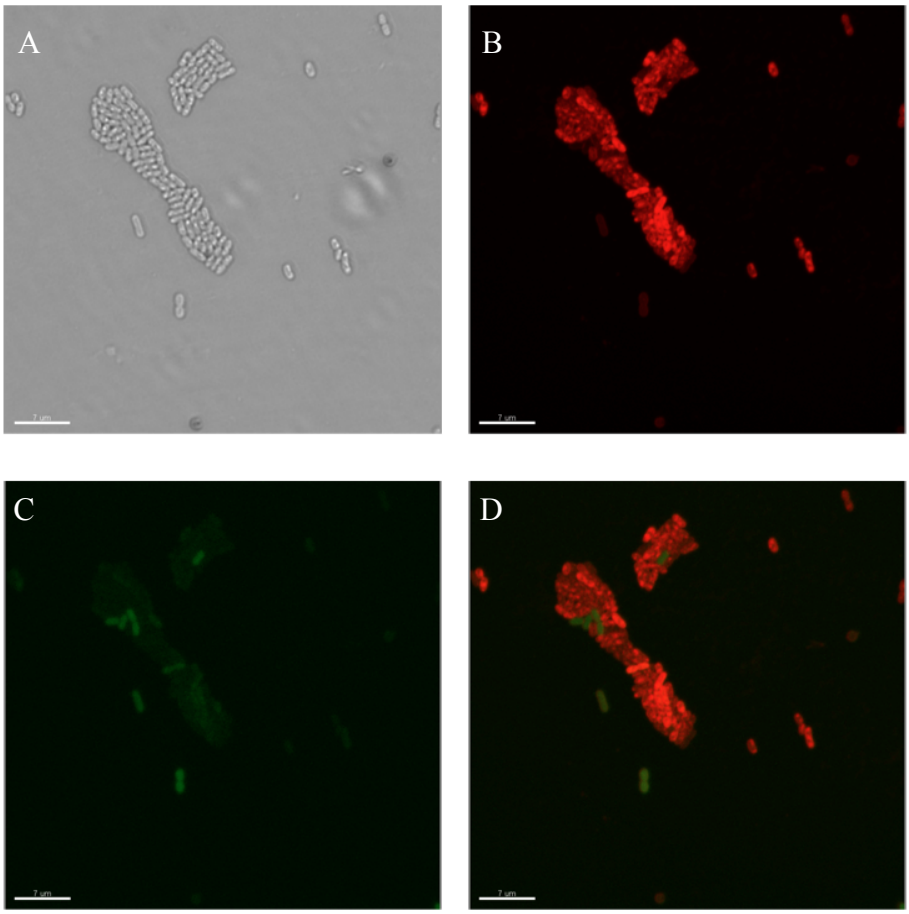

Figure 35: . Phase contrast (A), red fluorescence (B), GFP fluorescence (C), and overlay of B and C (D) of a bacteria mixture (*B. cenocepacia* mutant *cepR*$^{+}$ and *B. cenocepacia* mutant Δ*cepR*-GFP) incubated with FLAQS **11** (244 μM).

Furthermore, the study of bacterial interspecies communication pathways based on a given AHL chemotype has become a hot topic and is explored by many research groups. In this regard, FLAQS could deliver the perfect tool for this research area and lead to the discovery of new common communication pathways used by different organisms. Furthermore, it could lead to *in vivo* visualization of pathogenic and symbiotic interactions between bacteria and their eukaryotic hosts.

4.3.3 3-Oxo FLAQS

After having achieved a method for the selective labeling of *B. cenocepacia*, we wondered if other QS receptors could be targeted by FLAQS. The selectivity of the synthetic analogues depends on the acyl side chain, so we hypothesized that other QS receptors could be labeled by changing the length or oxidation state at C3-position of the FLAQS. We were especially interested in the labeling of LasR, which is one of the QS receptors used by *P. aeruginosa*. Such a LasR selective FLAQS could, in combination with FLAQS, lead to an extremely fast, simple and inexpensive tool to analyze sputa of CF patients, since co-infection of both species is often observed in clinical infection. LasR is target in the natural habitat by OdDHL, an AHL signaling molecule with a ketone at C3 position. For this reason, we synthesized various AHL analogues **12-16** with this oxidation pattern as shown in Figure 36.

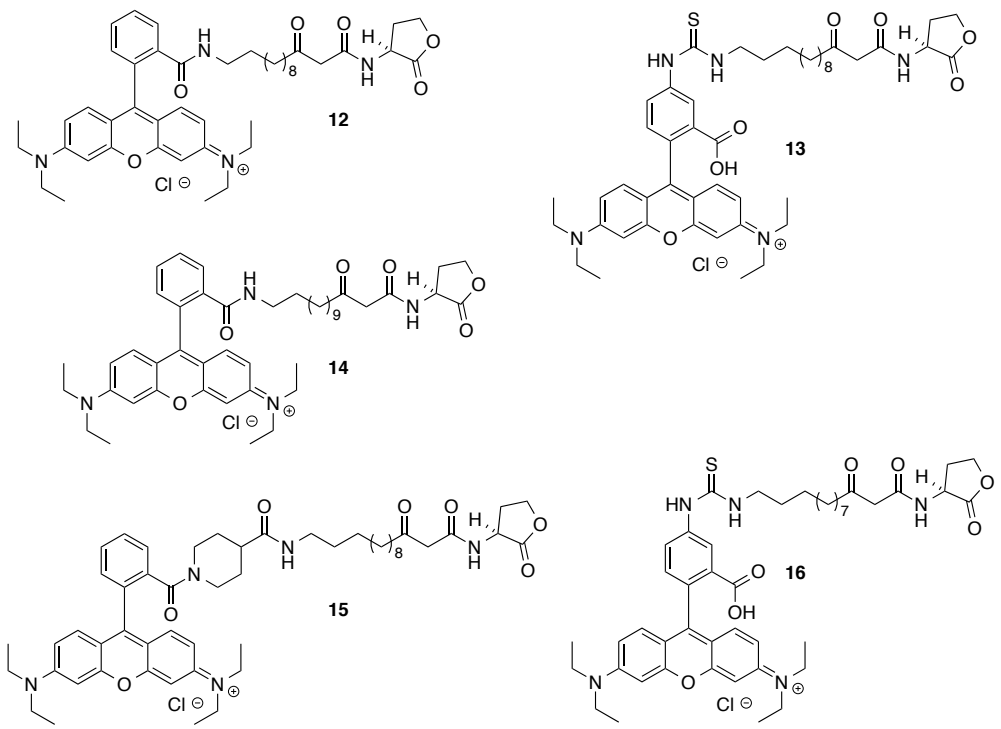

Figure 36: Synthesized 3-oxo FLAQS with different rhodamine dyes and chain lengths.

The biological evaluation was performed on the *P. putida* ISO F117 (pKR-C12) reporter strain, which expresses the desired LasR receptor. As this biosensor is based on the production of GFP upon activation, we used the rhodamine dyes as fluorophores in order to distinguish the activity from the labeling. The most promising preliminary results were obtained with hybrid **15** bearing the fluorophore **10** and a

chain length of C_{14}. This analogue was obtained in six steps and with an overall yield of 30% after purification by preparative reverse phase HPLC.

We were next interested in the fluorescent properties of this compound. The measured fluorescence spectrum is shown in Figure 37 and the results are similar to the previous one obtained with the same fluorescent dye. The absorption maximum is located at 561 nm and the emission maximum at 591 nm.

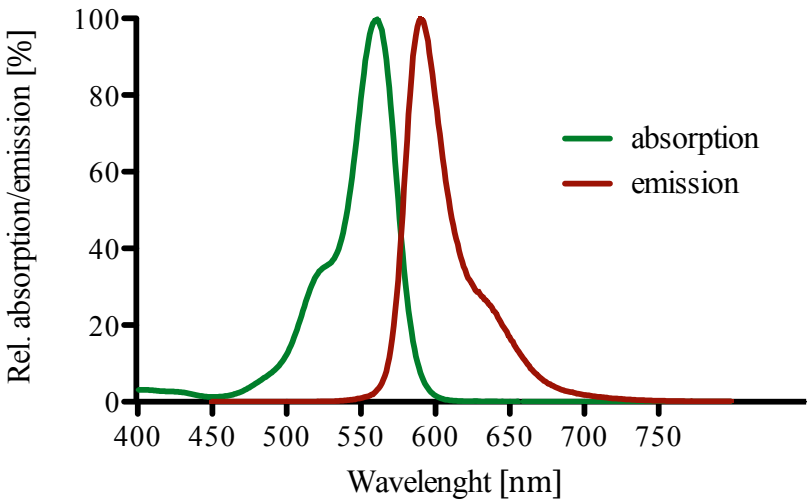

Figure 37: Fluorescence spectrum of **15**.

We subsequently determined the concentration dependency of QS induction in the reporter strains. Therefore, activity tests were performed with the pAS-C8 and pKR-C12 biosensors over a large concentration range (Figure 38 and 39). Surprisingly, FLAQS **15** was able to induce QS in both biosensors, although higher activity could be observed for the pKR-C12 sensor. Unfortunately, both positive controls (blue) showed an unusual concentration behavior. The problem associated with these assays was the quality of the added native AHLs. Nevertheless, both assays showed a remarkable concentration dependent response of the sensors with FLAQS **15** with activity maxima at about 15 µM for the pAS-C8 and between 2 and 8 µM for the pKR-12 sensor. This shows that this hybrid is recognized by both types of receptors (CepR and LasR), in contrast to compound **11**, which was only accepted by CepR.

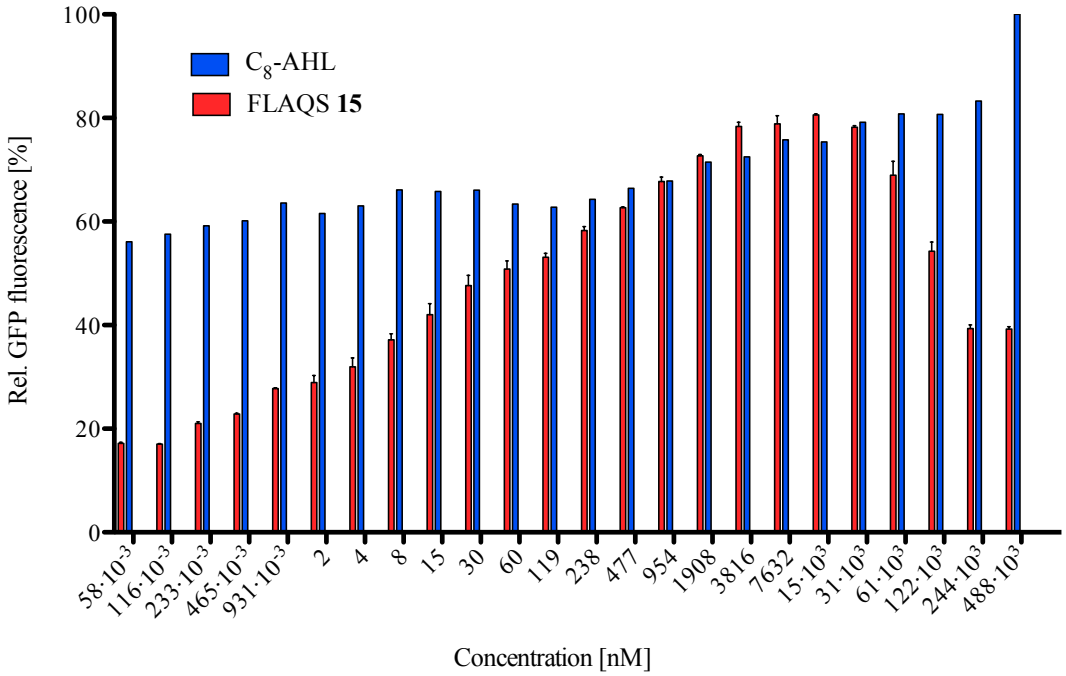

Figure 38: Activity tests with the *P. putida* F117 (pAS-C8) biosensor comparing FLAQS **15** and the natural C_8-AHL (data is reported as mean ± SEM, $N = 2$).

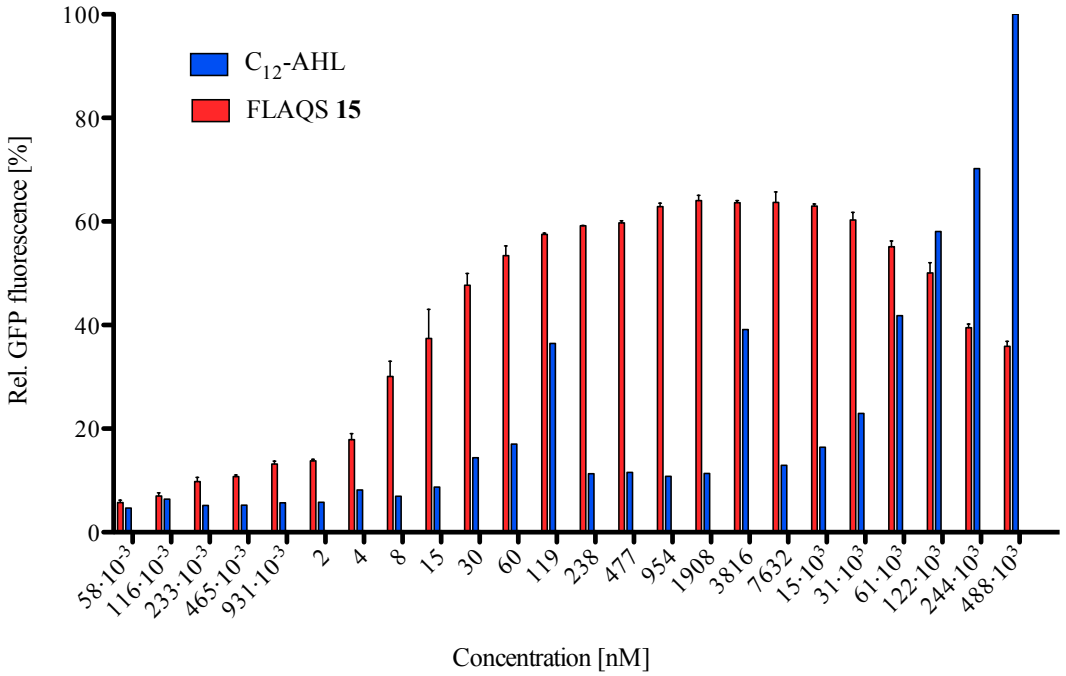

Figure 39: Activity tests with the *P. putida* F117 (pKR-C12) biosensor comparing FLAQS **15** and the natural C_{12}-AHL (data is reported as mean ± SEM, $N = 2$).

However, since QS could be induced in both reporter strains, in contrast to the previously analyzed FLAQS, we carried out our investigations using fluorescence microscopy to distinguish green and red fluorescence from GFP and rhodamine, respectively. Therefore, the pKR-C12 reporter strain was incubated with a 244 µM concentration of FLAQS **15** for 3 hours. We were pleased to discover that overlapping green and red fluorescence could be observed as shown in Figure 40. However, QS could not be induced in the entire population and not all the bacteria showed red fluorescence. Nevertheless, these first results are extremely promising and higher concentrations of FLAQS could lead to an even better level of labeling. Furthermore, different labeling stages were observed by confocal microscopy. Smaller bacteria showed red fluorescence only at the poles of the cells, whereas larger bacteria demonstrated a unitary fluorescence distribution. The former observation is in agreement with the findings by Meijler and co-workers with their two-step approach (see section 6.2). The results indicate a possible cell division dependent labeling of the cells. However, further experiments are required to investigate these observations in detail and clarify the mode of labeling.

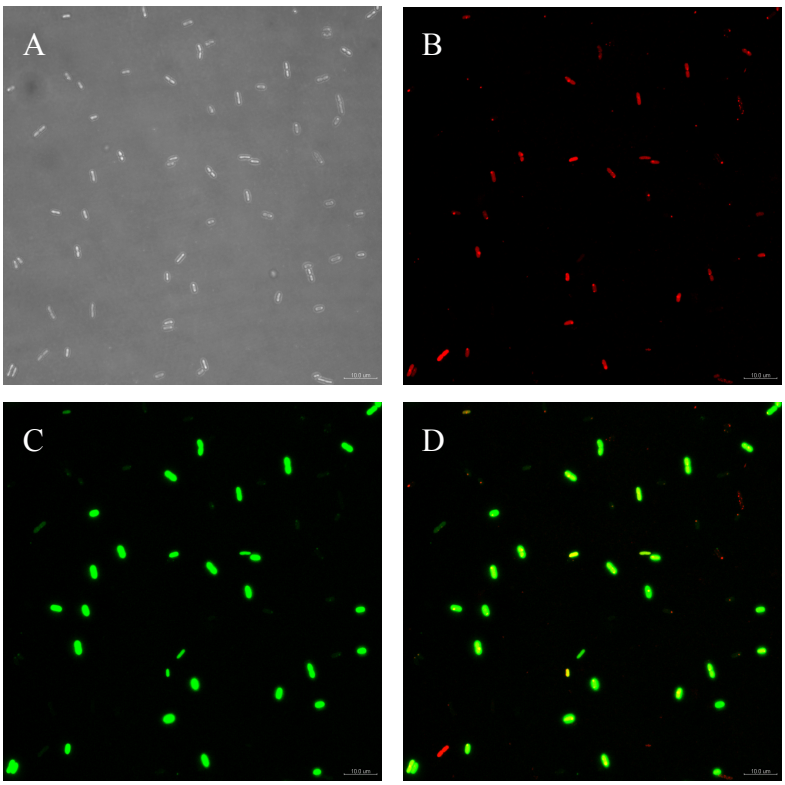

Figure 40: Phase contrast (A), red fluorescence (B), GFP fluorescence (C) and overlay of phase contrast, A, B, and C (D) of pKR-C12 sensor incubated with **15** (244 µM).

FLAQS **15** was also incubated with the pAS-C8 sensor to verify the selectivity of this AHL mimic for LasR. The obtained results shown in Figure 41 were surprising, because the red and green signals did not overlap at all. Even though QS was induced in some bacteria, none of those showed red labeling. The higher the concentration of FLAQS **15**, the less green cells could be observed. These results are especially interesting because CF patients with bacterial lung infections are often co-infected with *P. aeruginosa* and *B. cenocepacia*. Investigations in the Eberl group showed that these two strains are capable to communicate with each other in a unidirectional way. Only *B. cenocepacia* is able to perceive AHLs from *P. aeruginosa* for activating QS. This mechanism might proceed though a different binding site of CepR. FLAQS **15** could play an essential role in elucidating this communication pathway.

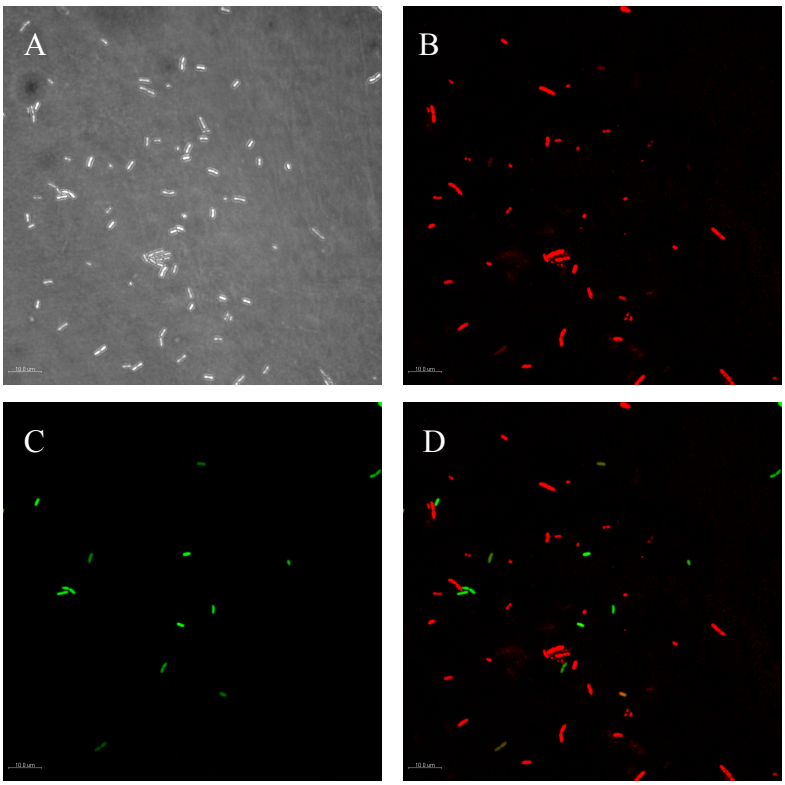

Figure 41: Phase contrast (A), red fluorescence (B), GFP fluorescence (C) and overlay of phase contrast, A, B, and C (D) of pAS-C8 sensor incubated with **15** (244 µM).

Our initial target was the labeling of wild-type bacteria with FLAQS. So we preceded our studies by using two different wild-type bacterial strains, namely *P. aeruginosa* PAO1 and *B. cenocepacia* H111 (Figure 42). A moderate labeling of *P. aeruginosa* could be achieved after co-incubation with the marked hybrid **15** at high concentrations (A and B). On the other hand, no fluorescent labeling of

B. cenocepacia H111 could be detected (C and D), demonstrating the potential of this AHL mimic.

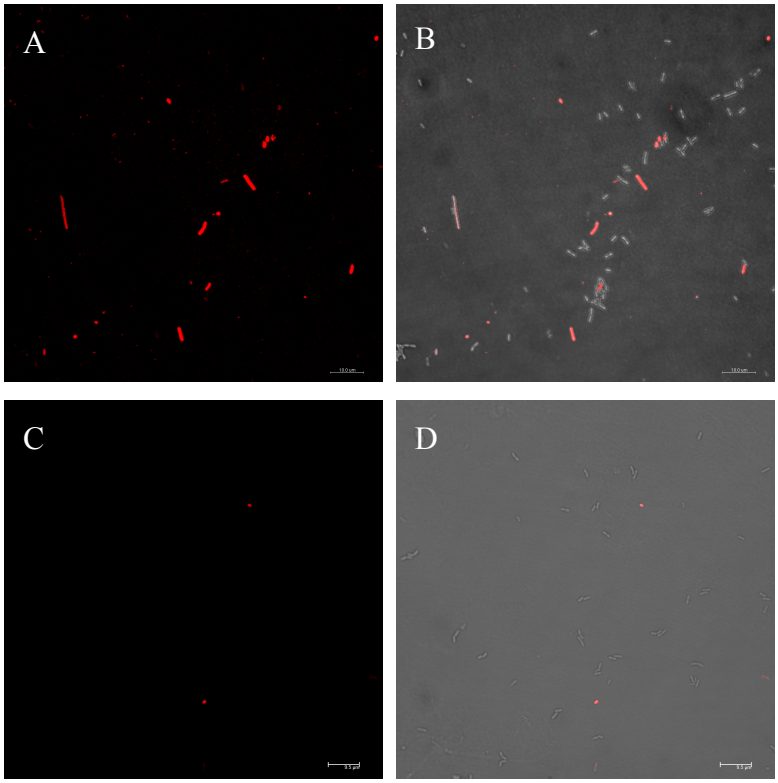

Figure 42: Red fluorescence (A) and overlay of A and phase contrast (B) of *P. aeruginosa* PAO1 incubated with **15** (2.44 mM). Red fluorescence (C) and overlay of C and phase contrast (D) of *B. cenocepacia* H111 incubated with **15** (244 µM).

4.3.4 Green FLAQS

FLAQS have the potential to become a powerful tool for the quick and inexpensive selective labeling of mixed bacterial strains. Therefore, differently labeled FLAQS with affinity for differing receptors could be used to identify mixed unknown bacterial samples. Therewith, bacteria with different QS receptors would be labeled with different colors and could be identified by fluorescence microscopy. In order to achieve this goal, various fluorescently tagged AHLs need to be prepared.

We decided to synthesize a green FLAQS by using our recognition pattern for *B. cenocepacia*. We hoped that this AHL mimic would behave just like its red counterpart. Dansyl was chosen as the fluorescent dye, as this moiety is widely used for biological evaluations. Hybrid **17** was achieved in four steps starting from

commercially available 12-aminododecanoicacid and dansyl chloride in 70% overall yield (Figure 43).

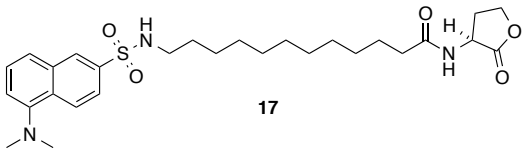

Figure 43: Structure of the green FLAQS **17**.

First, we investigated the fluorescent properties of hybrid **17**. The corresponding spectrum is shown in Figure 44. The maximum absorption is located at 335 nm, whereas the maximum emission can be found at 517 nm. The maximum excitation peak is situated at a much lower wavelength, compared with GFP. Thus, activity assays with the GFP reporter strains can still be performed.

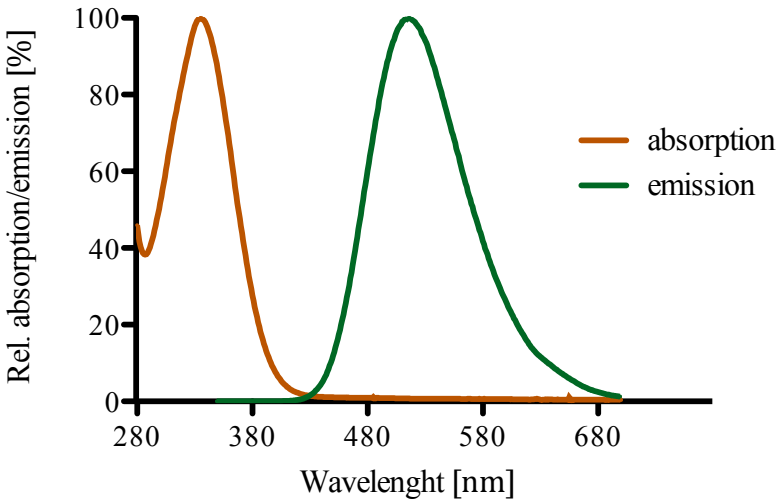

Figure 44: Fluorescence spectrum of **17**.

QS induction was tested for the two biosensors *P. putida* Iso F117 pAS-C8 and pKR-C12. As expected, better activity as obtained with the pAS-C8 sensor (Figure 45), whereas only weak QS induction was observed with the latter (Figure 46). However, compound **17** does not possess the same binding capacities as its rhodamine counterpart **11**. In order to further investigate the potential of the green FLAQS **17**, a more detailed study is required.

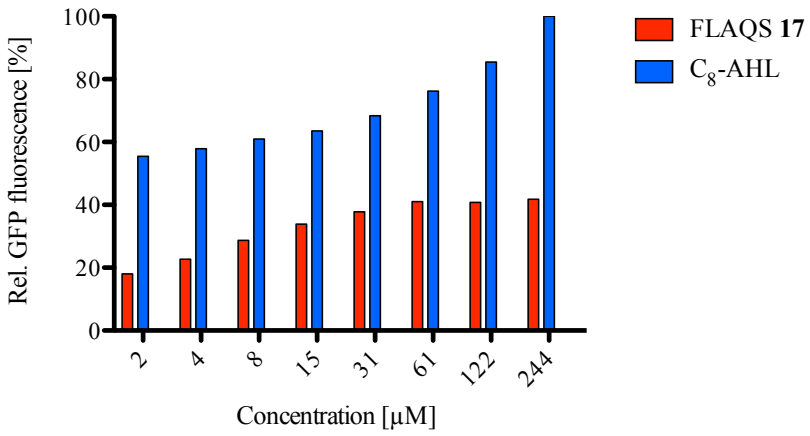

Figure 45: Activity tests with the *P. putida* F117 (pAS-C8) biosensor comparing FLAQS **17** and the natural C_8-AHL.

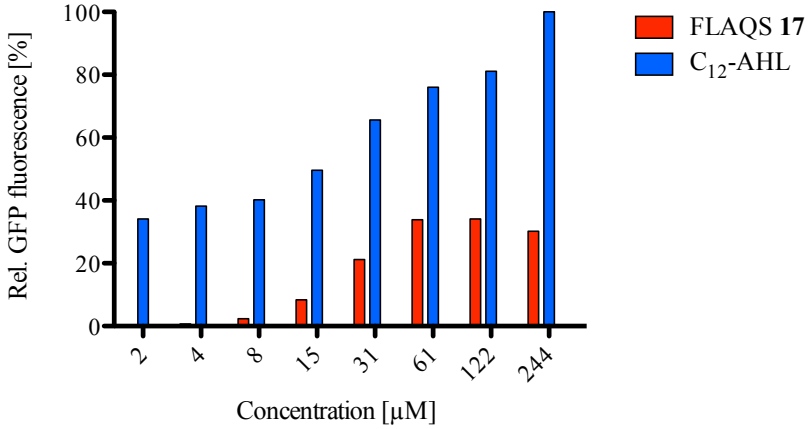

Figure 46: Activity tests with the *P. putida* F117 (pKR-C12) biosensor comparing FLAQS **17** and the natural C_{12}-AHL.

We continued our studies with the labeling of the wild-type strain *B. cenocepacia* H111, which was previously already successfully labeled with red FLAQS. Therefore, green FLAQS **17** was incubated with the WT strain as shown in Figure 47. Unfortunately, only very moderate labeling could be visualized by fluorescent microscopy analysis. The observed results cannot be solely attributed to deficient properties of the labeling compound, since labeling of the incubated cells was clearly seen in normal daylight. We could not improve the quality of the labeling due to limitations of the available instruments, especially the absence of an adequate filter. However, enhanced labeling is expected with the right equipment. Nevertheless, we

were able to synthesize a green FLAQS and the preliminary activity and labeling results obtained are highly promising and should be further investigated.

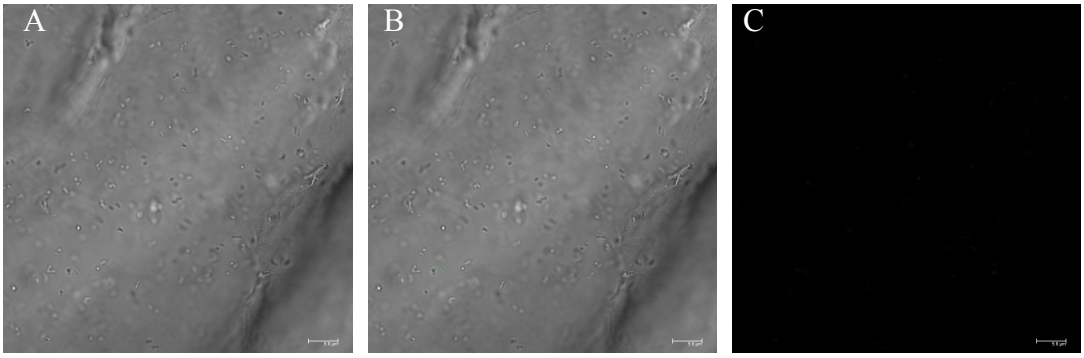

Figure 47: Phase contrast (A), overlay of phase contrast and green fluorescence (B) and green fluorescence (C) of *Burkholderia cenocepacia* H111 incubated with **17** (244 µM).

4.4 Conclusion

Our results demonstrate that easily synthesized FLAQS can be successfully used for the operationally simple and selective labeling of QS receptors. We could achieve two types of FLAQS that possess different properties for this purpose. Hybrids bearing a C_{12}-linker are selective for CepR and the labeling of *B. cenocepacia* H111, a pathogen isolated from a cystic fibrosis patient, was achieved with remarkable quality. Furthermore, application of FLAQS **11** suggested the presence of CepR as a soluble cytoplasmic protein. The selectivity of FLAQS **11** has been applied to specific QS labeling in a mixed bacterial culture.

The second type of FLAQS bearing 3-oxo functionality in the acyl side chain proved to be recognized by CepR and LasR. FLAQS **15** was successfully used for the fluorescent labeling of the wild-type *P. aeruginosa* PAO1. Even though we could not achieve the same level of labeling as with CepR, the obtained results are extremely promising. In addition, we successfully expanded the FLAQS library by introducing a green labeling agent.

We think that FLAQS could be utilized for the fast analysis of QS in various environmental and clinical samples, such as *e.g.* sputa from CF patients. Furthermore, FLAQS could potentially be applied for the investigation and visualization of bacteria-host communication pathways. This is especially interesting as only very little is known about this phenomenon.

5 SYNTHESIS OF MAJUCIN-TYPE SESQUITERPENES

5.1 Introduction

5.1.1 Neurodegenerative Diseases

Since ancient times, people have been seeking for agents that could preserve their youth and give eternal life. The search for the fountain of youth has not only been part of stories and tales but has been the focus of research by a variety of scientists. The most remarkable progress has been accomplished by medicine. Due to novel drugs, improved treatments and hygiene standards, a longer average lifetime has been achieved. However, there is a downside to this enormous success since the human body, especially the brain, has evolutionary not experienced such a long life span. The most serious concern in our aging society is the enormous increase of neurodegenerative diseases, which has become a major medical threat over the last century.[160] Many different disorders are attributed to this family, such as Parkinson's and Huntington's disease, amyotrophic lateral sclerosis and peripheral neuropathy. However, the most prevalent disorder among those is the Alzheimer's disease (AD), which affects approximately 36 million people worldwide.[161] This malady is characterized by the formation of amyloid plaques, dysfunctional neurons and loss of cognitive functions, thereby making a normal life impossible.[162] The pathogenesis of AD is not yet fully understood, but both genetic and environmental factors are believed to contribute to the progress of the illness.[163] Current therapies of dementia consist of administrating acetylcholine esterase inhibitors in order to prevent the breakdown of acetylcholine.[164] This results in cognitive improvement in most patients, often for 6 to 9 months or longer.[165] However, this simply delays the progression and does not lead to a cure and re-establishment of the brain function.[166]

---

[160] M. C. Via, Neurodegenerative Diseases: Next-Generation Drugs for Four Major Disorders, *Pharma Reports* **2008**.

[161] World Alzheimer Report, Alzheimer's Disease International, **2012**.

[162] (a) G. Vantini, D. Skaper, *Pharmacol. Res.* **1992**, *26*, 1; (b) H. W. Querfurth, F. M. LaFerla, *N. Engl. J. Med*. **2010**, *362*, 329.

[163] D. K. Lahiri, B. Maloney, M. R. Basha, Y. W. Ge, N. H. Zawia, *Curr. Alzheimer Res.* **2007**, *4*, 219.

[164] T. Mohamed, P. P. N. Rao, *Curr. Med. Chem*. **2011**, *18*, 4299.

[165] E. Giacobini, *Neurochem. Int.* **1998**, *32*, 413.

[166] (a) C. Holden, *Science* **1987**, *236*, 253; (b) J. L. Cummings, *N. Engl. J. Med*. **2004**, *351*, 56.

In recent studies, the progression of neurodegenerative diseases have been linked to decreased neurotrophic support.[167] It was previously believed that nerve regeneration in the central nervous system was irreversible, but recently it has become apparent that neurotrophins, a class of polypeptidyl agents, are involved in the survival of developing neurons and in the maintenance of mature neurons throughout life.[167]

The first neurotrophin to be isolated and characterized was the *nerve growth factor* (NGF) in 1948.[168] NGF is released by target tissue of sympathetic and sensory fibers and is taken up by the fibers where it increases the length and volume of neuron cells.[169] It is then retrogradely transported to the cell body. Initially regarded as promising therapeutic agents for the cure of neurodegenerative diseases, neurotrophins are large molecules that cannot penetrate into the target brain through the blood-brain barrier and suffer from a lack of bioavailability and stability.[170]

An attractive alternative approach is based on the search for orally available small organic molecules that could mimic or enhance neurotrophin action. Some recent examples of neuroregeneration by small natural products will be discussed in the following section.

5.1.2 Small Molecules

The search for small molecules that are able to mimic the biological effect of the natural neurotrophic factors or to stimulate their synthesis and secretion has promoted the interest of many research groups. Current literature suggests that the combination of NGF and compounds from natural sources could be employed for that purpose.[171] Hence, natural products may successfully be used for the treatment of neuronal injuries. Recently, many compounds isolated from natural sources have been determined to exhibit neuroprotective and neurotrophic properties and to enhance the neurite outgrowth activity of NGF in various experimental models.[171] In contrast to

[167] (a) M. R. Bennett, W. G. Gibson, G. Lemon, *Auton. Neurosci-Basic Clin.* **2002**, *95*, 1; (b) D. Dawbarn, S. J. Allen, *Neuropathol. Appl. Neurobiol.* **2003**, *29*, 211.

[168] E. D. Bueker, *Anat. Rec.* **1948**, *102*, 369.

[169] B. L. Irwin, K. K. Leonard, *Neuron Cell Mol. Biol.* **2002**, *3*, 410.

[170] R. M. Wilson, S. J. Danishefsky, *Acc. Chem. Res.* **2006**, *39*, 539.

[171] For current reviews, see: (a) F. M. Longo, S. M. Massa, *Nature Rev.* **2013**, *12*, 507; (b) S. V. More, S. Koppula, I.-S. Kim, H. Kumar, B.-W. Kim, D.-K. Choi, *Molecules* **2012**, *17*, 6728; (c) J. Xu, M. H. Lacoske, E. A. Theodorakis, *Angew. Chem. Int. Ed*. **2014**, *53*, 956.

the relatively structurally large neurotrophins, small molecules have the advantage to be generally easier available by synthesis and can therefore lead to new drugs for medical treatment.[172]

Various different classes of natural products have been shown to possess neuritotrophic properties. The first non-protein neurotrophic factor to be discovered was (+)-lactacystin (**LXXIX**, Figure 48), a sulfur-containing γ-lactam produced by a culture broth of *Streptomyces* sp. OM-6519.[173] This compound was shown to exhibit significant neuritogenic activity at a concentration of 1.3 μM in mouse neuroblastoma cell line Neuro 2A. Shortly after, Corey and Reichard reported its first total synthesis.[174] Another example for such a target is littoralisone (**LXXX**), a natural product from the iridoid glycoside family. Originally isolated from *Verbena littoralis* in 2001,[175] the first total synthesis was reported by MacMillan and co-workers in 2005 using organocatalysis in various key steps.[176] Many more complex natural products have been synthesized for this purpose, such as scabronine G (**LXXI**)[177] and merrilactone A (**LXXII**),[178] both reported first by Danishefsky and co-workers.

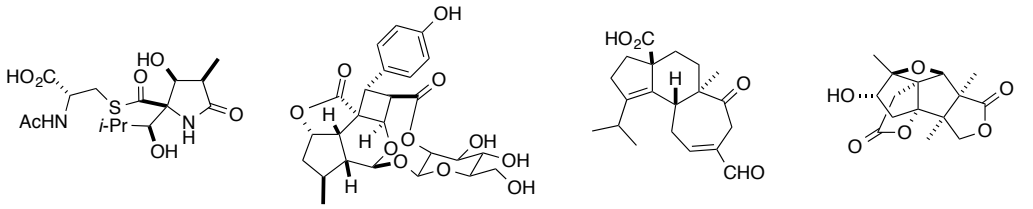

lactacystin (**LXXIX**) littoralisone (**LXXX**) scabronine G (**LXXXI**) merrilactone A (**LXXXII**)

Figure 48: Examples of synthesized neuritotrophic natural products.

Due to the importance of such molecules for the understanding of neurodegenerative diseases, it is imperative to have access to larger quantities of material, which is mostly not possible by extraction from the natural source. The Gademann research group has been successful in the synthesis of natural products

[172] S. S. Gill, N. K. Patel, G. R. Hotton, K. O'Sullivan, R. McCarter, M. Bunnage, D. J. Brooks, C. N. Svendsrem, P. Heywood, *Nature Med.* **2003**, *5*, 589.

[173] S. Omura, T. Fujimoto, K. Otoguro, K. Matsuzaki, R. Moriguchi, H. Tanaka, Y. Sasaki, *J. Antibiot*. **1991**, *44*, 113.

[174] E. J. Corey, G. A. Reichard, *J. Am. Chem. Soc*. **1992**, *114*, 10677.

[175] Y. S. Li, K. Matsunaga, M. Ishibashi, Y. Ohizumi, *J. Org. Chem*. **2001**, *66*, 2165.

[176] I. K. Mangion, D. W. C. MacMillan, *J. Am. Chem. Soc*. **2005**, *127*, 3696.

[177] S. P. Waters, Y. Tian, Y.-M. Li, S. J. Danishefsky, *J. Am. Chem. Soc*. **2005**, *127*, 13514.

[178] V. B. Birman, S. J. Danishefsky, *J. Am. Chem. Soc.* **2002**, *124*, 2080.

exhibiting neuritotrophic properties. The total synthesis and biological evaluation of various natural products such as withanolide A (Figure 49, **LXXXIII**),[179] militarinone D (**LXXXIV**),[180] cyrneine A (**LXXXV**),[181] and gelsemiol (**LXXXVI**)[182] have been accomplished in elegant strategies.

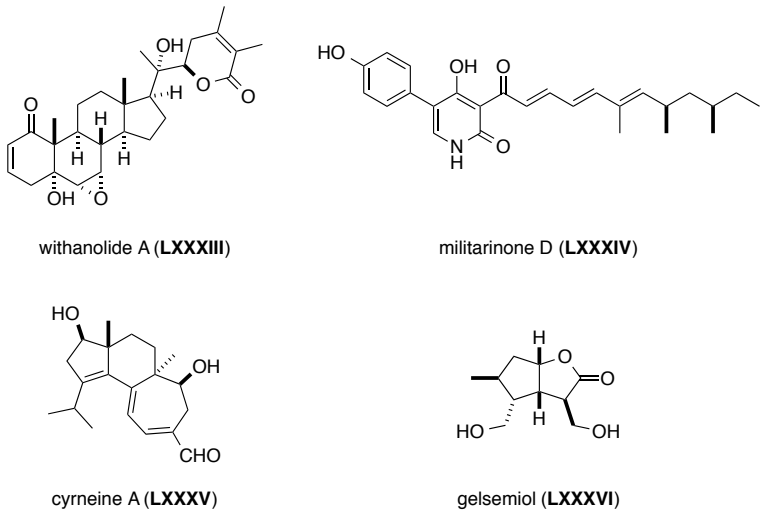

Figure 49: Synthesized neuritotrophic natural products by the Gademann group.

Even though structurally diverse molecules have been shown to possess neuritotrophic properties in model systems, the mode of action of most substrates still remains unknown. In order to enable possible drug candidates, further studies are essential and require further biochemical and synthetic efforts. That is why we were interested in a new class of natural products to expand the neuritotrophic chemical library.

[179] C. K. Jana, J. Hoecker, T. M. Woods, H. J. Jessen, M. Neuburger, K. Gademann, *Angew. Chem. Int. Ed.* **2011**, *50*, 8407.

[180] H. J. Jessen, A. Schumacher, T. Shaw, A. Pfaltz, K. Gademann, *Angew. Chem. Int. Ed.* **2011**, *50*, 4222.

[181] E. Elamparuthi, C. Fellay M. Neuburger, K. Gademann, *Angew. Chem. Int. Ed.* **2012**, *51*, 4071.

[182] M. Binaghi, P. Burch, M. Scherer, C. Wentzel, D. Bossert, L. Eberhardt, M. Neuburger, P. Scheiffele, K. Gademann, *Chem. Eur. J.* **2013**, *19*, 2589.

5.2 The Genus *Illicium*

5.2.1 Overview

Plants hold a breath-taking amount of different chemical compounds. We became interested in natural products derived from the genus *Illicium*, a species of flowering plants, evergreen shrubs and trees that occur in the West Indies, eastern North America, Mexico, and eastern Asia due to their impressive chemical diversity.[183] The fruits of *Illicium* species are distinctive star-shaped follicles with a characteristic refreshing flavor. The best-known example is the Chinese star anise, also known as *Illicium verum*, which has been traditionally used in Asian cooking as spice throughout ages. However, not all fruits from this species can be used for culinary purposes, as some have been known for several centuries to contain toxic compounds, such as the fruits of *Illicium anisatum*, better known as Japanese star anise. These toxic substances have been the focus of many researchers since the mid-19th century. It was not before 1952 that the toxic principle component was identified by Lane *et al*. and the pure toxic ingredient was named anisatin (Figure 50, **LXXXVII**).[184] The structure elucidation was recalcitrant and was only completed in 1968 by Yamada and Hirata.[185] Anisatin is recognized as one of the most potent neurotoxins of plant origin.[186]

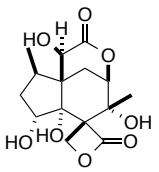

anisatin (**LXXXVII**)

Figure 50: Structure of anisatin.

Since the discovery of anisatin, components of the *Illicium* family have been intensively chemically investigated and many biologically active compounds have been identified to date.[187] It was shown that a number of these natural products have

[183] A. C. Smith, *Sargentia* **1947**, *7*, 1.

[184] J. F. Lane, W. T. Koch, N. S. Leeds, G. Gorin, *J. Am. Chem. Soc*. **1952**, *74*, 3211.

[185] K. Yamada, S. Takeda, S. Nakamura, Y. Hirata, *Tetrahedron* **1968**, *24*, 199.

[186] T. J. Schmidt, M. Gurrath, Y. Ozoe, *Bioorg. Med. Chem*. **2004**, *12*, 4159.

[187] Y. Fukuyama, J.-M. Huang, *Illicium, Pimpinella, and Foeniculum*; M. M. Jodral, Ed.; CRC LLC; New York, **2004**, p 31.

potent neurite outgrowth activity in primary cultured rat cortical neurons.[187] Further studies on chemical components in *Illicium* plants were carried out by Kawano,[188] and later by Schmidt[189] and Fukuyama[190] and their corresponding research groups. A variety of unique *seco*-prezizaane-type sesquiterpenes or so called *Illicium* sesquiterpenes were found exclusively in these plants. The majority of the active compounds were determined to be sesquiterpenes bearing a bicyclo[4.3.0]nonane carbon skeleton. These chemical moieties were further classified into six subgroups depending on the lactone-type. In the following section, structures, classes, and variety of these sesquiterpenes from *Illicium* species will be discussed.

5.2.2 *seco*-Prezizaane-Type Sesquiterpenes

The core structure of this class of natural products has been proposed to be derived from farnesol pyrophosphate (FPP, **LXXXVIII**) as shown in Scheme 6.[190] The proposed biosynthetic pathway suggests that FPP (**LXXXVIII**) can rearrange through intermediate **LXXXIX** and acorane (**XC**) to *allo*-cedrane (**XCI**). The *seco*-prezizaane core structure **XCII** is then finally formed by breaking the C-6-C-11 bond.

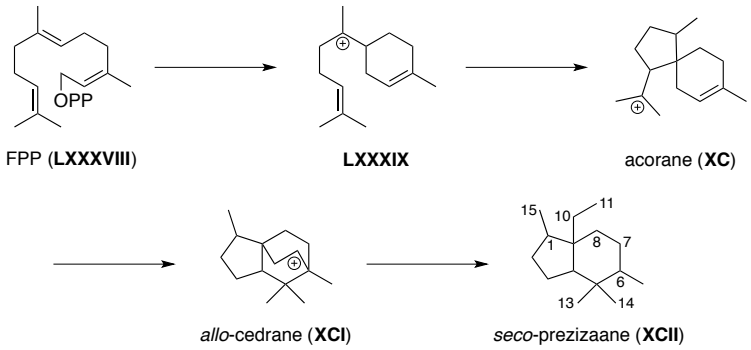

Scheme 6: Plausible biosynthesis of *seco*-prezizaane (**XCII**) through a common key biosynthetic intermediate, *allo*-cedrane (**XCI**).

seco-Prezizaane-type sesquiterpenes all have the same carbon skeleton but, depending on the subgroup, possess diverse lactone moieties. The structures of natural products that the six subtypes are named after (**LXXXVII**, **XCIII-XCVII**) are shown

[188] I. Kouno, N. Kawano, *J. Chem. Cos. Perkin Trans.* **1988**, 1537.

[189] T. J. Schmidt, H. M. Schmidt, E. Müller, W. Peters, F. R. Fronczek, A. Truesdale, N. H. Fischer, *J. Nat. Prod.* **1998**, *61*, 230.

[190] Y. Fukuyama, J.-M. Huang, *Studies in Natural Products Chemistry*; A. Rahman, Ed.; Elsevier: New York, **2005**, Vol. 32, p 395.

in Figure 51. The following section will focus on the subtype of our interest in the present work, namely the majucin-type sesquiterpenes.

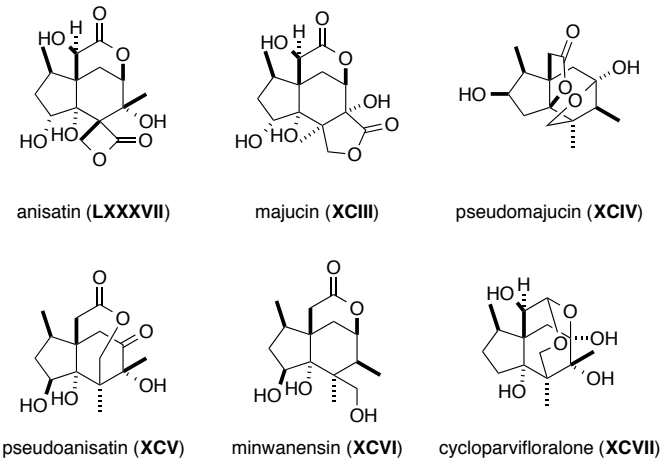

Figure 51: Six subtypes of seco-prezizaane-type sesquiterpenes from *Illicium* species.

5.2.3 Majucin-Type Sesquiterpenes

The common feature of this subtype is the presence of a γ-lactone ring (Figure 52). Majucin (**XCIII**) was the first compound to be structurally assigned by extensive spectroscopic analysis in 1988.[191] Ever since, many more natural products from this subgroup have been isolated and fully characterized.[190] Amazingly, several of these molecules have been shown to be neurotrophically active. The most active members of this family are jiadifenin (**XCVIII**),[192] jiadifenolide (**IC**),[193] (2*S*)-hydroxy-3,4-dehydroneomajucin (**C**),[192] jiadifenoxolane A (**CI**),[193] and the norsesquiterpenoid (2*R*)-hydroxy-norneomajucin (**CII**).[194] Furthermore, also the synthetic carboxylic acid derivative of jiadifenin **CIII** showed potent neurite outgrowth promoting activity in primary cultured rat cortical neurons.[190]

[191] C.-S. Yang, I. Kuono, N. Kawano, S. Sato, *Tetrahedron Lett*. **1988**, *29*, 1165.
[192] R. Yokoyama, J.-M. Huang, C. Yang, Y. Fukuyama, *J. Nat. Prod*. **2002**, *65*, 527.
[193] M. Kubo, C. Okada, J.-M. Huang, K. Harada, H. Hioki, Y. Fukuyama, *Org. Lett*. **2009**, *11*, 5190.
[194] M. Kubo, K. Kobayashi, J.-M. Huang, K. Harada, Y. Fukuyama, *Tetrahedron Lett*. **2012**, *53*, 1231.

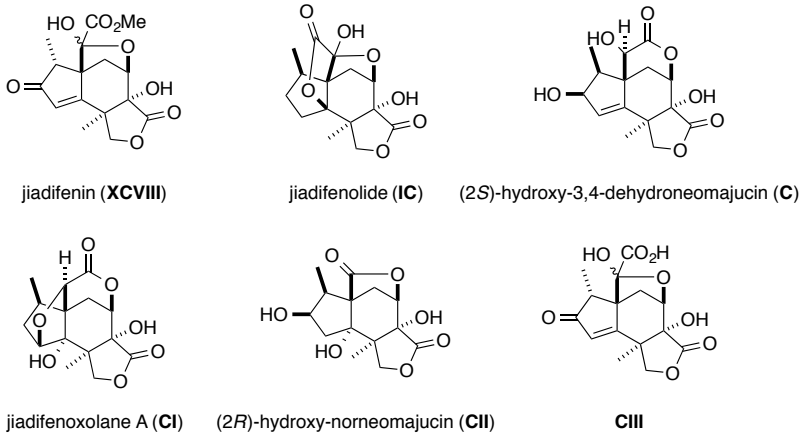

Figure 52: Majucin-type sesquiterpenes possessing neurotrophic activity.

With over 20 majucin-type sesquiterpenes having been isolated and characterized to date, only two of them have been synthesized so far. Therefore, further synthetic efforts are required in order to provide the required access to this class of natural products. Furthermore, no insight in the mode of action of these natural products has been obtained from previous research, making a more detailed structure-reactivity study necessary. The pharmacophore of these compounds may be found and used for additional investigations towards a real drug candidate.

A particularly interesting member of the majucin-type family of sesquiterpenes is jiadifenolide (**IC**). It does not only possess a highly oxidized and caged pentacyclic core structure, it also promotes neurite outgrowth at 10 nM concentrations.[193] Jiadifenolide (**IC**) has the same origin as jiadifenin (**XCVIII**) as both natural products were isolated from the East-Asian plant *Illicium jiadifengpi*. The architectural complexity combined with the desired bioactivity makes jiadifenolide the ideal target for total synthesis.

As previously mentioned, two of the majucin-type sesquiterpenes have already been synthesized. The following section will be focused on the successfully accomplished syntheses.

5.3 Previous Total Syntheses of Majucin-Type Sesquiterpenes

The synthesis of majucin-type sesquiterpenes has awaked the interest of various research groups.[195] However, only two have been accomplished to date, namely jiadifenin (**XCVIII**) and jiadifenolide (**IC**). The majority of the synthetic efforts have been directed to the preparation of **XCVIII**. The first racemic total synthesis was reported by Danishefsky and co-workers in 2004.[196] Since then, various enantioselective approaches towards this class of natural compounds have been reported in literature.[197] Theodorakis and co-workers reported the first enantioselective synthesis in 2011.[198] Another elegant total synthesis of (–)-jiadifenin (**XCVIII**) was reported by Zhai and coworkers shortly after.[199] Very recently, Xu *et al*. reported the first total synthesis of (–)-jiadifenolide (**IC**).[200]

5.3.1 Danishefsky's Total Synthesis of (±)-Jiadifenin[197]

The first synthesis of a majucin-type sesquiterpene was elegantly accomplished by Danishefsky and co-workers (Scheme 7).[196] The synthesis began with the commercially available cyclohexanone **CIV** and the authors obtained ketone **CV** as a 3:1 mixture of diastereoisomers in five steps by stepwise stereoselective alkylation. An intramolecular Horner-Wadsworth-Emmons reaction formed the A ring of **CVI**, which was followed by an intramolecular Claisen condensation to form the tricycle motif **CVII**. Oxidation of the β-keto ester with *m*-CPBA introduced the C-6 hydroxyl group as a single isomer. The formation of the *trans*-diol **CVIII** was achieved *via* stereo- and regioselective reduction of the C-7 ketone followed by methylation. Ozonolysis of the terminal alkene and subsequent Jones oxidation and stereoselective reduction of the ketone moiety led to the formation of lactone **CIX**. The introduction of the C-10 hydroxyl group of **CX** was achieved by treatment with Davis oxaziridine.[201] The synthesis of (±)-jiadifenin (**XCVIII**) was completed by Jones

[195] D. Urabe, M. Inoue, *Tetrahedron* **2009**, *65*, 6271.

[196] Y. S. Cho, D. A. Carcache, Y. Tian, Y. M. Li, S. J. Danishefsky, *J. Am. Chem. Soc*. **2004**, *126*, 14358.

[197] (a) K. Harada, A. Imai, K. Uto, R. G. Carter, M. Kubo, H. Hioki, Y. Fukuyama, *Org. Lett.* **2011**, *13*, 988; (b) G. Mehta, H. M. Shinde, R. S. Kumaran, *Tetrahedron Lett.* **2012**, *53*, 4320.

[198] L. Trzoss, J. Xu, M. H. Lacoske, W. C. Mobley, E. A. Theodorakis, *Org. Lett*. **2011**, *13*, 4554.

[199] Y. Yang, X. Fu, J. Chen, H. Zhai, *Angew. Chem. Int. Ed*. **2012**, *51*, 9825.

[200] J. Xu, L. Trzoss, W. K. Chang, E. A. Theodorakis, *Angew. Chem. Int. Ed*. **2011**, *50*, 3672.

[201] F. A. Davis, O. D. Stringer, *J. Org. Chem*. **1982**, *47*, 1774.

oxidation. The mono-oxidized intermediate **CXI** was also isolated and could be further oxidized to the natural product.

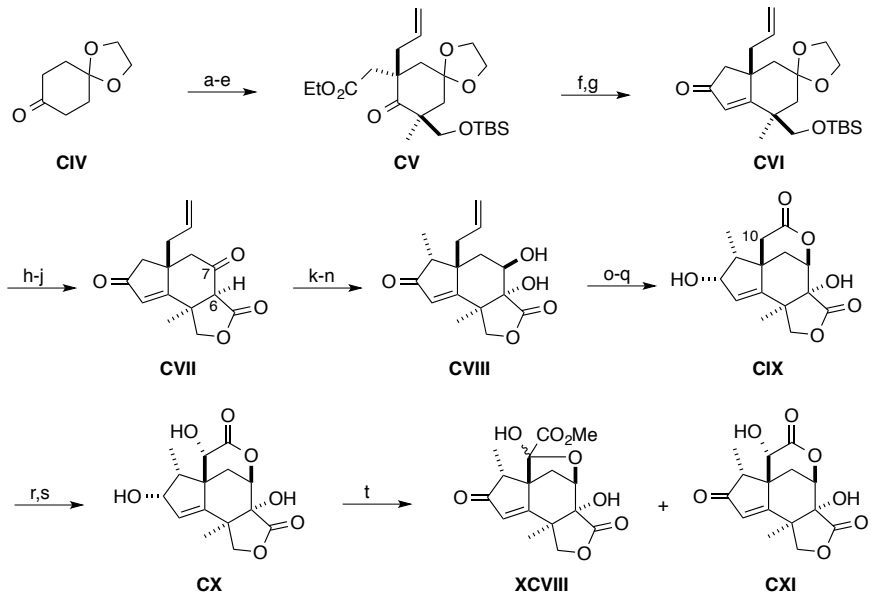

Scheme 7: a) LiHMDS, THF, -78 °C; MeI, -78°C to r.t.; b) 10% KOH, MeOH, HCHO (aq.), 0 °C; c) TBSOTf, 2,6-lutidine, CH_2Cl_2, 0 °C, 64% over three steps; d) LiHMDS, THF, –78 °C; allyl bromide, –78 °C to r.t., 73%; e) LDA, THF, –78 °C to –20 °C; $BrCH_2CO_2Et$, HMPA, –78 °C, 97%, *d.r.* = 3:1; f) $LiCH_2P(O)(OMe)_2$, THF, –78 °C, 81%; g) NaH, THF, reflux, 91%; h) 2 M HCl, THF, 94%, i) $ClCO_2Et$, pyridine, DMAP, CH_2Cl_2, 0 °C to r.t., 93%; j) NaH, THF, reflux, 94%; k) *m*-CPBA, CH_2Cl_2, 90%; l) $NaBH_4$, THF/MeOH (1:1), –78 °C, 93%; m) LDA, THF, –40 °C to –15 °C; n) MeI, HMPA, –35 °C, 64% over two steps; o) O_3, Sudan 7B Red, CH_2Cl_2/EtOH (1:1), –78 °C; p) Jones reagent, acetone, 90%; q) $NaBH_4$, $CeCl_3 \cdot 7H_2O$, THF/MeOH (3:1), –65 °C, 88%; r) NaHMDS, THF, –78 °C; s) Davis's oxaziridine, THF, –78 °C, 42% over two steps; t) Jones reagent, acetone; MeOH, 40% **XCVIII** and 29% **CXI**.

The first total synthesis of (±)-jiadifenin (**XCVIII**) was accomplished in 18 linear steps with an overall yield of 1.9% and provided several synthetic analogues to establish an initial SAR profile of this family. Interestingly, the fully synthetic intermediate **CXI** displayed even stronger neurotrophic activity in the assay than the natural product. However, these results should be considered with caution since the biological evaluations were performed on the racemic mixtures.

5.3.2 Theodorakis' Total Synthesis of (–)-Jiadifenolide[201]

Recently, Xu *et al.* reported on the first enantioselective total synthesis of a majucin-type sesquiterpene (Scheme 8).[200] Commercially available diketone **CXII** was used as the starting point for the synthesis, which was transformed into the prochiral triketone **CXIII** by allylation and subsequent Michael addition to methyl vinyl ketone. Following the Tu/Zhang protocol,[202] the authors could prepare the Parrish-type[203] diketone **CXIV** in optically enriched form (> 90% *e.e.*). Highly diastereoselective alkylation gave **CXV**, possibly controlled by the steric bulk of the allyl group. Further transformations afforded **CXVI**, which was treated with the McMurry reagent and then carbomethoxylated to the lactone **CXVII**. The tricyclic intermediate **CXVII** was epoxidized with alkaline hydrogen peroxide solution followed by oxidation to give the carboxylic acid that spontaneously triggered a "6-*exo*-tet" epoxide opening to furnish the *bis*-lactone **CXVIII**. Epoxidation of the double bond upon silyl deprotection and subsequent treatment the resulting epoxide with Dess-Martin periodinane triggered the key oxidative rearrangement to give rise to lactone **CXIX**. Even though the rearranged **CXIX** was susceptible to further oxidation, it could be secured in a 38% yield. Hydrogenation and protection led to ketone **CXX**, which was treated with Comins reagent and the resulting enol triflate was coupled with excess Me_3Al employing palladium catalysis to furnish compound **CXXI**. Hydrogenation of the trisubstituted alkene at 90 bar overpressure and hydroxylation of the lactone with Davis oxaziridine[204] afforded intermediate **CXXII**, which reacted with Jones reagent to complete the total synthesis of (–)-jiadifenolide (**IC**).

[202] X.-M. Zhang, M. Wang, Y.-Q. Tu, C.-A. Fan, Y.-J. Jiang, S.-Y. Zhang, F.-M. Zhang, *Synlett* **2008**, 2831.

[203] Z. G. Hajos, D. R. Parrish, *J. Org. Chem*. **1974**, *39*, 1615 .

[204] F. A. Davis, S. Chattopadhyay, J. C. Towson, S. Lal, T. Reddy, *J. Org. Chem*. **1988**, *53*, 2087.

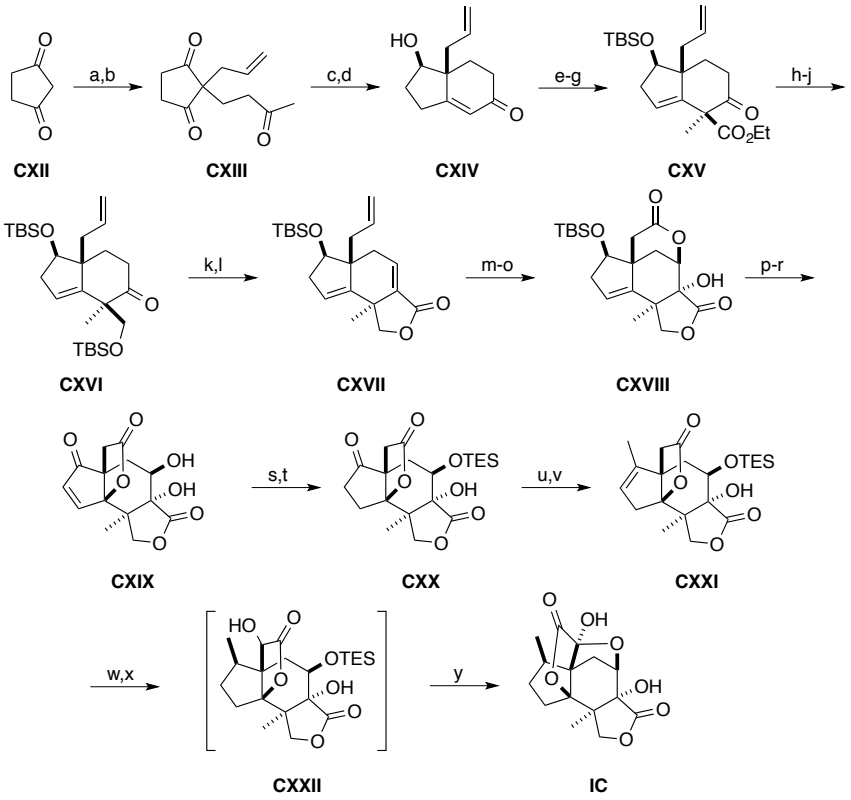

Scheme 8: a) Allyl acetate, $[PdC_3H_5Cl_2]_2$, BSA, cat. NaOAc, THF, reflux 24 h, 90%; b) methyl vinyl ketone, H_2O, r.t., 54%; c) D-prolinamide (30 mol %), PPTS (30 mol %), MeCN, 40 °C, 14 d, 74% (>90% *e.e.*); d) $NaBH_4$ (0.25 eq.), EtOH, 0 °C, 1 h; e) TBSCl, NH_4NO_3, DMF, r.t., 12 h, 92% for two steps; f) MMC, DMF, 130 °C, 3 h; $Et_3O^+BF_4^-$, *i*-Pr_2NEt, CH_2Cl_2, 0 °C, 5 min; g) TMSOTf, 2,6-lutidine, CH_2Cl_2, 0 °C to r.t., 1 h; TBAF (1.0 eq.), MeI, THF, –78 °C to r.t., 3 h, 43% for two steps; h) $LiAlH_4$, THF, 0 °C to r.t., 1 h; i) TBSCl (1.0 eq.), imidazole, CH_2Cl_2, 0 °C, 30 min; j) IBX, DMSO, 80 °C, 1 h, 85% for three steps; k) KHMDS, $PhNTf_2$, THF, –78 °C, 1 h; l) CO (1 atm), $[Pd(PPh_3)_4]$ (1 mol%), MeOH, DMF, Et_3N, 50 °C, 2 h; TFA, CH_2Cl_2, r.t., 5 h, 69% for two steps; m) H_2O_2, 3M NaOH, THF, 0 °C to r.t., 5 h, 99%; n) OsO_4 (1 mol%), $NaIO_4$, 1,4-dioxane, H_2O, r.t., 12 h; o) Jones reagent, acetone, 0 °C, 30 min, 70% for two steps; p) TBAF, THF, r.t., 30 min, 95%; q) *m*-CPBA, THF, 50 °C, 3 h; r) Dess-Martin periodinane, acetone, r.t., 2h, 38% for two steps; s) H_2 (6 atm), 10% Pd/C (5 mol%), MeOH, r.t., 24 h; t) TESOTf, 2,6-lutidine, THF, 0 °C to r.t., 30 min, 90% for 2 steps; u) KHMDS, Comins reagent, THF, –78 °C, 1.5 h; v) $AlMe_3$, $[Pd(PPh_3)_4]$ (50 mol%), THF, r.t., 2 h, 57% for two steps; w) H_2 (90 atm), PtO_2 (20 mol%), MeOH, r.t., 24 h; x) NaHMDS, (±)-*trans*-2-(phenylsulfonyl)-3-phenyloxaziridine, THF, –78 °C to r.t., 1.5 h; g) Jones reagent, acetone, 0 °C, 15 min, 33% for three steps.

The first total synthesis of (–)-jiadifenolide (**IC**) was accomplished in 25 linear steps in 0.5% overall yield from the commercially available cyclopentane 1,3-dione (**CXII**).

5.3.3 Theodorakis' Total Synthesis of (–)-Jiadifenin[199]

The first enantioselective total synthesis of (–)-jiadifenin (**XCVIII**) was reported by the research group of Theodorakis shortly after the initial jiadifenolide synthesis as shown in Scheme 9.[200] The previously described methods were employed to construct the tetracyclic lactone **CXXIII**, an intermediate from the synthetic route towards jiadifenolide (**IC**). Starting compound **CXXIII** was first dehydrated using Martin's sulfurane and the derived diene was hydrogenated to yield alkene **CXXIV**. Allylic oxidation at the C-2 position gave rise to the α,β-unsaturated ketone **CXXV**, which was then hydroxylated with Davis' oxaziridine to give lactone **CXXVI**. The final synthetic strategy is analog to the one described by Danishefsky and co-workers in the synthesis the racemic natural product.[196] Methylation with LDA/MeI/HMPA furnished the C-1 methylated product **CXXVII** with the required configuration. Alcohol **CXXVII** was then finally oxidized and rearranged under Jones conditions giving rise to (–)-jiadifenin (**XCVIII**) after methanolic work up, as described in the previous reports.[196]

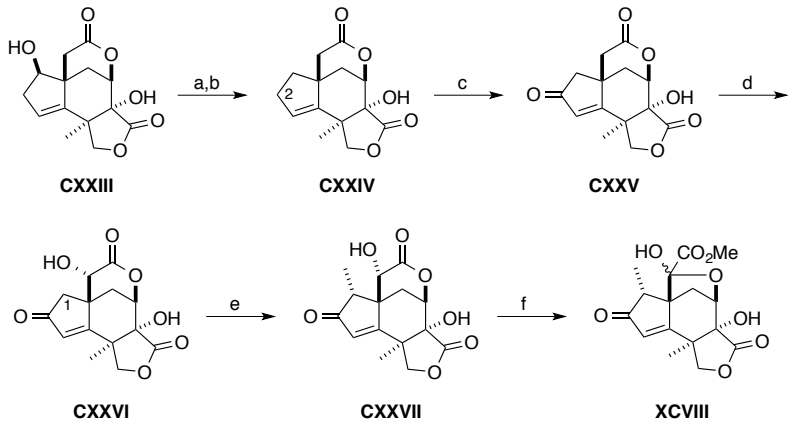

Scheme 9: a) Martin's sulfurane, THF, r.t., 2 h; b) H_2, Pd/C, MeOH, r.t., 1 h, 72% over two steps; c) $MnO(OAc)_9$, *t*-BuOOH, EtOAc, 3 Å MS, 40 °C, 16 h, 65%; d) NaHMDS, Davis' oxaziridine, THF, –78 °C, 1 h, 61%; e) LDA, MeI, THF, HMPA, –78 °C to –10 °C, 4 h, 60% *brsm*; f) Jones reagent, acetone, r.t., 20 min; MeOH, r.t., 15 min, 45%.

The first enantioselective total synthesis of (–)-jiadifenin (**XCVIII**) could be accomplished in six chemical steps from the previously described intermediate **CXXIII**. Overall, the synthesis preceded over 19 linear steps from readily available diketone **CXII** with an overall yield of 1.1%.

5.3.4 Zhai's Total Synthesis of (–)-Jiadifenin[200]

Another enantioselective route toward (–)-jiadifenin (**XCVIII**) was recently reported by the Zhai research group (Scheme 10). Their approach started with the coupling of readily available allylic bromide **CXXVIII** with lithiated propyne. Asymmetric dihydroxylation followed by a two-step acetal protection and deprotection of the terminal alcohol led to acetal **CXXIX** in good enantiomeric purity (> 93% *e.e.*). Jones oxidation and coupling of the corresponding carboxylic acid to the known alcohol **CXXX**[205] delivered ester (*E*)-**CXXXI**. Closure of the C ring was achieved using an Ireland-Claisen rearrangement with a good diastereoselective ratio of product **CXXXII** (*d.r.* = 7:1). Dihydroxy deprotection and selective silylation of the secondary hydroxy group led to enyne **CXXXIII**, which was then used for the key step, a Pauson–Khand reaction, to form the tricyclic intermediate **CXXXIV**. Subsequently, an interesting [2+2] cycloaddition between the enone moiety and allene furnished the head-to-head photocycloproduct **CXXXV** in a diastereoselective manner. Ozonolysis and ring opening with methanolic NaOMe led to **CXXXVI** as a fragmentation product upon oxidation applying the Ito-Saegusa protocol.[206] After exposure to TBAF, tandem desilylation and lactonization of enone **CXXXVI** furnished the according dilactone. The synthesis was completed by α-hydroxylation and Jones oxidation of this intermediate as already described by the Danishefsky[196] and Theodorakis[200] research groups.

Overall, Zhai's group completed the synthesis of (–)-jiadifenin (**XCVIII**) in 18 steps and 0.7% overall yield from allylic bromide **CXXVIII** in comparison to 19 steps and 1.1% yield in Theodorakis' synthesis.

---

[205] A. Reichenberg, M. Hintz, Y. Kletschek, T. Kuhl, C. Haug, R. Engel, J. Moll, D. N. Ostrovsky, H. Jomaa, M. Eberl, *Bioorg. Med. Chem. Lett*. **2003**, *13*, 1257.

[206] Y. Ito, T. Hirao, T. Saegusa, *J. Org. Chem*. **1978**, *43*, 1011.

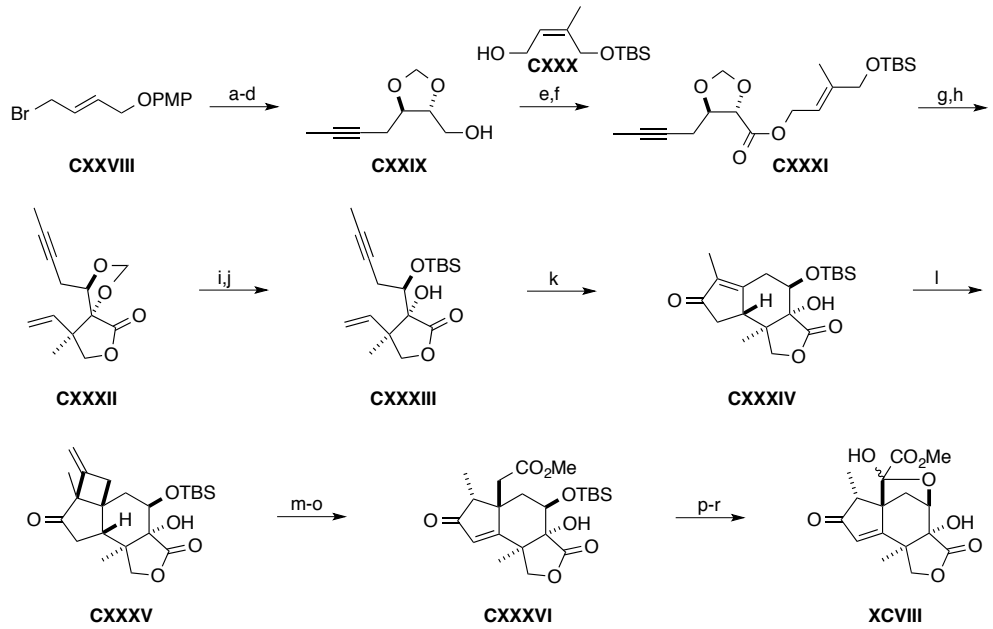

Scheme 10: a) 1-Bromo-1-propene, *n*-BuLi, CuI, THF, –78 °C to r.t., 74%; b) AD-mix-β, $MeSO_2NH_2$, *t*-BuOH/H_2O (1:1), 0 °C, 95%, >93% *e.e.*; c) KOH, CH_2I_2, [18]-crown-6, CH_2Cl_2, reflux, 80%; d) CAN, MeCN/H_2O (2.5:1), 90%; e) Jones reagent, acetone, -78 °C to r.t.; f) DCC, DMAP, **LI**, THF, r.t., 70% for two steps; g) LDA, TMSCl, THF, –78 °C to r.t. to reflux; h) TsOH·H_2O, MeOH, reflux, 54% for two steps, *d.r.* = 7:1; i) Ph_3CBF_4, CH_2Cl_2, reflux, 60%; j) TBSOTf, Et_3N, CH_2Cl_2, RT, 85%; k) [$Co_2(CO)_8$], Bu_3PS, toluene, RT to 75 °C, 67%; l) *hv*, allene, THF, –78 °C, 87%, *d.r.* = 4.8:1; m) O_3, MeOH, CH_2Cl_2; Me_2S, –78 °C to RT; NaOMe, MeOH, 89%; n) LDA, TMSCl, Et_3N, THF, –78 °C to –20 °C; o) $Pd(OAc)_2$, O_2, DMSO, 75 °C, 92% over two steps; p) TBAF, THF, RT, 96%; q) NaHMDS, (–)-*trans*-2-(phenylsulfonyl)-3-phenyloxaziridine, THF, -78 °C, 55%; r) Jones reagent, acetone, 0 °C; MeOH, RT, 46%.

5.4 Synthetic Studies on *Illicium* Sesquiterpenes

5.4.1 Retrosynthetic Analysis

Jiadifenolide (**18**) is a highly oxygenated sesquiterpene featuring a unique *seco*-prezizaane-type skeleton. Densely embedded in the framework of this cage-shaped molecule are seven stereocenters, including two separate all-carbon quaternary centers (C-5 and C-9). The previously described syntheses of majucin-type sesquiterpenes by the groups of Danishefsky,[196] Theodorakis,[200] and Zhai[199] were accomplished with a ring-construction sequence of B→AB→ABC, A→AB→ABC, and of C→BC→ABC, respectively. We propose a different strategy by first attaching the C ring to the A ring and then use an intramolecular ring-closing strategy to obtain the ABC core-structure as shown in Scheme 11.

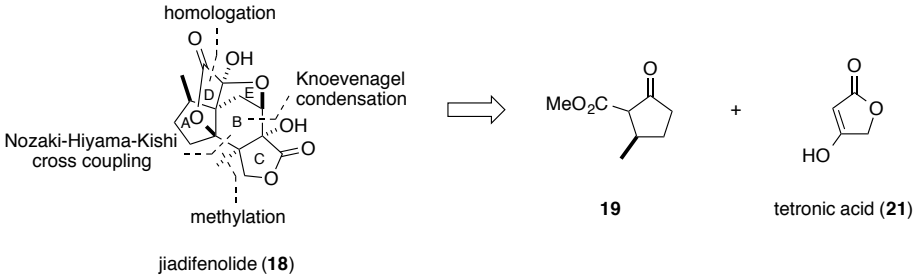

Scheme 11: Retrosynthetic analysis of (–)-jiadifenolide (**18**).

As outlined in Scheme 11, we envisioned that jiadifenolide (**18**) may be accessible through a series of transformations including an intramolecular and diastereoselective Nozaki-Hiyama-Kishi (NHK) cross coupling. We decided to start with the known keto ester **19**,[207] which can be obtained from D-pulegone (**20**) in three synthetic steps. The methyl group in **19** possesses the necessary (*R*) configuration of the A ring methyl in jiadifenolide. Starting with a natural product from the chiral pool has the advantage that we do not have to take into account any enantioselective step. Time-consuming optimization efforts to find the perfect chiral ligand and reaction conditions can be avoided by carefully choosing a suitable starting material. Nature offers us an enormous variety of chiral molecules, which many of them have been commercialized and can be used as a starting point for total syntheses.

[207] R. M. Coates, P. R. Vettel, *J. Org. Chem.* **1980**, *45*, 5430.

Tetronic acid (**21**) was envisioned to serve as the C ring moiety, which should be coupled to the A ring *via* a C_2-linker. The key step of the synthesis was planned to be a NHK cross coupling to form the C-4-C-5 bond. NHK reactions are frequently used in synthetic chemistry to couple vinylic halides or triflates to aldehydes. Even though rarely applied, some examples in literature demonstrate that ketones can be used as coupling reagents.[208] The reported yields are rather poor, but our intramolecular variation might effectively furnish the desired tricyclic core structure.

Insertion of the remaining C-14 methyl group was planned to be derived from a 1,4-addition to the unsaturated γ-lactone or *via* a two-step procedure including Corey-Chaykovsky cyclopropanation and subsequent Birch reduction.[209] Further oxidation of the core structure and homologation of the ester moiety should deliver the second γ-lactone after hydrolysis. The hydroxyl group at C-6 position was expected to be derived from the corresponding epoxide between C-6 and C-7.

It is noteworthy that the desired stereoselectivity of the complete synthesis is supposed to be directed by the methyl group of D-pulegone (**20**) by diastereoselective transformations.

5.4.2 Attachment of the C Ring

The synthesis started with the preparation of keto ester **19** as shown in Scheme 12. Bromination of D-pulegone (**20**) and subsequent treatment of the double brominated intermediate with methanolic NaOMe triggered the Favorskii rearrangement and ester **22** was obtained as a 1:1 mixture of diastereoisomers. Ozonolysis of **22** gave the known keto ester **19** in an excellent 76% overall yield. Modifications of the literature protocols[207] were necessary in order to obtain the desired product in satisfactory yield.

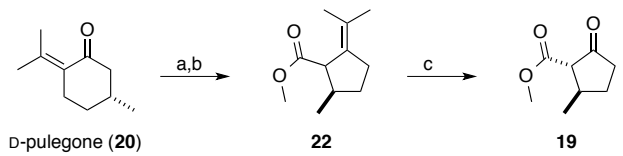

Scheme 12: a) Br_2, $NaHCO_3$, Et_2O, 0 °C, 40 min; b) NaOMe, MeOH, reflux, 2.5 h, 76% over two steps; c) O_3, CH_2Cl_2/MeOH (5:1), –78 °C; Zn, AcOH, –78 °C to r.t., 97%.

[208] (a) J. J. Miller, M. S. Sigman, *J. Am. Chem. Soc*. **2007**, *129*, 2752; (b) P. Knochel, C. J. Rao, *Tetrahedron* **1993**, *49*, 29; (c) R. Angell, P. J. Parsons, A. Naylor, *Synlett* **1993**, 189; (d) K. Suzuki, H. Takayama, *Org. Lett*. **2006**, *8*, 4605; (e) K. Takai, K. Kimura, T. Kuroda, T. Hiyama, H. Nozaki, *Tetrahedron Lett*. **1983**, *24*, 5281.

[209] T. E. Janini, P. Sampson, *J. Org. Chem*. **1997**, *62*, 5069.

With the A ring in hand, the next step was the attachment of the C ring. We decided to use linker **23**, prepared in a single step following a known procedure,[210] to attach the C ring moiety. Alkylation of keto ester **19** gave the desired silyl ether in a good diastereomeric ratio of 7:1, which was further iodinated to **24** using *in situ* prepared TMSI following the Olah/Narang protocol[211] (Scheme 13). The primary iodide **24** quickly decomposed to a single crystalline product under normal light exposure. X-ray crystal structure analysis showed that spiro compound **25** was formed. Even though the obtained product did not serve any synthetic purpose, it still verified that the desired configuration was introduced in C-9 position. Direct alkylation of **24** with 1,2-diiodoethane did not yield the expected product **24** and only complex mixtures were obtained under various reaction conditions.

Next, iodide **24** was reacted with tetronic acid (**21**) under basic conditions. However, preliminary results showed that the *O*-alkylated vinyl ether **26** was formed exclusively and not the desired *C*-alkylated product. Due to the moderate yields and undesired regioselectivity of the reactions, we decided to seek for a better synthetic strategy.

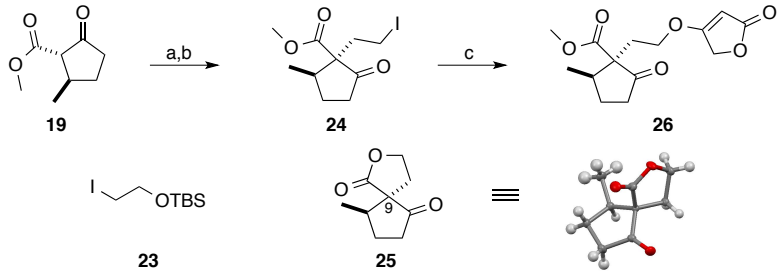

Scheme 13: a) K_2CO_3, **23**, acetone, r.t. to reflux, 2d, 53%, *d.r.* = 7:1; b) TMSI, MeCN, r.t., 1 h, 52%; c) tetronic acid (**21**), LiI, DBU, THF, reflux, 36 h; DMPU, reflux, 2 d.

Alternatively, keto ester **19** was allylated as shown in Scheme 14. The desired product **27** was obtained in superb 92% yield as an 11:1 mixture of diastereoisomers, which were easily separated by flash chromatography on silica gel. The improved selectivity can be explained by the milder reaction conditions applied due the superior electrophilic reactivity of allyl bromide compared to **23**. Ozonolysis gave pure aldehyde **28** after simple filtration over celite in quantitative yield. With aldehyde **28** in hand, we next envisioned to couple tetronic acid (**21**) *via* a Knoevenagel

[210] C. Desroches, C. Lopes, V. Kessler, S. Parola, *Dalton Trans.* **2003**, 2085.
[211] G. A. Olah, S. C. Narang, *Tetrahedron*, **1982**, *38*, 2225.

condensation.[212] However, no desired product could be isolated due to the strong electrophilic properties of the formed intermediate, which quickly reacted with the remaining **21** in solution to form the corresponding Michael adduct.

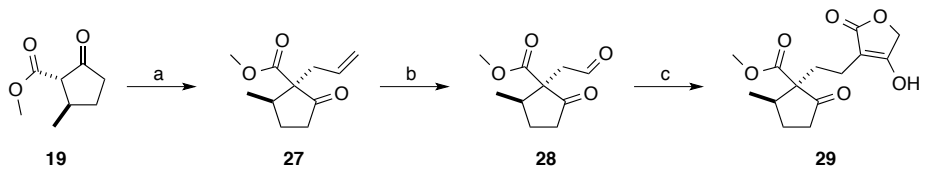

Scheme 14: a) NaH, THF/DMPU (4:1), r.t., 1 h; allyl bromide, 0 °C to r.t., 13 h, 92%, *d.r.* = 11:1; b) O_3, CH_2Cl_2/MeOH (5:1), -78 °C; Zn, AcOH, –78°C to r.t., quant.; c) Hantzsch' ester, tetronic acid (**21**), L-proline (10 mol%), MeOH, 24 h, r.t., 81%.

Facing a similar problem, Ramachary and co-workers reported a cascade three-component reductive alkylation using Hantzsch' ester as reducing agent to couple tetronic acid to carbonyl moieties.[213] Optimized reaction conditions using this procedure led to product **29** in 81% yield.[212] Best results were obtained using 0.1 equivalents of L-proline and 2.2 equivalents of Hantzsch' ester, as reducing the amounts of any of the reagents led to a significant drop in yield.

As an alternative, we envisaged to couple tetronic acid to a higher oxidized substrate in order to overcome later oxidation state adjustments. Thus, aldehyde **28** was oxidized to the corresponding carboxylic acid **30** using sodium chlorite in quantitative yield (Scheme 15). For the ensuing acylation step we tested a method reported by Yoshii *et al*., which allows a one-pot acylation procedure involving a DMAP-mediated Fries rearrangement of the kinetic *O*-acylation product.[214] Following the reported method, **31** could be isolated by preparative HPLC separation in 19% yield since decomposition of the substrate was observed on silica gel. Even with a successful isolation of the product, it was shown to be very unstable and decomposition could be detected after short time, even under protecting atmosphere at 4 °C. Therefore, we decided to pursue our synthetic strategy with the more stable product **29**.

[212] E. Kaufmann, Master Thesis, Basel, **2011**.

[213] D. P. Ramachary, M. Kishor, *Org. Biomol. Chem.* **2008**, *6*, 4176.

[214] K. Nomura, K. Hori, M. Arai, E. Yoshii, *Chem. Pharm. Bull.* **1987**, *35*, 4368.

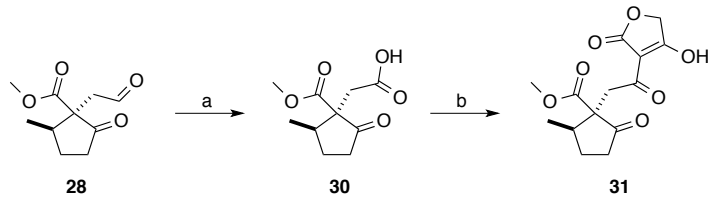

Scheme 15: a) 2-Methyl-2-butene, sodium chlorite, sodium phosphate, *t*-BuOH/H_2O (1:2), r.t., 2 h, quant.; b) DMAP, DCC, **21**, *N*,*N*-diisopropylethylamine, CH_2Cl_2, 0 °C to r.t., 16 h, 19%.

After having attached the C ring moiety, we turned our attention towards the key step of the synthesis, the formation of the B ring.

5.4.3 Formation of the B Ring

5.4.3.1 Nozaki-Hiyama-Kishi Approach

The formation of the six-membered B ring was addressed next. For this, we envisioned to use a NHK cross coupling reaction to obtain the tricyclic core structure. First, C-5 position had to be activated in order to allow oxidative addition of nickel during the process. Vinyl halides and triflates are most commonly used as starting reagents for NHK reaction. Therefore, substrate **29** was triflated to yield compound **32** in quantitative yield (Scheme 16). The resulting triflate **32** was treated with $CrCl_2$ and a catalytic amount of $NiCl_2$ in degassed DMF at 50 °C for 24 h to give the desired product **33** as a single stereoisomer in 69% yield, which was confirmed by X-ray crystal structure analysis as shown in Figure 16.

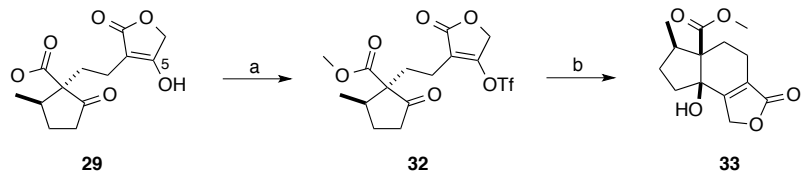

Scheme 16: a) 2,6-Lutidine, Tf_2O, CH_2Cl_2, –78 °C to r.t., 7 h, quant.; b) $NiCl_2$ (10 mol%), $CrCl_2$, 3 Å MS, DMF, 50 °C, 24 h, 69%.

To the best of our knowledge, this represents the first completely diastereoselective and intramolecular NHK coupling with a ketone. In order to further optimize these excellent results and reduce the required excess of chromium needed, we investigated some variations of the NHK reaction.

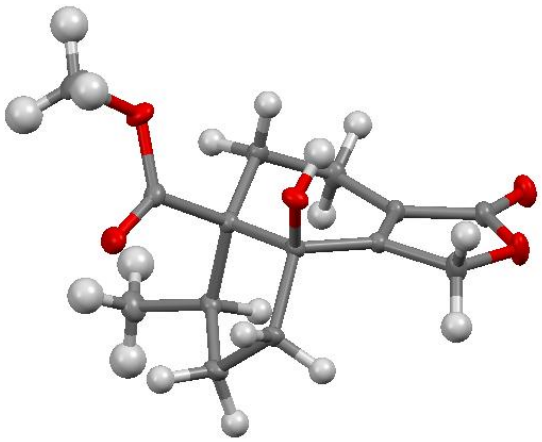

Figure 53: X-ray crystallographic analysis of the tricyclic intermediate **33**. Red = O, grey = C, white = H.

Fürstner and co-workers presented catalytic in chromium variation of the NHK reaction.[215] The authors used manganese as reducing agent in the presence of less hygroscopic $CrCl_3$ and TMSCl to cleave the formed chromium oxygen bond due to the stronger silyl-oxygen bonding properties. In order to reduce the high amount of Cr(II), which is toxic and relatively expensive, different reaction conditions were screened as shown in Table 3.[216]

First, we tested if $CrCl_2$ could be replaced by $CrCl_3$ by addition of manganese (entries 1 and 2). Unfortunately, the obtained yields were not better than with $CrCl_2$. Also the use of a $CrCl_2$ and $CrCl_3$ mixture did not improve the results (entry 3). Interestingly, by mixing a large excess of $CrCl_2$ with manganese afforded lower yields compared to manganese free reaction conditions (entry 4). Furthermore, addition of TMSCl and LiCl in presence of catalytic amount of chromium sources did not improve the results (entries 5-7).

In conclusion, the NHK reactions catalytic in chromium were not to be applicable to this specific example. However, first results demonstrate that $CrCl_3$ serves as an alternative to $CrCl_2$ in the presence of manganese.

[215] (a) A. Fürstner, N. Shi, *J. Am. Chem. Soc.* **1996**, *118*, 2533; (b) A. Fürstner, N. Shi, *J. Am. Chem. Soc*. **1996**, *118*, 12349.

[216] C. Daeppen, Master Thesis, Basel, **2012**.

Table 3: Screening different reaction conditions for the NHK reaction.

Entry[a]	$CrCl_2$ (eq.)	$CrCl_3$ (eq.)	Mn (eq.)	Additive (eq.)	Yield of **33** (%)
1	-	2.3	1.5	-	28
2	-	4.0	2.0	-	55
3	3.0	1.0	-	-	43
4	10.0	-	2.0	-	31
5	0.2	-	1.7	TMSCl, 2.4	0
6	-	0.2	1.5	TMSCl, 1.3	12
7	-	0.5	2.0	LiCl, 2.5	3

[a)] All reaction were performed in DMF at 50 °C for 5 hours with 10 mol% of $NiCl_2$.

5.4.3.2 Shapiro Approach

Although excellent results were obtained with the NHK approach, we wondered if we could circumvent the use of large amounts of chromium needed for the scale-up of the synthesis. An intriguing alternative approach would be an intramolecular Shapiro reaction to form the six-membered B ring. Shapiro reactions are typically used to couple tosylhydrazones and ketones under strongly basic conditions.[217] However, these reactions are generally used for intermolecular coupling of rather unfuctionalized starting materials. Nevertheless, we expected that the corresponding hydrazone might be formed, which can eventually be used for the Shapiro reaction.

Therefore, substrate **29** was treated with tosylhydrazine in ethanol at 50 °C for two days as shown in Scheme 17.[212] The desired product **34** was obtained in relatively poor yield along with a crystalline side-product, which was characterized by X-ray crystal structure analysis as the tetracyclic diazo compound **35** (Figure 54). We assume that the formation of the 1-pyrazoline ring is derived from decomposition of tosylhydrazone at C-4 position to the corresponding diazoalkane, which then undergoes a 1,3-dipolar cycloaddition to the α,β-unsaturated lactone. Such intramolecular 1,3-dipolar cycloaddition reactions were first reported by Padwa in 1980 by heating ω-alkenyltosylhydrazones in the presence of NaH to give 1-pyrazolines.[218] Very recently, Valdés and co-workers reported on a one-pot

[217] R. H. Shapiro, M. F. Lipton, K. J. Kolonko, R. L. Buswell, L. A. Capuano, *Tetrahedron Lett.* **1975**, *16*, 1811.

[218] A. Padwa, H. Ku, *J. Org. Chem.* **1980**, *45*, 3756.

diastereoselective synthesis of bicyclic 1-pyrazolines under basic conditions.[219] It is noteworthy, that the construction of such a tetracyclic ring system with three newly formed stereocenters using tosylhydrazone in a one-pot reaction is to the best of our knowledge unprecedented.

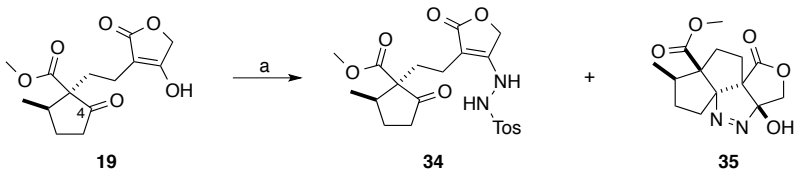

19 **34** **35**

Scheme 17: a) 4-Methylbenzenesulfonhydrazide, EtOH, 50 °C, 2 d, 38% for **34** and 15% for **35**.

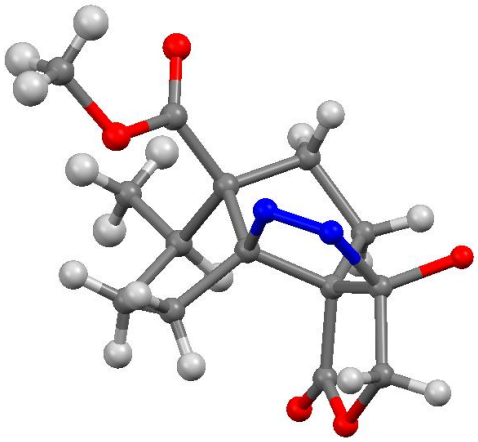

Figure 54: X-ray crystallographic analysis of the tetracyclic side-product **35**. Blue = nitrogen, red = O, grey = C, white = H.

Despite the beauty of this new [5,5,5,5]-tetracyclic compound **35**, it did not serve for the planed synthetic strategy. However, with hydrazone **34** in hand, we decided to examine the planned intramolecular Shapiro reaction. Unfortunately, treatment of **34** with *n*-BuLi at –78 °C did not lead to the desired tricyclic intermediate **33** as only a complex mixture was obtained under these reaction conditions. Due to these results obtained with this strategy, we decided to consider another approach.

[219] R. Barroso, M. Escibano, M.-P. Cabal, C. Valdés, *Eur. J. Org. Chem*. **2014**, DOI: 10.1002/ejoc.201301587.

5.4.3.3 Vinyl bromide Approach

As another alternative, we decided to study ring closure *via* vinyl bromide **36**, which was obtained either by direct bromination of enol **29** using the Vilsmeier-Haack reagent[220] or by treatment of vinyl triflate **32** with TBAB in a toluene/THF mixture as shown in Scheme 18.[212] The desired product **36** was obtained under both reaction conditions in 42% and 51% yield, respectively.

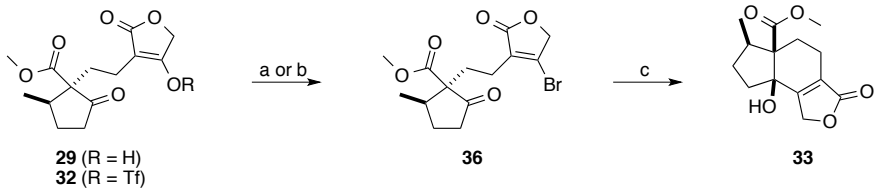

Scheme 18: For **29**: a) DMF, oxalylbromide, CH_2Cl_2, 0 °c to r.t., 5 d, 42%; For **32**: b) TBAB, toluene/THF (1:1), 50 °C to 60 °C, 24 h, 51%; c) *n*-BuLi, THF, –78 °C to r.t., 1 h, 26%.

With **36** in hand, radical cyclization was tested using 2,2′-azo*bis*(2-methylpropionitrile) (AIBN) and tributyltin hydride in benzene at reflux. Surprisingly, no conversion could be observed under different reaction conditions and with careful exclusion of oxygen. Therefore, transmetallation with organo lithium reagent and subsequent cyclization was employed as an alternative. The reaction using *n*-butyllithium in THF at –78 °C gave the desired product **33** along with a multitude of side-products. Due to the insufficient yields for the formation of the vinyl bromide **36** and for the cyclization step, we decided to pursue our synthetic strategy using the NHK coupling reaction as key step.

5.4.4 Formation of the D Ring

In accordance to our A→AC→ABC approach, we continued our efforts with the formation of the D ring moiety. Therefore, we intended to reduce the ester group to the corresponding primary alcohol, which should then be oxidized to the aldehyde **37**. A variety of reduction conditions were tested for this purpose. The use of $LiAlH_4$ proved to be too harsh as several product were detected by crude NMR analysis, whereas reactions with $NaBH_4$ in ethanol at 60 °C and superhydride ($LiEt_3BH$) in THF at 0 °C selectively reduced the lactone part of the molecule while the

[220] A. Vilsmeier, A. Haack, *Ber. Dtsch. Chem. Ges*. **1927**, *60*, 119.

methylester remained untouched. However, reduction with borane dimethyl sulfide led to aldehyde **37** in 76% yield as shown in Scheme 19.[212] Only traces of the corresponding alcohol could be isolated. We assume that the arrangement of the tertiary alcohol and the ester group might lead to a stable complex in the transition state with the borane, thus preventing further reduction to the alcohol. This reaction outcome is an advantage discovered by serendipity.

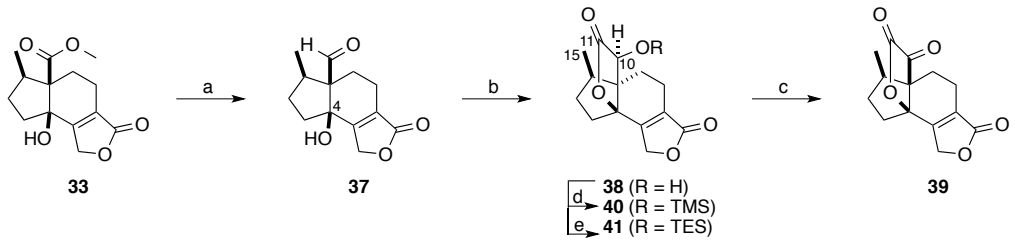

33 37 39

Scheme 19: a) Borane dimethyl sulfide, THF, 0 °C to 45 °C, 2.5 h, 76%; b) KCN, THF/H_2O (1:1), r.t., 2 d, 65%; c) PCC, CH_2Cl_2, r.t., 16 h, 83%; d) 2,6-lutidine, TMSOTf, CH_2Cl_2, 0 °C, 3 h, 99%; e) Et_3N, imidazole, TESCl, CH_2Cl_2, 0 °C to r.t., 14 h, 77%.

For the completion of the second γ-lactone, we planned to install the remaining C-11 carbon by cyanide addition followed by hydrolysis, leading to lactonization. Cyanidation with TMSCN and Et_3N did not give the desired product. As an alternative, potassium cyanide was added to an aqueous THF solution of aldehyde **37**. To our great delight, not the expected cyanohydrin could be isolated after completion of the reaction, but a different crystalline product was obtained. X-ray crystal structure analysis of the resulting product showed that the tetracyclic lactone **38** was formed (Figure 55, left). Astonishingly, the obtained product **38** suited our synthetic pathway and could be achieved in a single step from aldehyde **37** in 65% yield.

To this point, the exact reaction mechanism is speculative, as no precedence can be found in literature for hydrolysis of cyanohydrins under neutral reaction conditions. We believe that the formation of the lactone moiety proceeds *via* nucleophilic attack of the neighboring C-4 hydroxy group to the cyanide to form the corresponding imine. As the reaction is conducted in aqueous organic solvent, hydrolysis of the imine leads the α-hydroxy lactone **38**. Surprisingly, the product was obtained as a single diastereoisomer. The reason for this observation is still unclear and various reasons might be responsible. Diastereoselective nucleophilic attack of the cyanide moiety to the aldehyde would explain the stereochemical outcome, but it is rather implausible due to the complete selectivity. A more reasonable explanation would be,

that both cyanohydrins are formed by addition of potassium cyanide by kinetic control in equilibrium with the aldehyde **37**, and only one of them can further react to the thermodynamic product **38**. Isomerization of the hydroxyl group due to steric effects with the proximate C-15 methyl group is possible, but rather improbable due to the poor acidity at C-10 position.

Lactone **37** was further oxidized to the α-keto lactone **39** with pyridinium chlorochromate in 83% yield to have the appropriate oxidation state at C-10 position, which was confirmed was X-ray crystal structure analysis (Figure 55, right).

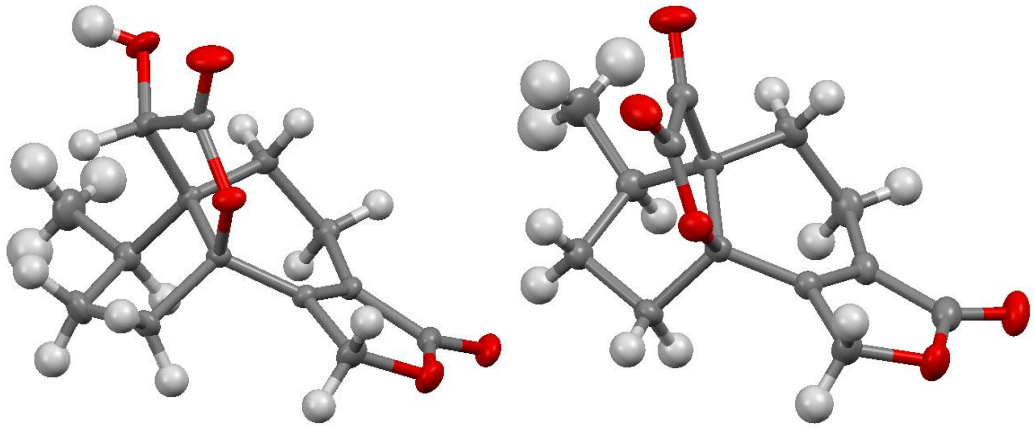

Figure 55: Left: X-ray crystallographic analysis of compounds **38** (left) and **39** (right). Red = O, grey = C, white = H.

With the key intermediates in hand, we addressed the introduction of the remaining C-14 methyl group. Moreover, silyl-protected lactones **40** and **41** were also prepared as further possible substrates, since the presence of the hydroxyl group in **38** could be incompatible for this purpose.

5.4.5 Methylation Efforts

Our initial strategy involved the insertion of the C-14 methyl group *via* 1,4-addition of a methyl cuprate reagent to the α,β-unsaturated lactone. However, all of the reaction condition studied with **33**, **38**, or **40** remained ineffective as shown in Table 4. The addition of TMSCl[221] (entries 2, 4, 5, and 8) and the use of higher order

[221] A. Alexakis, J. Berlan, Y. Besace, *Tetrahedron Lett.* **1986**, *27*, 1047.

cyanocuprates[222] (entries 6 and 10) did not promote conjugate addition of the cuprates.

Table 4: Screening different reaction condition for insertion of the C-14 methyl group.

Entr	Substrate	Methyl source	Copper Source	Additive	Solvent
1	**33**	MeLi, 3.0 eq	CuI, 1.5 eq	-	Et_2O
2	**33**	MeLi, 2.2 eq	CuI, 1.1 eq	TMSCl	CH_2Cl_2
3	**38**	MeLi, 2.4 eq	CuI, 1.2 eq	-	Et_2O
4	**38**	MeLi, 2.4 eq	CuI, 1.2 eq	TMSCl	CH_2Cl_2
5	**38**	MeLi, 5.0 eq	CuI, 2.5 eq	TMSCl	CH_2Cl_2
6	**38**	MeLi, 5.0 eq	CuCN, 5.5 eq	*n*-Bu_3P	Et_2O
7	**38**	MeMgBr, 1.5 eq	CuI, 4.0 eq	-	Et_2O
8	**40**	MeLi, 5.0 eq	CuI, 2.5 eq	TMSCl	CH_2Cl_2
9	**40**	MeLi, 3.0 eq	CuI, 3.0 eq	BF_3	Et_2O
10	**40**	MeLi, 5.0 eq	CuCN, 5.5 eq	*n*-Bu_3P	Et_2O

Sampson and co-workers described a similar scenario and attributed the lack of reactivity to a competitive γ-deprotonation pathway, which affords an aromatic furan oxide rather than the conjugate addition.[223] To overcome this side-reaction, the authors applied an efficient cyclopropanation/reduction protocol for introducing a methyl group at the 4-position of a 3,4-disubstituted 2(*5H*)-furanone *via* a Corey-Chaykovsky reaction followed by a Birch reduction. Identical reaction conditions as described in literature were applied to **33**, **38**, **40** and **41**, however, no conversion could be observed in any case. In addition, epoxidation of the conjugated double bond with large excess of several epoxidating reagents only resulted in recovery of the starting material. Therefore, we concluded that steric interactions protect the β,β-disubstituted lactone to allow for reaction with active reagents.

To prove our hypothesis, a less bulky model system was tested. The commercially available cyclic anhydride **42** was therefore reduced by $NaBH_4$ in THF to give the known butenolide **43**.[224] The electronic properties of **43** should be comparable with our synthetic intermediates, though, lacking the bulky A ring and ester moieties. Various conjugate addition reactions were tested using organocopper reagents. In

[222] B. H. Lipshutz, *Tetrahedron Lett.* **1983**, *24*, 127.
[223] T. E. Janini, P. Sampson, *J. Org. Chem.* **1997**, *62*, 5069.
[224] D. Butina and F. Sondheimer, *Synthesis* **1980**, 543.

contrast to previous results (Table 4, entries 2, 4 and 8), Me_2CuLi in the presence of TMS in CH_2Cl_2 afforded the desired methylated lactone **44** in 41% yield (Scheme 20). Reactions performed in Et_2O as solvent did only result in recovery of unreacted starting material. Yamamoto and co-workers reported that the described reaction conditions are especially powerful for the methylation of sterically congested α,β-enoates.[225] Facing a similar problem, we resolved to apply the described reaction conditions to our system.

We decided reduce the steric bulk of our substrate, which mainly arises from the A ring. Thus, compound **33** was dehydrated under mild reaction conditions to diene **45**, which was then further regioselectively hydrogenated to lactone **46** in 93% yield over both steps. Hydrogenation occurred exclusively from the less hindered face of the molecule, leaving the convex face completely free from bulky residues.

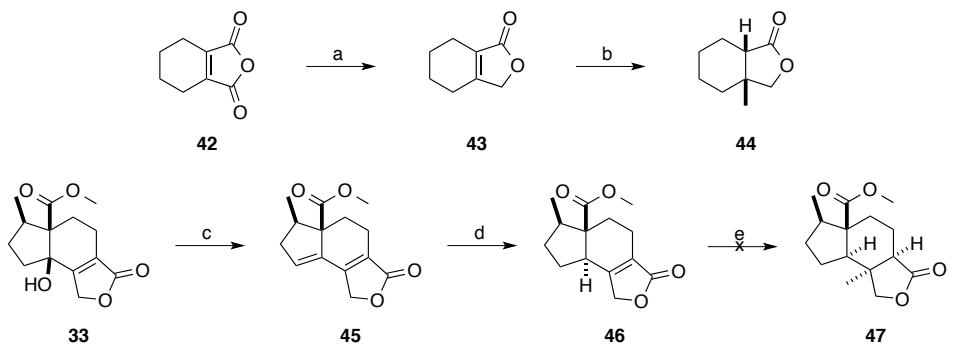

Scheme 20: a) $NaBH_4$, THF, 0 °C to r.t., 4 h, 75%; b) CuI, MeLi, TMSCl, CH_2Cl_2, –78 °C to r.t., 14 h, 41%; c) Burgess reagent, THF, r.t., 3.5 h, 93%; d) Pd/C, H_2 (5 bar), 45 min, r.t., quant.; e) CuI, MeLi, TMSCl, CH_2Cl_2, –78 °C to r.t., 16 h.

X-ray crystal structure analysis of diene **45** showed that the convex face of the molecule is planar due to the conjugated diene moiety and should therefore not sterically influence conjugate addition reactions of organocuprates.

[225] N. Asao, S. Lee, Y. Yamamoto, *Tetrahedron Lett*. **2003**, *44*, 4265.

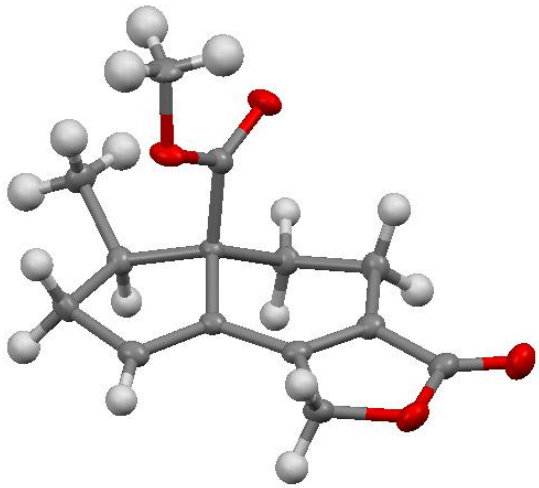

Figure 56: X-ray crystallographic analysis of diene **45**. Red = O, grey = C, white = H.

With **45** in hand, 1,4-addition reaction conditions were tested as shown in Table 5.[216] Various methyl cuprates were prepared *in situ* and added to diene **45** under the described reaction conditions. The results were either complex mixtures (entries 2 and 3) or double alkylation at the C-12 carbonyl position (entries 1, 4, and 5).

Table 5: Screening for methylation of diene **45**.

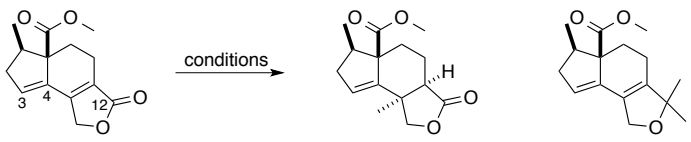

45 **48** **49**

Entry	Conditions	Observation
1	3.0 eq. MeLi, 1.5 eq. CuI, –78 °C to r.t., Et_2O	Only **49** obtained
2	3.0 eq. MeLi, 1.5 eq. CuI, –78 °C to r.t., THF	Complex mixture
3	1.5 eq. MeMgBr, 4.0 eq. CuI, 0 °C to r.t., Et_2O	Complex mixture
4	2.0 eq. $AlMe_3$, 0.2 eq. $Cu(CO_3CF_3)_2$, –30 °C to r.t., toluene	Only **49** obtained
5	2.0 eq. $AlMe_3$, 0.2 eq. $Cu(CO_3CF_3)_2$, –30 °C to r.t., Et_2O	Only **49** obtained

Corey-Chaykovsky cyclopropanation of **45** could serve as an alternative reaction pathway. Even though full conversion was obtained using the same conditions as applied by Janini *et al.*,[223] cyclopropanation only occurred between C-3 and C-4, leaving the tetrasubstituted double bond untouched.

Since diene **45** was not electrophilic enough at C-5 position, we continued our studies with the hydrogenated lactone **46**. Same reaction conditions as described by

Asao *et al*.[225] were applied to **46**. However, no conversion of the starting material was observed and **46** was recovered after the work-up.

In summary, the introduction of the methyl group proved not to be applicable to our substrate scope. As all attempts to introduce it *via* conjugate addition or cyclopropanation and subsequent Birch reduction failed, we considered alternative strategies for the completion of the natural product.

5.4.6 Alternative Cyclization Efforts

5.4.6.1 Paternò-Büchi Cycloaddition

Since conjugate addition and other reactions were ineffective with the α,β-unsaturated lactone, we opted for introducing the remaining methyl group before construction of the B ring. Thus, vinyltriflate **32** was an ideal starting material for this purpose. Fürstner and co-workers demonstrated that inexpensive and readily available iron salts could serve as excellent precatalysts for the cross-coupling of Grignard reagents with alkenyl triflates.[226] Following this protocol, β-methyl lactone **50** was obtained in excellent 96% yield as shown in Scheme 21.[216]

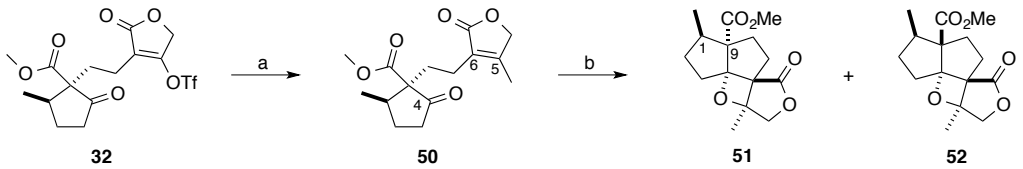

Scheme 21: a) MeMgBr, $Fe(acac)_3$, NMP, THF, –30 °C, 1 h, 96%; b) h*v* (300 nm), benzene, r.t., 3 h, 19% for **51** and 14% for **52**.

With **50** in hand, the formation of the C-4-C-5 bond was studied. The Paternò-Büchi reaction was chosen as a potential pathway for this purpose.[227] Intramolecular Paternò-Büchi photoaddition reactions between α,β-unsaturated carbonyl and ketone moieties have been used for the formation of oxetanes.[228] Therefore, we were optimistic that the desired carbon-carbon bond could be formed by this approach.

---

[226] B. Scheiper, M. Bonnekessel, H. Krause, A. Fürstner, *J. Org. Chem*. **2004**, *69*, 3943.

[227] G. Büchi, C. G. Inman, E. S. Lipinsky, *J. Am. Chem. Soc*. **1954**, *76*, 4327.

[228] J. Iriondo-Alberdi, J. E. Perea-Buceta, M. F. Greaney, *Org. Lett*. **2005**, *7*, 3969.

The reaction was performed under inert conditions with degassed benzene in a Rayonet® UV-reactor and **50** was irradiated for 3 hours at 300 nm wavelength. Two cyclized products were isolated after purification by flash chromatography. The structure of the major product was determined by X-ray crystallographic analysis. Unfortunately, the undesired regioisomer was obtained, after bond formation between C-4 and C-6. Surprisingly, the methyl group at C-1 and the ester group at C-9 position were *trans* configured. We assume that this *cis* to *trans* isomerization occurs *via* an α-cleavage induced by a Norrish type I reaction.[229] Norrish type I and II are known side-reactions in Paternò-Büchi cycloaddition reactions. A possible reaction mechanism is shown in Scheme 22. α-Cleavage in the excited state of **50** leads to the acyl-alkyl diradical species **53**. Due to the formation of this diradical intermediate, radical recombination can lead to the isomerized compound **54**. Paternò-Büchi reaction of both **50** and **54** gives the corresponding oxetanes **52** and **51**, respectively.

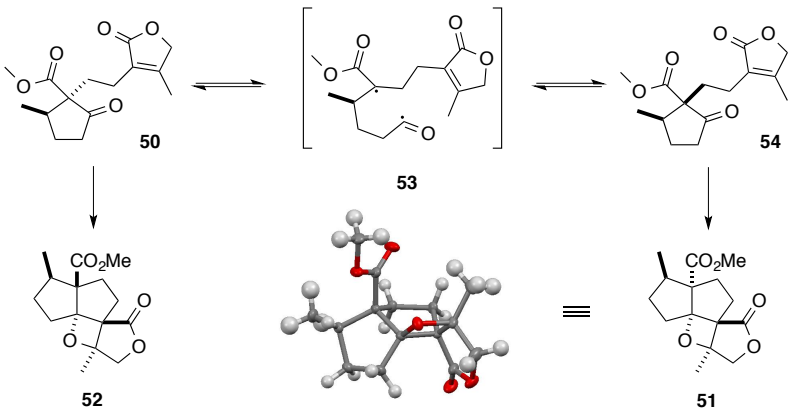

Scheme 22: Isomerization mechanism and Paternò-Büchi reaction.

Although we could not verify the structure of the minor product by X-ray crystallographic analysis, we are confident that oxetane **52** was formed based on intense NMR studies. These results imply that the desired *endo*-oxetane cannot be formed under Paternò-Büchi conditions. Therefore, we continued our efforts towards another cyclization method.

[229] T. Laue, A. Plagens, *Named Organic Reactions*, 2nd Ed., John Wiley & Sons Ltd., West Sussex England, **2005**.

5.4.6.2 Heck Coupling

Alternatively, we examined an intramolecular Heck coupling reaction for the formation of the B ring. Therefore, ketone **50** was modified to the corresponding enol triflate **55** in 34% yield as shown in Scheme 23. The reaction conditions for this transformation were not further optimized.

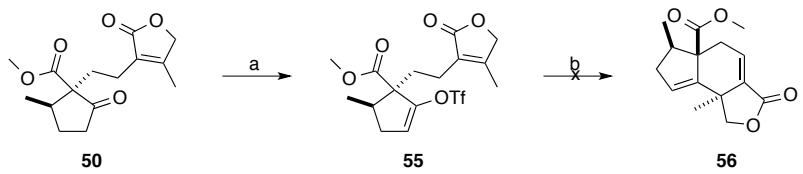

Scheme 23: a) LiHMDS, *N*-phenyl*bis*(trifluoromethanesulfonimide), THF, –20 °C to 0 °C, 3.5 h, 34%; b) $Pd(OAc)_2$, TBAC, $NaHCO_3$, DMF, 50 °C, 3 d.

With triflate **55** in hand, we decided to use Jeffery conditions for the Heck reaction.[230] This protocol is especially advantageous as it accelerates the rate of the reaction to the extent that lower reaction temperatures are possible by using a combination of tetraalkylammonium salts (phase transfer catalysts) and insoluble bases. However, Heck reaction of **55** showed no conversion to the desired alkene **56**. NMR analyses of the major products suggest that the mechanism follows first a 5-*exo*-*trig* instead of a 6-*endo*-*trig* cyclization. This intermediate can then further react *via* a cascade 3-*exo*-*trig* reaction and/or β-hydride elimination. We abandoned this approach due the observed undesired regioselectivity of the Heck coupling with this substrate and turned our attention to another approach.

5.4.6.3 SmI_2 Approach

Ketone-alkene coupling reactions using samarium(II) diiodide have been shown to be incredibly useful in synthetic chemistry. Samarium-induced reduction of ketones gives rise to ketyl radicals, which may be coupled to a variety of alkenic species. Furthermore, excellent diastereoselectivities can be achieved with intramolecular coupling of ketyl radical with α,β-unsaturated esters.[231]

---

[230] T. Jeffery, *Tetrahedron*, **1996**, *52*, 10113.

[231] (a) S. Fukuzawa, M. Iida, A. Nakanishi, T. Fujinami, S. Sakai, *J. Chem. Soc., Chem. Commun.* **1987**, 920; (b) S. Fukuzawa, A. Nakanishi, T. Fujinami, S. Sakai, *J. Chem. Soc., Perkin Trans. 1* **1988**, 1669; (c) E. J. Enholm, A. Trivellas, *Tetrahedron Lett.* **1989**, *30*, 1063; (d) E. J. Enholm, H. Satici, A. Trivellas, *J. Org. Chem.* **1989**, *54*, 5841.

Thus, radical carbon-carbon bond formation between C-4 and C-5 of the pre-methylated lactone **50** was investigated next. According to Baldwin rules, both 5-*exo-trig* and 6-*endo-trig*-type cyclizations are favored in this case.[232] However, in our case a 6-*endo-trig* cyclization is expected to be dominating due to the stability of the resulting conjugated α-carbonyl radical intermediate. Therefore, different reaction condition were applied to ketone **50** using SmI_2 as shown in Table 6. Reaction with the reagent in THF without any further additives led mostly to the formation of an unidentified side-product at 0 °C as well as at reflux (entries 1 and 2). Despite HMPA is known to effectively promote intramolecular coupling of inactivated alkenic ketones,[233] no reaction could be observed with HMPA as shown in entry 3. Also the addition of protic additives such as MeOH and *t*-BuOH did not lead to the formation of the desired product **57** (entries 4, 6 and 7). Some reactions of SmI_2 can be efficiently accelerated by the addition of catalytic amount of NiI_2.[234] However, this did not lead to lactone **57** in our case (entry 5).

Table 6: Different reaction conditions for SmI_2-induced radical cyclization of **50**.

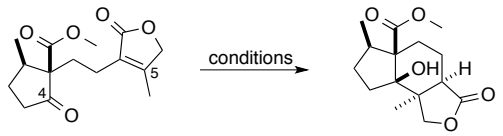

50 **57**

Entry	Conditions	Observation
1	3 eq. SmI_2, THF, 0 °C to r.t., 1 h	Mostly side-product isolated
2	3 eq. SmI_2, THF, 0 °C to 75 °C, 1 h	Mostly side-product isolated
3	3 eq. SmI_2, 4 eq. HMPA, THF, 0 °C to r.t., 2 h	Starting material recovered
4	3 eq. SmI_2, 10 eq. MeOH, THF, 0 °C to r.t., 4 h	Mostly side-product isolated
5	3 eq. SmI_2, 1 eq. NiI_2, THF, 0 °C to r.t., 3 h	Mostly side-product isolated
6	4 eq. SmI_2, 2 eq. MeOH, THF, r.t. to 75 °C, 40 min	Mostly side-product isolated[a]
7	3 eq. SmI_2, 2 eq. *t*-BuOH, THF, –78 °C to r.t., 5 h	Mostly side-product isolated[a]

[a] Also reduced ketone isolated.

Since the intramolecular SmI_2 cyclization did not lead to the expected tricyclic intermediate **57**, other cyclization methods were more promising.

[232] J. E. Baldwin, *J. Chem. Soc., Chem. Commun.* **1976**, 734.

[233] G. A. Molander, J. A. McKie, *J. Org. Chem.* **1992**, *57*, 3132.

[234] F. Machrouhi, B. Hamann, J.-L. Namy, H. B. Kagan, *Synlett* **1996**, 633.

5.4.6.4 Further Cyclization Efforts

As already mentioned in section 5.4.3.2, we envisioned that ring closure might be achieved *via* an intramolecular Shapiro reaction. The required hydrazone was formed at C-4 position of the pre-methylated ketone **50** as shown in Scheme 24. The reaction was performed in ethanol at room temperature and the desired tosylhydrazone **58** was obtained in 50% yield.

With **58** in hand, the Shapiro reaction was performed by addition of *n*-BuLi in hexane at –78 °C. However, no conversion was observed under the describe reaction conditions and starting material was recovered. We assume that the low solubility of the starting material in hexane contributed to this effect. However, further addition of TMEDA did not lead to any observable conversion.

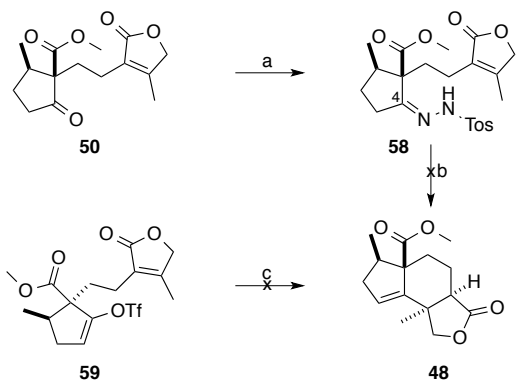

Scheme 24: a) 4-Methylbenzenesulfonhydrazide, 1 M HCl, EtOH, r.t., 25 h, 50%; b) *n*-BuLi, TMEDA, hexane, –78 °C to r.t., 17 h; c) $NiCl_2$ (10 mol%), $CrCl_2$, 3 Å MS, DMF, 100 °C, 4 h.

Inspired by our previous results with the NHK reaction, we wondered if this approach would allow the B ring formation with the methylated precursor **50**. In contrast to the non-methylated substrate **32**, no conversion was observed under the established reaction conditions even at 100 °C.

Attempts to convert ketone **50** into the corresponding vinyl bromide or iodide, which could then be further used for Barbier-type cyclizations remained inefficient. Since all performed reaction with pre-methylated intermediates showed either undesired regioselectivity or no reactivity at all, we decided to pursue a radical change in the approach by modification of the A ring.

5.4.7 Hydroxyl-Directed Cyclopropanation Approach

As an alternative to the Corey-Chaykovsky reaction, a directed cyclopropanation was studied. A variety of stereoselective cyclopropanation reactions have been intensively investigated over the last decades.[235] For our purpose, we were especially interested in hydroxyl-directed variations of this reaction type. Therefore, the configuration of the tertiary hydroxyl group of the tricyclic intermediate **33** needed to be inverted. Diene **45** was epoxidized with *m*-CPBA to give compound **60** in 90% yield as shown in Scheme 25. The stereoselective outcome of the reaction was confirmed by X-ray crystal structure analysis of **60**.

Next, reduction of epoxide **60** to alcohol **61** was attempted. However, reactions with lithium aluminum hydride and L-selectride did not lead to the desired product but resulted in complex mixtures after work-up.

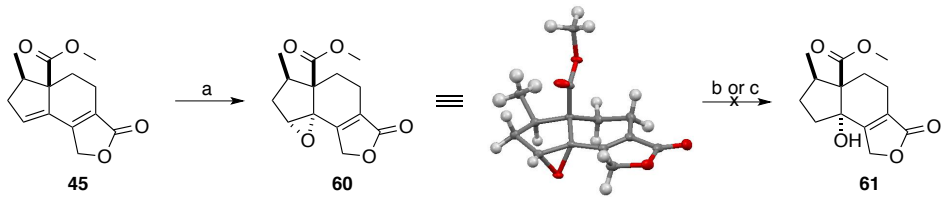

Scheme 25: a) *m*-CPBA, CH_2Cl_2, 0 °C to r.t., 3 d, 90%; b) L-selectride, THF, r.t., 2.5 h; c) lithium aluminium hydride, THF, r.t., 1 h.

Next, we investigated bismuth(III) chloride mediated epoxide opening reactions,[236] but no desired product was observed after completion of the reaction. Since the introduction of the hydroxy group proved to be more problematic than expected, we decided to head for the dihydroxylated lactone **62**.

Dihydroxylation was performed with catalytic OsO_4 and NMO as co-oxidant in a *t*-BuOH/water mixture. The desired diol **62** was obtained in 84% yield in a diastereomeric ratio of 10:1 as shown in Scheme 26. To verify the configuration of the formed diol moiety, **62** was further protected to acetal **63**, which was obtained as a crystalline compound. X-ray crystal structure analysis confirmed our assumption that dihydroxylation occurs from sterically less hindered bottom face.

In order to overcome possible coordinative effects of the secondary hydroxyl group, diol **62** was protected as the corresponding silyl ether and **64** was isolated in

[235] For review on stereoselective cyclopropanation reactions, see: H. Lebel, J.-F. Marcoux, C. Molinaro, A. B. Charette, *Chem. Rev.* **2003**, *103*, 977.

[236] R. M. A. Pinto, J. A. R. Salvador, C. L. Roux, *Tetrahedron* **2007**, *63*, 9221.

68% yield. The allylic alcohol moiety was believed to be the perfect directing group for cyclopropanation reactions on the α,β-unsaturated lactone.

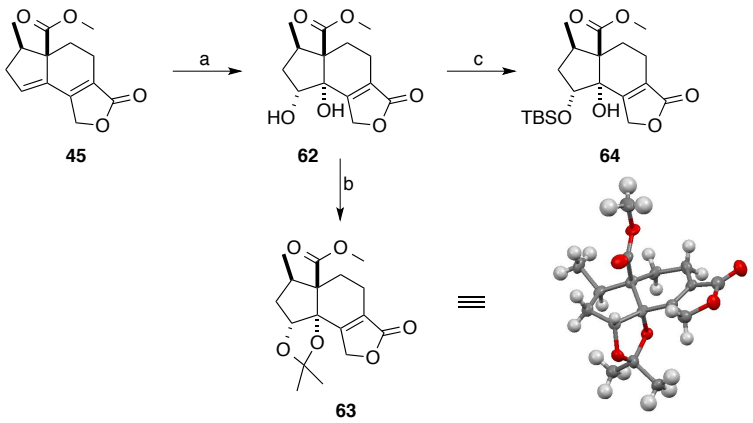

Scheme 26: a) OsO_4 (5 mol%), NMO, *t*-BuOH/H_2O (3:1), 0 °C to r.t., 3 d, 84%, *d.r.* = 10:1; b) 2-methoxypropene, *p*-TSA, THF, r.t., 14 h, 71%; c) TBSOTf, 2,6-lutidine, 0 °C to r.t., 4 h, 68%.

Cyclopropanation of the allylic alcohol **64** was investigated under a variety of reaction conditions as shown in Table 7.[216] Initial results with the Nishimura variation[237] of the Simmons-Smith reaction led to recovery of the stating material or deprotection (entries 1 and 2). Further experiments with more reactive chloroiodomethane[238] and different solvents only yielded in the unprotected diol **62** (entries 3 and 4).

The use of samarium/mercury [239] and chromium [240] in conjugation with diidomethane or chloroiodomethane to initiate cyclopropanation did not form isolatable amounts of product **65** (entries 5-7). Moreover, the treatment of trialkylaluminium with chloroiodomethane[241] in the presence of **64** was investigated. However, the reaction did not afford any cyclopropane **65** (entry 8).

Since none of the reactions described in Table 7 formed any measurable amount of cyclopropanated product **65**, we chose to modify the starting material **64**.

[237] J. Furukawa, R. Kawabata, J. Nishimura, *Tetrahedron Lett*. **1966**, *28*, 3353.
[238] S. E. Denmark, J. P. Edwards, *J. Org. Chem*. **1991**, *56*, 6974.
[239] G. A. Molander, L. S. Harring, *J. Org. Chem*. **1989**, *54*, 3525.
[240] J. M. Concellón, H. Rodríguez-Solla, C. Méjica, E. G. Blanco, *Org. Lett*. **2007**, *9*, 2981.
[241] D. B. Miller, *Tetrahedron Lett.* **1964**, 989.

Table 7: Directed cyclopropanation efforts of **64**.

64 **65**

Entry	Conditions	Observation
1	5 eq. $Zn(CH_2CH_3)_2$, 10 eq. CH_2I_2, CH_2Cl_2, –15 °C to r.t.	No conversion
2	10 eq. $Zn(CH_2CH_3)_2$, 10 eq. CH_2I_2, DCE, –27 °C to r.t.	Deprotection
3	10 eq. $Zn(CH_2CH_3)_2$, 10 eq. CH_2ICl, CH_2Cl_2, –15 °C to r.t.	Deprotection
4	5 eq. $Zn(CH_2CH_3)_2$, 10 eq. CH_2ICl, THF, –15 °C to r.t.	Deprotection
5	4 eq. $CrCl_2$, 4 eq. CH_2ICl, THF, 83 °C	No conversion
6	4 eq. Sm, 0.4 eq. $HgCl_2$, 4 eq. CH_2I_2, THF, –78 °C to r.t.	No conversion
7	4 eq. Sm, 0.4 eq. $HgCl_2$, 4 eq. CH_2ICl, THF, –78 °C to r.t.	No conversion
8	1 eq. $AlMe_3$, 1 eq. CH_2ICl, THF, 0 °C	No conversion

We assumed that the lacking reactivity might either be attributed to steric hindrance of the allylic alcohol moiety or to aromatization of the γ-lactone ring under the reaction conditions.

To address the second scenario, lactone **64** was reduced to the sensitive lactol **66** in quantitative yield as shown in Scheme 27.[216] The product was obtained in a diastereomeric ration of 1:1.6 and subsequently cyclopropanated following the Nishimura protocol.[237] However, the anticipated product **67** could not be isolated and only decomposition of the starting material was observed under the reaction conditions.

Due to the instability of the lactol moiety, **66** was etherificated with methanol to give the stable acetal **68** in 67% yield. Unfortunately, acetal **68** also proved to be unstable under cyclopropanation conditions and a variety of side-products were obtained after completion of the reaction without formation of **69**.

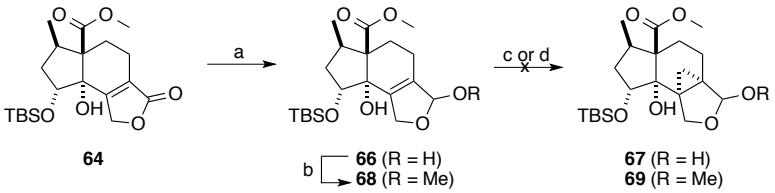

64 b → **66** (R = H), **68** (R = Me) **67** (R = H), **69** (R = Me)

Scheme 27: a) DIBAL-H, CH_2Cl_2, –78 °C to r.t., 3 h, quant., *d.r.* = 1.6:1; b) MeOH, *p*-TSA monohydrate, r.t., 15 h, 67%; c) diethylzinc, CH_2Cl_2, –15 °C to r.t., CH_2ICl, 3 h; d) diethylzinc, CH_2Cl_2, –15 °C to r.t., CH_2I_2, 5 h.

As no evidence for a successful cyclopropanation reaction could be observed, we decided to look for a different strategy for the introduction of the methyl group.

5.4.8 Oxidative A Ring Opening

As described in the previous section, we assumed that the lacking reactivity of the α,β-unsaturated lactone might be derived from steric hindrance of the A ring moiety. Therefore, the σ-bond between C-3 and C-4 of the diol **62** was oxidatively cleaved in the presence of sodium periodate to give ketoaldehyde **70** in quantitative yield after simple work-up as shown in Scheme 28. Aldehyde **70** proved to be somewhat unstable, for which reason it was protected either as the corresponding acetal **71** or 1,3-dithiolane **72**.

While the acetal moiety in **71** was envisioned solely as a protecting group to prevent decomposition of the starting material, dithiolane groups may serve as reactive intermediates for further umpolung reactions[242] in a later re-closure of the A ring. However, the initial goal was the introduction of the required methyl group. Cyclopropanation reactions of α,β-unsaturated ketoester by a Corey-Chaykovsky reaction have been described in literature.[243] Hence, both protected aldehydes **71** and **72** were treated under the same reaction conditions. However, cyclopropanation to product **73** or **74** was not observed after completion of the reaction as both substrates proved not to be stable under the applied reaction conditions.

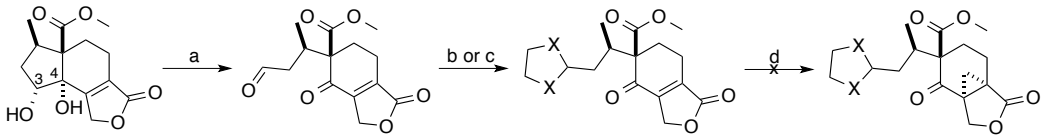

Scheme 28: a) $NaIO_4$, THF/H_2O (2:1), r.t., 1 h, quant.; b) 1,2-ethanedithiol, $BF_3 \cdot Et_2O$, CH_2Cl_2, r.t., 20 min, 54%; c) ethylene glycol, *p*-TSA monohydrate, 3 Å MS, benzene, 90 °C, 6 h, 83%; d) trimethylsulfoxonium iodide, NaH, DMSO, r.t., 3 h.

Since introduction of the methyl group *via* nucleophilic attack of the α,β-unsaturated carbonyl moiety was inefficient, it was decided to alter the strategic perception.

---

[242] D. Seebach, E. J. Corey, *J. Org. Chem*. **1975**, *40*, 1975.

[243] P. H. Lee, B. Lee, J. Lee, S. K. Park, *Tetrahedron Lett*. **1999**, *40*, 3427.

In order to alter the electronic properties at C-5 position, we chose to reduce the carbon-carbon double bond while having a carbonyl group at C-4 position. This would introduce the desired nucleophilic properties for the trapping of methylating agents. Thus, diol **62** was hydrogenated to the corresponding lactone **75** (Scheme 29). Reactions with Pd/C and $Pd(OH)_2$ as catalyst (EtOH, 60 bar H_2, 2.5 h, r.t.) resulted in complex mixtures, whereas the Crabtree catalyst[244] (CH_2Cl_2, 2.5 h, 60 bar H_2) showed no reactivity. Reduction with $NaBH_4/NiCl_2$[245] led to the desired product **75**. However, the reaction did not reach full conversion even with large excess of reagent. Finally, best results were obtained with $Rh/C/Al_2O_3$-catalyst at 60 bar hydrogen pressure in EtOAc. Compound **75** was isolated in quantitative yield after a short filtration of the crude reaction mixture over celite. The desired product **75** was obtained as a single diastereoisomer, which was confirmed by X-ray crystal structure analysis.

Diol **75** was further oxidized to keto aldehyde **76** using sodium periodate in quantitative yield. Slow decomposition of the resulting aldehyde was observed over time. NMR and LC-MS analyses indicated that side-product **77** was formed *via* intramolecular aldol reaction. In order to prevent this side-reaction, aldehyde **76** was protected as the corresponding acetal **78** or 1,3-dithiolane **79**.

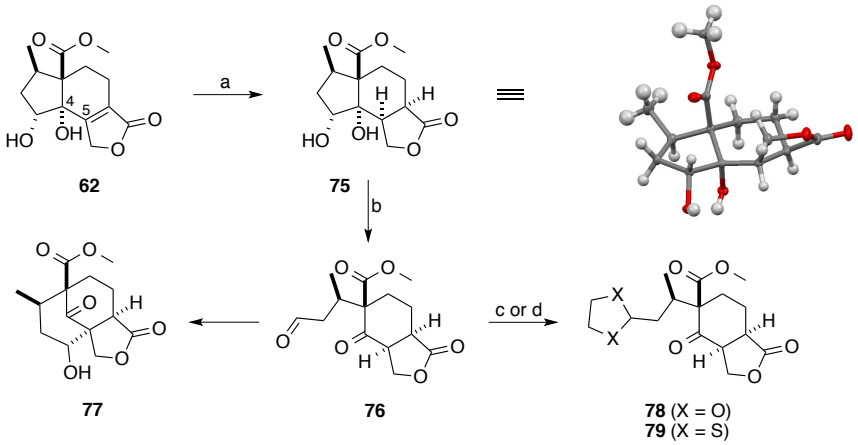

Scheme 29: a) $Rh/C/Al_2O_3$ (10 mol%), H_2 (60 bar), EtOAc, r.t., 3 h, quant.; b) $NaIO_4$, THF/H_2O (2:1), r.t., 1.5 h, quant.; c) 1,2-ethanedithiol, $BF_3 \cdot Et_2O$, CH_2Cl_2, r.t., 1 h, 56%; d) ethylene glycol, *p*-TSA monohydrate, benzene, 90 °C, 2 h, quant.

[244] R. Crabtree, *Acc. Chem. Res*. **1979**, *12*, 331.

[245] N. Abe, F. Fujisaki, K. Sumoto, S. Miyano, *Chem. Pharm. Bull*. **1991**, *39*, 1167.

5.4.9 Successful Methyl Insertion

Having installed ketone functionality at C-4 position, we envisaged inserting the methyl group to the α-position. The formation of the aldol decomposition product **77** implies that the C-5 position possesses the desired nucleophilic properties for this purpose.

Initially, we planed to use iodomethane as the electrophilic partner for this accomplishment. Various bases such as DBU and LDA were tested with **78** and **79** for this purpose. However, basic conditions resulted in opening of the lactone ring upon deprotonation of the α-hydrogen. As a result, complex mixtures were obtained after reaction completion in accordance with literature on similar substrates.[246] Furthermore, amine catalyzed methylation was attempted, however, decomposition of starting material was observed.

Since direct methylation did not yield the desired product due to decomposition under basic and deprotection under acidic conditions, we decided to search for a more reactive electrophilic species.

Inspired by the formation of the intramolecular side-product **77**, α-hydroxymethylation of **78** using formaldehyde was tested next. The results of the extensive screening are summarized in Table 8.[247]

[246] J. López-Pérez, E. del Olmo, B. de Pascual-Teresa, M. Merino, S. Martín, A. San Feliciano, *Tetrahedron* **1995**, *51*, 6343.

[247] A. Heikinheimo, Master Thesis, Aalto, **2012**.

Table 8: Screening of hydroxymethylation conditions for the formation of **80**.

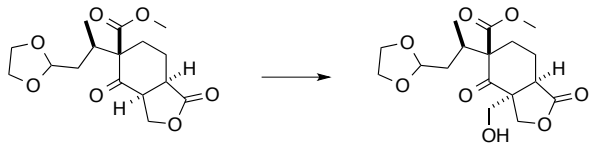

78 **80**

Entry	Reagent	Additive	Solvent	Temperature	Time	Observation
1	Formaline (2 eq.)	$KHCO_3$	THF	r.t.	3 d	Decomposition
2	Formaline (270 eq.)	*p*-TSA	THF	r.t.	2 d	Traces of **77**
3	Formaline (260 eq.)	-	THF	r.t.	2 d	No conversion
4	Formaline (230 eq.)	-	THF	60 °C	4 h	No conversion
5	Formaline (230 eq.)	-	THF	70 °C	3 d	40% **80**, 50% **78**
6	Formaline (130 eq.)	-	THF	70 °C	3 d	Only **78** observed
7[a]	Formaline (150 eq.)	-	THF	100 °C	2 d	Complex mixture
8[a]	Formaline (150 eq.)	-	THF	120 °C	21 h	Complex mixture
9	Formaline (100 eq.)	-	THF	70 °C	3 d	No conversion
10[a]	Paraformaldehyde (20 eq.)	-	THF	70 °C	3 d	No conversion
11	Formaline (84 eq.)	-	THF	70 °C	4 d	Only **78** observed
12[a]	Paraformaldehyde (50 eq.)	-	THF	160 °C	18 h	Complex mixture
13[a]	Paraformaldehyde (170 eq.)	$AlCl_3$	THF	160 °C	18 h	Complex mixture
14	Formaline (220 eq.)	-	THF	70 °C	12 d	Only **78** observed
15	Formaline (230 eq.)	-	THF pH 6	70 °C	3 d	92% **80**
16	Formaline (230 eq.)	-	THF pH 7	70 °C	3 d	Complex mixture
17	Formaline (230 eq.)	-	THF pH 8	70 °C	3 d	Complex mixture
18	Formaline (230 eq.)	-	THF pH 6	40 °C	14 h	94% **80**

[a] Reaction performed in a sealed pressure tube.

The use of a weak base such as $KHCO_3$ resulted in nearly complete decomposition of the starting material, underlining the poor tolerance of **78** towards basic conditions (entry 1). On the other hand, addition of catalytic amount of *p*-TSA led to slow conversion to several products along with side-product **77** (entry 2). Reactions without addition of further reaction partners were performed with formaline as co-solvent. However, no conversion could be detected at room temperature and raising the temperature to 60 °C for four hours (entries 3 and 4). A exceptional discovery was, that reactions performed at 70 °C for three days proved to deliver the desired hydroxymethylated product **80** in 40% yield along with 50% unreacted starting material (entry 5).

A variety of different conditions were tested to further improve the results (entries 6-14). Conditions free of water were investigated by using solid paraformaldehyde in dry THF and high temperatures (entries 10, 12 and 13). However, omission of water led to either to recovery of the starting material or complex mixtures. By careful analysis of the performed reactions, we found out that the pH of the reaction mixture slightly dropped after prolonged reaction time and the longer reactions were carried out, the more side-product **77** was obtained.

In order to avoid the increase of acidity of the reaction mixture, a variety of aqueous buffer solutions were prepared from citric acid and sodium biphosphate. Thus, hydroxymethylation was performed by addition of different buffer solutions. Reactions over three days in buffers of pH 7 and 8 resulted in complex mixtures (entries 16 and 17). Delightfully, at pH 6 and stirring at 70 °C over three days gave the desired product **80** in excellent yield as a single diastereoisomer (entry 15). After further optimization efforts, the reaction was found to proceed in nearly full conversion at 40 °C over night giving the hydroxymethylated product **80** in 94% yield (entry 18). The pH was found to be crucial for this reaction to proceed.

The stereochemical outcome of the reaction was verified by 2D-NMR studies. Hydroxymethylation was expected to be stereospecific due to the formation of the thermodynamically favorable *cis*-fused bicyclic ring system.[248]

For the deoxygenation of **80**, we considered the Barton-McCombie reaction to be suitable for this purpose.[249] This reaction sequence begins with the formation of a

[248] D. A. Lightner, J. E. Gurst, *Organic Conformational Analysis and Stereochemistry from Circular Dichroism Spectroscopy*; Wiley-VCH: New York, **2000**, 173.

[249] D. H. R. Barton, S. W. McCombie, *J. Chem. Soc., Perk. Trans. 1* **1975**, 1574.

xanthate or oxothiocarbonly from the corresponding alcohol. Radical cleavage of the inserted thiocarbonyl moiety by a trialkyl tin radical is subsequently initiated by AIBN to form an alkyl radical, which can then be reduced by a tinhydride reagent.[250] This protocol has been widely used for an impressive range of total syntheses due to its large tolerance towards various functional groups.

In order to test this reaction, thiocarbonyl and xanthate formation were attempted on alcohol **80**. However, neither of them could be formed under any reaction condition studied and only starting material was recovered in each case. The lacking reactivity might be attributed to steric hindrance of the neopentyl alcohol moiety. More reactive thiocarbonyl reagents, such as pentafluoro- or trichlorophenoxy thiocabonyls,[251] were not investigated for this purpose.

An alternative sequence would include halogenation of the alcohol and subsequent radical dehalogenation to form the desired intermediate. Halogenation under standard Appel conditions[252] using CCl_4 in combination with PPh_3 resulted in no conversion and complete recovery of the starting material. Due to the relatively wide scope described for the PPh_3/CCl_3CN reagent couple,[253] this protocol was tested on hydroxymethylated substrate **80**. Indeed, chlorinated product **81** was isolated in 85% yield with only traces of side-products present in the crude material (Scheme 30).

Radical dehalogenation of **81** was initially attempted with *n*-Bu_3SnH and catalytic amounts of AIBN under oxygen-free conditions, however, no conversion was observed. Nonetheless, changing to Ph_3SnH under the same reaction conditions gave **82** in 16% yield. We assume that Ph_3SnH is more suitable for this reaction due to the reduced steric bulk compared to the tributyl derivative. To improve the yield of the dehalogenation step, it was decided to introduce the more reactive iodide instead of the chloride moiety.

Iodination was achieved in 75% yield from the starting substrate **80**. Radical dehalogenation of iodide **83** with *n*-Bu_3SnH gave the methylated product **82** in 84% yield. The reaction gave a second product, which was identified as ring-expanded

[250] For mechanistic studies on Barton-McCombie reactions, see: (a) D. H. R. Barton, D. Crich, A. Löbberding, S. Z. Zard, *Tetrahedron* **1986**, *42*, 2329; (b) D. Crich, *Tetrahedron Lett*. **1988**, *29*, 5805.

[251] D. H. R. Barton, J. C. Jaszberenyi, A. I. Morrell, *Tetrahedron Lett*. **1991**, *32*, 311.

[252] R. Appel, *Angew. Chem. Int. Ed*. **1975**, *14*, 801.

[253] E. D. Matveeva, A. I. Yalovskaya, I. A. Cherepanov, Y. G. Bundel, A. L. Kurts, *Zh. Org. Khim*. **1991**, *27*, 1611.

7,5-bicyclic product **84** (Figure 57). This product is formed *via* a Beckwith-Dowd-type rearrangement after initial primary radical formation.[254] Attempts to suppress this side-reaction by excessive addition of tin hydride reagent were not effective giving the same ration of **82**:**84** due to kinetic reaction control.

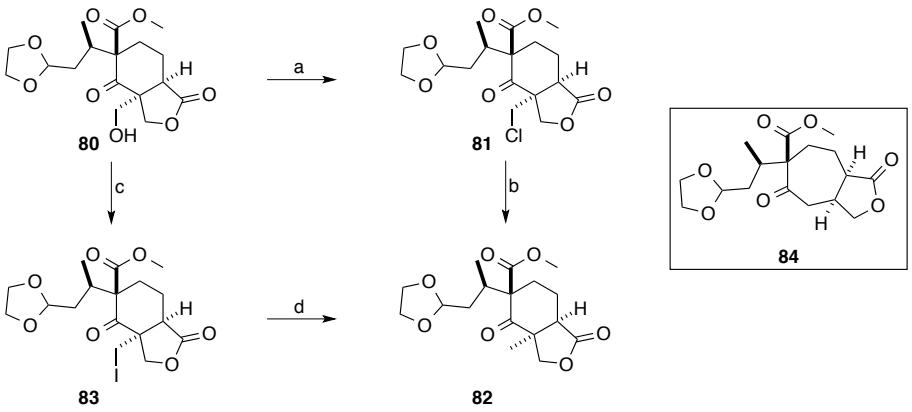

Scheme 30: a) PPh_3, trichloroacetonitrile, MeCN, 85 °C, 16 h, 82%; b) Ph_3SnH, AIBN, benzene, 85 °C, 22 h, 16%; c) PPh_3, imidazole, I_2, benzene, r.t., 12 h, 75%; d) *n*-Bu_3SnH, AIBN, benzene, 85 °C, 3 h, 84% and 16% **84**.

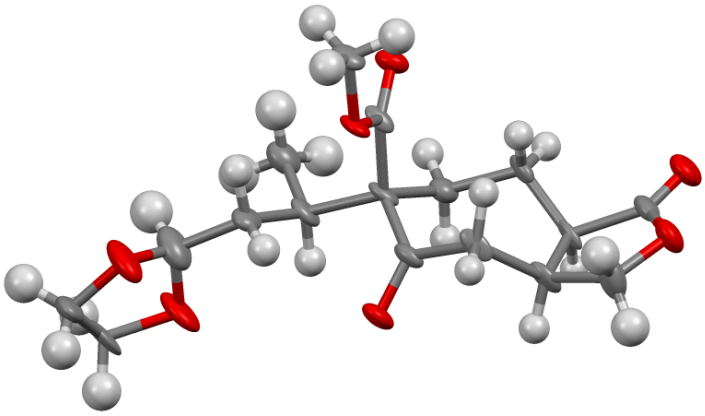

Figure 57: X-ray crystallographic analysis **84**. Red = O, grey = C, white = H.

In summary, the methyl group was successfully introduced in a stereoselective manner after numerous approaches.

[254] (a) A. L. J. Beckwith D. M. O'Shea, S. W. Westwood, *J. Am. Chem. Soc*. **1988**, *110*, 2565; (b) P. Dowd, S.-C. Choi, *J. Am. Chem. Soc.* **1987**, *109*, 3493.

5.4.10 Reclosure of the A Ring

Having introduced the C-14 methyl group, we turned our focus on reclosure of the A ring. First, acetal deprotection was carried out in acidified aqueous acetone and aldehyde **85** was isolated after extraction in quantitative yield without the need for further purification (Scheme 31).

The shortest route to provide the desired tricyclic alkene **48** would be a McMurry coupling of the aldehyde and ketone moieties.[255] This reaction is characterized by coordination of both carbonyl oxygens to low-valent titanium and subsequent C-C bond formation. Reduction of this intermediate gives then the olefinic product. Therefore, titanium chloride is typically combined with a reducing agent such as zinc.

Treatment of aldehyde **85** under McMurry conditions gave a single product. Surprisingly, it was not the expected alkene **48**, but β-keto ester **86**. Further studies on this reaction showed that aldehyde **85** undergoes fast *retro*-Michael addition upon addition of a Lewis acid and is therefore not suitable for McMurry coupling reactions.

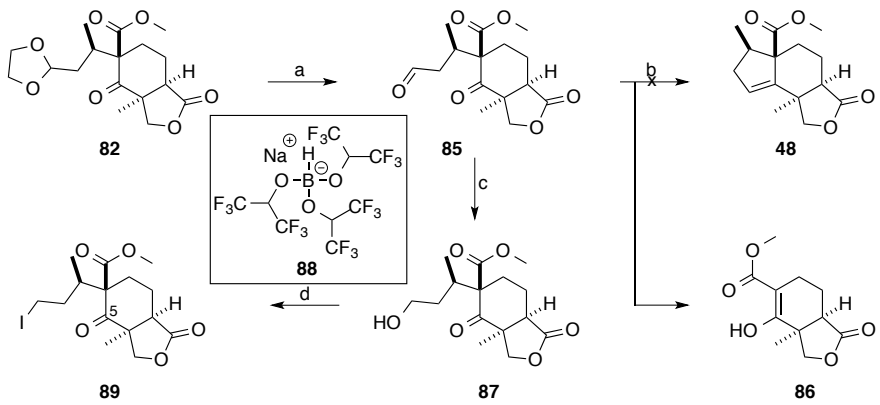

Scheme 31: a) 1 M HCl, acetone, r.t., 14 h, quant.; b) $TiCl_4$, Zn, DME, 90 °C, 3 h; c) **88**, hexafluoro-2-propanol, r.t., 16 h, 85%; d) PPh_3, imidazole, I_2, r.t., 16 h, 95%.

Sodium borohydride reduction of **85** to alcohol **87** at –78 °C in a CH_2Cl_2/ethanol mixture gave not very robust results ranging from 97% to 0% yield. Toshima and co-workers recently described the preparation of a chemoselective reducing agent under especially mild conditions.[256] Sodium *tris*(hexafluoroisoproopoxy)borohydride (**88**), can be easily synthesized from sodium borohydride and hexafluoro-2-propanol and showed smooth reduction of aldehydes in presence of ketones in excellent yields

[255] (a) J. E. McMurry, *Acc. Chem. Res*. **1974**, *7*, 281; (b) J. E. McMurry, *Chem. Rev*. **1989**, *89*, 1513.
[256] Y. Kuroiwa, S. Matsumura, K. Toshima, *Synlett* **2008**, *16*, 2523.

at room temperature. Reduction of **85** following this protocol gave alcohol **87** in 85% yield and with excellent reproducibility. Intermediate **87** was subsequently iodinated to **89** using Appel conditions. Iodinated product **89** was isolated in 95% yield as a crystalline substance. X-ray crystal structure analysis finally proved the desired configuration of the methyl group at C-5 position as shown in Figure 58.

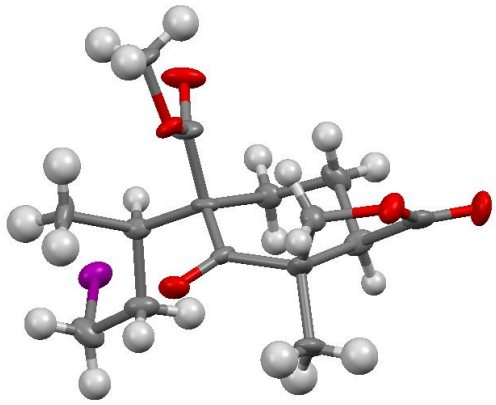

Figure 58: X-ray crystallographic analysis of iodide **89**. Red = O, grey = C, purple = I, white = H.

Having iodide **89** in hand, we turned our attention towards the critical reclosure of the A ring. Different reaction mechanisms are feasible for this transformation. A variety of different reaction conditions are summarized in Table 9. First, we envisaged using a Barbier-type cyclization for this purpose. Therefore, iodide **89** was treated with *t*-BuLi and *n*-BuLi at –78 °C in THF for 20 min before quenching of the reaction (entries 1 and 2). However, mostly complex mixtures were obtained after reaction completion. Addition of an organolithium reagent proved to be extremely reactive, even at –78 °C. Nevertheless, minor amounts of **57** could be isolated in the *t*-BuLi promoted reaction.

An alternative approach by a radical cyclization was examined as this method allows higher chemoselectivity for the ketone moiety as the organolithium approach. A variety of radical initiators have been studied for this purpose. First, we investigated the Et_3B/O_2 induced reaction, as this would provide a mild and tin-free approach.[257] Thus, a 1 M Et_3B solution was added to iodide **88** dissolved in toluene and oxygen was passed through the reaction mixture for one hour at 0 °C (entry 3).

[257] For review on organoboranes as source of radicals, see: C. Ollivier, P. Renaud, *Chem. Rev.* **2001**, *101*, 3415.

Even though some traces of **57** were formed during the reaction, most of the starting material remained unreacted after extended reaction period.

SmI_2-mediated cyclization reactions have been demonstrated to efficiently promote formation of medium-sized rings.[258] Addition of SmI_2 to iodide **89** led to the formation of a complex mixture, while no conversion of the starting was observed with NiI_2 as further additive (entries 4 and 5). Gratifyingly, addition of HMPA provided the compound **57** in remarkable 76% yield (entry 6). The product was isolated as a single diastereoisomers due to the formation of the thermodynamically favorable *cis*-fused bicyclic 6,5 ring system. As a side-reaction of this transformation, radical decomposition of **89** to **86** and monomethyl cyclopropane was observed. Though, a mild and efficient cyclization method for the formation of **57** could be established.

Table 9: Different reaction conditions for the cyclization and reclosure of the A ring.

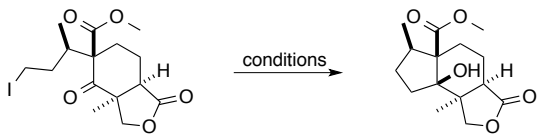

89 **57**

Entry	Conditions	Observation
1	1 eq. *t*-BuLi, THF, –78 °C, 20 min	Minor amount of **57** isolated
2	2 eq. *n*-BuLi, pentane/Et_2O (3:2), –78 °C, 1 h	Complex mixture
3	20 eq. Et_3B, O_2, toluene, 0 °C, 1 h	Traces of **57**, mostly **89** recovered
4	6 eq. SmI_2, THF to r.t., 0 °C 1 h	Complex mixture
5	3 eq. SmI_2, 1 eq. NiI_2, 0 °C, 1h	Recovery of staring material
6	3 eq. SmI_2, 10 eq. HMPA, THF, r.t., 1 h	76% **89** and 9% **86**

As an alternative strategy, we wondered if the *bis*-halogenated product **90** could be used as a feasible intermediate. We assumed that a four-step synthesis from aldehyde **76** would be possible. However, since we still had some remaining chloride **81** in hand, we decided to use it as starting material due to faster access. For that reason, **81** was deprotected under aqueous acidic conditions and the resulting aldehyde was reduced with sodium borohydride to alcohol **91** in excellent 73% yield over both steps (Scheme 32). The iodination step was performed under standard conditions and **90**

[258] (a) P. Girard, J. L. Namy, H. B. Kagan, *J. Am. Chem. Soc.* **1980**, *102*, 2693; (b) G. A. Molander, J. A. McKie, *J. Org. Chem.* **1993**, *58*, 7216.

was isolated in a compromised yield of 12%. In addition, product **90** proved to be unstable and fast decomposition was observed.

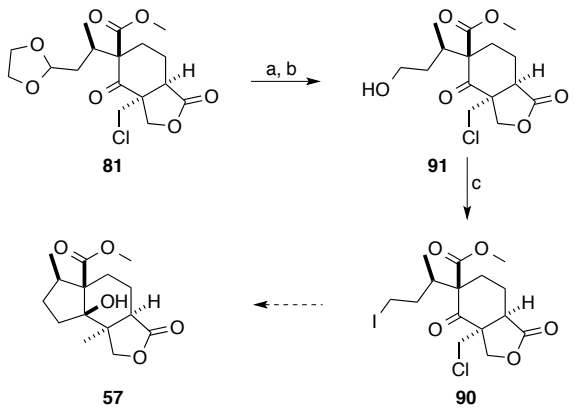

Scheme 32: a) 1 M HCl, acetone, r.t., 14 h; b) $NaBH_4$, EtOH/CH_2Cl_2 (1:4), –78 °C, 2.5 h, 73% over two steps; c) PPh_3, imidazole, I_2, r.t., 2 h, 12%.

Due to the unsatisfactory yield and instability of the *bis*-halogenated product **90**, we focused on the completion of the total synthesis.

5.4.11 Formation of the D Ring – Part II

Tricyclic lactone **57** is structurally similar to the methyl-free intermediate **33**. Therefore, we envisaged that the same reaction sequence could be applied for the formation of the D ring. To prove this assumption, methylester **57** was reduced with borane dimethyl sulfide to give aldehyde **92** in 66% yield after chromatographic separation on silica gel.

To further improve this reaction, crude aldehyde **92** was used for the follow-up cyanide addition and lactone **93** could be isolated in outstanding 63% yield over two steps as a single diastereoisomer (Scheme 33). The (*S*) configuration of the carbinol C-10 position was verified by NOESY experiments. Lactone **93** features the complete carbon-skeleton of jiadifenolide (**18**) with other oxidation states at C-6, C-7 and C-10.

The first oxidation was performed at C-10 using Dess-Martin periodinane and **94** was obtained in quantitative yield.

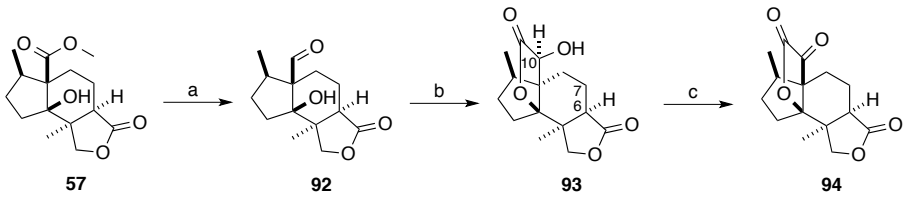

Scheme 33: a) Borane dimethyl sulfide, THF, 0 °C to 45 °C, 2.5 h; b) KCN, THF/H_2O (1:1), r.t., 2 d, 63% over two steps; c) DMP, CH_2Cl_2, r.t., 2 h, quant.

The tetracyclic core-structure of jiadifenolide was achieved in 22 linear steps from the enantiomerically pure natural product D-pulegone. For the investigation of the remaining chemical steps we decided to use model-substrates.

5.4.12 Model Studies for the E Ring Formation

Looking for a model to investigate the remaining steps, we decided to use the previously synthesized tetracyclic intermediate **38**. This product was obtained in ten linear steps as shown in section 5.4.4 and can therefore be produced in larger amounts than the methylated counterpart **93**.

To further improve the structural resemblance of the model system, **38** was hydrogenation to **95** in quantitative yield as shown in Scheme 34. The diastereoselectivity of the reduction was confirmed by X-ray crystal structure analysis as shown in Figure 59. In terms of conformation and electronic properties at C-6 position, **95** and the methylated **93** should have assimilable properties.

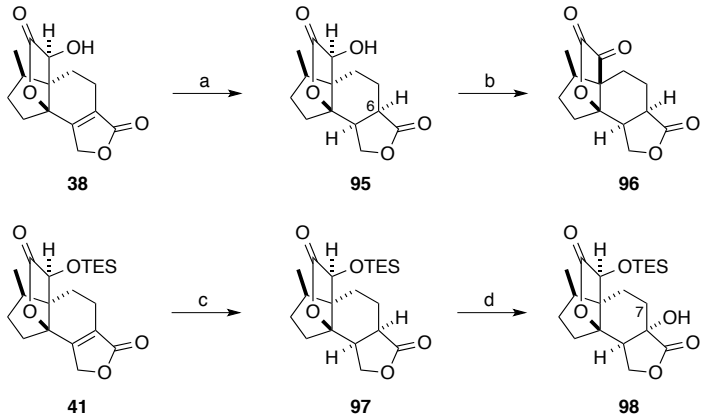

Scheme 34: a) Rh/C (10 mol%), H_2 (60 bar), EtOH, 16 h, r.t., quant.; b) DMP, CH_2Cl_2, r.t., 2 h, quant.; c) $Pd(OH)_2$/C (10 mol%), H_2 (70 bar), 16 h, r.t., quant.; d) LiHMDS, O_2, $P(OPh)_3$, –78 °C, 2 h, 47%.

Two more advanced model compounds were prepared, namely α-keto lactone **96** and silylether **97**. Both compounds were synthesized in quantitative yield from their precursors **38** and **41**, respectively. Diversified model studies allow to access the intricate details of the reaction.

Initial trials with TES-protected lactone **97** showed that the hydroxyl group at C-6 position could be effectively installed. Therefore, **97** was deprotonated with LiHMDS at –78 °C and oxygen was passed through the reaction mixture. Addition of triphenyl phosphite finally reduced the formed peroxide and alcohol **98** was isolated in 47% yield along with some amounts of starting material. The desired oxidation state at C-6 position was therefore successfully introduced. The drawback of this approach is the fact that oxidation of the C-7 position is no longer possible, unless the hydroxyl moiety would eliminate, accumulating additional steps to the synthesis.

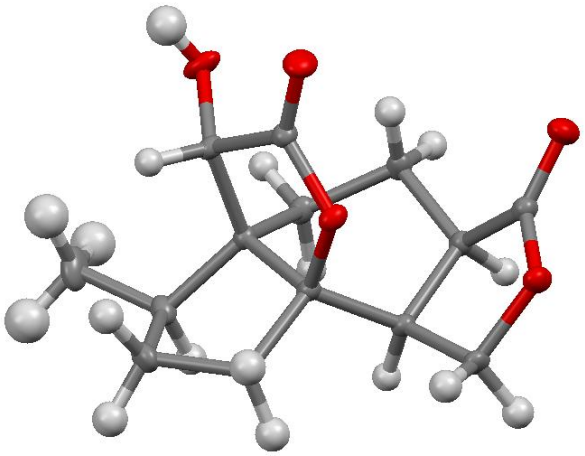

Figure 59: X-ray crystallographic analysis of hydrogenated lactone **95**. Red = O, grey = C, white = H.

Oxidation at C-6 position was investigated with the test substrate **96**. Our initial goal was α-selenation of this position, which could then be oxidized to the corresponding selenoxide and subsequently eliminated after basic work-up to the α,β-unsaturated lactone.[259] This approach has been widely used in various total syntheses including the recently published synthesis of virosaine A by Miyatake-Ondozabal *et al*.[260]

[259] H. J. Reich, S. Wollowitz, *Org. React.* **1993**, *44*, 1.

[260] H. Miyatake-Ondozabal, L. Bannwart, K. Gademann, *Chem. Commun*. **2013**, *49*, 1921.

The reactions studied with α-keto lactone **96** are summarized in Table 10. Reactions performed with diphenyl diselenide or chloroselenobenzene after α-deprotonation of the lactone moiety led to either formation of a complex mixture of recovery of the starting material (entries 1-3). Furthermore, hydroxylation applying the $(PhO)_3P$, O_2 conditions did not yield any desired product (entry 4). As no product could be obtained, we tested the stability of **96** upon deprotonation with LiHMDS and quenching with deuterated methanol as shown in entry 5. Surprisingly, decomposition of the starting material was observed. Therefore, another model system was studied in the following reactions.

Table 10: Different reaction conditions for the oxidation of **96**.

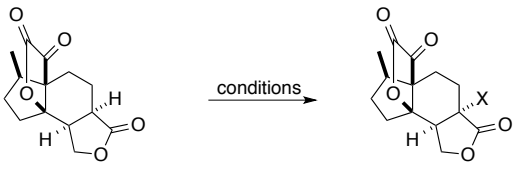

96 X = SePh, OH or D

Entry	Conditions	Observation
1	1.5 eq. LiHMDS, 1.3 eq. $(PhSe)_2$, THF, –78 °C to 0 °C, 2.5 h	Complex mixture
2	1.5 eq. LDA, 1.3 eq. PhSeCl, THF, –78 °C to r.t., 1.5 h	Starting material recovered
3	1.5 eq. LDA, 1.3 eq. $(PhSe)_2$, THF, –78 °C to 0 °C, 2.5 h	Complex mixture
4	1.5 eq. LiHMDS, 1.5 eq. $(PhO)_3P$, O_2, THF, –78 °C to r.t., 16 h	Starting material recovered
5	1.5 eq. LiHMDS, d_4-MeOD, THF, –78 °C to r.t., 14 h	Complex mixture

α-Selenation was tested on the two model structures **95** and **97**. However, both compounds proved to be unstable under the applied reaction conditions and complex mixtures were obtained upon work-up.

As we already had some methylated tetracyclic substrate **93** in hand, we decided to investigate oxidative reactions with this substrate in order to promote the progress of the project.

5.4.13 Formation of the E Ring

α-Selenation of **93** was carried out in THF at –78 °C by addition of LDA and subsequent treatment with phenylselenyl bromide (Scheme 35). ^{1}H NMR analysis of the crude material showed a newly formed product corresponding to the expected selenated intermediate along with some unreacted starting material. The resulting mixture was treated with H_2O_2 in acetic acid for two hours to form the selenoxide derivative, which was eliminated by basic work-up. Even though traces of the expected α,β-unsaturated lactone could be detected in the crude material, another major product was formed during work-up. Intensive NMR analysis and finally X-ray crystal structure analysis of the isolated product showed that the cyclized substrate **99** was formed in 48% yield (Figure 60). The formation of the remaining E ring moiety occurred *via* intramolecular oxa-Michael addition due to the basic work-up conditions applied. From a structural point of view, **99** is very similar to the natural product jiadifenolide (**18**) solely missing both hydroxy groups at the C-6 and C-10 position.

At first, we wanted to introduce the C-6 hydroxy group. Therefore, α-oxidation of lactone **99** was tested using our established LiHMDS, O_2 and $(PhO)_3P$ procedure as described in the previous section. Curiously, deprotonation of the α-proton led to E ring opening, which could be trapped as the corresponding silyl ethers **100** or **101**. These transformations were carried out on a small scale of less than 1 mg, which is why we were not able to determine the exact yield for each step. However, NMR analysis of the crude reaction mixtures showed the obtained compounds as sole products and good yields are expected for larger scale reactions. This exciting structural behavior is extremely interesting, since both forms can be isolated depending on the reaction conditions. Addition of lithium amide bases favor the tetracyclic structure due to the strong Li-O-bond formed, which can be trapped with various oxophilic electrophiles. On the other hand, addition of weaker bases or acids to the E ring-open substrate leads to oxa-Michael addition and reclosure of the E ring. These observations are exceedingly advantageous as they add flexibility to the synthetic strategy.

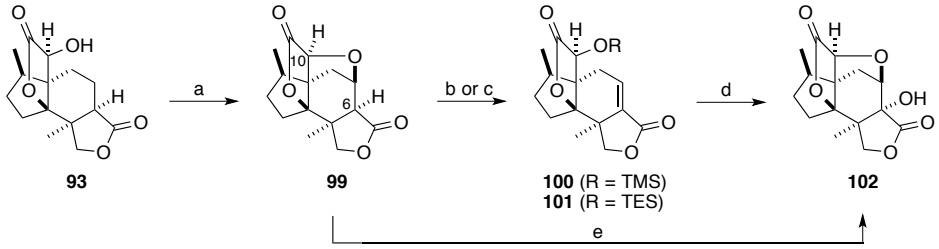

Scheme 35: a) LDA, PhSeBr, H_2O_2, THF, –78 °C to 0 °C, 1.5 h, 48%; b) LiHMDS, TMSCl, –78 °C to 0 °C, 1 h; c) LiHMDS, TESCl, –78 °C to 0 °C, 1 h; d) NaOH, H_2O_2, MeOH/THF (3:1), 0 °C to r.t., 16 h; e) NaOH, H_2O_2, MeOH/THF (3:1), 0 °C to r.t., 14 h.

Due to these observations, we decided to epoxidize the carbon-carbon double bond, which was expected to be diastereoselective due to the strong steric bias. Therefore, the TMS-protected substrate **100** was treated with a methanolic alkaline hydrogen peroxide solution as described by Theodorakis and co-workers for a similar intermediate.[200] The TMS protecting group was cleaved under the applied reaction condition. Nevertheless, the epoxidation of the double bond was successful. Interestingly, the C-10 hydroxyl moiety spontaneously triggered a "5-*exo*-tet" epoxide opening to furnish the E ring and **102** was obtained as the sole reaction product. Reactions with the TES-protected substrate **101** as starting material gave the pentacyclic compound **102** as major product along with smaller amounts of epoxidized protected alcohol. Treatment of the crude material with TBAF solution led to **102** as the sole product. As no unprotected epoxide could be detected after these reactions, we concluded that epoxide opening occurred rapidly after silyl deprotection of the alcohol.

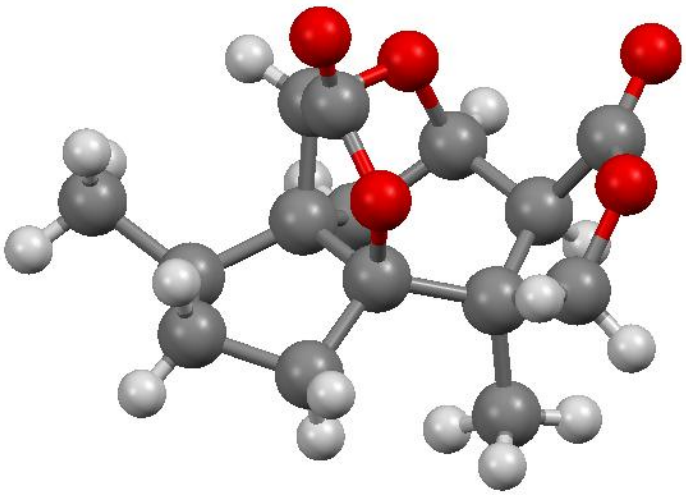

Figure 60: X-ray crystallographic analysis of pentacyclic substrate **99**. Red = O, grey = C, white = H.

Interestingly, epoxidation of the TMS-protected compound **100** led to full conversion of the starting material and no oxa-Michael product **99** could be detected after the reaction. Nevertheless, the protecting group proved to be labile and easily cleavable. Therefore, we assumed that the E ring closure to **102** is reversible in basic methanolic solution. This implies that a one-pot epoxidation of **99** to **102** should be possible.

To test this assumption, little amounts of **99** (< 1 mg) were treated with sodium hydroxide and hydrogen peroxide in methanol for 5 h and ^{1}H NMR analysis of the crude product showed that formation of **102** was achieved. Nevertheless, these preliminary results demonstrate that this strategy allows a simpler access to 10-deoxy-jiadifenolide (**102**) compared to the previous route, as no protecting group manipulation is required.

Due to the resemblance of **102** and the natural product jiadifenolide (**18**), we decided to compare the NMR spectra of both products as shown in Table 11.

Table 11: ^{1}H NMR and ^{13}C NMR datum comparison of jiadifenolide (**18**) with synthetic 10-deoxy-jiadifenolide (**102**).

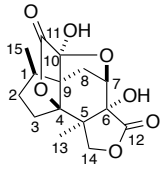

jiadifenolide (**18**)

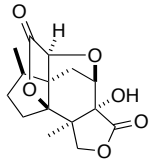

10-deoxy-jiadifenolide (**102**)

Position	δ ^{1}H (**18**) (d_4-MeOD)	δ ^{1}H (**102**) (d_4-MeOD)	δ ^{13}C (**18**) (d_4-MeOD)	δ ^{13}C (**102**) (d_4-MeOD)
1	2.21 (qdd, 12.3, 12.3, 7.1)	2.25 (m)	41.6	38.6
2α	1.27 (dddd, 12.3, 12.3, 12.3, 6.0)	1.19 (m)	33.0	32.5
2β	1.88 (brdddd, 12.3, 12.3, 12.3, 4.1)	1.99 (m)	-	-
3α	2.08 (ddd, 12.9, 12.3, 6.0)	2.08 (m)	35.2	34.3
3β	2.00 (brdd, 12.9, 4.1)	2.06 (m)	-	-
4	-	-	97.5	100.5
5	-	-	48.1	47.6
6	-	-	77.6	78.4
7	4.41 (d, 5.8)	4.39 (d, 5.8)	79.1	81.2
8α	2.09 (d, 12.9)	2.12 (d, 13.0)	32.1	33.0
8β	2.46 (dd, 12.9, 5.8)	2.24 (dd, 13.0, 6.0)	-	-
9	-	-	58.8	60.4
10	-	3.97 (s)	101.9	78.3
11	-	-	173.6	174.6
12	-	-	178.3	177.9
13	1.22 (s, 3H)	1.22 (s, 3H)	19.9	19.3
14α	3.79 (d, 9.3)	3.82 (d, 9.4)	74.6	74.5
14β	4.60 (d, 9.3)	4.63 (d, 9.4)	-	-
15	1.20 (d, 7.1, 3H)	1.07 (d, 7.0, 3H)	14.7	15.3

Both carbon and proton NMR shifts perfectly match except for the C-10 signals. This is due to the lacking hydroxyl group of the synthetic intermediate. In order to obtain the natural product, various approaches were conducted on different substrates as discussed in the following section.

5.4.14 The Missing Last Step

To complete the total synthesis of jiadifenolide (**18**), oxidation at C-10 position is necessary. Inspired by the ring-opening capability of the closely related substrate **99**, we envisaged that **102** would behave similarly under basic conditions and allow epoxide formation between C-6 hydroxyl group and C-7 position. Oxidation of the resulting alcohol moiety at C-10 position would subsequently lead to the formation of jiadifenolide (**18**) upon E ring formation under aqueous conditions. Furthermore, this epoxide was suggested to be an intermediate in the biosynthesis of jiadifenolide from neomajucin as described by Fukuyama and co-workers.[193] Technically, E ring opening can be realized under basic or acidic conditions *via* deprotonation of C-6 hydroxyl group or *via* protonation of the tetrahydrofuran moiety, respectively. Thus, several reaction conditions were tested as shown in Table 12.

We assumed that **102** might be in equilibrium with its corresponding epoxide in solution. If so, oxidation of the latter and subsequent aqueous work-up would lead to **18**. Thus, **102** was treated with Dess-Martin periodinane in sub-milligram scales in CH_2Cl_2 and dioxane at room temperature or at 50 °C, respectively (entries 1 and 2). However, no conversion of the starting material could be observed. Next, Jones oxidation was attempted at room temperature and at 70 °C, however, only starting material could be detected after work-up (entries 3 and 4).

Since acidic reaction conditions did not lead to the desired result, we attempted the application of basic reaction conditions. Therefore, **102** was deprotonated with sodium hydride and subsequently treated with Dess-Martin periodinane (entry 5). However, only **102** could be recovered in this reaction. Given that our first trials did not affect conversion of the starting material, we sought of more practical oxidative procedures. Zhang and co-workers reported on effective oxidation conditions using iodobenzene dichloride as stoichiometric oxidant in the presence of 2,2,6,6-tetramethylpiperidin-1-yloxy (TEMPO) and pyridine.[261] Iodobenzene dichloride was prepared as described by the authors and the reaction was carried out in chloroform at 50 °C for 5 hours (entry 6). Unfortunately, no product could be detected after the reaction and unreacted starting material was recovered. As an alternative, we tested the Mukaiyama protocol[262] using *N*-chlorosuccinimide (NCS) and a catalytic amount

[261] X.-F. Zhao, C. Zhang, *Synthesis* **2007**, 551.

[262] T. Mukaiyama, J.-I. Matsuo, D. Iida, H. Kitagawa, *Chem. Lett*. **2001**, *30*, 846.

of commercially available *N-tert*-butylbenzenesulfenamide, however, no product was formed (entry 7).

As none of the performed reactions led to any detectable formation of jiadifenolide (**18**), **102** was deprotonated using the same conditions as with the 6-deoxy derivative **99** to eventually isolate the E ring opened intermediate (entry 8). However, only starting material was obtained. Furthermore, trapping of the potentially formed alcoholate with TMSCl as applied to **102** was not successful and only traces of TMS-protected C-6 hydroxyl group were detected by NMR analysis (entry 9).

Due to the lacking reactivity of **102** an attempt to oxidize the molecule using the Fenton's reagent was tested.[263] The combination of iron(II) and hydrogen peroxide produces iron(III), hydroxyl anions and hydroxyl radicals. The free radicals generated by this process are highly reactive, non-selective oxidation agents. Thus, Fenton's reagent is used industrially for the destruction of harmful organic compounds. Due to its high reaction potential, Fenton's reagent has been rarely used in organic synthesis. An exceptional example involves the oxidation of barbituric acid to alloxane.[264] Therefore, we hoped that **102** would eventually react under these conditions and lead to the natural product *via* oxidation at C-10 position.

To test the reaction, substrate **102** and iron sulfate were dissolved in an acetonitrile/water mixture at room temperature (entry 10). Hydrogen peroxide was slowly added to the mixture and the solution changed the color from green to orange and gas formation was observed. The crude material was filtered over celite and silica gel after two hours reaction time. Curiously, the subsequent ^{1}H NMR analysis revealed that the starting material did not react under these rather harsh conditions.

Due to the stability of **102**, we decided to search for a different approach.

[263] H. J. H. Fenton, *J. Chem. Soc. Trans*. **1894**, *65*, 899.

[264] H. J. Brömme, W. Mörke, E. Peschke, *J. Pineal. Res*. **2002**, *33*, 239.

Table 12: Different reaction conditions tried for the last step of the total synthesis.

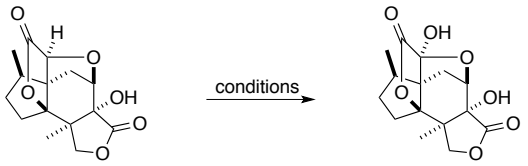

102 **18**

Entry	Conditions	Observation
1	3 eq. DMP, CH_2Cl_2, r.t., 1.5 h	No conversion
2	3 eq. DMP, dioxane, 50 °C, 14 h	No conversion
3	10 eq. Jones reagent, acetone, r.t., 3 h	No conversion
4	10 eq. Jones reagent, acetone, 70 °C, 3 h	No conversion
5	3 eq. NaH, 3 eq. DMP, dioxane, r.t. to reflux, 2 h	No conversion
6	1.5 eq. iodobenzene dichloride, 8 mol% TEMPO, 3 eq. pyridine, $CHCl_3$, 50 °C, 5 h	No conversion
7	10 eq. K_2CO_3, 1.5 eq. NCS, 0.5 eq. *N-tert*-butylbenzenesulfenamide, CH_2Cl_2, r.t., 3 h	No conversion
8	3 eq. LiHMDS, THF, –78 °C to r.t., 2 h	No conversion
9	1 eq. LiHMDS, TMSCl, THF, –78 °C to r.t., 1 h	Mostly **102**[a]
10	$FeSO_4$, H_2O_2, MeCN/H_2O 1:1, r.t., 2 h	No conversion

[a] Traces of TMS-protected C-6 hydroxyl group detected by ^{1}H NMR.

Since 10-deoxy-jiadifenolide (**102)** proved to be unreactive, we investigated earlier oxidations of the C-10 hydroxyl moiety. Thus, **99** was deprotonated and the derived E ring opened intermediate **103** was directly oxidized to α-keto lactone **104** as shown in Scheme 36. The yield could not be determined due to the small reaction scale of less than 1 mg, but **104** was obtained as sole product. Moreover, direct oxidation of **99** with Dess-Martin periodinane to give **104** was investigated, but the starting material did not react and was completely recovered after the reaction. Nevertheless, with **104** in hand, we hoped that epoxidation of the α,β-unsaturated lactone and subsequent aqueous work-up would lead to jiadifenolide (**18**). Epoxidation was performed in methanol by addition of NaOH and H_2O_2 and the mixture was stirred over night at room temperature but only decomposition products were observed in this reaction. We concluded that the electrophilic properties of the ketone dominate over the Michael acceptor capability, which could lead to endoperoxides and Baeyer-Villiger oxidation products.

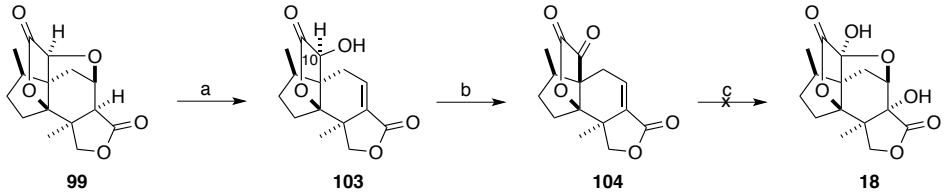

Scheme 36: a) LiHMDS, –78 °C to r.t., 2 h; b) DMP, CH_2Cl_2, r.t., 16 h; c) NaOH, H_2O_2, MeOH/THF (3:1), 0 °C to r.t., 14 h.

These findings suggest that the reaction order is crucial for accomplishment of the natural product. Since the presence of the C-10 ketone is not compatible with the epoxidation conditions, protection of this functional group as the ethylene glycol acetal was examined. Unfortunately, acetal formation was not effective as only traces of the desired product could be observed by ^{1}H NMR analysis even after several days of reaction time at reflux and using ethylene glycol as solvent.

Karimi and co-workers reported on an efficient aerobic oxidation of TBS-silyl ethers to carbonyl compounds catalyzed with *N*-hydroxyphthalimide and Co(II) complexes.[265] TBS protecting groups are in the order of 10^3 more stable than TES in basic media and should therefore be stable during the applied epoxidation conditions. Oxidative deprotection would then finally give jiadifenolide (**18**) upon aqueous work-up. To test this hypothesis, **103** was treated with TBSCl and TBSOTf, but no alcohol protection could be detected. TBS showed to be too sterically hindered for substrate **103**.

As an alternative, we envisaged to invert the C-10 hydroxyl group of **103**. The advantage of this approach is that the targeted inverted alcohol moiety cannot attack at C-7 position upon epoxidation to cyclize and could be oxidized to the corresponding ketone as the final step. Therefore, **99** was mesylated to **105** and subsequently treated with sodium hydroxide to give a single product (Scheme 37). ^{1}H NMR analyses of the obtained product suggest that the desired inverted alcohol **106** was formed. Due to the small scale of the reaction (< 1 mg) it was used for the epoxidation reaction without further purification.

[265] B. Karimi, J. Rajabi, *Org. Lett.* **2004**, *6*, 2841.

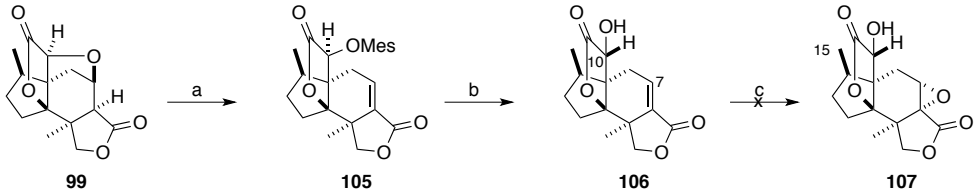

Scheme 37: a) LiHMDS, MesCl, –78 °C to r.t., 2 h; b) 1 M NaOH, H_2O/EtOH (2:1), r.t., 1 h; c) NaOH, H_2O_2, MeOH/THF (3:1), 0 °C to r.t., 14 h.

Treatment of crude **106** with sodium hydroxide and hydrogen peroxide in methanol for 14 hours led to the formation of a major product. ^{1}H NMR analysis of the obtained product in deuterated methanol was in accordance with the desired compound **107** (blue in Figure 61 A). Unfortunately, the obtained product decomposed in the NMR tube over night. Analysis of the proton NMR spectra showed that a major product was formed after one day in the deuterated solvent (green in Figure 61 B). Most surprisingly, formation of a third product was observed and ^{1}H-NMR analysis after two days showed the third product as major compound in solution (red in Figure 61 C). This phenomenon was rather surprising since epoxidation of **106** was performed in methanol for 14 hours without formation of any measurable side-products. So far, the mechanism involved in this transformation it is not entirely clear. Nucleophilic attack of the solvent at the α,β-unsaturated lactone *via* Michael addition could be one explanation, but NOESY experiments of the final product showed strong correlation between C-15 methyl group and C-10 hydroxyl moiety, which suggests that a rearrangement has occurred in this process. Furthermore, Jones oxidation of the crude product instantly after epoxidation did not show any formation of the natural product.

With the analytic data suggesting that desired **107** was formed initially and then decomposed into unknown compounds, further investigations are required to understand the process involved in these observations.

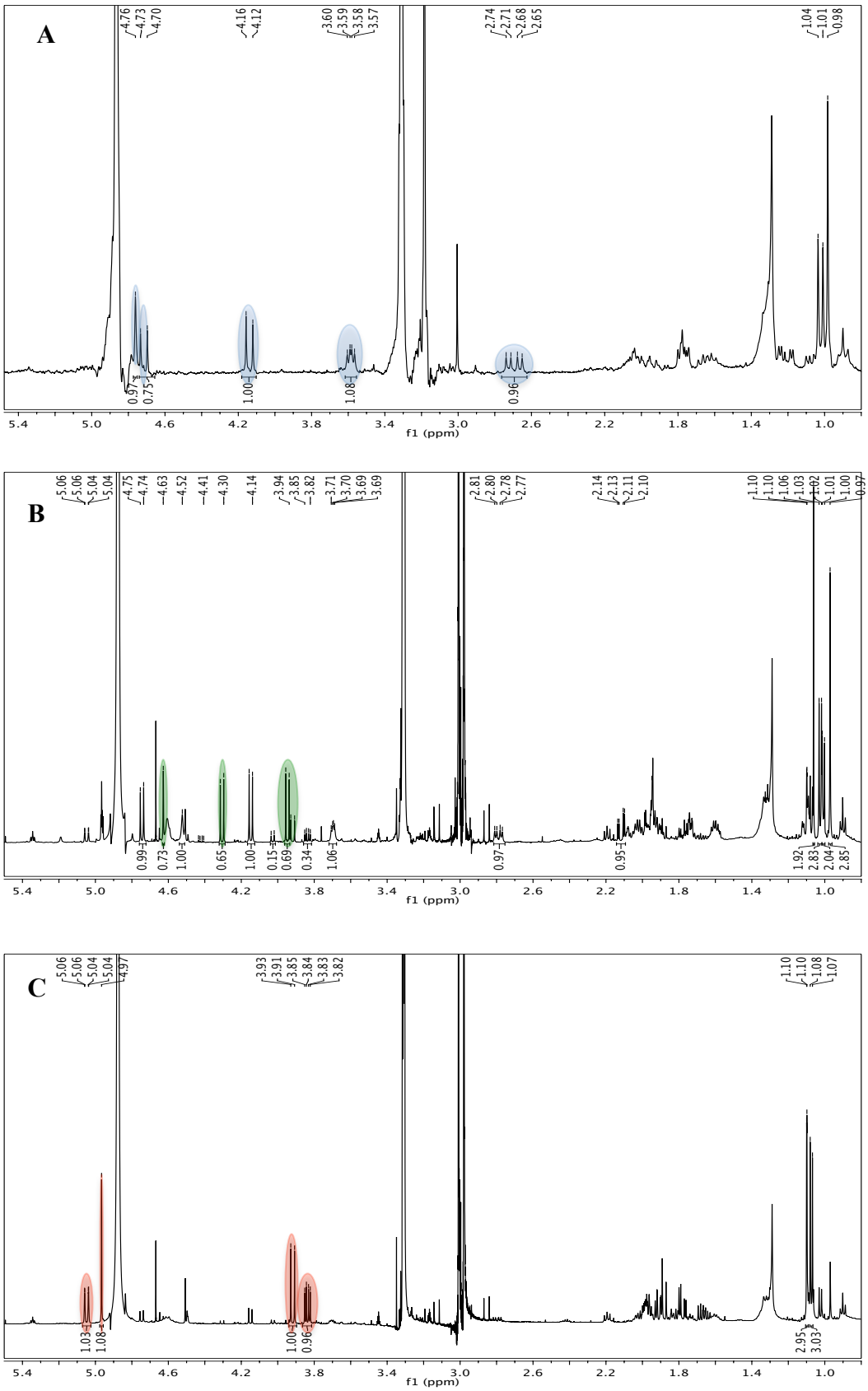

Figure 61: ^{1}H NMR spectra of decomposition of **107** in d_4-MeOD (A) directly after epoxidation, (B) after 1 day, and (C) after 2 days.

As an alternative, we intended to introduce both hydroxyl groups at C-6 and C-7 position prior to D and E ring formation. Thus, lactone **57** was oxidized to the α,β-unsaturated lactone **108** *via* α-selenation and subsequent oxidative elimination in 54% yield (81% *brsm*) as shown in Scheme 38. Next, we envisaged to oxidize **108** to the corresponding epoxide and subsequently transform it to the *trans*-diol under acidic aqueous conditions. However, epoxidation using hydrogen peroxide and sodium hydroxide followed by acidic work-up did not lead to the desired product. Instead, tetracyclic substrate **109** was obtained according to ^{1}H NMR analysis. The formation of **109** can be explained by hydrolysis of the ester moiety to the carboxylic intermediate followed by lactonization, or by lactonization of the formed diol. Product **109** is not a useful intermediate for the total synthesis of jiadifenolide (**18**). Interestingly, **109** is structurally related to the neurotrophically active natural product (2*R*)-hydroxy-norneomajucin (**110**).

In search of a milder epoxidation procedure, **108** was treated with *m*-CPBA. The reaction was initially tested in dichloromethane at room temperature, but no conversion of the starting material was observed. Heating the reaction mixture to 50 °C in chloroform for 19 h proved to be more efficient and full conversion was finally achieved. The desired product **111** could be obtained as a nearly 1:1 mixture of diastereoisomers as shown in Figure 62. We assume that the loss of regioselectivity is due to the coordinating effect of the methyl ester to *m*-CPBA compared to the hydrogen peroxide epoxidation procedure.

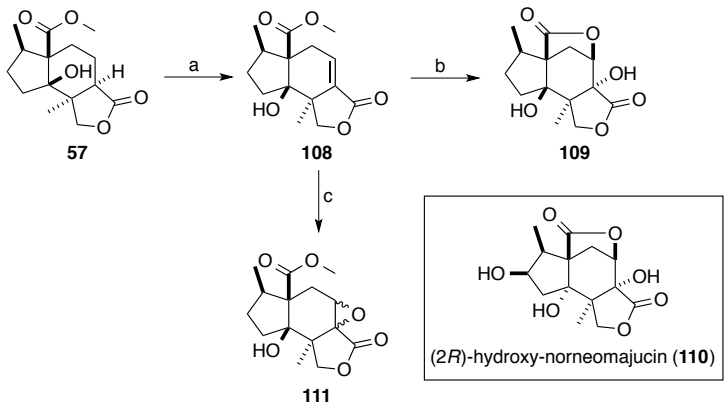

Scheme 38: a) LDA, PhSeBr, H_2O_2, THF, –78 °C to 0 °C, 1.5 h, 54% (81% *brsm*); b) NaOH, H_2O_2, MeOH/THF (3:1), 0 °C to r.t., 14 h; c) *m*-CPBA, $CHCl_3$, 50 °C, 19 h.

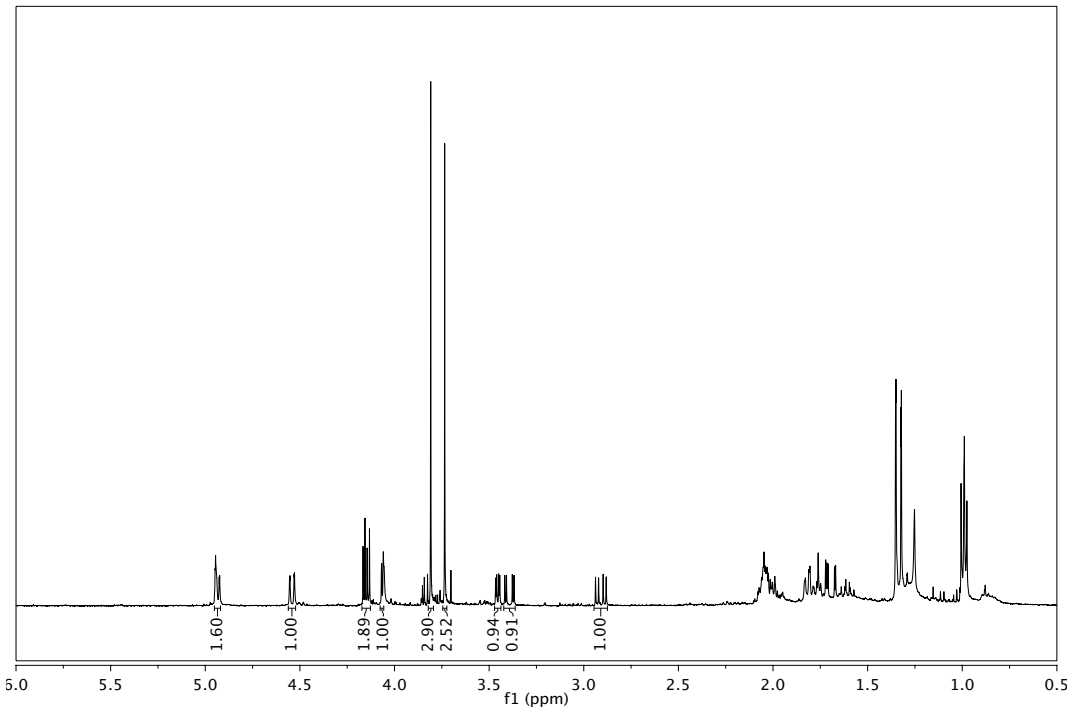

Figure 62: ^{1}H NMR spectra of the epoxidation product **111** in $CDCl_3$.

Unfortunately, we could not pursue this promising approach due to short of further starting material and lack of time. However, we are confident that other non-coordinative epoxidation methods will lead to the desired epoxidized product.

5.5 Conclusion and Outlook

In this chapter the synthetic studies on majucin-type sesquiterpenes from *Illicium* species are described. Due to the exceptional biological activity of various members of this family of natural products, these compounds can be considered as powerful neuritotrophic agents sparking great interest in chemistry, biology and medicine. Jiadifenolide (**18**) was chosen as target molecule due to its highly oxidized and caged structure combined with its exceptional neuritogenic properties.

We started our synthetic efforts from a member of the chiral pool, which overcomes the need for an enantioselective transformation. Starting from D-pulegone (**20**) we could access the tricyclic core intermediate **33** in eight linear steps including a cascade three-component reductive alkylation using Hantzsch' ester and a diastereosective intramolecular Nozaki-Hiyama-Kishi coupling with a ketone in 39%

overall yield. The studies were carried on towards the formation of the D ring moiety, which was astonishingly accomplished in two unprecedented steps *via* reduction of the ester group to the corresponding aldehyde with borane dimethyl sulfide and cyanide addition and hydrolysis under neutral conditions. Several methyl insertion approaches were tested on various substrate and alternative cyclization methods with pre-methylated substrates, such as Paternò-Büchi cycloaddition, Heck coupling or Shapiro reaction, showed either undesired regioselectivity or lacking reactivity. The missing methyl group was finally successfully installed in 12 steps through oxidative A ring opening, hydroxymethylation and ring reclosure *via* SmI_2-promoted intramolecular Barbier-type reaction. D ring formation was accomplished using our established reduction and cyanide addition protocol. Selenation of **93** and subsequent oxidative elimination of the resulting selenoxide gave the pentacyclic product **99**, which was then further oxidized to 10-deoxy-jiadifolide (**102**). Tragically, the final oxidation did not succeed due the inertness of **102** under various reaction conditions up to Fenton conditions.

Further promising preliminary results towards the completion of the total synthesis using different final approaches were established and could lead to the completion of the synthesis. These results should be replicated in larger scales as they were only tested on sub-milligram scales so far. As an alternative, aldehyde **92** could be vinylated to **112** and thereafter oxidized to **113** *via* selenation and subsequent oxidative elimination as shown in Scheme 39. Epoxidation to **114** and subsequent oxidative cleavage of the terminal double bond using sodium periodate combined with $RuCl_3$[266] has the potential to give the natural product **18** with **115** as reactive intermediate. Furthermore, other natural products, such as majucin, could be prepared from intermediate **57**. This would be especially interesting, as most of these natural products have not been synthesized to date.

[266] For review on Ru-catalyzed reactions, see: T. Naota, H. Takaya, S.-I. Murahashi, *Chem. Rev.* **1998**, *98*, 2599.

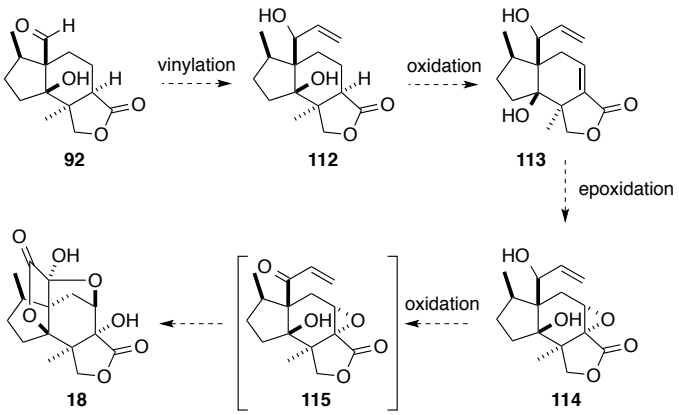

Scheme 39: Proposed total synthesis of jiadifenolide (**18**).

In summary, we accomplished the synthesis of 10-deoxy-jiadifolide (**102**) in 25 linear steps from the chiral pool molecule D-pulegone (**20**) with an overall yield of 3.7% for the first 24 steps. These results prompt further investigation of new neuroactive derivatives and the completion of the natural product.

6 CONCLUSION

This thesis entitled "*Synthesis of Majucin-Type Sesquiterpenes and Immobilization and Visualization of Quorum Sensing Signaling Molecules*" showcases the utility of modern synthetic chemistry in addressing fundamental human needs. The main focus of this work is the combination of synthetic chemistry with biological applications to investigate and improve healthcare-associated problems. Natural products served as inspiration for the design of new tools in the search for new therapeutics due to their evolutionary wisdom richness.

The first chapter described the synthesis and evaluation of dopamine-based natural product hybrids with dual properties. A nitro-dopamine anchor served for the surface functionalization, whereas an acylated homoserine lactone was used as the bioactive signaling moiety. These synthetic hybrids were immobilized by a simple dip-and-rinse procedure on titanium dioxide, a biocompatible metal frequently used in the field of medical devices, and the functionalized beads were shown to modulate quorum sensing in bacterial reporter strains. Quorum sensing is an important communication pathway used by bacteria to determine the density of their population and is responsible for various pathogenic properties, such as biofilm maturation or virulence. The length of the linker was shown to be crucial for bacterial recognition and a C_{12}-chain length was determined as ideal for the recognition of the CepR receptor, the quorum sensing receptor used by *Burkholderia cenocepacia*. The mode of action was determined to be *via* slow release of the bioactive hybrid compounds. This method is a highly attractive approach for the preparation of coated surfaces in medical devices capable to interrupt the quorum sensing signaling pathway.

The application of quorum sensing modulating hybrids was expanded in the second chapter of this thesis. Knowledge of the temporal and spatial production of quorum sensing signaling molecules within biofilms or within the infection host is scarce, but current techniques lack the possibility to visualize acylated homoserine lactone-mediated communication at the single cell level. To overcome this deficit, fluorescent labeling agents for quorum sensing (FLAQS) were developed by combining the determined recognition pattern for quorum sensing receptors with

rhodamine dyes. This concept was successfully applied to the selective labeling of the CepR in live cells. Further improvement of the FLAQS allowed the labeling of *B. cenocepacia* H111, a pathogenic wild-type strain isolated from a cystic fibrosis patient, with remarkable quality and the results suggest that CepR is a soluble cytoplasmic protein. The selectivity was also successfully applied to the specific labeling of mixed bacterial cultures. Second generation FLAQS bearing 3-oxo functionality in the acyl side chain proved to be recognized by CepR and LasR. The later is one of the quorum sensing receptors used by *Pseudomonas aeruginosa*. Even though the same level of labeling as with CepR could not be achieved, extremely promising results were obtained with the wild-type *P. aeruginosa* PAO1. In addition, the FLAQS library was expanded by introducing a green labeling agent. FLAQS could be used for the fast analysis of quorum sensing in various environmental and clinical samples and enable investigation and visualization of bacteria-host communication pathways.

The last chapter was dedicated to the synthesis of majucin-type sesquiterpenes from *Illicium* species. Due to the exceptional biological activity of various members of this family of natural products, these compounds can be considered as powerful neuritotrophic agents sparking great interest in chemistry, biology and medicine. Jiadifenolide was chosen as target molecule due to its highly oxidized and caged structure combined with its exceptional neuritogenic properties. The synthesis of 10-deoxy-jiadifenolide was accomplished in 25 steps with an overall yield of 3.7% for the first 24 steps. The reaction sequence was initiated from D-pulegone and the key features include a cascade three-component reductive alkylation, a diastereoselective intramolecular Nozaki-Hiyama-Kishi coupling with a ketone, and an unprecedented cyanide addition to an aldehyde with subsequent lactonization under neutral conditions. Even though 10-deoxy-jiadifenolide could not be further transformed to the natural product, a variety of structurally related products were accomplished. These derivatives can be used to study the mode of action and the structure-activity relationship for this class of natural products.

7 EXPERIMENTAL PART

7.1 General Methods and Materials

Unless otherwise stated, chemicals were purchased from Sigma-Aldrich, Acros, Alfa Aesar, or Fluka and used without further purification. Solvents for work-up and chromatography were distilled from technical quality. Solvents used for chemical transformations were either *puriss.* quality or dried by filtration through activated aluminium oxide under argon or nitrogen (H_2O content < 30 ppm, *Karl-Fisher* titration). All non-aqueous reactions were run in oven-dried or flame dried glassware under a positive pressure of argon or nitrogen. Concentration under reduced pressure was performed by rotary evaporation at 40 °C (unless otherwise specified). Yields refer to purity, dried and spectroscopically pure compound.

Analytical thin layer chromatography (TLC) was performed on Merck silica gel 60 F_{254} plates (0.25 mm thickness) precoated with fluorescent indicator. The developed plates were examined under UV light (254 nm or 366 nm) and stained with ceric ammonium molybdate or aqueous $KMnO_4/Na_2CO_3$ solution followed by heating.

Flash chromatography was performed using silica gel 60 (230-240 mesh) from Fluka using a forced flow eluent at 0.3-0.5 bar pressure.

All ^1H and ^{13}C NMR spectra were recorded using either Varian Gemini 300 MHz (^1H) or 75 MHz (^{13}C), Varian Mercury 300 MHz (^1H) or 75 MHz (^{13}C), Bruker DRX 500 MHz (^1H) or 125 MHz (^{13}C), Bruker DRX 400 MHz (^1H) or 100 MHz (^{13}C), Bruker DRX 600 MHz (^1H) or 150 MHz (^{13}C), Bruker Advance 800 MHz (^1H) or 200 MHz (^{13}C) FT spectrometers at room temperature. Chemical shifts δ are reported in ppm, multiplicity is reported as follows: s = singlet, d = doublet, t = triplet, q = quartet, quint. = quintet, sext. = sextet, sept. = septet, m = multiplet or unresolved and coupling constant *J* in Hz. Spectra were calibrated related to solvent's residual proton chemical shift ($CHCl_3$, δ = 7.26; d_4-MeOD, δ = 4.78, 3.31; d_6-DMSO, δ = 2.50) and solvent's residual carbon chemical shift ($CDCl_3$, δ = 77.16; d_4-MeOD, δ = 49.00; d_6-DMSO, δ = 39.52),

Analytical high-performance liquid chromatography (HPLC) was performed on a *Dionex Chromatography System* (Interface Chromeleon, ASI-100 automated sample injector, UV detector 170U or PDA-100 photodiode array detector, pump P680, TCC

thermostated column compartment, degaser, MSQ-ESI mass spectrometric detector). The *flow rate* was 1 mL / min. *Column*: Phenomenex Gemini (5 µm) (C18 (150 x 4.6 mm)), solvent A: H_2O, solvent B: MeOH).

Photoluminescence measurements were performed with a *Shimadzu RF-5301PC fluorometer*.

IR spectra were recorded using a *Varian 2000 FT-IR ATR Spectrometer* or *Varian 800 FT-IR ATR Spectrometer*. The absorption is reported in cm^{-1}.

Optical rotation $[\alpha]_D$ were measured at the sodium D line using a 1 mL cell with a 1 dm path length on a *Jasco P-2000* digital polarimeter and the concentration *c* is given in g/100 mL and the used solvent is $CHCl_3$ or MeOH.

Elementary analysis were performed by Mikroanalyse Labor of the Laboratorium für Organische Chemie at the University of Basel.

Melting points (M.p.) were determined using a *Büchi B-545* apparatus in open capillaries and are uncorrected. Photoluminescence measurements were performed with a Shimadzu RF-5301PC fluorometer.

Mass spectra (HRMS ESI) were recorded by the Mass spectrometric Service of the University of Bern on a *Sciex QSTAR Pulsar mass spectrometer* or by H. Nadig at the University of Basel on a *Bruker maXis 4G* using electrospray ionization in both cases.

X-ray analyses: Data collections for both crystal structures were performed at low temperature (123 K) using Mo-K_a radiation on a *Bruker KappaAPEX diffractometer*. Integration of the frames and data reduction was carried out using APEX2.[267] The structures were solved by direct methods using SIR92.[268] All non-hydrogen atoms were refined using anisotropically by full-matrix least squares on *F* using CRYSTALS.[269] Hydrogen atoms were placed in calculated positions by means of the "riding" model.

Preparative HPLC purification was performed on an *Ultimate 3000 RS Variable Wavelength Detector* using a Gemini C18, 10µm (250 mm x 2.12 mm) column at a flow rate of 20 mL/min and a gradient of 2.5-100% water/ACN in 1 h.

Reaction indicated with [154], [212], [216] and [247] were performed and characterized by [154]

[267] Bruker Analytical X-ray Systems, Inc., **2006**. *Apex2*, Version 2 User Manual, M86-E01078, Madison, WI.

[268] A. Altomare, G. Cascarano, C. Giacovazzo, A. Guagliardi, M. C. Burla, G. Polidori, M. Camalli, *J. Appl. Cryst.* **1994**, *27*, 435.

[269] P. W. Betteridge, J. R. Carruthers, R. I. Cooper, K. Prout, D. J. Watkin, *J. Appl. Cryst.* **2003**, *36*, 1487.

Natalie Huber, [212] Elias Kaufmann, [216] Christophe Daeppen, or [247] Annakaisa Heikinheimo.

Compounds not mentioned in the theoretical part, but in the experimental part are labeled as **EPX** starting with X = 1 and are shown in order of affiliation.

7.2 Catechol-Based Immobilization of QS Modulators

7.2.1 Material Preparation

All glassware used for surface modification was cleaned in "piranha solution" (H_2SO_4/H_2O_2 = 7:3; Fluka/Sigma-Aldrich) and extensively rinsed with ultrapure water (sterile filtered, Sigma).

Preparation of MOPS buffer: 2.09 g *N*-morpholinopropanesulphonic acid (≥ 99.5 %, Sigma), 3.52 g sodium chloride (≥ 99.5 %, Sigma-Aldrich), and 10.46 g potassium sulfate (≥ 99.0 %, Sigma-Aldrich) were dissolved in 100 mL ultrapure water (sterile filtered, Sigma).

The TiO_2 particles were cleaned using toluene (HPLC quality), 2 x 10 min ultrasonication and 2-propanol (HPLC quality), 2 x 7 min ultrasonication, dried under a nitrogen stream and finally put overnight in an oven at 120 °C.

7.2.2 Functionalization of TiO_2 beads

General procedure for functionalization of TiO_2 particles: 50 mg cleaned particles (99.6 %, ~325 mesh powder, Alfa Aesar) were placed into glass vials with 3 mL of buffer and 1.5 mg of the natural product hybrids. After 4 h incubation at 50 °C, the resulting particles were centrifuged for 5.5 min at 4'500 rpm, and the aqueous layer was decanted. The resulting particles were washed with water and dried with a stream of nitrogen. Further washing with methanol and water was carried out the same way (particles suspended in H_2O or MeOH for 5-20 min, and centrifugation 10-30 min at 4'500 rpm).

7.2.3 Sensor Strains

***Pseudomonas putida* Iso F117** (*putI*-knockout) **pAS-C8**; highly sensitive towards OHL (*N*-octanoyl-L-homoserine lactone), less sensitive for DHL (*N*-decanoyl-L-homoserine lactone), almost no sensitivity for BHL (*N*-butyryl-L-homoserine lactone). The quorum-sensing regulated promoter p_{cepI} is from *Burkholderia cenocepacia*, and controls expression of green-fluorescent protein (GFP). Plasmid-encoded resistance to gentamycin.

Pseudomonas putida **Iso F117** (*putI*-knockout) **pKR-C12**; highly sensitive towards Od-DHL (*N*-(3-oxo-decanoyl)-L-homoserine lactone), almost no sensitivity for shorter AHLs. The quorum-sensing regulated promoter p_{lasB} is from *Pseudomonas aeruginosa*, and controls expression of GFP. Plasmid-encoded resistance to gentamycin.

Culture conditions: The sensor strains were initially cultivated on LB-agar plates with gentamycin (20ug/mL). Single colonies were suspended in 5 mL LB (Luria-Bertani broth) for overnight cultivation (with gentamycin). These stationary phase starter cultures were diluted 1:100 into fresh LB and grown to mid logarithmic phase (OD600nm = 0.8) at 30°C with shaking (Infors HT incubator, Bottmingen, Switzerland). At this point, cultures were used for inoculation with test compounds.

7.2.4 Assessment of Biological Activity

The TiO_2-conjugated AHLs were suspended as a 10% slurry (w/v) in 1:1 DMSO/H_2O. Initial sensor activation experiments were conducted with a final concentration range of 0.05% - 0.25% conjugated beads added to mid-log phase sensor cultures (a total of 200 mL culture volume). After these initial tests, a final conjugated beads concentration of 0.1% was used throughout for further activation assays and for microscopy.

Culture/beads suspensions were incubated in black lidded 96-well microtiter plates (Nunc, Denmark), in the dark at 30°C for two hours, and induction of GFP fluorescence was assessed by spectrofluorimetry, with excitation and emission wavelengths at 485nm at 520nm, respectively (Microplate reader, BioTek Instruments, VT, USA) or by fluorescence microscopy (DM6000B, Leica, Germany).

Positive control: OHL (10 nM – 1 mM, diluted from 10mM stock solutions in ethyl acetate) was incubated with the sensor cultures in the same way.

Negative control: Sensor cultures with corresponding aliquots of 1:1 DMSO/H_2O or ethyl acetate.

7.2.5 Dialysis Experiments

Dialysis experiments were conducted to assess the chemical stability of the conjugated TiO_2-beads in the presence and absence of *P. putida* pAS-C8 sensor cells.

Briefly, 1% suspensions of conjugated beads were prepared in either 1 mL PBS pH 6.5, or phosphate-buffered LB medium containing 10^5 - 10^6 CFU/mL sensor cells and placed inside 1 mL-capacity dialysis tubes (SpectraPor „Float-a-lyzer“, 1 mL, 3.5-5 kDa MWCO). The dialysis tubes were tightly capped and were then allowed to float freely inside culture flasks containing 30 mL sterile LB supplemented with 20mg/mL gentamycin. As a positive control, 10mM OHL in 1 mL PBS pH 6.5 was dialyzed under the same conditions.

The culture flasks were placed in a slow-shaking incubator in the dark at 30°C. Aliquots were removed from the LB dialysis medium at various time intervals during incubation and stored at -20°C. After the final dialysis period of 16 hours, the frozen aliquots were thawed and used to each resuspend ca. 10^8 CFU/mL uninduced sensor cells. Induction of GFP fluorescence was subsequently assayed as described above.

7.2.6 Synthetic Part

Nitro-dopamine (EP1): A mixture of 3-hydroxytyramine hydrochloride (946.6 mg, 5.0 mmol, 1.0 eq.) and sodium nitrite (757.5 mg, 11 mmol, 2.2 eq.) was dissolved in water (13 mL) and cooled down to 0 °C. Sulfuric acid (8.7 mmol in 5 mL of water) was added slowly to the mixture, and a yellow precipitate was formed. After stirring at r.t. overnight, the precipitate was filtered and recrystallized from water. The product was dried under high vacuum to yield **EP1** (641.1 mg, 1.6 mmol, 64%) as the brown hemisulfate salt.

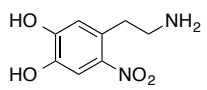

^{1}H-NMR (400 MHz, D_2O) δ = 7.69 (s, 1H), 6.85 (s, 1H), 3.30 (t, *J* = 7.0 Hz, 2H), 3.19 (t, *J* = 7.0 Hz, 2H).

Analytical according to reference: S. Knaggs, H. Malkin, H. M. I. Osborn, N. A. O. Williams, P. Yaqoob, *Org. Biomol. Chem*. **2005**, *3*, 4002.

Activated C_{12}-linker (EP2): Dodecandioic acid (**2**, 235.0 mg, 1.0 mmol, 1.0 eq.) was

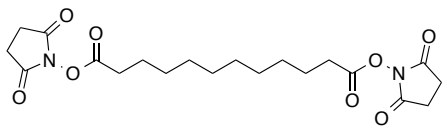

dissolved in MeCN (3 mL) and pyridine (0.16 mL, 2.0 mmol, 2.0 eq.) and *N*,*N*'-disuccinimidyl carbonate (539.0 mg, 2.0 mmol, 2.0 eq.) were added at room temperature. After 7 h, the solvent was removed by rotary evaporation. The residue was poured into a 1M aqueous HCl solution and extracted with CH_2Cl_2. The organic layer was evaporated to yield the desired product **EP2** (423.7 mg, 1.0 mmol, quant.) as a white solid.

^{1}H-NMR (400 MHz, $CDCl_3$) δ = 2.84 (s, 8H), 2.60 (t, *J* = 7.54 Hz, 4H), 1.79-1.69 (m, 4H), 1.40-1.30 (m, 12H). **^{13}C-NMR** (101 MHz, $CDCl_3$) δ = 169.3, 168.8, 31.1, 29.3, 29.1, 28.9, 25.7, 24.7.

Analytical according to reference: Fujimoto, K.; Oimoto, N.; Katsuno, K.; Inouye, M. *Chem. Commun.* **2004**, 1280.

Nitro-dopamine-C_{12}-AHL-hybrid (1): To a solution of dodecanedioic acid

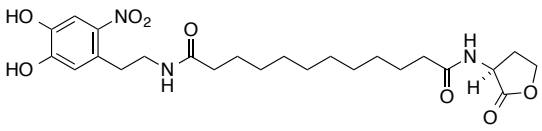

(69.2 mg, 0.3 mmol, 1.0 eq.) in THF/DMSO (7.0 mL/0.4 mL) were added EDC hydrochloride (116.6 mg, 0.6 mmol, 2.0 eq.) and *N*-hydroxysuccinimine (69.6 mg, 0.6 mmol, 2.0 eq.). The resulting mixture was stirred overnight at r.t. Hemisulfate **EP1** (74.9 mg, 0.15 mmol, 0.5 eq.) and Et_3N (0.13 mL, 0.9 mmol, 3.0 eq.) were added and the resulting mixture was stirred for 20 h before addition of (*S*)-α-amino-γ-butyrolactone hydrobromide (54.6 mg, 0.3 mmol, 1.0 eq.). After further 24 h, the mixture was filtrated and concentrated *in vacuo*. The crude was extracted with EtOAc (3 x) and water. Combined organic layers were subsequently washed with brine, dried over Na_2SO_4 and concentrated *in vacuo*. The crude product was purified by size exclusion chromatography (Sephadex LH-20, MeOH) to afford **1** (107.2 mg, 0.2 mmol, 72 %) as an orange solid.

Optical rotation: $[\alpha]_D = -7.3$ (c = 0.49, $CHCl_3$). **FTIR** ν = 2921, 2852, 2488, 2437, 1776, 1697, 1636, 1526, 1467, 1287, 1222, 1173, 1007, 946 cm^{-1}. **^{1}H NMR** (400 MHz, d_4-MeOD) δ = 7.54 (s, 1H), 6.71 (s, 1H), 4.58 (t, J = 10.0 Hz, 1H), 4.43 (td, J = 9.0, 1.8 Hz, 1H), 4.29 (ddd, J = 10.5, 9.0, 6.5 Hz, 1H), 3.43 (t, J = 7.0 Hz, 2H), 3.31 (dt, J = 3.3, 1.6 Hz, 2H), 3.02 (t, J = 6.9 Hz, 2H), 2.58-2.49 (m, 1H), 2.30-2.19 (m, 5H), 2.13 (t, J = 7.6 Hz, 2H), 1.66-1.50 (m, 4H), 1.39-1.22 (m, 12H). **^{13}C NMR** (101 MHz, d_4-MeOD) δ = 177.8, 176.4, 174.9, 152.3, 145.3, 141.7, 129.3, 119.3, 113.4, 67.2, 49.9, 40.7, 37.2, 36.7, 34.9, 34.2, 30.5, 30.4, 30.3, 30.2, 30.1, 29.7, 27.0, 26.8, 26.3, 26.1. **HRMS ESI** calc. for $C_{24}H_{36}N_3O_8$ $[M-H]^+$: 494.2497, found: 494.2487.

Rhodamine derivative (EP3): EDC hydrochloride (200.1 mg, 1.04 mmol, 1.0 eq.) and *N*-hydroxysuccinimine (186.3 mg, 1.57 mmol, 1.5 eq.) were added to a solution of rhodamine B (**5**, 500.0 mg, 1.04 mmol, 1.0 eq.) in dry MeCN (10 mL) at r.t. and under argon atmosphere. The resulting mixture was stirred overnight before *N*-alpha-Boc-L-lysine (260.2 mg, 1.04 mmol, 1.0 eq.) and Et_3N (0.29 mL, 2.09 mmol, 2.0 eq.) were added and the mixture was stirred for 2 days at r.t. The solvent was removed by rotary evaporation. Water and EtOAc were added and the aqueous layer was extracted with EtOAc and CH_2Cl_2. Combined organic layers were dried over Na_2SO_4, filtered and concentrated under reduced pressure. The crude product was purified by flash chromatography (CH_2Cl_2/MeOH 10:1) to afford **EP3** (428.0 mg, 0.64 mmol, 61%) as a pink solid.

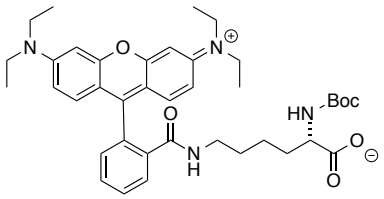

M.p.: Decomposes at 220 °C. $\mathbf{R}_f$ = 0.48 (CH_2Cl_2/MeOH 10:1). **FTIR** ν = 2971, 2929, 1669, 1613, 1513, 1469, 1401, 1358, 1328, 1265, 1219, 1168, 1117, 1091, 1019, 864, 819, 786, 702 cm^{-1}. **^{1}H NMR** (400 MHz, d_4-MeOD) δ = 7.87 (s, 1H), 7.56-7.54 (m, 2H), 7.10-7.08 (m, 1H), 6.46-6.40 (m , 2H), 6.39-6.33 (m, 4H), 3.92-3.90 (m, 1H), 3.40 (q, J = 7.0 Hz, 8H), 3.13-3.09 (m, 2H), 1.56-1.48 (m, 2H), 1.37-1.30 (m, 2H), 1.18 (t, J = 6.9 Hz, 12H), 1.10-1.06 (m, 2H). **^{13}C NMR** (101 MHz, d_4-MeOD) δ = 170.0, 157.9, 155.2, 154.8, 150.4, 134.1, 132.1, 129.7, 129.5, 125.1, 123.8, 109.5,

109.5, 106.1, 99.1, 80.3, 67.3, 45.4, 39.0, 32.5, 28.9, 28.8, 24.0, 13.0. **HRMS ESI** calc. for $C_{39}H_{51}N_4O_6$ $[M-H]^+$: 671.3803, found: 671.3816.

Rhodamine-nitro-dopamine-hybrid (3): Carboxylic acid **EP3** (270.0 mg, 0.40 mmol, 1.0 eq.) was dissolved MeCN (5 mL) and THF (2 mL) under argon atmosphere. *N*,*N*'-Disuccinimidyl carbonate (109.1 mg, 0.40 mmol, 1.0 eq.) and pyridine (33 µL, 0.40 mmol, 1.0 eq.) were added to the red solution. The resulting mixture was stirred for 4 h before **EP1** (99.5 mg, 0.20 mmol, 0.5 eq.) and Et_3N (113 µL, 0.81 mmol, 2.0 eq.) were added. The mixture was stirred overnight and the solvent was removed by rotary evaporation. Water and EtOAc were added and the aqueous layer was extracted two times with EtOAc. Combined organic layers were dried over Na_2SO_4, filtered and concentrated under reduced pressure. The crude product was purified by flash chromatography (CH_2Cl_2/MeOH 25-10:1) to afford **3** (145.0 mg, 0.17 mmol, 41%) as a red solid.

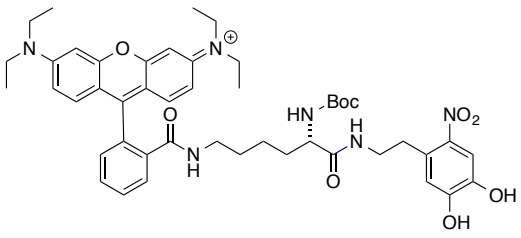

M.**p**.: 84.0 °C. $\mathbf{R_f}$ = 0.49 (CH_2Cl_2/MeOH 10:1). **FTIR** ν = 3400, 3358, 3121, 3085, 2928, 2852, 1712, 1633, 1591, 1527, 1332, 1289, 1181, 1130, 978, 933, 886, 813, 759, 672, 636 cm^{-1}. **^{1}H NMR** (400 MHz, d_4-MeOD) δ = 8.55-8.52 (m, 1H), 7.86-7.82 (m, 1H), 7.57-7.50 (m, 2H), 7.07 (d, *J* = 7.1 Hz, 1H), 6.69 (s, 1H), 6.42 (t, *J* = 2.0 Hz, 2H), 6.39-6.30 (m, 4H), 3.83-3.75 (m, 1H), 3.41-3.34 (m, 8H), 3.16-3.06 (m, 2H), 3.03-2.94 (m, 2H), 1.41 (s, 9H), 1.15 (t, *J* = 7.0 Hz, 12H). **^{13}C NMR** (101 MHz, d_6-DMSO) δ = 172.6, 165.7, 164.1, 157.1, 155.5, 152.1, 152.0, 152.0, 147.5, 144.1, 139.5, 132.7, 130.1, 130.0, 128.6, 128.5, 127.6, 127.5, 122.8, 121.4, 121.1, 117.4, 111.3, 107.3, 96.4, 95.1, 78.0, 50.5, 44.4, 42.8, 39.2, 38.1, 36.0, 31.9, 27.9, 27.2, 24.3, 12.8, 11.4. **HRMS ESI** calc. for $C_{47}H_{59}N_6O_9$ $[M]^+$: 851.4338, found: 851.4354.

Rhodamine derivative (6): To a solution of rhodamine B (**5**, 1.0 g, 2.3 mmol, 1.0 eq.) in MeCN (50 mL) *N*-hydroxysuccinimid (580.0 mg, 5.0 mmol, 2.1 eq.) and EDC hydrochloride (900.0 mg, 4.7 mmol, 2.0 eq.) were added under argon atmosphere at r.t., and the resulting mixture was stirred overnight. 1,2-Diaminoethan (2.0 mL, 29.9 mmol, 13 eq.) and Et_3N (3.2 mL, 23.0 mmol, 10.0 eq.) were added. The solution was stirred for 6 h and the solvent was removed by rotary evaporation. The residue was dissolved in CH_2Cl_2 and extracted with H_2O. The aqueous layer was extracted three times with CH_2Cl_2. Combined organic phases were washed with brine, dried over Na_2SO_4, filtered and the solvent was removed under reduced pressure. The crude compound was purified by flash chromatography (MeOH/CH_2Cl_2 1:25) to afford **6** (625.5 mg, 1.3 mmol, 56%) as brownish crystals.

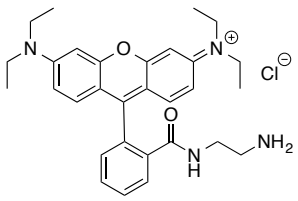

$\mathbf{R_f}$ = 0.44 (MeOH/CH_2Cl_2 1:7). **FTIR** ν = 3085, 3056, 3028, 2970, 2928, 2896, 1727, 1682, 1615, 1545, 1513, 1466, 1428, 1378, 1352, 1330, 1307, 1267, 1218, 1153, 1117, 1077, 1019, 969, 916, 813, 785, 764 cm^{-1}. **^{1}H NMR** (400 MHz, $CDCl_3$) δ = 7.93-7.87 (m, 1H), 7.47-7.41 (m, 2H), 7.12-7.06 (m, 1H), 6.45-6.41 (m, 2H), 6.38-6.35 (m, 2H), 6.29-6.25 (m, 2H), 3.33 (q, *J* = 7.2 Hz, 8H), 3.18 (t, *J* = 6.7 Hz, 2H), 2.40 (t, *J* = 6.7 Hz, 2H), 1.16 (t, *J* = 7.0 Hz, 12H). **^{13}C NMR** (126 MHz, d_4-MeOD) δ = 168.8, 153.3, 148.9, 132.5, 131.1, 128.9, 128.7, 128.1, 123.9, 122.8, 108.2, 105.5, 97.7, 65.1, 44.4, 43.5, 40.9, 12.6. **HRMS ESI** calc. for $C_{30}H_{37}O_2N_4$ $[M]^+$: 485.2911, found: 485.2924.

Rhodamine-nitro-dopamine-hybrid (EP4): To a solution of **EP2** (87.2 mg, 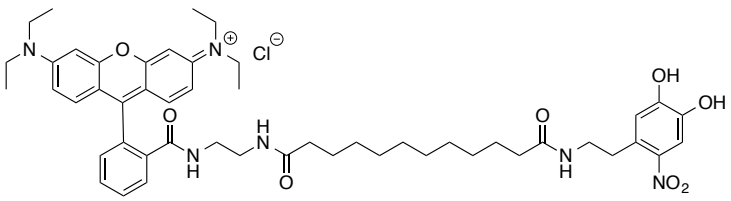 0.21 mmol, 1.0 eq.) in THF/DMSO (5 mL, 1:1) were added **6** (52.7 mg, 0.21 mmol, 1.0 eq.) and Et_3N (0.053 mL, 0.42 mmol, 2.0 eq.) under argon atmosphere. The resulting mixture was stirred overnight at r.t. Rhodamine B (**5**, 100.0 mg, 0.21 mmol, 1.0 eq.) and Et_3N (0.053 mL, 0.4 mmol, 2.0 eq.) were added at r.t. and the mixture was stirred for 4 h. The reaction mixture was diluted with EtOAc. After addition of water, the organic layer was extracted 7 times with water. Combined organic layers were washed with brine, dried over Na_2SO_4, filtered, and concentrated by rotary evaporation. The crude compound was purified by flash chromatography (CH_2Cl_2/MeOH 50-13:1) yielding **4** (95.0 mg, 0.11 mmol, 52%) as brown crystals.

R_f = 0.40 (MeOH/CH_2Cl_2 1:7). **FTIR** ν 3311, 2972, 2926, 2855, 2362, 2340, 1633, 1614, 1514, 1468, 1425, 1399, 1356, 1328, 1296, 1265, 1216, 1143, 1116, 1091, 1044, 1017, 949, 885, 818, 787, 758, 717, 703, 668 cm^{-1}. **^{1}H NMR** (400 MHz, d_4-MeOD) δ = 7.90-7.83 (m, 1H), 7.58-7.49 (m, 3H), 7.07-7.04 (m, 1H), 6.70 (s, 1H), 6.43 (s, 2H), 6.38 (s, 4H), 3.46-3.41 (m, 2H), 3.38 (q, *J* = 7.1 Hz, 8H), 3.22 (t, *J* = 6.4 Hz, 2H), 3.01 (q, *J* = 7.1 Hz, 4H), 2.12 (t, *J* = 7.6 Hz, 2H), 1.98 (t, *J* = 7.5 Hz, 2H), 1.62-1.43 (m, 4H), 1.30-1.21 (m, *J* = 13.3 Hz, 12H), 1.16 (t, *J* = 7.0 Hz, 12H). **HRMS ESI** calc. for $C_{50}H_{65}O_6N_8$ $[M]^+$: 877.4858, found: 877.4869.

7.3 Labeling of QS Pathways

7.3.1 Bacterial Strains and Plasmids

The used bacterial strains and plasmids are listed in Table 13.

Table 13: Bacterial strains and plasmids used.

Strain or plasmid	Relevant characteristic(s)	Reference
Bacterial strains		
B. cenocepacia H111	Clinical isolate	[270]
B. cenocepacia H111-ΔcepR + pBAH27	pBBR1MCS-5 containing the *cepR* genes of *B. cenocepacia* H111; Gm^r	[157]
B. cenocepacia H111-ΔcepR/I	cepI/R::FRT	Eberl *et al.*, unpublished
B. cenocepacia H111-ΔcepR-pBAH8 (GFP)	pBBR1MCS-5 containing $PA_{1/04/03}$-*gfp mut3*-T_o-T_1	[271]
P. putida F117	AHL-negative derivative of IsoF; $PpuI^-$	[64]
E. coli XL1-Blue	*recA1 endA1 gyrA96 thi-1 hsdR17 supE44 relA1 lac* [F *proAB lacI*^{q} *Z*ΔM15 Tn*10* (Tet^r)]	Stratagene
Plasmids		
pAS-C8	pBBR1MCS-5 carrying P_{cepI}-gfp(ASV)-P_{lac}-*cep*R; Gm^r	[64]
pKR-C12	pBBR1MCS-5 carrying P_{lasB}-gfp(ASV)-P_{lac}-*las*R; Gm^r	[64]

7.3.2 Preparation of Bacterial Strains

Scrapes of glycerol stocks were added into LB-medium and raised over night at 30 °C (plasmids pAS-C8 and pKR-C12) or 37 °C (*B. cenocepacia, E. coli*). Antibiotics were added as required at final concentrations of 25 mg of gentamycin/liter, 50 mg of kanamycin/liter, 100 mg of ampicillin/liter and 20 mg of chloramphenicol/liter. Overnight cultures (5 mL) were diluted into fresh LB medium (25 mL) and grown under vigorous shaking for around 1 h until an optical density (OD_{600nm}) between 0.6-1.0 was reached.

[270] (a) S. Walter, P. Gudowius, J. Bosshammer, U. Römling, H. Weissbrodt, W. Schürmann, H. von der Hardt, B. Tummler, *Thorax* **1997**, *52*, 318; (b) K. Riedel, C. Arevalo-Ferro, G. Reil, A. Görg, F. Lottspeich, L. Eberl, *Electrophoresis* **2003**, *24*, 740.

[271] C. R. Wulff-Strobel, A. W. Williams, S. C. Straley, *Mol. Microbiol.* **2002**, *43*, 411.

7.3.3 *In vivo* Incubation with Test Compounds

FLAQS were dissolved in DMSO and 1% acetic acid. FLAQS **4** was activated with TFA due to its pH dependence. Bacterial cultures were distributed into the wells of a 96 well microtiter plate. Wells of the first row were charged with 200 µL of bacterial culture and all other wells with 100 µL. Test-substances (5 µL) with a concentration of 10 mM were added to first row wells. The first column was used as negative control without addition of any AHL analog and the last column was used as positive control with addition of the corresponding natural AHL (5 µL) with a concentration of 100 µM. From the first row 100 µL were taken out and mixed with the well in row two. This dilution procedure was done from top to the bottom. The filled plates with bacteria cultures and the test compounds were incubated for a further 2 h at the corresponding temperatures.

7.3.4 *In vivo* Activity Tests

Activity tests were performed on a microtiter plate reader Synergy HT (MWG Biotech, Germany). Emission was measured at 515 nm with an excitation wavelength at 474 nm. Data were processed with KC4 software (BioTek Instruments) and corrected for auto fluorescence by subtracting the mean value of negative controls. The signals from well 1 of the positive controls with the natural AHL were set as 100% relative green fluorescence.

7.3.5 Microscopic Analysis in Live Cells

For microscopic analysis bacteria samples were washed with 0.9% NaCl solution and centrifuged for 5 min at 5000 r.p.m. To detect motile bacteria a smear of bacterial cultures was fixed with 1% agarose on a glass slide. Fluorescence pictures were taken on a fluorescence microscope (DM6000, Leica) with a x100 oil objective. For red fluorescent pictures a RFP channel was used with an excitation filter BP546/12 and suppression filter BP605/75. Green fluorescence was measured with GFP (excitation filter: BP470/40; suppression filter: BP525/50) or GFG (excitation filter: D480/20; suppression filter: D520/20) channel. Additionally, a confocal laser scanning microscope (DM5500Q, Leica) equipped with a x100 oil objective was used. Data

were analyzed with Leica Application Suite (Mannheim, Germany) and the Imaris software package (Bitplane, Switzerland).

7.3.6 Synthesis of FLAQS

C_{12}-FLAQS (4):[154] To a solution of rhodamine B (**5**, 75.0 mg, 0.157 mmol, 1.0 eq.) in MeCN (4.0 mL) was added *N*-hydroxysuccinimid (19.3 mg, 0.167 mmol, 1.1 eq.) and 1-(3-dimethyl aminopropyl)-3-ethyl-carbodiimide (32.1 mg, 0.167 mmol, 1.1 eq.). The resulting mixture was stirred at room temperature for 15 h. 1,2-Diaminoethane (0.2 mL, 3.040 mmol, 20.0 eq.) and freshly distilled Et_3N (0.4 mL, 3.040 mmol, 20.0 eq.) were added to the reaction mixture and it was stirred at room temperature for additional 6 h. The solvent was concentrated and the residue was extracted with H_2O and CH_2Cl_2. The organic layer was washed with brine, dried over Na_2SO_4, filtered, and concentrated *in vacuo*. The crude compound was purified by flash chromatography (SiO_2, CH_2Cl_2/MeOH 2-8%) and subsequently dissolved in MeCN (4.0 mL). Activated linker **EP2** (65.0 mg, 0.157 mmol, 1.0 eq.) and freshly distilled Et_3N (0.1 mL, 0.761 mmol, 5.0 eq.) were added and the mixture was stirred at room temperature for 4 h. Subsequently, (*S*)-α-amino-γ-butyrolactone hydrobromide (27.7 mg, 0.157 mmol, 1.0 eq.) was added and the mixture was stirred at room temperature for 19 h. The solvent was concentrated *in vacuo* and the residue was extracted with H_2O and CH_2Cl_2. The organic layers was washed with brine, dried over Na_2SO_4, filtered, and concentrated *in vacuo*. The crude compound was purified by size-exclusion chromatography (Sephadex LH-20, MeOH) to yield the title compound (103.0 mg, 0.132 mmol, 88%) as a pink solid.

M.p. = 98.2-101.9 °C. $\mathbf{R_f}$ = 0.30 (CH_2Cl_2/MeOH 7:1). **FTIR** ν 3383, 3315, 3075, 2969, 2927, 2855, 2359, 2323, 2288, 2234, 2191, 2121, 2082, 1778, 1634, 1614, 1546, 1514, 1468, 1427, 1377, 1356, 1330, 1304, 1266, 1219, 1117, 1017, 950, 820, 787, 759, 703 cm^{-1}. **^{1}H-NMR** (400 MHz, d_4-MeOD) δ = 7.90-7.84 (m, 1H), 7.59-7.48 (m, 2H), 7.06 (d, *J* = 7.4 Hz, 1H), 6.43 (s, 2H), 6.40-6.33 (m, 4H), 4.63-4.55 (m, 1H), 4.47-4.40 (m, 1H), 4.33-4.22 (m, 1H), 3.42-3.33 (m, 8H), 3.26-3.10 (m, 2H),

2.99-2.92 (m, 2H), 2.53 (dddd, *J* = 9.0, 6.3, 4.0, 1.9 Hz, 1H), 2.31-2.19 (m, 3H), 2.00 (t, *J* = 7.5 Hz, 2H), 1.63-1.56 (m, 2H), 1.53-1.43 (m, 2H), 1.38-1.20 (m, 12H), 1.18-1.12 (m, 12H). **^{13}C-NMR** (101 MHz, d_4-MeOD) δ = 179.8, 176.4, 173.4, 169.1, 154.8, 150.5, 131.8, 129.5, 128.5, 126.7, 125.2, 123.6, 109.6, 101.4, 99.10, 67.1, 49.9, 45.4, 40.7, 39.4, 36.7, 30.5, 30.4, 30.3, 30.2, 30.1, 30.0, 29.9, 29.6, 26.7, 12.9. **HRMS-ESI** calc. for $C_{49}H_{66}O_6N_5$ $[M]^+$: 780.4695, found: 780.4713.

FLAQS (11):[154] Fluorophore **10**[159] (50.0 mg, 0.066 mmol, 1.0 eq.) was dissolved in

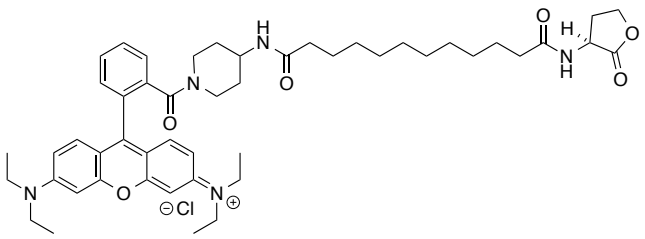

CH_2Cl_2 (3.0 mL) and TFA (3.0 mL) and stirred at room temperature for 5 h. The reaction was concentrated *in vacuo*. To a mixture of **EP2** (28.2 mg, 0.066 mmol, 1.0 eq.) in MeCN (4.0 mL) was added (*S*)-α-amino-γ-butyrolactone hydrobromide (12.1 mg, 0.066 mmol, 1.0 eq.) and Et_3N (0.02 mL, 0.133 mmol, 2.0 eq.) and the resulting mixture was stirred at room temperature for 10 h. The previously deprotected fluorescent dye was dissolved in MeCN (1.0 mL) and added to the reaction mixture. The resulting mixture was stirred for additional 15 h at room temperature. The mixture was concentrated *in vacuo* and the residue was extracted with H_2O and CH_2Cl_2 (3 x 15 mL). The combined organic layers were washed with brine, dried over Na_2SO_4, filtered and concentrated *in vacuo*. The crude compound was purified by preparative RP HPLC (2.5-100% water/ACN over 1 h) to yield the title compound (39.0 mg, 0.047 mmol, 71%) as purple solid.

M.p.: 97.6-100.3 °C. $\mathbf{R_f}$ = 0.30 (CH_2Cl_2/MeOH 7:1). **FTIR** ν = 3311, 3071, 2927, 2854, 2360, 2338, 1777, 1737, 1690, 1642, 1587, 1550, 1466, 1412, 1336, 1273, 1247, 1177, 1128, 1074, 1011, 977, 922, 823, 798, 717, 683 cm^{-1}. **^{1}H NMR** (400 MHz, d_4-MeOD) δ = 8.53 (s, 1H), 7.79-7.73 (m, 2H), 7.66 (dt, *J* = 4.0, 3.1 Hz, 1H), 7.53-7.48 (m, 1H), 7.28 (dd, *J* = 9.5, 2.0 Hz, 2H), 7.07 (t, *J* = 9.7 Hz, 2H), 6.97 (d, *J* = 2.3 Hz, 2H), 4.63-4.53 (m, 1H), 4.47-4.39 (m, 1H), 4.34-4.23 (m, 1H), 4.13 (d, *J* = 12.5Hz, 1H), 3.78-3.64 (m, 9H), 3.09-2.95 (m, 1H), 2.71-2.61 (m, 1H), 2.59-2.47 (m, 1H), 2.27-2.19 (m, 3H), 2.12 (t, *J* = 7.4 Hz, 2H), 1.77 (t, *J* = 13.4 Hz, 2H), 1.58

(dd, *J* = 13.4, 6.7 Hz, 4H), 1.40-1.26 (m, 24H), 1.21-1.11 (m, 2H). **^{13}C NMR** (101 MHz, d_4-MeOD) δ = 177.4, 176.3, 174.4, 169.4, 157.2, 157.0, 137.0, 133.2, 131.9, 131.7, 131.3, 131.1, 128.5, 115.3, 114.8, 97.3, 67.3, 49.5, 47.8, 47.5, 46.9, 41.8, 37.0, 36.7, 33.1, 31.8, 30.5, 30.4, 30.2, 30.1, 29.6, 27.0, 26.7, 12.9. **HRMS ESI** calc. for $C_{49}H_{66}N_5O_6$ $[M]^+$: 820.5008, found: 820.5026.

***N*-Boc-C_{12}-AHL (EP5):**[154] A mixture of 12-aminododecanoic acid (444.0 mg, 2.06 mmol, 1.0 eq.), di-*tert*-butyl dicarbonate (629.0 mg, 2.88 mmol, 1.4 eq.), NaOH (107.0 mg, 2.68 mmol, 1.3 eq.) in H_2O (14.0 mL) and *tert*-butanol (7.0 mL) was stirred at room temperature for 23 h. The mixture was diluted with H_2O and 1 M HCl solution and was extracted with EtOAc (3 x 15 mL). The combined organic layers were washed with brine, dried over Na_2SO_4, filtered, and concentrated *in vacuo.* The residue was dissolved in MeCN (15.0 mL). *N*,*N*'-Disuccinimidyl carbonate (833.0 mg, 3.09 mmol, 1.5 eq.) and pyridine (0.3 mL, 4.12 mmol, 2.0 eq.) were added to the solution. The mixture was stirred at room temperature for 18 h, concentrated *in vacuo,* and the residue was extracted with 1 M HCl solution and CH_2Cl_2 (3 x 15 mL). The combined organic layers were dried over Na_2SO_4, filtered, concentrated *in vacuo.* The residue was dissolved in MeCN (15.0 mL). (*S*)-α-Amino-γ-butyrolactone hydrobromide (562 mg, 3.09 mmol, 1.5 eq.) and freshly distilled Et_3N (0.6 mL, 4.12 mmol, 2.0 eq.) were added and the mixture was stirred at room temperature for 18 h. The resulting mixture was concentrated and the residue was extracted with H_2O and CH_2Cl_2 (3 x 15 mL). The combined organic layers were washed with brine, dried over Na_2SO_4, filtered, and concentrated *in vacuo*. The crude product was purified by flash-chromatography (SiO_2, EtOAc/pentane 1:1) to yield the title compound (395.0 mg, 1.03 mmol, 50%) as white solid.

M.p.: 110.9-111.3 °C. $\mathbf{R_f}$ = 0.60 (EtOAc/pentane 2:1). **Optical rotation**: $[\alpha]_D$ = 0.0 (*c* = 0.96, CH_2Cl_2). **FTIR** ν = 3325, 2922, 2852, 1776, 1688, 1645, 1538, 1469, 1446, 1385, 1365, 1280, 1251, 1226, 1168, 1138, 1106, 1072, 1042, 1014, 997, 976, 948, 871, 722, 656 cm^{-1}. **^{1}H NMR** (400 MHz, $CDCl_3$) δ = 6.26 (brs, 1H), 4.56 (ddd, *J* = 11.4, 9.1, 7.4 Hz, 2H), 4.45 (t, *J* = 9.0 Hz, 1H), 4.27 (ddd, *J* = 10.9, 9.4, 6.0 Hz,

1H), 3.15-3.00 (m, 1H), 2.90-2.72 (m, 1H), 2.23 (t, *J* = 7.6 Hz, 1H), 2.12 (ddd, *J* = 20.5, 11.5, 5.7 Hz, 1H), 1.62 (dt, *J* = 14.4, 7.3 Hz, 2H), 1.43 (s, 11H), 1.24 (s, 14H). **^{13}C NMR** (101 MHz, $CDCl_3$) δ = 175.8, 173.9, 156.1, 79.1, 66.2, 49.2, 40.7, 36.2, 30.5, 30.1, 29.6, 29.5, 29.4, 29.3, 28.5, 26.9, 25.5.

Protected C_{14}-3-oxo AHL (EP6):[154] A mixture of 12-aminododecanoic acid 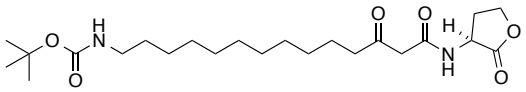 (71.5 mg, 0.332 mmol, 1.0 eq.), di-*tert*-butyl dicarbonate (101.0 mg, 0.465 mmol, 1.4 eq.) and NaOH (17.3 mg, 0.432 mmol, 1.3 eq.) in H_2O (3 mL) and *tert*-butanol (1.5 mL) was stirred at room temperature for 23 h. The mixture was diluted with H_2O and 1 M aqueous HCl solution and was extracted with EtOAc (3 x 10 mL). The combined organic layers were washed with brine, dried over Na_2SO_4, filtered, concentrated and subsequently dissolved in CH_2Cl_2 (3 mL) and Meldrum`s acid (47.8 mg, 0.332 mmol, 1.0 eq.), *N*,*N*'-dicyclohexylcarbodiimide (75.3 mg, 0.365 mmol, 1.1 eq.) and 4-dimethyl-aminopyridine (44.6 mg, 0.365 mol, 1.1 eq.) were added. The mixture was stirred at room temperature for 18 h and then filtered and the filtrate was concentrated. DMF (2 mL) and (*S*)-α-amino-γ-butyrolactone hydrobromide (61.0 mg, 0.332 mg, 1.0 eq.) were added to the residue. The mixture was heated to 60 °C, stirred for 4 h, and subsequently cooled down to room temperature. The mixture was diluted with EtOAc and washed with saturated $NaHCO_3$ solution (10 mL), 1 M HCl solution (10 mL) and brine (10 mL). The organic layer was concentrated and the crude product was purified by flash-chromatography (SiO_2, EtOAc/pentane 1:1 to 2:1) to yield **EP6** (72.1 mg, 0.169 mmol, 51%) as a white solid.

M.p. = 82.8-84.3 °C. **R_f** = 0.23 (EtOAc/pentane 2:1). **Optical rotation**: $[\alpha]_D$ = 0.0 (*c* = 0.69, CH_2Cl_2). **FTIR** ν = 3345, 3297, 3065, 2920, 2853, 2167, 1776, 1718, 1681, 1645, 1525, 1470, 1364, 1322, 1274, 1251, 1180, 1107, 1015, 950, 870, 719, 652 cm^{-1}. **^{1}H-NMR** (400 MHz, $CDCl_3$) δ = 13.23 (s, 1H), 7.70 (d, *J* = 5.0 Hz, 1H), 4.59 (ddd, *J* = 11.5, 8.8, 6.8 Hz, 1H), 4.51 (brs, 1H), 4.46 (td, *J* = 9.1, 1.2 Hz, 1H), 4.26 (ddd, *J* = 11.0, 9.3, 6.1 Hz, 1H), 3.11-3.04 (m, 2H), 2.80-2.65 (m, 1H), 2.51 (t, *J* = 7.4 Hz, 2H), 2.23 (ddd, *J* = 23.6, 11.3, 9.0 Hz, 1H), 1.59-1.53 (m, 2H), 1.42 (s,

9H), 1.24 (s, 16H). **^{13}C-NMR** (101 MHz, $CDCl_3$) δ = 206.7, 174.9, 166.5, 79.1, 66.0, 49.2, 48.2, 45.9, 44.0, 40.7, 30.2, 29.8, 29.6, 29.5, 29.4, 29.3, 29.0, 28.5, 26.9, 23.4. **HRMS ESI** calc. for $C_{23}H_{41}N_2O_6$ $[M-H]^+$: 441.2959, found: 441.2971.

***N*-Boc-C$_{11}$-AHL (EP7):**[154] A mixture of 11-aminoundecanoic acid (91.0 mg, 0.452 mmol, 1.0 eq.), di-*tert*-butyl dicarbonate (13.8 mg, 0.633 mmol, 1.4 eq.), NaOH (23.5 mg, 0.588 mmol, 1.3 eq.) in H_2O (4.0 mL), and *tert*-butanol (2 mL) was stirred at room temperature for 23 h. The mixture was diluted with H_2O and 1 M HCl solution before it was extracted with EtOAc (3 x 15 mL). The combined organic layers were washed with brine, dried over Na_2SO_4, filtered, and concentrated *in vacuo*. The residue was dissolved in MeCN (5.0 mL). *N*,*N*'-Disuccinimidyl carbonate (146.0 mg, 0.542 mmol, 1.1 eq.) and pyridine (0.1 mL, 0.904 mmol, 2.0 eq.) were added. The mixture was stirred at room temperature for 18 h after which time it was concentrated. The residue was extracted with 1 M HCl solution and CH_2Cl_2 (3 x 10 mL). The combined organic layers were dried over Na_2SO_4, filtered, concentrated *in vacuo,* and subsequently dissolved in MeCN (5.0 mL). (*S*)-α-Amino-γ-butyrolactone hydrobromide (123.0 mg, 0.678 mmol, 1.5 eq.) and freshly distilled Et_3N (0.1 mL, 0.903 mmol, 2.0 eq.) were added and the resulting mixture was stirred at room temperature for 18 h. The reaction mixture was concentrated *in vacuo* and the residue was extracted with H_2O and CH_2Cl_2 (3 x 10 mL). The combined organic layers were washed with brine, dried over Na_2SO_4, filtered, and concentrated under reduced pressure. The crude product was purified by flash-chromatography (SiO_2, EtOAc/pentane 1:1) to yield the title compound (155.0 mg, 0.403 mmol, 89%) as white solid.

M.p. = 121.3-121.7 °C. **R_f** = 0.40 (EtOAc/pentane 2:1). **Optical rotation**: $[\alpha]_D$ = 0.0 (*c* = 0.72, CH_2Cl_2). **FTIR** ν = 3323, 2922, 2853, 1775, 1681, 1644, 1525, 1470, 1448, 1425, 1385, 1366, 1339, 1284, 1274, 1248, 1226, 1167, 1108, 1042, 1013, 964, 948, 869, 782, 721, 655, 633 cm^{-1}. **^{1}H-NMR** (400 MHz, $CDCl_3$) δ = 6.28 (brs, 1H), 4.55 (ddd, *J* = 11.6, 8.5, 5.9, 1H), 4.46 (t, *J* = 9.0 Hz, 1H), 4.28 (ddd, *J* = 11.2, 9.4, 5.9 Hz, 1H), 3.16-3.00 (m, 2H), 2.84 (dt, *J* = 12.5 Hz, 1H), 2.24 (t, *J* = 7.6 Hz, 2H), 2.14 (ddd, *J* = 23.8, 11.5, 8.9 Hz, 1H), 1.63 (dt, *J* =14.8, 7.4 Hz, 2H), 1.43 (s, 11H), 1.26 (s,

12H). **^{13}C-NMR** (101 MHz, $CDCl_3$) δ = 175.7, 174.0, 66.2, 49.3, 40.7, 36.2, 30.6, 30.1, 29.5, 29.4, 29.3, 29.2, 28.5, 26.8, 25.5. **HRMS ESI** calc. for $C_{20}H_{36}N_2O_5$ $[M-H]^+$: 385.2697, found: 385.2710.

***N*-Boc-C$_{13}$-3-Oxo-AHL (EP8):**[154] A mixture of 11-aminoundecanoic acid (30.4 mg, 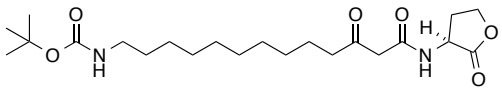 0.151 mmol, 1.0 eq.), di-*tert*-butyl dicarbonate (46.1 mg, 0.211 mmol, 1.4 eq.) and NaOH (7.85 mg, 0.196 mmol, 1.3 eq.) in H_2O (3 mL) and *tert*-butanol (1.5 mL) was stirred at room temperature for 23 h. The mixture was diluted with H_2O and 1 M HCl and was extracted with EtOAc (3 x 10 mL). The combined organic layers were washed with brine, dried over Na_2SO_4, filtered and concentrated and subsequently dissolved in CH_2Cl_2 (3 mL) and Meldrum`s acid (21.8 mg, 0.151 mmol, 1.0 eq.), *N*,*N*'-dicyclohexylcarbodiimide (34.3 mg, 0.166 mmol, 1.1 eq.) and 4-dimethyl-aminopyridine (20.3 mg, 0.166 mol, 1.1 eq.) were added. The mixture was stirred at room temperature for 18 h and then filtered and the filtrate was concentrated. DMF (2 mL) and (*S*)-α-amino-γ-butyrolactone hydrobromide (30.2 mg, 0.166 mg, 1.1 eq.) were added to the residue. The mixture was heated to 60 °C, stirred for 4 h and subsequently cooled down to room temperature. The mixture was diluted with EtOAc and washed with saturated $NaHCO_3$ solution (10 mL), 1 M HCl solution (10 mL) and brine (10 mL). The organic layer was concentrated and the crude product was purified by flash chromatography (SiO_2, EtOAc/pentane 1:1 to 2:1) to yield **EP8** (60.8 mg, 0.143 mmol, 94%) as a white solid.

M.p. = 85.4-86.5 °C. **R_f** = 0.14 (EtOAc/pentane 2:1). **Optical rotation**: $[\alpha]_D$ = –1.8 (*c* = 0.59, CH_2Cl_2). **FTIR** ν = 3355, 3318, 2922, 2851, 1776, 1717, 1682, 1643, 1523, 1469, 1409, 1365, 1277, 1251, 1171, 1106, 1013, 949, 871, 784, 725 cm^{-1}. **^{1}H-NMR** (400 MHz, $CDCl_3$) δ = 13.24 (s, 1H), 7.70 (d, *J* = 4.6 Hz, 1H), 4.59 (ddd, *J* = 11.5, 8.7, 6.7 Hz, 1H), 4.50 (brs, 1H), 4.47 (t, *J* = 9.1 Hz, 2H), 4.27 (ddd, *J* = 11.0, 9.3, 6.1 Hz, 1H), 3.09 (dd, *J* = 12.4, 6.0 Hz, 2H), 2.81-2.69 (m, 1H), 2.52 (t, *J* = 7.3 Hz, 2H), 2.23 (ddd, *J* = 23.6, 11.4, 9.0 Hz, 1H), 1.61-1.52 (m, 2H), 1.43 (s, 11H), 1.26 (s, 10H). **^{13}C-NMR** (101 MHz, $CDCl_3$) δ = 206.7, 174.9, 166.5, 79.1, 66.0, 49.2, 48.2, 45.9, 44.0, 30.2, 30.0, 29.5, 29.4, 29.1, 28.6, 26.9, 23.4. **HRMS ESI** calc. for

$C_{22}H_{39}N_2O_6$ [M-H]$^+$: 427.2803, found: 427.2811.

***N*-Boc-C_{14}-3-oxo-AHL (EP9):**[154] Linker **EP6** (149.6 mg, 0.341 mmol, 1.0 eq.) was

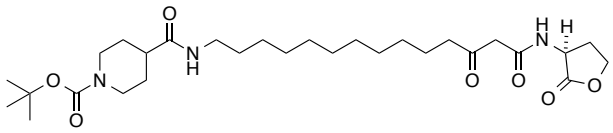

dissolved in CH_2Cl_2 (0.5 mL) and TFA (0.5 mL) at r.t. and the resulting mixture was stirred for 5 h. The solvent was removed under rotary evaporation and the crude was redissolved in dry CH_2Cl_2 (2 mL). *N*-Boc-4-piperidinecarboxylic acid (78.2 mg, 0.341 mmol, 1.0 eq.) was dissolved in dry MeCN (4 mL) and cooled down to 0 °C before *N*-hydroxysuccinimide (43.2 mg, 0.375 mmol, 1.1 eq.) and *N*,*N*'-dicyclohexylcarbodiimide (77.4 mg, 0.375 mmol, 1.1 eq.) were added. The mixture was stirred at r.t. for 16 h. The deprotected AHL analogue and triethylamine (96 µL, 0.682 mmol, 2.0 eq.) were added subsequently and the reaction mixture was stirred at r.t. for 3 h and 15 min. The solvent was evaporated and the residue was extracted with H_2O and CH_2Cl_2 (3 x). The organic layers were combined, dried over Na_2SO_4, filtered and evaporated under reduced pressure. The residue was purified by flash chromatography (EtOAc/pentane 1:1) to yield the desired product (117.0 mg, 0.212 mmol, 62%) as a white solid.

M.p.: 108.2-110.9 °C. $\mathbf{R_f}$ = 0.05 (EtOAc/pentane 2:1). **FTIR** ν = 3296, 3076, 2920, 2851, 1777, 1719, 1685, 1635, 1544, 1467, 1429, 1383, 1364, 1337, 1278, 1261, 1246, 1216, 1176, 1130, 1104, 1067, 1016, 1003, 946, 872, 818, 763, 720, 688, 609 cm^{-1}. **^{1}H NMR** (500 MHz, $CDCl_3$) δ = 13.54 (s, 1H), 7.71 (d, *J* = 5.8 Hz, 1H), 5.51 (s, 1H), 4.58 (ddd, *J* = 11.4, 8.7, 6.6 Hz, 1H), 4.47 (td, *J* = 9.1, 1.2 Hz, 1H), 4.27 (ddd, *J* = 11.0, 9.3, 6.1 Hz), 4.13 (d, *J* = 13.3 Hz, 2H), 3.23 (dd, *J* = 12.8, 6.9 Hz, 2H), 2.75 (ddd, *J* = 21.3, 12.0, 1.8 Hz, 3H), 2.52 (t, *J* = 7.3 Hz, 2H), 2.26-2.17 (m, 2H), 1.83-1.75 (m, 2H), 1.61 (ddd, *J* = 16.2, 12.7, 5.5 Hz, 6H), 1.45 (s, 9H), 1.30-1.21 (m, 18H). **^{13}C NMR** (101 MHz, $CDCl_3$) δ = 206.7, 174.9, 166.5, 154.8, 79.8, 66.0, 49.2, 44.0, 43.6, 396, 30.0, 29.8, 29.7, 29.5, 29.4, 29.0, 28.8, 28.6, 27.0, 23.4. **HRMS ESI** calc. for $C_{29}H_{49}N_3NaO_7$ [M-Na]$^+$: 574.3465, found: 574.3463.

C_{12}-FLAQS (EP10):[154] To a solution of **EP5** (8.0 mg, 0.020 mmol, 1.0 eq.) in

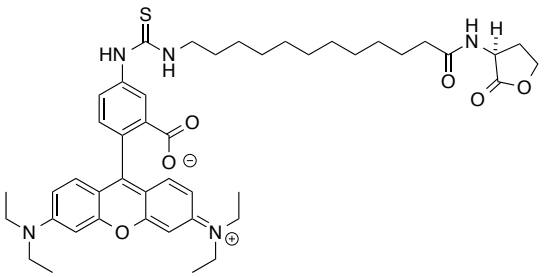

CH_2Cl_2 (0.5 mL) was added TFA (0.5 mL) and the mixture was stirred at room temperature for 3 h. The reaction mixture was concentrated *in vacuo* and subsequently dissolved in MeCN (2.0 mL). Rhodamine B isothiocyanate (**8**, 10.1 mg, 0.020 mmol, 1.0 eq.) and freshly distilled Et_3N (5.0 µL, 0.04 mmol, 2.0 eq.) were added and the resulting mixture was stirred at room temperature for 17 h. The solvent was removed with a nitrogen stream at room temperature. The residue was dissolved in a little amount of CH_2Cl_2 and precipitated in Et_2O to yield 13.5 mg of the impure title compound as a purple solid.

M.p. = 86.9-90.1 °C. **R_f** = 0.30 (CH_2Cl_2/MeOH 7:1). **FTIR** ν = 3240, 3047, 2977, 2928, 2855, 2623, 2607, 2499, 1778, 1756, 1646, 1588, 1529, 1465, 1398, 1337, 1273, 1246, 1178, 1130, 1073, 1037, 1015, 976, 923, 825, 683 cm^{-1}. **^{1}H-NMR** (400 MHz, d_4-MeOD) δ = 8.54-6.59 (m, 9H), 4.63-4.53 (m, 1H), 4.44 (td, *J* = 9.0, 1.8 Hz, 1H), 4.35-4.23 (m, 1H), 3.73-3.57 (m, 8H), 2.95-2.87 (m, 2H), 2.53 (ddd, *J* = 11.0, 9.6, 4.4 Hz, 1H), 2.29-2.21 (m, 3H), 1.72-1.55 (m, 4H), 1.36-1.26 (m, 25H). **UPLC-MS (+*ESI*)** *m/z* = 799.0 $(M+H)^+$.

C_{12}-FLAQS (EP11):[154] To a solution of **EP5** (8.3 mg, 0.021 mmol, 1.0 eq.) in

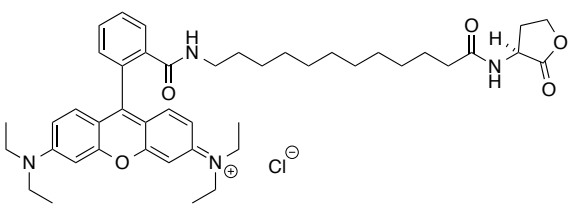

CH_2Cl_2 (0.5 mL) was added TFA (0.5 mL) and the mixture was stirred at room temperature for 3 h. The reaction mixture was concentrated under reduced pressure. To a solution of rhodamine B (**5**, 10.0 mg, 0.021 mmol, 1.0 eq.) in MeCN (2.0 mL) was added *N*-hydroxysuccinimide (2.4 mg, 0.021 mmol, 1.0 eq.) and 1-(3-dimethylaminopropyl)-3-ethylcarbo-diimide hydrochloride (4.0 mg, 0.021 mmol, 1.0 eq.) and the resulting mixture was stirred at room temperature for 4 h. The previously deprotected **EP5** and freshly distilled Et_3N (6.0 µL, 0.042 mmol, 2.0 eq.) were added to the mixture and was stirred at room temperature for 15 h. The solvent

was evaporated under reduced pressure and the residue was extracted with H_2O and CH_2Cl_2 (3 x 5 mL). The combined organic layers were washed with brine, dried over Na_2SO_4, filtered, and concentrated *in vacuo*. The crude product was purified by size-exclusion chromatography (MeOH) to yield 20.9 mg of the impure title compound as a purple solid.

R_f = 0.25 (CH_2Cl_2/MeOH 7:1). **^{1}H-NMR** (400 MHz, d_4-MeOD) δ = 7.89-7.83 (m, 1H), 7.72 (dd, *J* = 5.5, 3.4 Hz, 1H), 7.62 (dd, *J* = 5.8, 3.1 Hz, 1H), 7.59-7.50 (m, 2H), 7.09 (dd, *J* = 6.0, 1.8 Hz, 1H), 6.48 (s, 2H), 6.37 (dd, *J* = 21.1, 8.0 Hz, 2H), 4.62-4.53 (m, 1H), 4.43 (td, *J* = 9.0, 1.6 Hz, 1H), 4.29 (ddd, *J* = 10.2, 9.2, 6.6 Hz, 1H), 3.40 (dd, *J* = 14.0, 7.0 Hz, 8H), 3.05 (t, *J* = 6.5 Hz, 2H), 2.59-2.48 (m, 1H), 2.27-2.18 (m, 3H), 1.63-1.57 (m, 2H), 1.34-1.27 (m, 4H), 1.16 (t, *J* = 7.0 Hz, 12H), 1.12-1.01 (m, 10H).

C_{18}-FLAQS (EP12):[154] To a solution of rhodamine B (**5**, 9.6 mg, 0.020 mmol, 1.0 eq.) in MeCN (2 mL) was added NHS (2.5 mg, 0.022 mmol, 1.1 eq.) and 1-(3-dimethylamino-propyl)-3-ethylcarbo-diimide hydrochloride (4.2 mg, 0.022 mmol, 1.1 eq.). This mixture was stirred at room temperature for 18 h. 6-Amino-hexanoic acid (2.6 mg, 0.020 mmol, 1.0 eq.) and freshly distilled Et_3N (6.0 µL, 0.040 mmol, 2.0 eq.) were added to the mixture and stirred at room temperature for 23 h. It was concentrated *in vacuo* and the residue was extracted with 1 M HCl solution and CH_2Cl_2 (3 x 5 mL). The combined organic layers were dried over Na_2SO_4, filtered, concentrated *in vacuo*, and purified by flash-chromatography (SiO_2, 10% MeOH in CH_2Cl_2). To a mixture of **EP5** (8.3 mg, 0.020 mmol, 1.0 eq.) in MeCN (2.0 mL) was added Et_3N (6.0 µL, 0.040 mmol, 2.0 eq.) and the mixture was stirred at room temperature for 7.5 h. The previously synthesized rhodamine B derivative in MeCN (1.0 mL) was added to the reaction mixture and stirred at room temperature for additional 15 h. The mixture was concentrated *in vacuo* and the residue was extracted with H_2O and CH_2Cl_2 (3 x 5 mL). The combined organic layers were dried over Na_2SO_4, filtered, and concentrated *in vacuo*. The crude product was purified by size-exclusion chromatography (MeOH) to yield 5.8 mg of the impure title compound as a purple solid.

R_f = 0.10 (CH_2Cl_2/MeOH 7:1). **^{1}H-NMR** (400 MHz, d_4-MeOD) δ = 8.37-6.74 (m, 10H), 4.58 (dd, *J* = 10.8, 9.3 Hz, 1H), 4.44 (td, *J* = 9.0, 1.7 Hz, 1H), 4.29 (ddd, *J* = 10.5, 9.1, 6.6 Hz, 1H), 3.69 (dt, *J* = 19.2, 7.0 Hz, 8H), 2.53 (dt, *J* = 13.7, 7.0 Hz, 4H), 2.27-2.20 (m, 9H), 2.06-2.00 (m, 1H), 1.64-1.52 (m, 14H), 1.34-1.30 (m, 18H).

C_{11}-FLAQS (EP13):[154] To a solution of **EP7** (8.3 mg, 0.021 mmol, 1.0 eq.) in

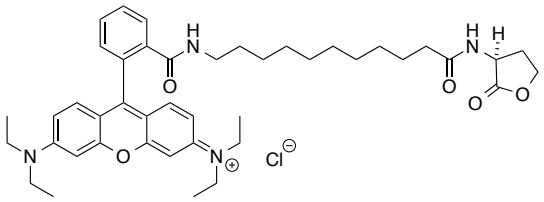

CH_2Cl_2 (0.5 mL) was added TFA (0.5 mL) and the mixture was stirred at room temperature for 3 h. The reaction mixture was concentrated and used without further purification. To a solution of rhodamine B (**5**, 10.0 mg, 0.021 mmol, 1.0 eq.) in MeCN (2 mL) was added *N*-hydroxysuccinimide (2.4 mg, 0.021 mmol, 1.0 eq.) and 1-(3-dimethylaminopropyl)-3-ethylcarbo-diimide hydrochloride (4.0 mg, 0.021 mmol, 1.0 eq.) and the mixture was stirred at room temperature for 4 h. To this mixture was added the previously deprotected **EP7** and Et_3N (6 µL, 0.042 mmol, 2.0 eq.) and the mixture was stirred at room temperature for 15 h. The solvent was evaporated under reduced pressure and the residue was extracted with H_2O and CH_2Cl_2 (3 x 5 mL). The combined organic layers were washed with brine, dried over Na_2SO_4, filtered, and concentrated. The crude product was purified by size exclusion chromatography (Sephadex LH-20, MeOH) to yield 20.9 mg of the impure product as a purple solid.

R_f = 0.25 (CH_2Cl_2/MeOH 7:1). **^{1}H-NMR** (400 MHz, d_4-MeOD) δ = 7.89-7.83 (m, 1H), 7.72 (dd, *J* = 5.5, 3.4 Hz, 1H), 7.62 (dd, *J* = 5.8, 3.1 Hz, 1H), 7.59-7.50 (m, 2H), 7.09 (dd, *J* = 6.0, 1.8 Hz, 1H), 6.48 (s, 2H), 6.37 (dd, *J* = 21.1, 8.0 Hz, 2H), 4.62-4.53 (m, 1H), 4.43 (td, *J* = 9.0, 1.6 Hz, 1H), 4.29 (ddd, *J* = 10.2, 9.2, 6.6 Hz, 1H), 3.40 (dd, *J* = 14.0, 7.0 Hz, 8H), 3.05 (t, *J* = 6.5 Hz, 2H), 2.59-2.48 (m, 1H), 2.27-2.18 (m, 3H), 1.63-1.57 (m, 2H), 1.34-1.27 (m, 4H), 1.16 (t, *J* = 7.0 Hz, 12H), 1.12-1.01 (m, 10H).

C_{11}-FLAQS (EP14):[154] To a solution of **EP7** (8.0 mg, 0.020 mmol, 1.0 eq.) in CH_2Cl_2 (0.5 mL) was added TFA (0.5 mL) and the mixture was stirred at room temperature for 3 h. The reaction mixture was concentrated and subsequently dissolved in MeCN (2 mL). Rhodamine B isothiocyanate (**8**, mixed isomers, 10.1 mg, 0.020 mmol, 1.0 eq.) and Et_3N (5 µL, 0.04 mmol, 2.0 eq.) were added and the mixture was stirred at room temperature for 17 h. The solvent was removed with a nitrogen stream. The residue was dissolved in a little amount of CH_2Cl_2 and precipitated in Et_2O to yield 13.5 mg of the impure product as a purple solid.

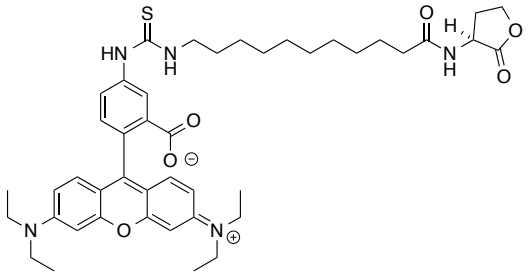

M.p. = 86.9-90.1 °C. $\mathbf{R_f}$ = 0.30 (CH_2Cl_2/MeOH 7:1). **FTIR** ν = 3240, 3047, 2977, 2928, 2855, 2623, 2607, 2499, 1778, 1756, 1646, 1588, 1529, 1465, 1398, 1337, 1273, 1246, 1178, 1130, 1073, 1037, 1015, 976, 923, 825, 683 cm^{-1}. **^{1}H-NMR** (400 MHz, d_4-MeOD) δ = 8.54-6.59 (m, 9H), 4.63-4.53 (m, 1H), 4.44 (td, *J* = 9.0, 1.8 Hz, 1H), 4.35-4.23 (m, 1H), 3.73-3.57 (m, 8H), 2.95-2.87 (m, 2H), 2.53 (ddd, *J* = 11.0, 9.6, 4.4 Hz, 1H), 2.29-2.21 (m, 3H), 1.72-1.55 (m, 4H), 1.36-1.26 (m, 21H). **UPLC-MS (+*ESI*)** *m/z* = 799.0 $(M+H)^+$.

C_{10}-FLAQS (EP15):[154] Fluorophore **10** (11.0 mg, 0.017 mmol, 1.0 eq.) was dissolved in CH_2Cl_2 (1.5 mL) and TFA (1.5 mL) and stirred at room temperature for 5 h. The reaction was concentrated *in vacuo*. To a mixture of activated decandioic acid (5.5 mg, 0.014 mmol, 0.8 eq.) in MeCN (1.0 mL) was added (*S*)-α-amino-γ-butyrolactone hydrobromide (3.1 mg, 0.017 mmol, 1.0 eq.) and freshly distilled Et_3N (5 µL, 0.034 mmol, 2.0 eq.) and the mixture was stirred at room temperature for 6.5 h. The previously deprotected **10** in MeCN (1.0 mL) was added and the mixture was stirred at room temperature for 15 h. It was concentrated under reduced pressure and the residue was extracted with H_2O and CH_2Cl_2 (3 x 5 mL). The combined organic layers

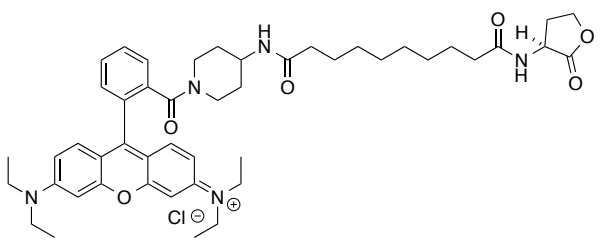

were washed with brine, dried over Na_2SO_4, filtered and concentrated *in vacuo*. The crude product was purified by size-exclusion chromatography (MeOH) to yield 12.6 mg of the impure title compound as a purple solid.

R_f = 0.25 (CH_2Cl_2/MeOH 7:1). **^{1}H-NMR** (400 MHz, d_4-MeOD) δ = 7.80-7.78 (m, 2H), 7.68-7.62 (m, 1H), 7.53-7.46 (m, 1H), 7.28 (dd, *J* = 9.5, 2.7 Hz, 2H), 7.07 (t, *J* = 8.4 Hz, 2H), 6.97 (d, *J* = 2.4 Hz, 2H), 4.62-4.52 (m, 1H), 4.43 (td, *J* = 9.0, 1.9 Hz, 1H), 4.33-4.23 (m, 1H), 4.13 (d, *J* = 12.3 Hz, 1H), 3.79-3.66 (m, 9H), 3.08-2.97 (m, 1H), 2.72-2.64 (m, 1H), 2.57-2.48 (m, 1H), 2.31-2.18 (m, 2H), 2.12 (t, *J* = 7.4 Hz, 2H), 1.83-1.71 (m, 3H), 1.63-1.52 (m, 4H), 1.32 (t, *J* = 6.2 Hz, 24H).

C_{13}-3-Oxo-FLAQS (12):[154] To a solution of **EP8** (5.0 mg, 0.011 mmol, 1.0 eq.) in CH_2Cl_2 (0.5 mL) was added TFA (0.5 mL) and the mixture was stirred at room temperature for 3 h. The reaction mixture was concentrated and used without further purification. To a solution of rhodamine B (**5**, 5.4 mg, 0.011 mmol, 1.0 eq.) in MeCN (2 mL) was added *N*-hydroxysuccinimide (1.31 mg, 0.011 mmol, 1.0 eq.) and 1-(3-dimethylaminopropyl)-3-ethylcarbo-diimide hydrochloride (2.18 mg, 0.011 mmol, 1.0 eq.) and the mixture was stirred at room temperature for 4 h. To this mixture was added the previously deprotected **EP8** and Et_3N (3 µL, 0.023 mmol, 2.0 eq.) and the mixture was stirred at room temperature for 15 h. The solvent was evaporated under reduced pressure and the residue was extracted with H_2O and CH_2Cl_2 (3 x 5 mL). The combined organic layers were washed with brine, dried over Na_2SO_4, filtered, and concentrated. The crude product was purified by size exclusion chromatography (Sephadex LH-20, MeOH) to yield 8.6 mg of impure product as a purple solid.

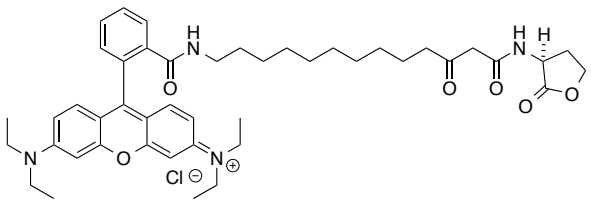

R_f = 0.45 (CH_2Cl_2/MeOH 7:1). **^{1}H-NMR** (400 MHz, d_4-MeOD) δ = 8.10 (dd, *J* = 7.4, 1.2 Hz, 1H), 7.91-7.81 (m, 1H), 7.63 (ddt, *J* = 8.9, 7.4, 3.7 Hz, 2H), 7.56-7.48 (m, 2H), 7.35-7.21 (m, 2H), 7.07 (dd, *J* = 5.2, 2.2 Hz, 1H), 6.99 (dd, *J* = 9.5, 2.5 Hz, 1H), 4.61 (dd, *J* = 10.9, 9.2 Hz, 1H), 4.44 (td, *J* = 9.0, 1.7 Hz, 1H), 4.29 (ddd, *J* = 10.6, 9.0,

6.5 Hz, 1H), 3.65 (q, *J* = 7.1 Hz, 8H), 3.04 (t, *J* = 6.9 Hz, 2H), 2.59-2.53 (m, 2H), 2.39-2.10 (m, 2H), 1.57-1.51 (m, 2H), 1.29 (t, *J* = 7.1Hz, 12H), 1.16 (t, *J* = 7.0 Hz, 16H).

C_{14}-3-Oxo-FLAQS (13):[154] To a solution of **EP6** (10.0 mg, 0.023 mmol, 1.0 eq.) in

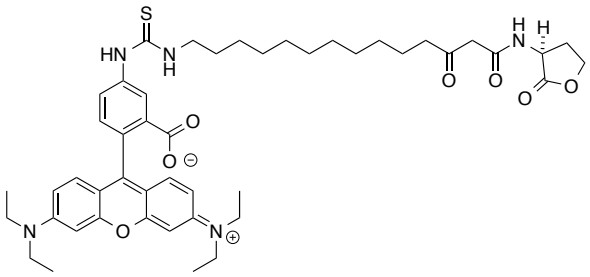

CH_2Cl_2 (0.5 mL) was added TFA (0.5 mL) and the mixture was stirred at room temperature for 3 h. The reaction mixture was concentrated and subsequently dissolved in MeCN (1.5 mL). Rhodamine B isothiocyanate (**8**, mixed isomers, 11.4 mg, 0.023 mmol, 1.0 eq.) and Et_3N (5 µL, 0.045 mmol, 2.0 eq.) were added and the mixture was stirred at room temperature for 17 h. The solvent was concentrated and the residue was extracted with H_2O and CH_2Cl_2 (3 x 5 mL). The combined organic layers were washed with brine, dried over Na_2SO_4, filtered, and concentrated. The crude product was recrystallized with CH_2Cl_2 in EtO_2 to yield 34.9 mg of impure product as a purple solid.

R_f = 0.20 (CH_2Cl_2/MeOH 7:1). **^{1}H-NMR** (400 MHz, d_4-MeOD) δ = 8.09-6.81 (m, 9H), 4.66-4.52 (m, 1H), 4.47-4.37 (m, 1H), 4.34-4.19 (m, 1H), 3.69-3.55 (m, 8H), 2.57 (ddd, *J* = 11.5, 6.0, 3.6 Hz, 2H), 2.33-2.08 (m, 2H), 1.61-1.50 (m, 2H), 1.39-1.21 (m, 14H), 1.10, (dt, *J* = 14.0, 7.0 Hz, 16H).

C_{14}-3-Oxo-FLAQS (14):[154] To a solution of **EP6** (7.7 mg, 0.023 mmol, 1.0 eq.) in

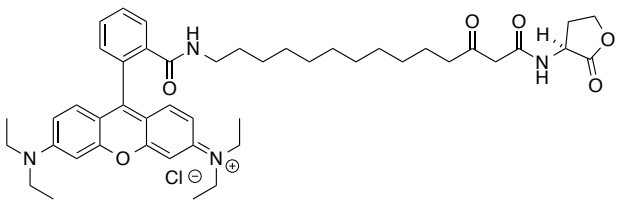

CH_2Cl_2 (0.5 mL) was added TFA (0.5 mL) and the mixture was stirred at room temperature for 3 h. The reaction mixture was concentrated under reduced pressure. To a solution of rhodamine B (**5**, 10.9 mg, 0.023 mmol, 1.0 eq.) in MeCN (1 mL) was added *N*-hydroxysuccinimide (2.6 mg, 0.023 mmol, 1.0 eq.) and 1-(3-dimethylaminopropyl)-3-ethylcarbo-diimide hydrochloride (4.35 mg, 0.023 mmol, 1.0 eq.) and the mixture was stirred at room

temperature for 4 h. To this mixture was added the previously deprotected **EP6** and Et_3N (6 µL, 0.045 mmol, 2.0 eq.) and the mixture was stirred at room temperature for 15 h. The solvent was evaporated under reduced pressure and the residue was extracted with H_2O and CH_2Cl_2 (3 x 5 mL). The combined organic layers were washed with brine, dried over Na_2SO_4, filtered, and concentrated. The crude product was purified by size exclusion chromatography (Sephadex LH-20, MeOH) to yield 37.2 mg of the impure title compound as a purple solid.

R_f = 0.30 (CH_2Cl_2/MeOH 7:1). **^{1}H-NMR** (400 MHz, d_4-MeOD) δ = 8.11 (dd, *J* = 7.5, 1.4 Hz, 1H), 7.70-7.59 (m, 2H), 7.26 (dd, *J* = 10.6, 5.5 Hz, 2H), 6.99 (dd, *J* = 9.5, 2.4 Hz, 2H), 6.91 (d, *J* = 2.4 Hz, 2H), 6.34 (ddd, *J* = 15.1, 5.7, 3.9 Hz, 1H), 4.66-4.52 (m, 1H), 4.44 (ddd, *J* = 15.1, 5.7, 3.9 Hz, 1H), 4.35-4.25 (m, 1H), 3.65 (q, *J* = 7.1 Hz, 8H), 3.22-3.10 (m, 2H), 2.63-2.49 (m, 2H), 2.43-2.21 (m, 2H), 2.43-2.21 (m, 2H), 1.29 (t, *J* = 7.0 Hz, 18H), 1.15 (dd, *J* = 13.0, 6.1, 12H).

C_{14}-3-Oxo-FLAQS (15): Hybrid **EP9** (100.0 mg, 0.181 mmol, 1.0 eq.) was dissolved in CH_2Cl_2 (1 mL) and TFA (1 mL) at r.t. and the resulting mixture was stirred for 5 h. The solvent was removed under rotary evaporation and the crude was redissolved in dry MeCN (1 mL). Rhodamine B (**5**, 87.2 mg, 0.182 mmol, 1.0 eq.) was dissolved in dry MeCN (5 mL) and *N*-hydroxysuccinimide (23.1 mg, 0.200 mmol, 1.1 eq.) and 1-(3-dimethylaminopropyl)-3-ethylcarbodiimide hydrochloride (38.4 mg, 0.200 mmol, 1.1 eq.) were added. The mixture was stirred at r.t. over night. The deprotected AHL analogue and triethylamine (51 µL, 0.364 mmol, 2.0 eq.) were added subsequently and the reaction mixture was stirred at r.t. over night. The solvent was evaporated and the residue was extracted with H_2O and CH_2Cl_2 (3 x). The combined organic layers were washed with brine, dried over Na_2SO_4, filtered, and concentrated. The crude compound was purified by preparative RP HPLC (2.5-100% water/ACN over 1 h) to yield the title compound (49.4 mg, 0.054 mmol, 30%) as purple solid.

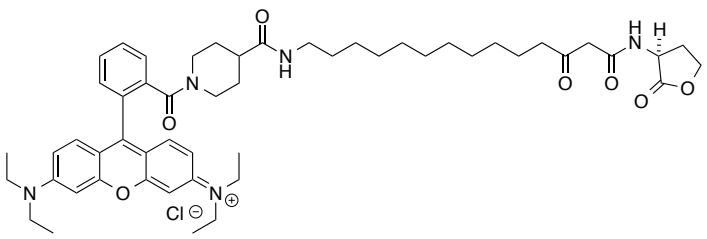

M.p.: 110.0-116.6°C. $\mathbf{R_f}$ = 0.15 (CH_2Cl_2/MeOH 7:1). **FTIR** ν = 2965, 2926, 2854, 1779, 1715, 1645, 1629, 1585, 1529, 1508, 1481, 1466, 1411, 1394, 1334, 1272, 1246, 1178, 1131, 1072, 1010, 978, 951, 921, 868, 820, 791, 758, 729, 710, 683, 664, 630 cm^{-1}. **^{1}H-NMR** (500 MHz, $CDCl_3$) δ = 7.78-7.74 (m, 2H), 7.68-7.65 (m, 1H), 7.51 (dd, *J* = 5.4, 3.3 Hz, 1H), 7.28 (t, *J* = 9.6 Hz, 2H), 7.07 (d, *J* = 9.6 HZ, 2H), 6.97 (d, *J* = 2.2 HZ, 2H), 4.61 (dd, *J* = 10.9, 9.3 Hz, 1H), 4.44 (td, *J* = 9.0, 1.7 Hz, 1H), 4.34-4.18 (m, 2H), 3.82 (d, *J* = 12.9 Hz, 1H), 3.70 (q, *J* = 7.1 Hz, 9H), 3.11 (t, *J* = 6.9 Hz, 2H), 3.06-2.59 (m, 1H), 2.60-2.52 (m, 4H), 2.38-2.22 (m, 2H), 1.71-1.58 (m, 2H), 1.57-1.51 (m, 2H), 1.49-1.40 (m, 2H), 1.34-1.27 (m, 24H). **^{13}C-NMR** (101 MHz, $CDCl_3$) δ = 206.3, 177.1, 176.6, 169.3, 159.3, 157.2, 157.1, 137.1, 133.3, 133.2, 132.0, 131.7, 131.3, 131.0, 128.7, 1156.6, 114.8, 97.4, 97.3, 67.2, 50.1, 46.9, 43.6, 43.4, 42.4, 40.3, 30.6, 30.6, 30.5, 30.5, 30.4, 30.3, 30.1, 29.6, 27.9, 24.4, 12.9. **HRMS ESI** calc. for $C_{52}H_{70}N_5O_7$ $[M]^+$: 876.5270, found: 876.5276.

C_{13}-3-Oxo-FLAQS (16):[154] To a solution of **EP8** (5.00 mg, 0.011 mmol, 1.0 eq.) in

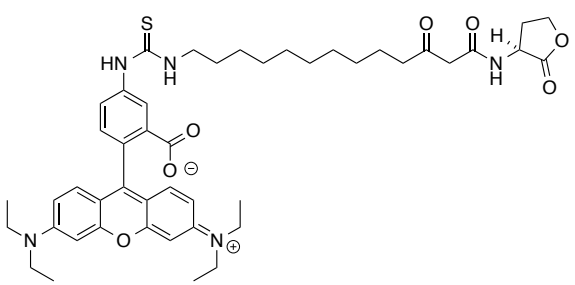

CH_2Cl_2 (0.5 mL) was added TFA (0.5 mL) and the mixture was stirred at room temperature for 3 h. The reaction mixture was concentrated and subsequently dissolved in MeCN (2.5 mL). Rhodamine B isothiocyanate (**8**, mixed isomers, 5.7 mg, 0.011 mmol, 1.0 eq.) and Et_3N (3 µL, 0.023 mmol, 2.0 eq.) were added and the mixture was stirred at room temperature for 17 h. The solvent was concentrated and the residue was extracted with H_2O and CH_2Cl_2 (3 x 5 mL). The combined organic layers were washed with brine, dried over Na_2SO_4, filtered, and concentrated. The crude product was recrystallized with CH_2Cl_2 in EtO_2 to yield 10.1 mg of impure product as a purple solid.

$\mathbf{R_f}$ = 0.23 (SiO_2, CH_2Cl_2/MeOH 7:1). **^{1}H-NMR** (400 MHz, d_4-MeOD) δ = 8.24-6.85 (m, 9H), 4.66-4.55 (m, 1H), 4.50-4.38 (m, 1H), 4.36-4.25 (m, 1H), 3.67 (d,

J = 6.6 Hz, 4H), 3.21 (dt, *J* = 7.0, 5.1 Hz, 2H), 2.96-2.86 (m, 1H), 2.64-2.51 (m, 2H), 2.38-2.22 (m, 1H), 1.73-1.48 (m, 4H), 1.31 (dd, *J* = 7.0, 4.9 Hz, 22H).

Green FLAQS (17): Hybrid **EP5** (14.0 mg, 0.035 mmol, 1.0 eq.) was dissolved in

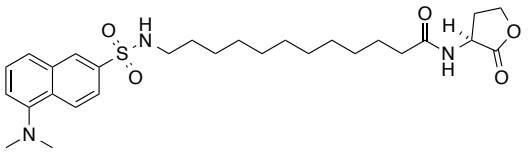

CH_2Cl_2 (0.5 mL) and TFA (0.5 mL) at r.t. and the resulting mixture was stirred for 3 h. The solvent was removed under rotary evaporation and the crude was redissolved in dry CH_2Cl_2 (2 mL). The solution was cooled down to 0 °C before triethylamine (5.0 µL, 0.035 mmol, 1.0 eq.) and dansyl chloride (9.5 mg, 0.035 mmol, 1.0 eq.) were added. After stirring for 1 h, the reaction mixture was allowed to warm up to r.t. and the stirring was continued for a further hour. TLC showed an incomplete conversion of the starting material, so more dansyl chloride (28.5 mg, 0.105 mmol, 3.0 eq.) was added and the mixture was stirred at r.t. overnight. The solvent was evaporated under reduced pressure and the residue was purified by flash chromatography (CH_2Cl_2/MeOH 10:1) to yield the desired product as a yellow solid (13.0 mg, 0.024 mmol, 70%).

M.**p**.: 69.4-71.4°C. $\mathbf{R_f}$ = 0.43 (EtOAc/pentane 2:1). **FTIR** ν = 3318, 3078, 2923, 2852, 2789, 1777, 1711, 1645, 1574, 1545, 1456, 1407, 1382, 1357, 1310, 1224, 1160, 1139, 1092, 1075, 1013, 946, 789, 725, 682, 625 cm^{-1}. **^{1}H-NMR** (500 MHz, $CDCl_3$) δ = 8.78-8.50 (m, 1H), 8.46-8.29 (m, 1H), 8.23 (d, *J* = 7.0 Hz, 1H), 7.55 (dd, *J* = 15.3, 7.2 Hz, 2H), 7.30-7.16 (m, 1H), 6.49-6.31 (m, 1H), 5.16-4.94 (m, 1H), 4.95 (ddd, *J* = 11.3, 8.6, 6.4 Hz, 1H), 4.44 (t, *J* = 8.7 Hz, 1H), 4.26 (ddd, *J* = 11.0, 9.3, 6.0 Hz, 1H), 2.99-2.84 (m, 6H), 2.77 (ddd, *J* = 13.1, 8.2, 5.2 Hz, 1H), 2.26-2.19 (m, 2H), 2.15 (dt, *J* = 2.06, 6.9 Hz, 1H), 1.61 (dt, *J* = 15.0, 7.5 Hz, 2H), 1.34 (dd, *J* = 13.8, 6.7 Hz, 2H), 1.29-1.00 (m, 16H). **^{13}C-NMR** (101 MHz, $CDCl_3$) δ = 175.9, 174.0, 135.1, 130.2, 129.8, 128.30 123.8, 115.6, 77.5, 77.2, 76.8, 66.2, 49.2, 45.7, 43.4, 36.2, 30.4, 29.6, 29.3, 29.3, 29.2, 28.9, 26.4, 25.5. **HRMS ESI** calc. for $C_{28}H_{42}N_3O_5S$ $[M-H]^+$: 532.2840, found: 532.2847.

7.4 Synthesis of Majucin-Type Sesquiterpenes

Alkene (22): To a 25 mL round-bottom flask was added (*R*)-pulegone (0.83 mL, 4.87 mmol, 1.0 eq.), sodium bicarbonate (131.1 mg, 1.55 mmol, 0.3 eq.), and Et_2O (5 mL). The mixture was cooled down to 0 °C and stirred under argon atmosphere. Bromine (0.26 mL, 5.05 mmol, 1.0 eq.) was added drop-wise over a 30 min period. The resulting mixture was stirred for 30 min at 0 °C, filtered, and added to a cold solution of sodium methoxide (594.2 mg, 11.00 mmol, 2.3 eq.) in MeOH (22 mL). The reaction mixture was heated under reflux for 2.5 h with stirring. After cooling, aq. 1 M HCl solution was added and the resulting aqueous mixture was extracted three times with Et_2O. The combined extracts were dried over Na_2SO_4, filtered, and concentrated under reduced pressure. The residue was purified by flash chromatography (pentane/Et_2O 100:1) to afford **22** (590.3 mg, 3.26 mmol, 67%, *d.r.* = 1:1) as a colourless liquid.

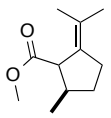

$\mathbf{R_f}$ = 0.44 (pentane/Et_2O 17:1). **FTIR**: ν = 2952, 2872, 1730, 1456, 1434, 1374, 1349, 1295, 1257, 1230, 1191, 1145, 1008, 907, 804, 741 cm^{-1}. **^{1}H NMR** (400 MHz, $CDCl_3$) δ = 3.67 (s, 3H) 3.65 (s, 3H), 3.41 (d, *J* = 8.0 Hz, 1H), 2.95 (d, *J* = 6.4 Hz), 2.14-2.50 (m, 6H), 1.93-2.01 (m, 1H), 1.62-1.81 (m, 2H), 1.66 (s, 3H), 1.63 (s, 3H), 1.61 (s, 3H), 1.57 (s, 3H), 1.31-1.29 (m, 1H), 1.04 (d, *J* = 6.7 Hz, 3H), 1.00 (d, *J* = 6.9 Hz, 3H). **^{13}C NMR** (101 MHz, $CDCl_3$) δ = 176.4, 174.7, 135.1, 134.4, 126.1, 125.9, 55.8, 52.9, 51.8, 51.2, 41.0, 39.1, 32.9, 30.6, 30.4, 21.7, 21.3, 21.2, 21.1, 19.8, 15.9. **HRMS ESI** calc. for $C_{11}H_{18}NaO_2$ $[M\text{-}Na]^+$: 205.1199, found: 205.1202.

Keto ester (19): Into a solution of **22** (360 mg, 1.98 mmol, 1 eq.) in MeOH (20 mL) and CH_2Cl_2 (100 mL) at -78 °C was bubbled ozone until the solution became light blue. Ozone addition was stopped and the solution was stirred under argon at -78 °C for 15 min and at r.t. for 10 min. Zinc powder (526 mg, 7.96 mmol, 4.0 eq.) and acetic acid (0.46 mL, 7.96 mmol, 4.0 eq.) were added to the solution. The resulting mixture was stirred at r.t. for 30 min and filtered over celite. The filtrate was neutralized with saturated $NaHCO_3$ solution and the aqueous layer was extracted two times with CH_2Cl_2. Combined organic layers were washed with water and brine, dried over Na_2SO_4, filtered and evaporated under

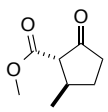

reduced pressure to afford **19** (300.6 mg, 1.92 mmol, 97%) as a colourless liquid.

R_f = 0.13 (pentane/Et_2O 9:1). **Optical rotation**: $[\alpha]_D$ = +93.5 (*c* = 0.46, $CHCl_3$). **FTIR**: ν = 2959, 2875, 1754, 1724, 1436, 1335, 1289, 1260, 1202, 1128, 1006 cm^{-1}. **^{1}H NMR** (400 MHz, $CDCl_3$) δ = 3.76 (s, 3H), 2.77 (d, *J* = 11.4 Hz, 1H), 2.67-2.53 (m, 1H), 2.48-2.39 (m, 1H), 2.38-2.26 (m, 1H), 2.20 (dddd, *J* = 12.7, 8.3, 6.2, 2.0 Hz, 1H), 1.48 (dtd, *J* = 12.6, 11.2, 8.5 Hz, 1H), 1.18 (d, *J* = 6.5 Hz, 3H). **^{13}C NMR** (101 MHz, $CDCl_3$) δ = 212.0, 169.7, 63.1, 52.5, 38.9, 36.5, 29.5, 19.4. **Elementary Analysis** calc. for $C_8H_{12}O_3$: C = 61.52, H = 7.74, N = 0.00, found: C = 61.49, H = 7.60, N = 0.00. **HRMS ESI** calc. for $C_8H_{13}O_3$ $[M-H]^+$: 157.0859, found: 157.0861.

Silyl ether (23): A mixture of 2-iodoethanol (0.39 mL, 5.0 mmol, 1.0 eq.) and imidazole (511.2 mg, 7.5 mmol, 1.5 eq.) were dissolved in dry CH_2Cl_2 (7 mL) under argon atmosphere. TBSCl (829.0 mg, 5.5 mmol, 1.1 eq.) was added at r.t. and the resulting mixture was stirred overnight. The reaction mixture was washed twice with water and brine. The organic layer was dried over Na_2SO_4, filtered and concentrated under reduced pressure to afford **23** (1.395 g, 4.88 mmol, 98%) as an orange liquid.

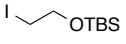

^{1}H NMR (400 MHz, $CDCl_3$) δ = 3.83 (t, *J* = 7.0 Hz, 2H), 3.20 (t, *J* = 7.0 Hz, 2H), 0.90 (s, 9H), 0.08 (s, 6H).

Analytical according to reference: C. Desroches, C. Lopes, V. Kessler, S. Parola, *Dalton Trans.* **2003**, 2085.

Silyl ether (EP16): Ketone **19** (300.0 mg, 1.92 mmol, 1.0 eq.) was dissolved in dry acetone (15 mL) under argon atmosphere. Linker **23** (630.1 mg, 2.20 mmol, 1.2 eq.) and potassium carbonate (611.2 mg, 4.40 mmol, 2.3 eq.) were added and the resulting mixture was stirred for 4 h at r.t., followed by stirring for 2 days at reflux. The solvent was removed by rotary

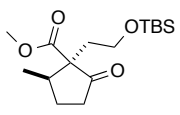

evaporation and the mixture was diluted with Et_2O and washed with water. The aqueous layer was extracted twice with Et_2O, and the combined organic layers were dried over Na_2SO_4, filtered and concentrated under reduced pressure. The crude product was purified by flash chromatography (pentane/Et_2O 10:1) to afford **EP16** (317.4 mg, 1.01 mmol, 53%, *d.r.* = 7:1) as colourless oil.

R_f = 0.44 (pentane/Et_2O 4:1). **Optical rotation**: $[\alpha]_D$ = +62.7 (*c* = 0.31, $CHCl_3$). **FTIR** ν = 2955, 2930, 2884, 2857, 1751, 1732, 1463, 1434, 1405, 1398, 1255, 1229, 1190, 1163, 1097, 1060, 1006, 970, 940, 906, 835, 810, 775, 729, 661 cm^{-1}. **^{1}H NMR** (400 MHz, $CDCl_3$) δ = 3.78-3.69 (m, 1H), 3.66 (s, 3H), 3.68-3.63 (m, 1H), 2.59-2.45 (m, 2H), 2.34-2.25 (m, 1H), 2.20-2.13 (m, 1H), 2.09-1.96 (m, 2H), 1.77 (ddd, *J* = 23.9, 11.8, 8.5 Hz, 1H), 1.02 (d, *J* = 6.9 Hz, 3H), 0.86 (s, 9H), 0.02 (d, *J* = 4.3 Hz, 6H). **^{13}C NMR** (101 MHz, $CDCl_3$) δ = 216.1, 171.4, 62.0, 59.2, 51.9, 39.0, 38.6, 34.0, 28.4, 26.0, 18.4, 15.9, -5.4, -5.4. **HRMS ESI** calc. for $C_{16}H_{31}O_4Si$ $[M-H]^+$: 315.1986, found: 315.1986.

Iodide (24): Sodium iodide (50.5 mg, 0.33 mmol, 1.1 eq.) was dissolved in MeCN (7 mL) under argon atmosphere. TMSCl (43 µL, 0.33 mmol, 1.1 eq.) was added drop-wise at r.t. The protected alcohol **EP16** (100.1 mg, 0.32 mmol, 1.0 eq.) was added and the resulting mixture was stirred for 1 h. The Reaction mixture was quenched with aq. sat. $NaHCO_3$ solution and diluted with Et_2O. The aqueous layer was extracted two times with Et_2O. Combined organic layers were dried over Na_2SO_4, filtered and evaporated under reduced pressure to afford **24** (50.9 mg, 0.16 mmol, 52%) as colourless oil, which slowly decomposed to the spiro compound **25.**

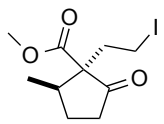

R_f = 0.25 (pentane/Et_2O 10:1). **^{1}H NMR** (400 MHz, $CDCl_3$) δ = 3.70 (s, 3H), 3.49 (ddd, *J* = 12.6, 9.2, 4.7 Hz, 1H), 3.14 (ddd, *J* = 12.7, 9.2, 4.8 Hz, 1H), 2.59-2.45 (m, 2H), 2.31-2.16 (m, 3H), 2.12-2.03 (m, 1H), 1.77 (qd, *J* = 11.9, 8.7 Hz, 1H), 1.05 (d, *J* = 6.8 Hz, 3H). **^{13}C NMR** (101 MHz, $CDCl_3$) δ = 215.5, 170.0, 64.6, 52.2, 41.3, 38.6, 38.2, 28.4, 16.1, -1.1.

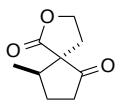

R_f = 0.50 (pentane/EtOAc 3:2). **Optical rotation**: $[\alpha]_D$ = 117.8 (*c* = 0.22, MeOH). **FTIR** ν = 2968, 2917, 2883, 1756, 1726, 1460, 1376, 1224, 1180, 1114, 1045, 1021, 973, 955, 911, 882, 832, 799 cm^{-1}. **^{1}H NMR** (500 MHz, $CDCl_3$) δ = 4.46 (td, *J* = 8.8, 6.2 Hz, 1H), 4.31 (td, *J* = 8.7, 6.2 Hz, 1H), 2.69 (dddd, *J* = 16.9, 8.3, 6.3, 3.9 Hz, 2H), 2.38-2.25 (m, 1H), 2.21 (ddd, *J* = 16.7, 9.8, 5.5 Hz, 2H), 2.14-2.00 (m, 2H), 1.23 (d, *J* = 6.3 Hz, 3H). **^{13}C NMR** (126 MHz, $CDCl_3$) δ = 213.8, 173.2, 66.7, 61.0, 41.9, 37.4, 30.2, 27.0, 14.8. **HRMS ESI** calc. for $C_9H_{13}O_3$ $[M-H]^+$: 169.0859, found: 169.0859. **X-ray crystal structure** is given in the appendices section.

Keto ester (26): To a stirred suspension of 2,4(3*H*,5*H*)-furandione (46.2 mg, 0.149 mmol, 1.0 eq.) and anhydrous LiI (22.0 mg, 0.164 mmol, 1.1 eq.) in dry THF (2 mL) was added DBU (24.7 µL, 0.164 mmol, 1.1 eq.). The resulting mixture was stirred for 30 min at r.t. before **24** (46.2 mg, 0.149 mmol, 1.0 eq.) dissolved in dry THF (2 mL) was added. The mixture was refluxed for 36 h with stirring, upon which time DMPU (0.5 mL) was added thereby dissolving the suspension in the reaction flask. The mixture was stirred at reflux for 2 days. Water and EtOAc were added and the aqueous layer was extracted twice times with EtOAc. The product was obtained after purification by flash chromatography on silica gel (pentane/EtOAc 3:2) giving the *O*-alkylated product **26** as the major product.

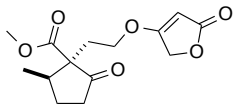

R_f = 0.24 (pentane/EtOAc 3:2). **^{1}H NMR** (400 MHz, $CDCl_3$) δ = 5.15 (s, 1H), 4.58 (d, *J* = 1.0 Hz, 2H), 4.38 (ddd, *J* = 10.1, 8.7, 5.5 Hz, 1H), 4.22-4.14 (m, 1H), 3.71 (s, 3H), 2.59 (ddd, *J* = 19.2, 8.7, 1.1 Hz, 1H), 2.38 (ddd, *J* = 14.8, 8.7, 6.4 Hz, 1H), 2.32-2.17 (m, 2H), 2.15-2.01 (m, 2H), 1.80 (ddt, *J* = 14.7, 12.4, 7.2 Hz, 1H), 1.06 (d, *J* = 6.8 Hz, 3H). **^{13}C NMR** (101 MHz, $CDCl_3$) δ = 215.6, 179.0, 173.5, 170.2, 89.4, 69.1, 67.9, 61.3, 52.4, 41.7, 38.4, 31.2, 28.4, 15.8.

Allylic ester (27): Ketone **19** (1.00 g, 6.4 mmol, 1.0 eq.) was dissolved in dry THF (14.0 mL) and freshly distilled DMPU (3.6 mL). Sodium hydride (60% dispersion in mineral oil, 307 mg, 7.7 mmol, 1.2 eq.) was added at r.t. and the grey suspension was stirred for 1 h after which it turned to a yellow solution. Allyl bromide (0.67 ml, 7.7 mmol, 1.2 eq.) was added at 0 °C and the milky mixture was stirred for 1 h at 0 °C before it was allowed to warm up to r.t. After 12 h the mixture was diluted with Et_2O (20 mL) and washed three times with water. The aqueous layers were reextracted twice with Et_2O. The combined organic layers were dried over Na_2SO_4, filtrated and evaporated under reduced pressure. Both diastereoisomers were separated by chromatography (pentane/Et_2O 9:1) giving the desired product **27** (1.06 g, 5.4 mmol, 84%) and *trans*-product (95 mg, 0.5 mmol, 8%) as a colourless liquids.

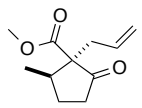

$\mathbf{R_f}$ = 0.48 (pentane/Et_2O 4:1). **Optical rotation**: $[\alpha]_D$ = +38.4 (*c* = 0.25, MeOH). **FTIR** ν = 3079, 2958, 2882, 1749, 1731, 1434, 1227, 1187, 1165, 998, 919 cm^{-1}. **^{1}H NMR** (400 MHz, $CDCl_3$) δ = 5.56-5.67 (m, 1H), 5.09-5.13 (m, 1H), 5.08 (s, 1H), 3.69 (s, 3H), 2.66 (dd, *J* = 14.2, 6.2 Hz, 1H), 2.47-2.58 (m, 2H), 2.27-2.38 (m, 1H), 2.00-2.18 (m, 2H), 1.72-1.84 (m, 1H), 1.02 (d, *J* = 6.9 Hz, 3H). **^{13}C NMR** (101 MHz, $CDCl_3$) δ = 216.2, 171.1, 133.2, 119.6, 63.1, 52.0, 39.1, 38.7, 35.8, 28.3, 15.6. **Elementary Analysis** calc. for $C_{11}H_{16}O_3$: C = 67.32, H = 8.22, N = 0.00, found: C = 67.29, H = 8.20, N = 0.00. **EI-MS** 70 eV, *m/z* (%) = 196.1 (22, M^+), 168.1 (100), 136.1 (63), 109.1 (90), 81.1 (68).

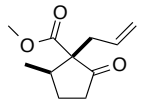

$\mathbf{R_f}$ = 0.24 (pentane/Et_2O 9:1). **Optical rotation**: $[\alpha]_D$ = +5.1 (*c* = 0.30, MeOH). **FTIR** ν = 2957, 2889, 1728, 1640, 1458, 1435, 1245, 1212, 1165, 1130, 1014, 993, 917, 848, 778 cm^{-1}. **^{1}H NMR** (400 MHz, $CDCl_3$) δ = 5.74-5.86 (m, 1H), 5.09-5.11 (m, 1H), 5.03-5.13 (m, 1H), 3.71 (s, 3H), 2.73-2.84 (m, 1H), 2.55 (ddt, *J* = 14.5, 6.7, 1.3 Hz, 1H), 2.32-2.46 (m, 1H), 2.32-2.46 (m, 3H), 2.05-2.15 (m, 1H), 1.65 (dq, *J* = 13.0, 8.8 Hz, 1H), 1.08 (d, *J* = 6.9 Hz, 3H). **^{13}C NMR** (101 MHz, $CDCl_3$) δ = 214.4, 172.0, 133.5, 118.4, 64.0, 52.6, 39.6, 37.1, 33.5, 27.6, 14.8. **HRMS ESI** calc. for $C_{11}H_{16}NaO_3$ $[M\text{-}Na]^+$: 219.0992, found: 219.0994.

Aldehyde (28):[212] Alkenyl **27** (2.50 g, 12.8 mmol, 1.0 eq.) was dissolved in a 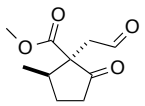 CH_2Cl_2/MeOH mixture (30 mL, 5:1) and cooled down to –78 °C. Ozone was bubbled through the stirring mixture until it turned slightly blue. The bubbling was stopped and the solution was stirred for 15 minutes at –78 °C during which time the mixture turned colourless again. Zinc powder (3.36 g, 51.0 mmol, 4.0 eq.) and acetic acid (2.6 mL, 51.0 mmol, 4.0 eq.) were added. The resulting mixture was allowed to warm up to r.t. overnight. The crude was filtrated over celite and washed with CH_2Cl_2. After evaporation of the solvent the filtrate was suspended with CH_2Cl_2, filtrated, and evaporated again giving aldehyde **28** (2.54 g, 12.8 mmol, quant.) as a colourless liquid.

R_f = 0.68 (pentane/Et_2O 9:1). **Optical rotation**: $[\alpha]_D$ = +16.4 (*c* = 0.51, MeOH). **FTIR**: ν = 2959, 2881, 2857, 2746, 1749, 1717, 1629, 1599, 1456, 1435, 1401, 1397, 1350, 1326, 1233, 1217, 1197, 1167, 1126, 1059, 1038, 1006, 904, 759 cm^{-1}. **^{1}H NMR** (400 MHz, $CDCl_3$) δ = 9.66 (d, *J* = 0.5 Hz, 1H), 3.71 (s, 3H), 3.13 (d, *J* = 18.8 Hz, 1H), 2.91 (dd, *J* = 18.8, 1.2 Hz, 1H), 2.54-2.60 (m, 2H), 2.36-2.47 (m, 1H), 2.08-2.18 (m, 1H), 1.79-1.92 (m, 1H), 1.01 (d, *J* = 6.9 Hz, 3H). **^{13}C NMR** (101 MHz, $CDCl_3$) δ = 215.3, 199.3, 170.3, 60.5, 52.4, 46.1, 40.1, 38.0, 28.6, 15.7. **HRMS ESI** calc. for $C_{10}H_{15}O_4$ $[M-H]^+$: 199.0965, found: 199.0963.

Lactone (29):[212] A solution containing the aldehyde **28** (0.49 g, 2.47 mmol, 1.0 eq.), 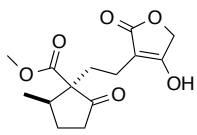 Hantzsch`ester (1.38 g, 5.44 mmol, 2.2 eq.), tetronic acid (0.26 g, 2.47 mmol, 1.0 eq.) and L-proline (28.5 mg, 0.25 mmol, 0.1 eq.) in methanol (30 mL) was stirred for 24 h at r.t. After evaporation under reduced pressure the crude product was purified by flash chromatography (CH_2Cl_2/MeOH 20:1) giving **29** (0.56 g, 1.99 mmol, 81%) as a beige solid.

M.p.: 125.5-125.9 °C. **R_f** = 0.23 (CH_2Cl_2/MeOH 10:1). **Optical rotation**: $[\alpha]_D$ = +12.8 (*c* = 0.27, MeOH). **FTIR**: ν = 2961, 2942, 2882, 2699, 1746, 1729, 1714, 1648, 1406, 1231, 1195, 1104, 1041, 988, 767 cm^{-1}. **^{1}H NMR** (400 MHz, d_4-MeOD) δ = 4.57 (s, 2H), 3.67 (s, 3H), 2.41-2.52 (m, 2H), 2.23-2.34 (m, 2H), 2.05-2.16 (m, 2H), 1.85-2.17 (m, 2H), 1.77 (ddd, *J* = 23.8, 11.5, 8.5 Hz, 1H), 1.05 (d,

J = 6.9 Hz, 3H). **^{13}C NMR** (126 MHz, d_4-MeOD) δ = 218.3, 178.4, 175.6, 172.6, 100.8, 68.3, 64.1, 52.2, 40.7, 39.7, 30.6, 29.3, 17.0, 16.1. **Elementary Analysis** calc. for $C_{14}H_{18}O_6$: C = 59.57, H = 6.43, N = 0.00, found: C = 59.27, H = 6.20, N = 0.00. **EI-MS** 70 eV, *m/z* (%) = 282.1 (1, M^+), 251.1 (9), 157.2 (77), 141.1 (100), 109.1 (40).

Carboxylic acid (30): Aldehyde **28** (0.555 g, 2.8 mmol, 1.0 eq.) was dissolved in

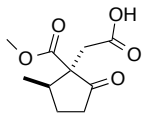

t-BuOH (10 mL) and 2-methyl-2-butene (0.1 mL). Sodium chlorite (3.165 g, 28.0 mmol, 10 eq.) and sodium phosphate (3.359 g, 28.0 mmol, 10 eq.) were dissolved in water (20 mL) and subsequently added to the mixture at r.t. The resulting mixture was stirred for 2 hours. Brine was added and the mixture was extracted three times with EtOAc. Combined organic layers were dried over Na_2SO_4, filtered and evaporated under reduced pressure. The acid **30** (600 mg, 2.8 mmol, quant.) was obtained in pure form as a colourless oil.

$\mathbf{R}_f$ = 0.21 (EtOAc/pentane 4:1). **Optical rotation**: $[\alpha]_D$ = +39.7 (c = 0.74, MeOH). **FTIR**: ν = 2959, 2883, 1710, 1455, 1434, 1401, 1336, 1220, 1199, 1159, 1122, 1069, 1052, 1002, 953, 877, 842, 809, 763, 736, 703 cm^{-1}. **^{1}H NMR** (400 MHz, $CDCl_3$) δ = 3.70 (s, 3H), 3.15 (d, J = 18.0 Hz, 1H), 2.84 (d, J = 18.0 Hz, 1H), 2.62-2.39 (m, 3H), 2.16-2.06 (m, 1H), 1.83 (dt, J = 23.6, 11.8 Hz, 1H), 1.03 (d, J = 6.9 Hz, 3H). **^{13}C NMR** (101 MHz, $CDCl_3$) δ = 215.4, 176.0, 170.1, 60.8, 53.6, 52.4, 39.6, 38.1, 35.9, 28.3, 24.6, 20.3, 15.6. **HRMS ESI** calc. for $C_{10}H_{14}NaO_5$ $[M\text{-}Na]^+$: 237.0733, found: 237.0735.

Lactone (31): Carboxylic acid **30** (32.0 mg, 0.149 mmol, 1.0eq.) was dissolved in dry

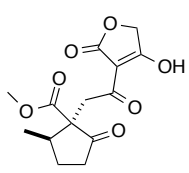

CH_2Cl_2 (2 mL) and 4-dimethylaminopyridine (5.5 mg, 0.0448 mmol, 0.3 eq.) and *N*,*N*'-dicyclohexylcarbodiimide (37.0 mg, 0.179 mmol, 1.2 eq.) were added. The mixture was cooled down to 0 °C before 4-hydroxy-2(5*H*)-furanone (15.6 mg, 0.149 mmol, 1.0 eq.) and *N*,*N*-diisopropylethylamine (27 µL, 0.164 mmol, 1.1 eq.) were added. The resulting mixture was stirred for 1 h at 0 °C and subsequently at r.t. overnight. The solution was filtered and the solid was washed with CH_2Cl_2. The filtrate was concentrated under

reduced pressure, and the residue was taken up in EtOAc. The organic phase was washed with a 1 M HCl solution and the aqueous layer was extracted twice with EtOAc. Combined organic layers were dried over Na_2SO_4, filtered and evaporated again. The crude compound was purified by preparative RP-HPLC (ACN/H_2O) to yield the desired product **31** (8.2 mg, 0.0277 mmol, 19%) as a yellow solid.

^{1}H NMR (400 MHz, $CDCl_3$) δ = 4.71 (s, 1H), 3.73 (s, 2H), 3.49 (t, *J* = 18.2 Hz, 1H), 2.61 (dd, *J* = 19.0, 9.1 Hz, 1H), 2.52–2.31 (m, 1H), 2.16–2.07 (m, 1H), 1.90-1.75 (m, 1H), 1.05 (d, *J* = 6.8 Hz, 2H). **HPLC/MS**: R_t = 2.6 min, *m/z* (ES^+) 297.1 (MH^+).

Vinyl triflate (32): Enolate **29** (228 mg, 0.81 mmol, 1.0 eq.) and 2,6-lutidine (95 µl, 0.81 mmol, 1.0 eq.) were dissolved in dry CH_2Cl_2 (10 mL) and cooled down to –78 °C. Trifluoromethanesulfonic anhydride (0.14 mL, 0.81 mmol, 1.0 eq.) was added dropwise in 20 minutes. The reaction mixture was allowed to warm up to r.t. over 7 h. The yellow solution was treated with pentane (10 mL), filtrated and the filtrate was extracted with EtOAc, washed with saturated $NaHCO_3$ solution and brine. The organic layers were dried over Na_2SO_4, filtrated and evaporated. Purification by flash chromatography (EtOAc/pentane 1:4) gave product **32** (334 mg, 0.81 mmol, quant.) as a slightly yellow solid.

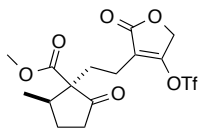

M.p.: 43.6-44.4 °C. $\mathbf{R_f}$ = 0.33 (EtOAc/pentane 1:4). **Optical rotation**: $[\alpha]_D$ = +7.2 (*c* = 0.28, MeOH). **FTIR**: ν = 2962, 2885, 2361, 2340, 1778, 1750, 1731, 1703, 1434, 1221, 1136, 1087, 1046, 816 cm^{-1}. **^{1}H NMR** (400 MHz, $CDCl_3$) δ = 4.90-4.92 (m, 2H), 3.71 (s, 3H), 2.72-2.52 (m, 2H), 2.41-2.20 (m, 3H), 2.01-2.14 (m, 2H), 1.73-1.95 (m, 2H), 1.07 (d, J = 6.8 Hz, 3H). **^{13}C NMR** (101 MHz, $CDCl_3$) δ = 215.7, 170.5, 169.8, 160.5, 120.3, 66.6, 62.2, 52.1, 41.2, 38.6, 29.4, 28.3, 17.8, 16.0. **^{19}F NMR** (376 MHz, $CDCl_3$) δ = –72.81. **Elementary Analyses** calc. for $C_{15}H_{17}F_3O_8S$: C = 43.48, H = 4.14, N = 0.00, found: C = 43.60, H = 3.95, N = 0.00. **EI-MS** 70 eV, *m/z* (%) = 281.1 (16), 249.1 (52), 221.1 (57), 166.2 (62), 141.1 (100), 109.1 (68).

Alcohol (33): Nickel(II) chloride (106 mg, 0.821 mmol, 0.1 eq.), chromium(II) chloride (3.12 g, 7.72 mmol, 6.0 eq.) and some 3Å molecular sieves were dried in a round bottom flask under reduced pressure with a heat gun. Triflate **32** (1.70 g, 4.110 mmol, 1.0 eq.) dissolved in dry DMF (40 mL) was degassed and subsequently added to the dried chromium and nickel-mixture. The green mixture was stirred at 50 °C for 24 h, then quenched by water (100 mL) and extracted with Et_2O until no more product could be detected in the aqueous layer. The combined organic layers were dried over Na_2SO_4, filtrated and evaporated. The crude was purified by flash chromatography (EtOAc/pentane 1:4) to afford the cyclized product **33** (749.0 mg, 2.81 mmol, 69%) as a white solid.

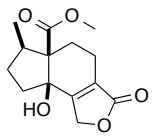

Or

To a colourless solution of vinyl bromide **36** (250 mg, 0.72 mmol, 1.0 eq.) in dry and degassed THF (7 mL) was added *n*-butyllithium (1.6 M solution in THF, 0.63 mL, 1.01 mmol, 1.4 eq.) dropwise at -78 °C. The yellow mixture was stirred subsequently for 1 h after which time it was allowed to warm up to r.t. and the resulting mixture was stirred over night. The solvent was evaporated and extracted with Et_2O and 1 M HCl solution. The organic layer was washed with water and brine and the aqueous layer reextracted with Et_2O. The combined organic layers were dried over Na_2SO_4, filtrated and evaporated. Purification was performed by flash chromatography (EtOAc/pentane 1:3) giving **33** (51 mg 0.19 mmol, 26%) as a white solid.

M.p.: 129.5-129.7 °C. $\mathbf{R_f}$ = 0.30 (EtOAc/pentane 1:3). **Optical rotation**: $[\alpha]_D = -37.0$ (*c* = 0.26, MeOH). **FTIR**: ν = 3346, 2956, 2899, 2360, 1728, 1675, 1443, 1245, 1194, 1153, 1100, 1058, 1015, 653 cm^{-1}. **^{1}H NMR** (400 MHz, $CDCl_3$) δ = 5.06 (d, *J* = 1.9 Hz, 1H), 4.96-5.03 (m, 1H), 4.78 (dt, *J* = 17.5, 2.8 Hz, 1H), 3.77 (s, 3H), 2.25-2.36 (m, 2H), 2.01-2.24 (m, 4H), 1.85-1.95 (m, 2H), 1.73-1.83 (m, 1H), 1.11 (d, *J* = 6.8 Hz, 3H). **^{13}C NMR** (126 MHz, $CDCl_3$) δ = 176.5, 173.4, 164.7, 124.8, 80.9, 64.9, 60.2, 52.4, 41.7, 38.5, 32.9, 31.2, 20.4, 18.7. **Elementary Analyses** calc. for $C_{14}H_{18}O_5$: C = 63.15, H = 6.81, N = 0.00, found: C = 63.02, H = 6.80, N = 0.00. **EI-MS** 70 eV, *m/z* (%) = 266.1 (45, M^+), 238.1 (31), 206.1 (82), 178.1 (100), 133.1 (39), 91.1 (26). **X-ray crystal structure** is given in the appendices section.

Hydrazone (34):[212] Enolate **29** (150 mg, 0.53 mmol, 1.0 eq.) and

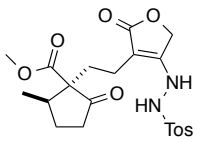

4-methylbenzenesulfonhydrazide (102 mg, 0.53 mmol, 1.0 eq.) were dissolved in dry ethanol (1.4 mL). The resulting brown solution was stirred for 2 days at 50 °C. The solvent was evaporated and the crude product was purified twice by flash chromatography (CH_2Cl_2/MeOH 20:1 and EtOAc/pentane 1:1) giving hydrazone **34** (90 mg, 0.20 mmol, 38%) and the diazo compound **35** (24 mg, 0.08 mmol, 15%) as white solids.

$\mathbf{R_f}$ = 0.24 (EtOAc/pentane 1:1). **FTIR**: ν = 3244, 2956, 1725, 1642, 1598, 1455, 1403, 1339, 1236, 1208, 1162, 1123, 1091, 1041, 994, 814, 764 cm^{-1}. **^{1}H NMR** (400 MHz, d_4-MeOD) δ = 7.81 (d, *J* = 8.3 Hz, 2H), 7.45 (d, *J* = 8.1 Hz, 2H), 4.75 (s, 2H), 3.65 (s, 3H), 2.46 (s, 3H), 2.36-2.49 (m, 3H), 2.19-2.33 (m, 2H), 2.05-2.14 (m, 1H), 1.92-2.02 (m, 1H), 1.70-1.87 (m, 3H), 1.03 (d, *J* = 6.9 Hz, 3H). **^{13}C NMR** (126 MHz, d_4-MeOD) δ = 218.6, 178.1, 172.8, 146.3, 135.5 (2C), 131.2 (2C), 129.5, 96.3, 67.6, 64.1, 52.4, 40.9, 39.6, 31.0, 29.3, 21.6, 17.7, 16.2. **HRMS ESI** calc. for $C_{21}H_{27}N_2O_7S$ $[M-H]^+$: 451.1533, found: 451.1528.

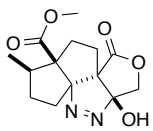

$\mathbf{R_f}$ = 0.35 (EtOAc/pentane 1:1). **Optical rotation**: $[\alpha]_D$ = –5.4 (*c* = 0.18, MeOH). **FTIR**: ν = 3250, 2954, 2873, 1716, 1562, 1463, 1431, 1377, 1255, 1243, 1223, 1190, 1172, 1124, 1057, 1030, 1008, 987, 968, 939, 853, 814, 790, 754, 711 cm^{-1}. **^{1}H NMR** (400 MHz, d_4-MeOD) δ = 4.36 (d, *J* = 11.0 Hz, 1H), 4.14 (d, *J* = 11.0 Hz, 1H), 3.75 (s, 3H), 2.60-2.70 (m, 1H), 2.34-2.46 (m, 1H), 2.12-2.18 (m, 2H), 2.02-2.10 (m, 2H), 1.76-1.82 (m, 2H), 1.53-1.62 (m, 1H), 0.99 (d, *J* = 6.9 Hz, 3H). **^{13}C NMR** (126 MHz, d_4-MeOD) δ = 177.7, 173.2, 121.8, 119.0, 75.9, 71.0, 61.0, 52.0, 41.1, 33.9, 30.8, 29.7, 26.2, 14.3. **HRMS ESI** calc. for $C_{14}H_{19}N_2O_5$ $[M-H]^+$: 295.1288, found: 295.1287. **X-ray crystal structure** is given in the appendices section.

Vinyl bromide (36):[212] To a stirred solution of **29** (100 mg, 0.35 mmol, 1.0 eq.) in

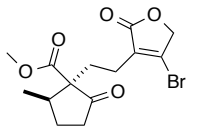

CH_2Cl_2 (1 mL) was added first DMF (50 µl, 0.71 mmol, 2.0 eq.) and subsequently oxalylbromide (40 µl, 0.43 mmol, 1.2 eq.) during 30 min at 0 °C. The resulting green solution was stirred for 1 h at 0 °C, allowed to warm up to r.t. and stirred overnight. More oxalylbromide (40 µl, 0.43 mmol, 1.2 eq.) was added at 0 °C and the mixture was stirred for 5 days at r.t. Water was added to the reaction mixture and the aqueous layer was separated and extracted three times with EtOAc. The organic layers were combined and washed with aq. sat. $NaHCO_3$ solution and brine, then dried over Na_2SO_4, filtrated and evaporated. The crude product was purified by flash chromatography (EtOAc/pentane 1:2) giving the vinyl bromide **36** (51 mg, 0.15 mmol, 42%) as slightly orange oil.

Or

Triflate **32** (54 mg, 0.13 mmol, 1.0 eq.) and TBAB (84 mg, 0.26 mmol, 2.0 eq.) were dissolved in dry toluene (1 mL) and dry THF (1 mL). The resulting colourless mixture was stirred at 50 °C overnight. Then it was heated to 60 °C and more TBAB (84 mg, 0.26 mmol, 2.0 eq.) was added. The reaction mixture was quenched with water after 2 h and subsequently extracted four times with Et_2O. The combined organic layers were dried over $MgSO_4$, filtrated and evaporated under reduced pressure. Purification was performed by flash chromatography (EtOAc/pentane 1:3) giving vinyl bromide **36** (23 mg, 0.07 mmol, 51%) as colourless oil.

$\mathbf{R_f}$ = 0.53 (pentane/EtOAc 2:1). **^{1}H NMR** (400 MHz, $CDCl_3$) δ = 4.76-4.78 (m, 2H), 3.71 (s, 3H), 2.52-2.66 (m, 2H), 2.20-2.38 (m, 3H), 1.88-2.15 (m, 3H), 1.80 (ddd, *J* = 24.0, 11.5, 8.6 Hz, 1H), 1.08 (d, *J* = 6.8 Hz, 3H). **^{13}C NMR** (126 MHz, $CDCl_3$) δ = 215.9, 171.0, 170.7, 140.1, 132.2, 73.1, 62.4, 52.0, 40.6, 38.7, 29.3, 28.3, 19.9, 16.1.

Aldehyde (37):[212] Borane dimethyl sulfide complex (2 M in THF, 0.826 mL, 1.65 mmol, 2.0 eq.) was added dropwise to a solution of the methylester **33** (220 mg, 0.826 mmol, 1.0 eq.) in dry THF (4 mL) at 0 °C. The colourless solution was stirred subsequently for 0.5 h and then warmed up to 45 °C for 2 h. After cooling down to r.t., ethanol was added until the exothermic reaction and bubbling ceased. After evaporation, the crude product was purified by flash chromatography (Et_2O/pentane 3:1) giving aldehyde **37** (149 mg, 0.63 mmol, 76%) as a white solid.

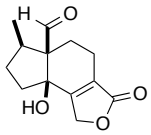

M.p.: 158.1-158.5 °C. $\mathbf{R_f}$ = 0.21 (Et_2O/pentane 3:1). **Optical rotation**: $[\alpha]_D$ = –49.3 (*c* = 0.23, MeOH). **FTIR**: ν = 3346, 2942, 2874, 2758, 1744, 1716, 1669, 1435, 1353, 1224, 1107, 1061, 1016, 929, 753 cm^{-1}. **^{1}H NMR** (400 MHz, $CDCl_3$) δ = 9.70 (s, 1H), 5.01 (ddd, *J* = 17.4, 3.4, 1.7 Hz, 1H), 4.80 (dt, *J* = 17.4, 2.7 Hz, 1H), 4.07 (d, *J* = 1.7 Hz, 1H), 2.04-2.36 (m, 6H), 1.72-1.99 (m, 3H), 1.17 (d, *J* = 7.1 Hz, 3H). **^{13}C NMR** (126 MHz, $CDCl_3$) δ = 206.8, 173.1, 163.5, 125.2, 80.1, 69.5, 61.9, 40.3, 37.7, 31.6, 28.6, 18.8, 17.7. **Elementary Analyses** calc. for $C_{13}H_{16}O_4$: C = 66.09, H = 6.83, N = 0.00, found: C = 65.90, H = 6.75, N = 0.00. **EI-MS** 70 eV, m/z (%) = 236.1 (13, M^+), 190.1 (100), 175.1 (66), 145.1 (42), 91.1 (27).

Lactone (38):[212] To the aldehyde **37** (43.0 mg, 0.18 mmol, 1.0 eq.), dissolved in THF/water (1:1, 5 mL), was added potassium cyanide (42.0 mg, 0.64 mmol, 3.5 eq.). The resulting mixture was stirred for 2 d at r.t. before the aqueous reaction mixture was extracted several times with EtOAc until no more product could be detected in the organic layer. The combined organic layers were dried over Na_2SO_4, filtrated and evaporated. The crude product was purified by flash chromatography (EtOAc/cyclohexane 1:1) giving tetracyclic compound **38** (31.0 mg, 0.12 mmol, 65%) as a white solid.

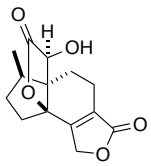

M.p.: 194.0-194.3 °C. $\mathbf{R_f}$ = 0.28 (EtOAc/cyclohexane 1:1). **Optical rotation**: $[\alpha]_D$ = –32.6 (*c* = 0.19, MeOH). **FTIR**: ν = 3479, 2953, 2929, 2874, 2361, 1785, 1725, 1682, 1442, 1359, 1217, 1191, 1133, 1086, 1046, 1022, 967 cm^{-1}. **^{1}H NMR** (400 MHz, $CDCl_3$) δ = 4.82-4.99 (m, 2H), 4.57 (d, *J* = 2.8 Hz, 1H), 2.91 (d,

J = 3.2 Hz, 1H), 2.45-2.54 (m, 2H), 2.21-2.30 (m, 1H), 2.00-2.10 (m, 3H), 1.83-1.98 (m, 2H), 1.62-1.70 (m, 1H), 1.42-1.53 (m, 1H), 1.16 (d, *J* = 6.7 Hz, 3H). **^{13}C NMR** (101 MHz, $CDCl_3$) δ = 176.3, 172.5, 157.5, 127.8, 87.4, 69.6, 68.9, 56.2, 36.2, 35.9, 30.7, 21.3, 15.8, 14.0. **HRMS ESI** calc. for $C_{14}H_{17}O_5$ $[M\text{-}H]^+$: 265.1071, found: 265.1065. **X-ray crystal structure** is given in the appendices section.

Keto lactone (39):[212] To a solution of the alcohol **38** (8.5 mg, 0.03 mmol, 1.0 eq.) in CH_2Cl_2 (1 mL) were added pyridinium chlorochromate (23.0 mg, 0.11 mmol, 3.3 eq.) and some silica gel. The resulting orange mixture was for 16 h at r.t. The reaction mixture was directly loaded onto a column. The column was eluted with CH_2Cl_2 first then with a 30:1 mixture of CH_2Cl_2/MeOH giving the α-ketolactone **39** (7.0 mg, 0.03 mmol, 83%) as colourless crystals.

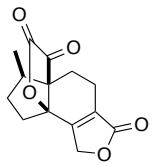

R_f = 0.36 (EtOAc/cyclohexane 1:1). **Optical rotation**: $[\alpha]_D$ = –83.2 (*c* = 0.17, $CHCl_3$). **FTIR**: ν = 2965, 2932, 2862, 1788, 1748, 1678, 1437, 1385, 1354, 1308, 1248, 1214, 1191, 1156, 1140, 1110, 1061, 1013, 969, 958, 896, 852, 831, 799, 764, 745 cm^{-1}. **^{1}H NMR** (400 MHz, $CDCl_3$) δ = 5.00-5.06 (m, 1H), 4.85-4.92 (m, 1H), 2.45-2.57 (m, 2H), 2.30-2.39 (m, 1H), 2.05-2.27 (m, 3H), 1.93-2.02 (m, 1H), 1.79 (ddd, *J* = 14.0, 10.1, 5.3 Hz, 1H), 1.54-1.61 (m, 2H), 1.05 (d, *J* = 6.9 Hz, 3H). **^{13}C NMR** (101 MHz, $CDCl_3$) δ = 196.7, 171.4, 159.0, 156.0, 130.5, 89.4, 68.9, 58.7, 46.6, 36.0, 32.7, 29.8, 18.0, 15.5. **HRMS ESI** calc. for $C_{14}H_{15}O_5$ $[M\text{-}H]^+$: 263.0914, found: 263.0912. **X-ray crystal structure** is given in the appendices section.

TMS ether (40):[212] To a solution of the alcohol **38** (23 mg, 0.09 mmol, 1.0 eq.) in CH_2Cl_2 (1.5 mL) were added 2,6-lutidine (0.3 mL, 0.26 mmol, 3.0 eq.) and trimethylsilane triflate (24 µl, 0.13 mmol, 1.5 eq.) at 0 °C. The colourless solution was stirred at this temperature for 3 h, quenched with water and extracted with EtOAc. The organic layer was dried over $MgSO_4$, filtrated and evaporated. The resulting crude product was purified by flash chromatography (Et_2O/pentane 2:1) to obtain the protected alcohol **40** (26 mg,

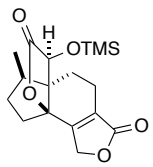

0.08 mmol, 99%) as a white solid.

R_f = 0.71 (EtOAc/cyclohexane 1:1). **^{1}H NMR** (400 MHz, $CDCl_3$) δ = 4.92-4.99 (m, 1H), 4.80-4.86 (m, 1H), 4.54 (s, 1H), 2.42-2.51 (m, 1H), 2.20-2.28 (m, 1H), 1.79-2.07 (m, 5H), 1.50-1.67 (m, 2H), 1.09 (d, *J* = 6.7 Hz, 3H), 0.22 (s, 9H). **^{13}C NMR** (101 MHz, $CDCl_3$) δ = 175.2, 172.7, 158.2, 127.7, 86.6, 70.7, 69.0, 55.6, 36.8, 36.3, 30.8, 22.3, 16.1, 14.1, 0.6.

Silyl ether (41):[212] To a solution of alcohol **38** (10.0 mg, 0.04 mmol, 1.0 eq.) in CH_2Cl_2 (1 mL) were added some drops of triethylamine and imidazole (7.7 mg, 0.11 mmol, 3.0 eq.). The mixture was treated with chlorotriethylsilane (20 µl, 0.11 mmol, 3.0 eq.) at 0 °C. The resulting colourless reaction mixture was allowed to warm up to r.t. overnight. As no reaction had occurred the solution was heated up to 35 °C and a catalytic amount of DMAP was added. After stirring for 2 h the reaction mixture was quenched with water. The aqueous reaction mixture was extracted four times with CH_2Cl_2 and the combined organic layers were dried over $MgSO_4$, filtrated and evaporated under reduced pressure. Purification was performed by flash chromatography (EtOAc/pentane 1:1) to yield the protected alcohol **41** (11.0 mg, 0.03 mmol, 77%) as a white powder.

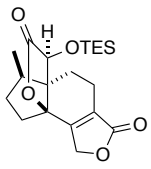

R_f = 0.29 (EtOAc/pentane 1:4). **^{1}H NMR** (400 MHz, $CDCl_3$) δ = 4.92-4.99 (m, 1H), 4.79-4.87 (m, 1H), 4.56 (s, 1H), 2.41-2.51 (m, 1H), 2.19-2.26 (m, 1H), 1.78-2.08 (m, 5H), 1.50-1.65 (m, 2H), 1.11 (d, *J* = 6.7 Hz, 3H), 0.98 (t, *J* = 7.9 Hz, 9H), 0.81-0.63 (m, 6H). **^{13}C NMR** (101 MHz, $CDCl_3$) δ = 175.1, 172.7, 158.3, 127.6, 86.5, 70.7, 69.0, 56.0, 36.9, 36.4, 30.8, 22.3, 16.1, 14.1, 7.0, 5.4. **HRMS ESI** calc. for $C_{20}H_{31}O_5Si$ $[M-H]^+$: 379.1935, found: 379.1932.

Butenolide (43): To a stirred suspension of 3,4,5,6-tetrahydrophthalic anhydride (**42**, 500.0 mg, 3.22 mmol, 1.0 eq.) in dry THF (8 mL) at 0 °C was added drop wise a solution of $NaBH_4$ in dry THF (12 mL) over 3 h under argon atmosphere. The mixture was stirred for an additional hour at r.t., cooled down to 0 °C and acidified with 1 M HCl solution until pH 3. Some more water and CH_2Cl_2 were added and the aqueous layer was extracted 2 times with CH_2Cl_2. Combined organic layers were dried over Na_2SO_4, filtered and evaporated under reduced pressure. Purification was performed by flash chromatography (EtOAc/pentane 1:3) to yield butenolide **43** (331.5 mg, 2.40 mmol, 75%) as slightly yellow solid.

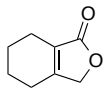

$\mathbf{R_f}$ = 0.32 (pentane/EtOAc 3:1). **^{1}H NMR** (400 MHz, $CDCl_3$) δ = 4.69-4.66 (m, 2H), 2.35-2.24 (m, 2H), 2.25-2.18 (m, 2H), 1.83-1.62 (m, 4H).

Analytical according to reference: D. Butina and F. Sondheimer, *Synthesis* **1980**, 543.

Lactone (44): Copper(I) iodide (84.4 mg, 0.434 mmol, 2.0 eq.) was heated up using a heating gun under vacuum. Dry Et_2O (1 mL) was added and the mixture was cooled down to 0 °C under argon atmosphere. Methyl lithium (1.6 M in Et_2O, 540 µL, 0.869 mmol, 4.0 eq.) was added dropwise and the colourless solution was stirred for 10 min. The solvent was removed under reduced pressure at 0 °C and dry CH_2Cl_2 (1 mL) was added. The resulting solution was stirred for 5 min at 0 °C and the solvent was removed again under reduced pressure. Dry CH_2Cl_2 (1 mL) was added and the mixture was cooled down to –78 °C. Chlorotrimethylsilane (0.057 µL, 0.434 mmol, 2.0 eq.) and **43** (dissolved in 0.5 mL CH_2Cl_2, 30.0 mg, 0.217 mmol, 1.0 eq.) were added to the yellow solution. The mixture was slowly heated up to r.t. overnight and subsequently quenched by addition of a saturated aqueous NH_4Cl solution, followed by extraction with CH_2Cl_2 (2 x). Combined organic layers were dried over Na_2SO_4, filtered and evaporated under reduced pressure. The crude product was purified by flash chromatography with pentane/EtOAc 5:1 to yield the desired product (13.7 mg, 0.089 mmol, 41%) in a 1:3.5 diastereoisomeric mixture of the *cis*/*trans* bicyclic ring system as a white solid and some unreacted starting material (4.8 mg, 0.035 mmol).

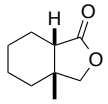

R_f = 0.47 (pentane/EtOAc 4:1). **^{1}H NMR** (400 MHz, $CDCl_3$) δ = 3.90 (d, *J* = 8.6 Hz, 1H), 3.80 (d, *J* = 8.6 Hz, 1H), 2.28-2.23 (m, 1H), 2.09-2.00 (m, 1H), 1.65-1.51 (m, 4H), 1.50-1.39 (m, 3H), 1.18 (s, 3H). **^{13}C NMR** (126 MHz, $CDCl_3$) δ = 178.7, 80.0, 46.2, 38.7, 33.1, 22.7, 21.6, 21.4, 21.3.

Analytical according to reference: A. B. Smith III, M. Visnick, J. N. Haseltine, P. A. Sprengeler, *Tetrahedron* **1986**, *42*, 2957.

Diene (45): Ester **33** (301 mg, 1.13 mmol, 1.0 eq.) was dissolved in dry THF (16 mL) and Burgess reagent (417 mg, 1.70 mmol, 1.5 eq.) was added. The clear solution was stirred for 3.5 h at r.t. After 1 h, a white precipitate was observable. Water (8 mL) was added and extracted with Et_2O (3 x 25 mL). The combined organic layers were washed with brine (13 mL) and then dried over Na_2SO_4, filtered and evaporated to obtain a white solid. The crude was purified by flash chromatography (pentane/EtOAc 3:1) to obtain the desired olefin **45** (262 mg, 1.06 mmol, 93%) as a white solid.

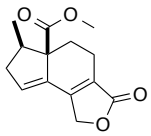

M.p.: 124.9-125.6 °C. **R_f** = 0.24 (pentane/EtOAc 4:1). **Optical rotation**: $[\alpha]_D$ = +193.5 (*c* = 0.16, $CHCl_3$). **FTIR** ν = 2952, 2936, 2846, 1740, 1715, 1644, 1439, 1346, 1239, 1172, 1042, 1014, 980, 761, 744 cm^{-1}. **^{1}H NMR** (400 MHz, $CDCl_3$) δ = 6.18 (s, 1H), 4.98-4.81 (m, 2H), 3.67 (s, 3H), 2.74-2.56 (m, 1H), 2.52-2.15 (m, 2H), 1.35 (ddd, *J* = 12.8, 11.7, 5.8 Hz, 1H), 1.07 (d, *J* = 7.0 Hz, 3H). **^{13}C NMR** (101 MHz, $CDCl_3$) δ = 173.8, 173.1, 151.8, 136.2, 133.2, 126.5, 69.1, 59.9, 52.0, 45.8, 40.6, 30.8, 19.7, 14.9. **HRMS ESI** calc. for $C_{14}H_{17}O_4$ $[M-H]^+$: 249.1121, found: 249.1119. **X-ray crystal structure** is given in the appendices section.

Lactone (46): Diene **45** (8.4 mg, 0.0338 mmol, 1.0 eq.) was dissolved in EtOH (2 mL). A catalytic amount of Pd/C (10 % Pd) was added and the mixture was stirred for 45 min at 5 bar H_2 atmosphere. The crude mixture was filtered over a pad of silica and celite and washed with EtOAc. The organic layer was evaporated under reduced pressure giving the reduced

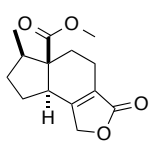

product **46** (8.5 mg, 0.0338 mmol, quant.) as colourless oil.

R_f = 0.21 (pentane/EtOAc 4:1). **Optical rotation**: $[\alpha]_D$ = +12.4 (*c* = 0.40, $CHCl_3$). **FTIR**: ν = 2957, 2925, 2853, 1722, 1436, 1380, 1351, 1259, 1196, 1078, 1017, 854, 797, 741 cm^{-1}. **^{1}H NMR** (400 MHz, $CDCl_3$) δ = 4.83-4.70 (m, 2H), 3.61 (s, 3H), 2.79-2.69 (m, 1H), 2.64 (dd, *J* = 13.3, 6.9 Hz, 1H), 2.51-2.40 (m, 1H), 2.39–2.27 (m, 1H), 2.26-2.18 (m, 1H), 2.18-2.08 (m, 1H), 1.99-1.90 (m, 1H), 1.88-1.81 (m, 1H), 1.53-1.45 (m, 2H), 0.99 (d, *J* = 6.9 Hz, 3H). **^{13}C NMR** (101 MHz, $CDCl_3$) δ = 174.0, 173.3, 164.8, 124.6, 70.4, 59.1, 51.4, 47.8, 42.6, 32.0, 30.3, 22.7, 20.1, 15.7. **HRMS ESI** calc. for $C_{14}H_{19}O_4$ $[M-H]^+$: 251.1278, found: 251.1279.

Lactone (50): To a dry and degassed solution of THF (12.0 mL) and NMP (0.6 mL)

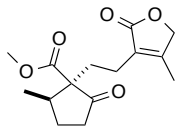

was added ester **32** (516.0 mg, 1.25 mmol, 1.0 eq.) and $Fe(acac)_3$ (22.0 mg, 62.3 μmol, 5 mol%) and cooled down to –30 °C. The mixture was stirred for 10 minutes at this temperature and MeMgBr (3.2 M in THF, 54.5 μl, 1.74 mmol, 1.4 eq.) was rapidly added to the orange solution. The mixture turned into a brown to green mixture, which ended in a colourless solution with brown precipitate. The reaction was quenched after 1 h with saturated NH_4Cl solution at –30 °C. The mixture was allowed to warm up to r.t. and water was added and the organic layer was separated. The aqueous layer was extracted with EtOAc (4 x 20 mL) and the combined organic layers were dried over Na_2SO_4, filtered and evaporated under reduced pressure. The crude was purified by flash chromatography (pentane/EtOAc 2:1 then 1:1) to obtain the desired β-methyl lactone **50** (333.9 mg, 1.19 mmol, 96%) as colourless oil.

R_f = 0.24 (EtOAc/pentane 1:2). **Optical rotation**: $[\alpha]_D$ = +61.0 (*c* = 0.29, $CHCl_3$). **FTIR**: ν = 2985, 1743, 1678, 1451, 1228, 1166, 1032, 762 cm^{-1}. **^{1}H NMR** (400 MHz, $CDCl_3$) δ = 4.61 (s, 2H), 3.69 (s, 3H), 2.59-2.45 (m, 2H), 2.42-2.32 (m, 1H), 2.29-2.08 (m, 3H), 2.05 (brs, 3H), 1.92-1.87 (m, 2H), 1.85-1.73 (m, 1H), 1.07 (d, *J* = 6.8 Hz, 3H). **^{13}C NMR** (101 MHz, $CDCl_3$) δ = 216.4, 174.9, 171.0, 157.7, 127.0, 72.7, 62.7, 52.0, 40.3, 38.9, 30.6, 28.4, 18.4, 16.1, 12.3. **HRMS ESI** calc. for $C_{15}H_{21}O_5$ $[M-H]^+$: 281.1384, found: 281.1383.

Oxetane (51 and 52):[216] Ester **50** (53.0 mg, 189.0 µmol, 1.0 eq.) was dissolved in dry and degassed benzene (19 mL) and added into a Quartz-tube under argon atmosphere and irradiated for 3 h. The crude was evaporated to obtain yellow oil, which was purified by flash chromatography (pentane/Et_2O 3:2) to obtain the oxetane **51** (10.0 mg, 35.7 µmol, 19%) and **52** (7.3 mg, 26.0 µmol, 14%) as white solids.

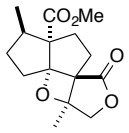

M.p.: 92.2-92.7 °C. $\mathbf{R_f}$ = 0.30 (Et_2O/pentane 1:1). **Optical rotation**: $[\alpha]_D$ = –1.4 (*c* = 0.30, $CHCl_3$). **FTIR** ν = 2955, 2927, 1759, 1722, 1452, 1274, 1249, 1130, 1015, 797 cm^{-1}. **^{1}H NMR** (500 MHz, $CDCl_3$) δ = 4.56 (d, *J* = 10.6 Hz, 1H), 4.05 (d, *J* = 10.6 Hz, 1H), 3.75 (s, 3H), 2.73-2.64 (m, 2H), 2.24-2.17 (m, 1H), 2.12-2.03 (m, 4H), 1.85-1.80 (m, 1H), 1.45 (s, 3H), 1.20-1.11 (m, 1H), 0.95 (d, *J* = 7.0 Hz, 3H). **^{13}C NMR** (126 MHz, $CDCl_3$) δ = 176.0, 174.3, 106.0, 83.1, 78.9, 64.9, 60.1, 52.4, 40.2, 34.3, 30.7, 30.6, 26.8, 19.7, 15.7. **X-ray crystal structure** is given in the appendices section.

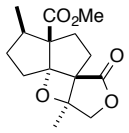

M.p.: 95.8-96.7 °C. $\mathbf{R_f}$ = 0.24 (Et_2O/pentane 1:1). **Optical rotation**: $[\alpha]_D$ = –15.0 (*c* = 0.02, $CHCl_3$). **FTIR** ν = 2955, 2947, 1760, 1725, 1438, 1246, 1151, 1114, 1025, 1002, 772 cm^{-1}. **^{1}H NMR** (500 MHz, $CDCl_3$) δ = 4.53 (d, *J* = 10.6 Hz, 1H), 4.04 (d, *J* = 10.6 Hz, 1H), 3.73 (s, 3H), 2.62 (ddd, *J* = 13.9, 12.5, 8.1 Hz, 1H), 2.25-2.16 (m, 2H), 2.14-2.06 (m, 2H), 2.02-1.98 (m, 1H), 1.88-1.69 (m, 3H), 1.47 (s, 3H), 0.91 (d, *J* = 6.6 Hz, 3H). **^{13}C NMR** (126 MHz, $CDCl_3$) δ = 176.0, 172.0, 105.0, 83.0, 79.3, 67.0, 59.5, 51.8, 40.0, 32.0, 31.4, 30.2, 23.9, 20.1, 15.3.

Vinyl triflate (55): Ketone **50** (165.0 mg, 0.589 mmol, 1.0 eq.) was dissolved in dry THF (5 mL) and cooled down to –40 °C under argon atmosphere. LiHMDS (1 mol/L in THF, 1.77 mL, 1.779 mmol, 3.0 eq.) was added drop wise while the reaction slowly rose to –20 °C. After stirring for 30 min, *N*-phenyl*bis*(trifluoromethanesulfonimide) (434.0 mg, 1.180 mmol, 2.0 eq.) was added and the reaction mixture was stirred for 3 h at 0 °C. A saturated $NaHCO_3$ solution was added drop wise (exothermic) to the brown solution, followed by water.

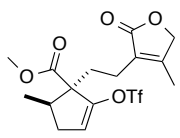

The crude was extracted three times with EtOAc. Combined organic layers were dried over Na_2SO_4, filtered and evaporated under reduced pressure. The residue was purified by flash chromatography (pentane/EtOAc 4:1) giving product **55** (82.3 mg, 0.200 mmol, 34%) as a colourless oil.

$\mathbf{R_f}$ = 0.33 (pentane/EtOAc 3:1). **Optical rotation**: $[\alpha]_D$ = +3.0 (*c* = 0.90, MeOH). **FTIR**: ν = 2960, 2934, 1734, 1678, 1599, 1496, 1421, 1381, 1338, 1203, 1138, 1082, 1047, 1005, 934, 900, 836, 767, 736, 696 cm^{-1}. **^{1}H NMR** (400 MHz, $CDCl_3$) δ = 5.86 (t, *J* = 2.5 Hz, 1H), 4.62 (d, *J* = 0.8 Hz, 2H), 3.72 (s, 3H), 2.65-2.52 (m, 2H), 2.41 (td, *J* = 12.7, 4.4 Hz, 1H), 2.25-2.10 (m, 2H), 2.03 (s, 3H), 2.01-1.94 (m, 1H), 1.86 (ddd, *J* = 14.1, 12.3, 5.0 Hz, 1H), 1.03 (d, *J* = 6.7 Hz, 3H). **^{13}C NMR** (101 MHz, $CDCl_3$) δ = 174.9, 171.9, 157.7, 148.2, 129.6, 126.6, 123.7, 118.7, 72.7, 60.8, 52.1, 39.7, 35.2, 31.7, 18.4, 16.5, 12.2. **HRMS ESI** calc. for $C_{16}H_{20}F_3O_7S$ $[M-H]^+$: 413.0876, found: 413.0875.

Hydrazone (58): Ketoester **50** (7.5 mg, 26.8 µmol, 1.0 eq.) was dissolved in dry EtOH (0.2 mL). Tosylhydrazide (44.8 mg, 0.24 mmol, 9.0 eq.) and 4 drops of an aqueous 1 M HCl solution were added. The resulting mixture was stirred for 25 h at r.t. To the clear solution was added water (1.0 mL) and then extracted three times with EtOAc. Combined organic layers were dried over Na_2SO_4, filtered and evaporated to obtain a colourless oil. The crude was purified by flash chromatography (pentane/EtOAc 3:1) to obtain the desired tosylhydrazone **58** (7.0 mg, 13.4 µmol, 50%) as a white solid.

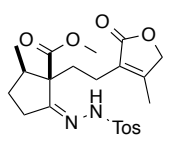

$\mathbf{R_f}$ = 0.18 (Et_2O/pentane 3:1). **^{1}H NMR** (400 MHz, $CDCl_3$) δ = 7.77 (d, *J* = 8.4 Hz, 2H), 7.27 (d, *J* = 7.5 Hz, 2H), 5.61 (brs, 1H), 4.62 (s, 2H), 3.50 (s, 3H), 2.40-2.38 (m, 4H), 2.23-2.11 (m, 3H), 2.07 (s, 3H), 2.01-1.86 (m, 4H), 1.67-1.56 (m, 1H), 0.94 (d, *J* = 6.8 Hz, 3H).

Epoxide (60): To a solution of the diene **45** (38.0 mg, 0.153 mmol, 1.0 eq.) in CH_2Cl_2 (5 mL) was added *m*-CPBA (70%, 60.4 mg, 0.245 mmol, 1.6 eq.) at 0 °C. The resulting mixture was stirred at 4 °C for 3.5 h and slowly heated up to r.t. and stirred for 3 days. The reaction mixture was poured into a mixture of aq. sat. $NaHCO_3$ and excess sodium thiosulfate, and extracted with ether. The organic layer washed with saturated sodium bicarbonate solution and brine, dried over Na_2SO_4, filtered and reduced under reduced pressure. The crude residue was purified by flash chromatography (pentane/EtOAc 4:1) giving epoxide **60** (36.2 mg, 0.137 mmol, 90%) as a crystalline compound.

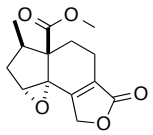

R_f = 0.24 (pentane/EtOAc 4:1). **^{1}H NMR** (400 MHz, $CDCl_3$) δ = 4.79-4.67 (m, 2H), 4.09 (s, 1H), 3.66 (s, 3H), 2.63-2.35 (m, 3H), 2.24 (dd, *J* = 13.6, 6.6 Hz, 1H), 1.83 (dp, *J* = 10.2, 7.0 Hz, 1H), 1.72-1.59 (m, 2H), 0.91 (d, *J* = 7.2 Hz, 3H). **^{13}C NMR** (101 MHz, $CDCl_3$) δ = 172.5, 172.3, 155.0, 135.3, 68.5, 63.8, 63.0, 55.5, 51.9, 35.5, 24.7, 20.1, 13.9. **X-ray crystal structure** is given in the appendices section.

Diol (62): Olefin **45** (80.0 mg, 0.322 mmol, 1.0 eq.) and NMO (49.7 mg, 0.483 mmol, 1.5 eq.) were dissolved in *tert*-butanol (3 mL) and water (1 mL). The clear solution was cooled to 0° C and OsO_4 (4% solution in water, 0.13 mL, 16.1 μmol, 5 mol%) was added dropwise. The clear solution was then allowed to warm up to r.t. and then stirred for 3 days. To the yellow solution was added saturated Na_2SO_3 solution (15 mL) and the orange to yellow emulsion was stirred for 30 minutes at r.t. The mixture was extracted with EtOAc (3 x 10 mL) and the combined organic layers were washed with brine (10 mL), dried over Na_2SO_4, filtered and evaporated to obtain a yellow oil. The crude was purified by flash chromatography (pentane/EtOAc 1:1) to obtain the desired diol **62** (76.7 mg, 0.272 mmol, 84%, *d.r.* = 10:1) as a white solid.

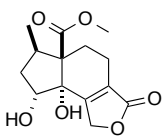

M.p.: 126.3-126.8 °C. **R_f** = 0.25 (pentane/EtOAc 1:1). **Optical rotation**: $[\alpha]_D$ = +45.6 (*c* = 0.16, $CHCl_3$). **FTIR** ν = 3449, 2959, 2929, 2360, 1727, 1714, 1660, 1429, 1351, 1255, 1202, 1037, 1021, 739 cm^{-1}. **^{1}H NMR** (400 MHz, $CDCl_3$) δ = 5.16 (dd, *J* = 12.2, 6.4 Hz, 1H), 5.03-4.70 (m, 2H), 3.69 (s, 1H), 3.62 (s, 3H), 2.72-2.53 (m,

1H), 2.50-2.40 (m, 1H), 2.40-2.22 (m, 3H), 2.22-2.09 (m, 1H), 1.90 (dd, *J* = 9.2, 7.0 Hz, 2H), 0.90 (d, *J* = 7.1 Hz, 3H). **^{13}C NMR** (101 MHz, $CDCl_3$) δ = 173.9, 173.5, 162.6, 128.0, 76.9, 71.5, 69.1, 63.3, 51.7, 41.4, 37.5, 22.4, 19.8, 15.7. **HRMS ESI** calc. for $C_{14}H_{19}O_6$ $[M-H]^+$: 283.1176, found: 283.1178.

Acetal (63): To a solution of the diol **62** (33.5 mg, 0.119 mmol, 1 eq.) in dry THF (3 mL) were added 2-methoxypropene (114 µL, 1.19 mmol, 10.0 eq.) and a catalytic amount of *p*-TSA and the reaction mixture was stirred at room temperature overnight under argon atmosphere. The reaction mixture was quenched with saturated $NaHCO_3$ solution and extracted three times with EtOAc. The combined organic layers were dried over Na_2SO_4, filtered and evaporated under reduced pressure. The crude product was purified by flash chromatography (pentane/EtOAc 3:1) to give the protected diol **63** (27.3 mg, 0.085 mmol, 71%) as a white solid.

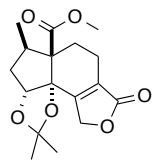

R_f = 0.67 (pentane/EtOAc 2:1). **Optical rotation**: $[\alpha]_D$ = +59.7 (*c* = 0.27, $CHCl_3$). **FTIR** ν = 3011, 2963, 2938, 2874, 1759, 1717, 1665, 1460, 1432, 1345, 1290, 1264, 1242, 1180, 1158, 1122, 1103, 1076, 1037, 1021, 972, 941, 897, 854, 813, 759, 744, 689 cm^{-1}. **^{1}H NMR** (400 MHz, $CDCl_3$) δ = 5.08-5.03 (m, 1H), 5.02-4.94 (m, 1H), 4.83 (dt, *J* = 17.4, 3.0 Hz, 1H), 3.60 (s, 3H), 2.58-2.29 (m, 4H), 2.09 (dt, *J* = 11.5, 7.7 Hz, 1H), 1.93 (ddd, *J* = 14.7, 7.9, 1.0 Hz, 1H), 1.80 (ddd, *J* = 14.7, 11.5, 8.2 Hz, 1H), 1.45 (s, 3H), 1.33 (s, 3H), 1.25 (s, 1H), 0.91 (d, *J* = 7.0 Hz, 3H). **^{13}C NMR** (101 MHz, $CDCl_3$) δ = 173.5, 173.2, 161.8, 128.9, 110.7, 87.3, 80.3, 69.9, 63.4, 51.9, 41.3, 37.5, 29.6, 28.2, 22.5, 19.6, 15.2. **HRMS ESI** calc. for $C_{17}H_{22}NaO_6$ $[M-Na]^+$: 345.1309, found: 345.1312. **X-ray crystal structure** is given in the appendices section.

TBS ether (64): Diol **62** (227.0 mg, 0.80 mmol, 1.0 eq.) was dissolved in dry CH_2Cl_2 (40 mL) and cooled down to 0 °C. To this solution was added 2,6-lutidine (0.10 mL, 0.89 mmol, 1.1 eq.) and then TBSOTf (0.20 mL, 0.89 mmol, 1.1 eq.) and stirred for 30 minutes at 0 °C. The clear solution was then allowed to warm up to r.t. for 3 h and was stirred for 1 h at this temperature. To the clear solution was added saturated NH_4Cl solution (20 mL) and then extracted with CH_2Cl_2 (2 x 20 mL). The combined organic layers were washed with brine (15 mL), dried over Na_2SO_4, filtered and evaporated to obtain a white to yellow solid. The crude was purified by flash chromatography on silica (pentane/EtOAc 7:1) to obtain the protected alcohol **64** (216.0 mg, 0.55 mmol, 68%) as a white solid.

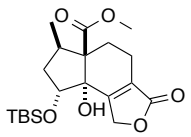

M.p.: 171.7-172.1 °C. $\mathbf{R_f}$ = 0.45 (cyclohexane/EtOAc 3:1). **Optical rotation**: $[\alpha]_D$ = +18.4 (*c* = 0.20, $CHCl_3$). **FTIR**: ν = 3506, 2955, 2860, 1742, 1712, 1354, 1254, 1119, 1038, 1021, 903, 837, 778 cm^{-1}. **^{1}H NMR** (400 MHz, $CDCl_3$) δ = 5.12 (dd, *J* = 8.3, 4.4 Hz, 1H), 4.91-4.68 (m, 2H), 4.31 (s, 1H), 3.62 (s, 3H), 2.69-2.55 (m, 1H), 2.48-2.41 (m, 1H), 2.38-2.21 (m, 2H), 2.21-2.11 (m, 1H), 1.92-1.72 (m, 2H), 0.92 (s, 9H), 0.89 (d, *J* = 7.1 Hz, 3H), 0.15 (s, 3H), 0.14 (s, 3H). **^{13}C NMR** (101 MHz, $CDCl_3$) δ = 173.8, 173.8, 162.8, 127.7, 77.0, 72.5, 68.9, 62.8, 51.6, 41.6, 37.5, 25.8, 22.3, 19.8, 17.8, 15.7, -4.0, -4.8. **Elementary Analyses** calc. for $C_{20}H_{32}O_6Si$: C = 60.58, H = 8.13, N = 0.00, found: C = 60.47, H = 8.03, N = 0.00. **HRMS ESI** calc. for $C_{20}H_{33}O_6Si$ $[M-H]^+$: 397.2041, found: 397.2036.

Lactol (66):[216] To a solution of ester **64** (31.0 mg, 78.2 μmol, 1.0 eq.) in CH_2Cl_2 (3.0 mL) was added DIBAL-H (1 M in toluene, 0.24 mL, 0.24 mmol, 3.0 eq.) at –78 °C. After 1.5 h at –78 °C additional DIBAL-H (1 M in toluene, 0.08 mL, 0.08 mmol, 1.0 eq.) was added and stirred for further 1.5 h. Water (1 mL) was added and the mixture was allowed to warm up to r.t., followed by addition of saturated $NaHCO_3$ solution (1.5 mL) and extraction with EtOAc (4 x). Combined organic layers were dried over Na_2SO_4, filtered and evaporated under reduced pressure. The crude was purified by flash chromatography (pentane/EtOAc 3:1) to obtain the desired lactol **66** (31.7 mg,

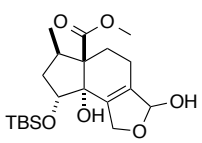

79.5 µmol, quant., *d.r.* = 1.6:1) as colourless oil.

R_f = 0.30 (EtOAc/pentane 1:3). **^{1}H NMR** (400 MHz, $CDCl_3$) δ = 5.78 (dd, *J* = 8.1, 3.4 Hz, 1H), 5.68 (dd, *J* = 10.5, 3.8 Hz, 1H), 5.05-5.01 (m, 2H), 4.77-4.73 (m, 1H), 4.68-4.63 (m, 1H), 4.59-4.55 (m, 1H), 4.48-4.57 (m, 1H), 4.35 (s, 1H), 4.19 (s, 1H), 3.83 (d, *J* = 10.7 Hz, 1H), 3.62, (s, 3H), 3.60 (s, 3H), 3.02 (d, *J* = 8.8 Hz, 1H), 2.59-2.48 (m, 2H), 2.34-2.21 (m, 5H), 2.17-2.06 (m, 3H), 2.03 (s, 1H), 1.94 (s, 1H), 1.81-1.76 (m, 4H), 0.89 (s, 18H), 0.11 (s, 6H), 0.09 (s, 6H). **^{13}C NMR** (101 MHz, $CDCl_3$) δ = 174.2, 173.8, 140.3, 139.8, 135.9, 135.5, 104.2, 73.2, 72.0, 71.83, 63.3, 62.9, 51.4, 51.3, 41.8, 41.7, 37.8, 37.7, 25.8, 25.8, 23.0, 22.5, 20.8, 17.9, 17.8, 15.7, 15.6, -4.1, -4.1, -4.9, -5.0.

Acetal (68):[216] Lactol **66** (32.8 mg, 82.3 µmol, 1.0 eq.) was dissolved in dry MeOH (28.5 mL) and *p*-TSA monohydrate (2.7 mg, 14.0 µmol, 0.2 eq.) was added at r.t. and the resulting mixture was stirred overnight. The clear solution was quenched with brine (10 mL) and extracted with EtOAc (15 mL) and water (10 mL). The aqueous layer was extracted with EtOAc (3 x 5 mL). Combined organic layers were washed with saturated $NaHCO_3$ solution and brine. The organic layer was dried over Na_2SO_4, filtered and evaporated under reduced pressure. Purification was performed by flash chromatography (pentane/EtOAc 15:1) to obtain acetal **68** (22.6 mg, 54.8 µmol, 67%) as a white solid.

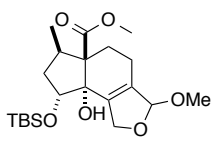

R_f = 0.30 (EtOAc/pentane 1:15). **^{1}H NMR** (400 MHz, $CDCl_3$) δ = 5.65 (t, *J* = 3.0 Hz, 1H), 5.52 (d, *J* = 4.2 Hz, 1H), 5.09-5.02 (m, 2H), 4.80-4.74 (m, 1H), 4.68-4.58 (m, 2H), 4.51 (d, *J* = 12.6 Hz, 1H), 4.23 (s, 1H), 4.12 (s, 1H), 3.61 (s, 6H), 3.30 (s, 3H), 3.14 (s, 3H), 2.63-2.53 (m, 2H), 2.30-2.09 (m, 8H), 1.83-1.77 (m, 4H), 0.90 (s, 9H), 0.90 (s, 9H), 0.86 (d, *J* = 7.1, 3H), 0.84 (d, *J* = 7.1, 3H), 0.12 (s, 3H), 0.11 (s, 3H), 0.10 (s, 3H), 0.10 (s, 3H). **^{13}C NMR** (101 MHz, $CDCl_3$) δ = 174.0, 141.8, 141.6, 133.5, 133.3, 109.8, 109.6, 73.4, 73.1, 72.7, 63.2, 63.0, 53.0, 51.6, 51.3, 51.3, 41.8, 41.7, 37.9, 37.8, 25.9, 25.8, 22.8, 22.7, 21.0, 20.9, 17.9, 15.7, -4.0, -4.9, -4.9.

Aldehyde (70):[216] Diol **62** (18.4 mg, 65.2 µmol, 1.0 eq.) was dissolved in THF/H_2O (2:1, 0.66 mL) and $NaIO_4$ (45.1 mg, 0.21 mmol, 3.2 eq.) was added at r.t. The reaction was diluted after 1 h with EtOAc (7 mL). The mixture was filtered over Na_2SO_4 and the crystals were vigorously washed with EtOAc (3 x 4 mL). Combined organic layers were evaporated to obtain a white solid. The crude was purified by flash chromatography (pentane/EtOAc 2:1) to obtain the desired aldehyde **70** (18.3 mg, 65.2 µmol, quant.) as a white solid.

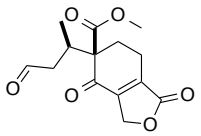

M.p.: 101.2-101.8 °C. $\mathbf{R_f}$ = 0.56 (EtOAc/pentane 1:1). **Optical rotation**: $[\alpha]_D$ = +64.0 (*c* = 0.15, $CHCl_3$). **FTIR** ν = 2957, 2826, 1755, 1725, 1685, 1435, 1234, 1203, 1026, 886, 737 cm^{-1}. **^{1}H NMR** (400 MHz, $CDCl_3$) δ = 9.72 (d, *J* = 1.2 Hz, 1H), 5.02-4.88 (m, 2H), 3.72 (s, 3H), 3.06-2.98 (m, 1H), 2.71-2.54 (m, 4H), 2.41 (ddd, *J* = 17.8, 8.8, 1.9 Hz, 1H), 2.17 (ddd, *J* = 13.5, 8.9, 6.3 Hz, 1H), 1.06 (d, *J* = 6.9 Hz, 3H). **^{13}C NMR** (126 MHz, $CDCl_3$) δ = 200.4, 191.7, 172.0, 170.3, 151.5, 143.5, 68.8, 61.2, 53.1, 46.8, 30.4, 29.0, 18.9, 16.8.

Acetal (71):[216] To ketoaldehyde **70** (4.7 mg, 16.8 µmol, 1.0 eq.) were added dry benzene (0.2 mL), ethylene glycol (62.5 mg, 1.01 mmol, 60.0 eq.), *p*-TSA monohydrate (3.2 mg, 33.5 µmol, 2.0 eq.) and 3 Å molecular sieves. The resulting mixture was heated to 90 °C for 6 h. The colourless solution was allowed to cool down to r.t. and EtOAc and an aqueous saturated $NaHCO_3$ solution were added. The aqueous layer was extracted three times with EtOAc and the combined organic layers were washed with brine. The organic layer was dried over Na_2SO_4, filtered and evaporated to obtain a slightly brown oil. The crude was purified by flash chromatography (pentane/EtOAc 2:1) to obtain the desired acetal **71** (3.5 mg, 13.9 µmol, 83%) as a white solid.

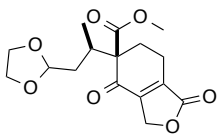

M.p.: 166.3-167.1 °C. $\mathbf{R_f}$ = 0.30 (pentane/EtOAc 2:1). **Optical rotation**: $[\alpha]_D$ = +34.8 (*c* = 0.18, $CHCl_3$). **FTIR**: ν = 3359, 3189, 2961, 2923, 2852, 1767, 1733, 1690, 1442, 1229, 1189, 1146, 1111, 1065, 1026, 954, 737 cm^{-1}. **^{1}H NMR** (500 MHz, $CDCl_3$) δ = 4.94 (qt, *J* = 17.5, 3.2 Hz, 2H), 4.90 (t, *J* = 4.8 Hz, 1H), 3.97-3.91 (m,

2H), 3.86-3.80 (m, 2H), 3.72 (s, 3H), 2.63-2.60 (m, 2H), 2.55-2.50 (m, 2H), 2.27-2.21 (m, 1H), 1.67-1.65 (m, 2H), 1.10 (d, J = 6.9 Hz, 3H). **^{13}C NMR** (101 MHz, $CDCl_3$) δ = 191.9, 172.2, 170.5, 151.6, 143.4, 103.6, 68.9, 65.1, 64.8, 62.3, 36.1, 32.9, 28.8, 19.0, 16.9.

Dithian (72):[216] Aldehyde **70** (6.6 mg, 23.5 µmol, 1.0 eq.) was dissolved in dry CH_2Cl_2 (0.1 mL) and 1,2-ethanedithiol (4.2 µl, 49.5 µmol, 2.1 eq.) and then BF_3 etherate (2.7 µl, 21.2 µmol, 0.9 eq.) were added at r.t. The colourless solution was stirred for 20 min at r.t. The reaction mixture was quenched with saturated $NaHCO_3$ solution and extracted three times with CH_2Cl_2. The combined organic layers were washed with brine, dried over Na_2SO_4, filtered and evaporated to obtain a white solid. The crude was purified by flash chromatography (pentane/EtOAc 4:1, then 1:1) to obtain the desired product **72** (4.5 mg, 10.4 µmol, 54%) as white to slightly green solid.

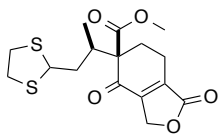

M.p.: 159.2-159.9 °C. $\mathbf{R_f}$ = 0.29 (EtOAc/pentane 1:4). **FTIR** ν = 2954, 2932, 2851, 1746, 1726, 1681, 1441, 1227, 1195, 1029, 900, 730 cm^{-1}. **^{1}H NMR** (400 MHz, $CDCl_3$) δ = 4.94 (qt, J = 17.5, 3.0 Hz, 2H), 4.52 (dd, J = 10.5, 4.0 Hz, 1H), 3.72 (s, 3H), 3.28-3.16 (m, 4H), 2.63-2.59 (m, 2H), 2.52 (dt, J = 13.9, 3.9 Hz, 1H), 2.45-2.37 (m, 1H), 2.27-2.20 (m, 1H), 1.94-1.83 (m, 1H), 1.79-1.69 (m, 1H), 1.08 (d, J = 6.8 Hz, 3H). **^{13}C NMR** (101 MHz, $CDCl_3$) δ = 191.7, 172.1, 170.4, 151.5, 143.5, 68.9, 62.2, 53.0, 52.0, 41.9, 38.7, 38.1, 37.3, 28.9, 19.0, 15.8.

Lactone (75):[216] Diol **62** (12.5 mg, 44.3 µmol, 1.0 eq.) and Rh/C/Al_2O_3 (5% Rh, 9.1 mg, 4.43 µmol 0.1 eq.) were dissolved in dry EtOAc (0.3 mL) and hydrogenated at r.t. under a 60 bar H_2 pressure. After 3 h, the reaction was filtered over celite and vigorously washed with EtOAc. The solvent was evaporated under reduced pressure to obtain a white solid. The crude was purified by flash chromatography (pentane/EtOAc 1:1) to obtain the desired hydrogenated lactone **75** (12.6 mg, 44.3 µmol, quant.) as a white solid.

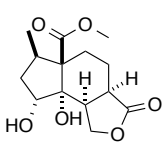

M.p.: 197.7-198.5 °C. $\mathbf{R_f}$ = 0.31 (EtOAc/pentane 1:1). **Optical rotation**: $[\alpha]_D$ = –110.8 (*c* = 0.12, $CHCl_3$). **FTIR** ν = 3498, 3425, 2955, 2871, 1743, 1708, 1366, 1202, 1038, 974, 716, 617 cm^{-1}. **^{1}H NMR** (500 MHz, $CDCl_3$) δ = 4.91 (dd, *J* = 9.2, 4.1 Hz, 1H), 4.24 (dd, *J* = 9.7, 8.3 Hz, 1H), 4.00 (dd, *J* = 11.5, 9.7 Hz, 1H), 3.69 (s, 3H), 3.43 (s, 1H), 2.93-2.84 (m, 2H), 2.63-2.55 (m, 1H), 2.22 (dt, *J* = 13.0, 3.6 Hz, 1H), 2.10 (brs, 1H), 2.06 (ddd, *J* = 10.6, 6.6, 3.5 Hz, 1H), 1.93-1.75 (m, 3H), 1.56-1.47 (m, 1H), 0.77 (d, *J* = 7.2 Hz, 3H). **^{13}C NMR** (126 MHz, $CDCl_3$) δ = 179.2, 174.3, 80.0, 72.53, 67.4, 59.6, 51.7, 44.1, 39.9, 39.3, 38.2, 24.9, 22.1, 14.7. **HRMS ESI** calc. for $C_{14}H_{21}O_6$ $[M-H]^+$: 285.1333, found: 285.1334. **X-ray crystal structure** is given in the appendices section.

Aldehyde (76):[216] Diol **75** (11.3 mg, 39.7 μmol, 1.0 eq.) was dissolved in THF/H_2O (2:1, 0.47 mL) and $NaIO_4$ (27.8 mg, 0.13 mmol, 3.2 eq.) was added at r.t. After 1.5 h, the reaction mixture was diluted with EtOAc (2 mL) and filtered over Na_2SO_4. The filtrate was vigorously washed with EtOAc (4 x 2 mL). The solvent was evaporated to obtain a white solid. The crude was purified by flash chromatography (pentane/EtOAc 2:1) to obtain the desired ketoaldehyde **76** (12.5 mg, 43.6 μmol, quant.) as colourless oil, which slowly decomposes to **77**.

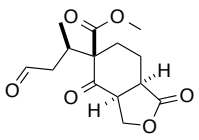

$\mathbf{R_f}$ = 0.38 (EtOAc/pentane 1:1). **Optical rotation**: $[\alpha]_D$ = –137.3 (*c* = 0.12, $CHCl_3$). **FTIR** ν = 2955, 1770, 1712, 1452, 1167, 998, 732, 626 cm^{-1}. **^{1}H NMR** (400 MHz, $CDCl_3$) δ = 9.71 (s, 1H), 4.86 (dd, *J* = 9.4, 1.9 Hz, 1H), 4.19 (dd, *J* = 9.4, 6.6 Hz, 1H), 3.70 (s, 3H), 3.30-3.18 (m, 2H), 2.93-2.84 (m, 1H), 2.82-2.68 (m, 2H), 2.29-2.17 (m, 2H), 2.15-2.04 (m, 2H), 1.07 (d, *J* = 6.7 Hz, 3H). **^{13}C NMR** (101 MHz, $CDCl_3$) δ = 205.4, 201.3, 176.7, 170.7, 66.2, 63.0, 52.5, 47.5, 45.6, 40.2, 29.1, 28.8, 18.8, 15.8.

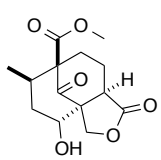

$\mathbf{R_f}$ = 0.31 (EtOAc/pentane 1:1). **^{1}H NMR** (500 MHz, $CDCl_3$) δ = 5.07 (d, *J* = 9.5 Hz, 1H), 4.18 (d, *J* = 9.5 Hz, 1H), 3.85 (dd, *J* = 10.8, 4.4 Hz, 1H), 3.75 (s, 3H), 3.39 (dd, *J* = 13.3, 6.0 Hz, 1H), 2.56-2.51 (m, 1H), 2.38-2.17 (m, 5H), 1.90 (ddd, *J* = 14.3, 5.4, 2.4 Hz, 1H), 1.00 (d, *J* = 7.1 Hz, 3H).

^{13}C NMR (126 MHz, $CDCl_3$) δ = 205.5, 177.3, 172.1, 71.3, 67.9, 59.5, 59.2, 52.5, 41.1, 35.8, 35.0, 34.9, 23.4, 16.1.

Acetal (78):[247] To the diol **75** (130.0 mg, 0.45 mmol, 1.0 eq.) dissolved in THF and

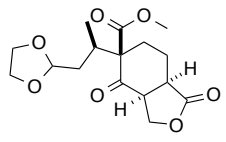

H_2O (3:1, 5 mL) was added sodium periodate (332.0 mg, 1.60 mmol, 3.4 eq.). The mixture was stirred at r.t. for 2 h and subsequently dried by filtrating the mixture through a patch of Na_2SO_4 and washed with EtOAc. The solvent was evaporated, and crude product was obtained as colourless oil. The crude ketoaldehyde **76** was dissolved in dry benzene (4 mL), and ethylene glycol (27 µL, 0.48 mmol, 1.1 eq.) was added, followed by *p*-TSA (9.2 mg, 0.05 mmol, 0.1 eq.). The resulting solution was heated to reflux (90 °C). After 1 h 45 min the solution was allowed to cool to r.t., and was then treated with saturated $NaHCO_3$ solution (3 mL) followed by extraction with EtOAc three times. The combined organic layers were washed with water, dried over Na_2SO_4 and evaporated under reduced pressure. The crude material was subjected to flash chromatography on silica (CH_2Cl_2/MeOH, 20:1) and concentrated to give protected aldehyde **78** (149.0 mg, 0.45 mmol, quant.) as a white solid.

R_f = 0.63 (CH_2Cl_2/MeOH 20:1). **Optical rotation**: $[\alpha]_D$ = –75.5 (*c* = 0.77, $CHCl_3$). **FTIR** ν = 2954, 2887, 1773, 1737, 1709, 1450, 1372, 1343, 1297, 1220, 1188, 1148, 1121, 1050, 1027, 998, 962, 734 cm^{-1}. **^{1}H NMR** (500 MHz, $CDCl_3$) δ = 4.95 (dd, *J* = 9.3, 1.8 Hz, 1H), 4.86 (dd, *J* = 6.4, 2.6 Hz, 1H), 4.14 (dd, *J* = 9.3, 6.5 Hz, 1H), 3.97-3.90 (m, 2H), 3.87-3.79 (m, 2H), 3.70 (s, 3H), 3.47 (ddd, *J* = 10.0, 6.4, 1.7 Hz, 1H), 3.18 (ddd, *J* = 10.1, 6.4, 5.1 Hz, 1H), 2.42-2.35 (m, 1H), 2.22-2.07 (m, 4H), 2.03 (ddd, *J* = 14.9, 9.8, 2.6 Hz, 1H), 1.54 (ddd, *J* = 14.9, 6.4, 0.8 Hz, 1H), 1.09 (d, *J* = 6.8 Hz, 3H). **^{13}C NMR** (101 MHz, $CDCl_3$) δ = 205.2, 176.8, 170.9, 103.3, 66.0, 65.1, 64.9, 64.2, 52.2, 45.7, 40.9, 36.8, 30.3, 29.1, 18.6, 15.4. **HRMS ESI** calc. for $C_{16}H_{23}O_7$ $[M-H]^+$: 327.1438, found: 327.1443.

Dithiolane (79):[216] Ketoaldehyde **76** (7.7 mg, 27.3 μmol, 1.0 eq.) was dissolved in dry CH_2Cl_2 (0.1 mL) and 1,2-ethanedithiol (3.3 mg, 35.5 μmol, 1.3 eq.) in dry CH_2Cl_2 (0.25 mL) and BF_3 etherate (3.5 mg, 24.5 μmol, 0.9 eq.) was added at r.t. After 1 h, the colourless solution was quenched with saturated $NaHCO_3$ solution and extracted three times with CH_2Cl_2. Combined organic layers were washed with brine, dried over Na_2SO_4, filtered and evaporated to obtain a white solid. The crude was purified by flash chromatography (pentane/EtOAc 3:1) to obtain the desired dithiolane **79** (5.5 mg, 15.3 μmol, 56%) as a white solid.

R_f = 0.71 (EtOAc/pentane 1:1). **Optical rotation**: $[\alpha]_D$ = –36.5 (*c* = 0.18, $CHCl_3$). **FTIR**: ν = 2927, 1772, 1736, 1709, 1450, 1227, 1197, 1165, 1060, 997, 908 cm^{-1}. **^{1}H NMR** (400 MHz, $CDCl_3$) δ = 4.93 (dd, *J* = 9.3, 2.0 Hz, 1H), 4.53 (dd, *J* = 11.4, 2.9 Hz, 1H), 4.18 (dd, *J* = 9.3, 6.7 Hz, 1H), 3.70 (s, 3H), 3.53 (ddd, *J* = 10.0, 6.7, 2.0 Hz, 1H), 3.29-3.10 (m, 5H), 2.29-2.08 (m, 6H), 1.61-1.55 (m, 1H), 1.08 (d, *J* = 6.4 Hz, 3H). **^{13}C NMR** (101 MHz, $CDCl_3$) δ = 204.8, 176.7, 170.7, 66.1, 64.1, 52.3, 52.1, 46.2, 42.4, 40.5, 38.6, 38.0, 35.6, 29.2, 18.7, 13.9.

Alcohol (80):[247] Keto acetal **78** (161.0 mg, 0.49 mmol, 1.0 eq.) was dissolved in THF (2.8 mL), and formaline (37% aq. solution, 8.3 mL, 112 mmol, 226 eq.) was added, followed by aq. citrate buffer solution (8.3 mL, pH 6.0). The resulting solution was heated up to 40 °C and stirred overnight. After cooling to r.t., the reaction mixture was diluted with EtOAc and water. The aqueous layer was extracted three times with EtOAc, and the combined organic layers were washed with water, dried over Na_2SO_4, and evaporated under reduced pressure. The crude residue was dissolved in a CH_2Cl_2/MeOH mixture (20:1) and filtered through a pad of silica. Purification by flash chromatography (CH_2Cl_2/MeOH 20:1) gave pure product **80** (164.3 mg, 0.46 mmol, 94%) as a white solid.

R_f = 0.30 (CH_2Cl_2/MeOH 20:1). **Optical rotation**: $[\alpha]_D$ = –23.5 (*c* = 0.30, $CHCl_3$). **FTIR**: ν = 3467, 2957, 2923, 2854, 1766, 1728, 1702, 1465, 1437, 1382, 1300, 1223,

1174, 1137, 1096, 1017, 952, 881, 860, 826, 751, 713 cm-1. **^{1}H NMR** (400 MHz, $CDCl_3$) δ = 4.87 (dd, *J* = 5.8, 3.5 Hz, 1H), 4.34 (d, *J* = 9.8 Hz, 1H), 4.13 (d, *J* = 9.8 Hz, 1H), 4.00-3.91 (m, 3H), 3.88-3.79 (m, 2H), 3.71 (s, 3H), 3.60 (d, *J* = 10.8 Hz, 1H), 3.02-2.93 (m, 1H), 2.38-2.19 (m, 3H), 2.05 (ddd, *J* = 12.9, 11.5, 2.3 Hz, 1H), 1.98-1.84 (m, 1H), 1.79-1.64 (m, 2H), 1.12 (d, *J* = 6.8 Hz, 3H). **^{13}C NMR** (101 MHz, $CDCl_3$) δ = 208.5, 177.5, 171.4, 103.7, 70.9, 67.0, 65.0, 64.8, 63.3, 56.6, 42.8, 35.8, 33.8, 30.5, 28.9, 20.8, 17.0. **HRMS ESI** calc. for $C_{17}H_{25}O_8$ $[M-H]^+$: 357.1544, found: 357.1552.

Chloride (81): To the hydroxymethylated ketoaldehyde **80** (169.0 mg, 0.47 mmol, 1.0 eq.) was added triphenylphosphine (176.0 mg, 0.66 mmol, 1.4 eq.), followed by dry acetonitrile (6 mL) and freshly distilled trichloroacetonitrile (166 μL, 0.24 mmol, 3.5 eq.). The resulting mixture was refluxed at 85 °C overnight. The reaction mixture was then cooled to r.t. and treated with a saturated $NaHCO_3$ solution, followed by extraction twice with EtOAc. The combined organic layers were dried over Na_2SO_4, filtered, and evaporated under reduced pressure. The crude material was subjected to flash chromatography on silica (EtOAc/pentane 1:3) and concentrated to give pure **81** (146.0 mg, 0.39 mmol, 82%) as colourless oil.

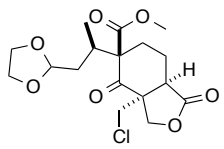

R_f = 0.26 (pentane/EtOAc 3:1). **Optical rotation**: $[\alpha]_D$ = +0.6 (*c* = 0.30, $CHCl_3$). **FTIR**: ν = 2960, 2882, 2361, 1767, 1705, 1588, 1437, 1413, 1382, 1293, 1221, 1175, 1128, 1080, 1018, 954, 891, 856, 819, 791, 758, 700 cm^{-1}. **^{1}H NMR** (400 MHz, $CDCl_3$) δ = 4.86 (dd, *J* = 5.7, 3.7 Hz, 1H), 4.39 (d, *J* = 10.3 Hz, 1H), 4.22 (d, *J* = 11.0 Hz, 1H), 4.03 (d, *J* = 10.3 Hz, 1H), 4.00-3.88 (m, 2H), 3.88-3.79 (m, 2H), 3.73 (s, 3H), 3.43 (d, *J* = 11.0 Hz, 1H), 3.27-3.17 (m, 1H), 2.45-2.36 (m, 1H), 2.37-2.27 (m, 2H), 2.09-1.96 (m, 1H), 1.80 (dd, *J* = 11.0, 2.1 Hz, 1H), 1.68-1.50 (m, 2H), 1.09 (d, *J* = 6.8 Hz, 3H). **^{13}C NMR** (101 MHz, $CDCl_3$) δ = 204.4, 176.4, 171.3, 103.5, 71.5, 65.1, 64.8, 63.7, 56.4, 53.0, 48.1, 43.4, 36.2, 35.8, 28.1, 21.1, 17.4. **HRMS ESI** calc. for $C_{17}H_{24}O_7Cl$ $[M-H]^+$: 375.1205, found: 375.1213.

Acetal (82): Iodide **83** (401.0 mg, 0.86 mmol, 1.0 eq.) was dissolved in dry and degassed benzene (30 mL) under argon atmosphere. Tri-*n*-butyltin hydride (348 µL, 1.29 mmol, 1.5 eq.) and AIBN (42.0 mg, 0.26 mmol, 0.3 eq.) were added and the mixture was stirred for 3 h at 85 °C. The solvent was removed *in vacuo* and the residue was purified by flash column chromatography (pentane/EtOAc 2:1) to give the protected aldehyde **82** (242.0 mg, 0.72 mmol, 84%) as a colourless oil the ring expended side product **84** (51.0 mg, 0.14 mmol, 16%).

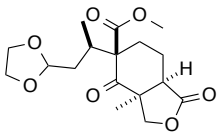

R_f = 0.18 (pentane/EtOAc 2:1). **Optical rotation**: $[\alpha]_D$ = –68.5 (*c* = 0.49, MeOH). **FTIR** ν = 2955, 2887, 1776, 1733, 1709, 1457, 1364, 1297, 1230, 1148, 1020, 963, 823, 733 cm^{-1}. **^{1}H NMR** (400 MHz, $CDCl_3$) δ = 4.85 (t, *J* = 4.8 Hz, 1H), 4.47 (d, *J* = 9.3 Hz, 1H), 3.95-3.84 (m, 3H), 3.83-3.75 (m, 2H), 3.64 (s, 3H), 2.61 (dd, *J* = 10.3, 6.1 Hz, 1H), 2.43-2.32 (m, 1H), 2.26-2.11 (m, 2H), 2.03-1.86 (m, 2H), 1.59-1.53 (m, 2H), 1.33 (s, 3H), 1.03 (d, *J* = 6.8 Hz, 3H). **^{13}C NMR** (101 MHz, $CDCl_3$) δ = 207.7, 177.5, 171.1, 103.5, 74.6, 65.0, 64.7, 63.3, 52.6, 50.9, 46.3, 36.1, 34.8, 27.7, 24.3, 19.5, 16.8. **HRMS ESI** calc. for $C_{17}H_{25}O_7$ $[M-H]^+$: 341.1595, found: 341.1591.

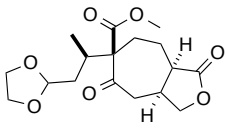

R_f = 0.14 (pentane/EtOAc 2:1). **Optical rotation**: $[\alpha]_D$ = +15.9 (*c* = 0.41, $CHCl_3$). **FTIR**: ν = 2982, 2960, 2932, 2883, 1737, 1696, 1468, 1445, 1396, 1355, 1323, 1256, 1236, 1214, 1202, 1181, 1138, 1117, 1081, 1029, 1014, 987, 963, 934, 880, 851, 797, 769, 706 cm^{-1}. **^{1}H NMR** (400 MHz, $CDCl_3$) δ = 4.96 (dd, *J* = 5.7, 4.2 Hz, 1H), 4.42 (dd, *J* = 9.4, 7.1 Hz, 1H), 4.02-3.94 (m, 3H), 3.90-3.84 (m, 2H), 3.76 (s, 3H), 2.90-2.78 (m, 1H), 2.70 (ddd, *J* = 8.7, 6.4, 2.8 Hz, 2H), 2.56 (dd, *J* = 11.8, 4.4 Hz, 1H), 2.46-2.33 (m, 2H), 2.10-1.94 (m, 2H), 1.76 (ddd, *J* = 13.9, 5.7, 1.7 Hz, 1H), 1.68 (ddd, *J* = 15.1, 9.4, 2.4 Hz, 1H), 1.45 (ddd, *J* = 14.1, 10.3, 4.2 Hz, 1H), 1.07 (d, *J* = 6.9 Hz, 3H). **^{13}C NMR** (126 MHz, $CDCl_3$) δ = 204.3, 177.9, 171.8, 104.0, 71.4, 67.3, 65.0, 64.7, 52.5, 43.6, 42.5, 37.4, 35.8, 33.3, 29.3, 22.9, 15.7. **HRMS ESI** calc. for $C_{17}H_{25}O_7$ $[M-H]^+$: 341.1595, found: 341.1591. **X-ray crystal structure** is given in the appendix.

Iodide (83): Alcohol **80** (408 mg, 1.14 mmol, 1.0 eq.), triphenylphosphine (600 mg, 2.29 mmol, 2.0 eq.) and imidazole (311 mg, 4.57 mmol, 4.0 eq.) were dissolved in dry benzene (30 mL) under argon atmosphere. Iodine (580 mg, 2.29 mmol, 2.0 eq.) was added at r.t. and the resulting mixture was stirred for 12 hours at that temperature. The **r**eaction was quenched with a 1:1 mixture of saturated $NaHCO_3$ and $Na_2S_2O_3$ solution and extracted three times with EtOAc. Combined organic layers were dried over Na_2SO_4, filtered and evaporated under reduced pressure. The residue was purified by flash chromatography on silica **(**pentane/EtOAc 5:2) giving iodide **83** (401.2 mg, 0.86 mmol, 75%) as a colourless oil.

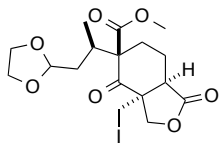

$\mathbf{R}_f$ = 0.23 (pentane/EtOAc 3:1). **Optical rotation**: $[\alpha]_D$ = +17.9° (*c* = 0.48, $CHCl_3$). **FTIR**: ν = 2954, 2886, 2360, 1781, 1731, 1710, 1436, 1366, 1225, 1162, 1030, 947, 824, 732 cm^{-1}. **^{1}H NMR** (400 MHz, $CDCl_3$) δ = 4.87 (dd, *J* = 5.8, 3.7 Hz, 1H), 4.39 (d, *J* = 10.2 Hz, 1H), 4.01 (d, *J* = 10.2 Hz, 1H), 3.98-3.87 (m, 3H), 3.86-3.78 (m, 2H), 3.72 (s, 3H), 3.15 (d, *J* = 10.3 Hz, 1H), 3.14-3.08 (m, 1H), 2.49-2.38 (m, 1H), 2.33-2.24 (m, 2H), 2.08-1.98 (m, 1H), 1.86 (tdd, *J* = 13.3, 8.3, 2.3 Hz, 1H), 1.72-1.55 (m, 2H), 1.11 (d, *J* = 6.8 Hz, 3H). **^{13}C NMR** (126 MHz, $CDCl_3$) δ = 203.7, 176.2, 171.1, 103.5, 72.9, 65.1, 64.8, 63.5, 55.3, 53.0, 46.9, 36.4, 35.6, 27.5, 20.8, 17.4, 11.3. **HRMS ESI** calc. for $C_{17}H_{24}IO_7$ $[M-H]^+$: 467.0561, found: 467.0557.

Aldehyde (85): The protected aldehyde **82** (227.0 mg, 0.67 mmol, 1.0 eq.) was dissolved in acetone (10 mL) before a 1 M aq. HCl solution (5 mL) was added. The resulting mixture was stirred overnight at r.t. The reaction was quenched by addition of a saturated aq. $NaHCO_3$ solution and extracted 3 times with EtOAc. The combined organic layers were dried over Na_2SO_4, filtered and evaporated under reduced pressure to yield already pure **85** (195.8 mg, 0.66 mmol, 99%) as colourless oil.

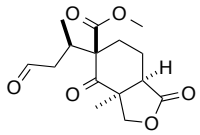

$\mathbf{R}_f$ = 0.56 (pentane/EtOAc 1:1). **Optical rotation**: $[\alpha]_D$ = –87.8 (*c* = 0.42, $CHCl_3$). **FTIR**: ν = 2956, 2360, 2339, 1776, 1717, 1457, 1385, 1295, 1234, 1155, 1022, 991, 787 cm^{-1}. **^{1}H NMR** (400 MHz, $CDCl_3$) δ = 9.72 (d, *J* = 1.7 Hz, 1H), 4.60 (d,

J = 9.4 Hz, 1H), 3.90 (d, *J* = 9.4 Hz, 1H), 3.68 (s, 3H), 2.94 (dqd, *J* = 9.8, 6.8, 3.0 Hz, 1H), 2.69 (t, *J* = 7.4 Hz, 1H), 2.67-2.60 (m, 1H), 2.52-2.43 (m, 1H), 2.31-2.19 (m, 2H), 2.08-1.94 (m, 2H), 1.36 (s, 3H), 1.00 (d, *J* = 6.8 Hz, 3H). **^{13}C NMR** (101 MHz, $CDCl_3$) δ = 208.1, 200.7, 177.3, 170.8, 74.7, 62.3, 52.8, 51.2, 46.8, 46.2, 31.3, 27.2, 24.5, 18.9, 16.6. **HRMS ESI** calc. for $C_{15}H_{21}O_6$ $[M-H]^+$: 297.1333 found: 297.1328.

Alcohol (87): Aldehyde **85** (78.1 mg, 0.264 mmol, 1.0 eq.) was dissolved in HFIP (1 mL). Borane **88**[256] (1 mol/L in THF, 790 µL, 0.791 mmol, 3.0 eq.) was added at r.t. under nitrogen atmosphere and stirred overnight. The reaction was quenched by addition of saturated NH_4Cl solution and extracted three times with EtOAc. Combined organic layers were dried over Na_2SO_4, filtered and evaporated under reduced pressure. The crude was purified by flash chromatography (pentane/EtOAc 2:3) giving alcohol **87** (66.9 mg, 0.224 mmol, 85%) as colourless oil.

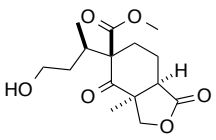

R_f = 0.26 (EtOAc/pentane 3:2). **Optical rotation**: $[\alpha]_D$ = –79.9 (*c* = 0.18, MeOH). **FTIR**: ν = 3529, 3407, 2955, 2884, 1775, 1731, 1708, 1456, 1385, 1364, 1293, 1231, 1187, 1154, 1055, 1021, 989, 916, 848, 732, 681 cm^{-1}. **^{1}H NMR** (400 MHz, $CDCl_3$) δ = 4.48 (d, *J* = 9.3 Hz, 1H), 3.94 (d, *J* = 9.3 Hz, 1H), 3.74 (ddd, *J* = 11.0, 8.8, 5.5 Hz, 1H), 3.69 (s, 3H), 3.67-3.58 (m, 1H), 2.64 (t, *J* = 8.4 Hz, 1H), 2.45-2.34 (m, 1H), 2.28 (dt, *J* = 9.3, 4.4 Hz, 1H), 2.25-2.17 (m, 1H), 2.07-1.92 (m, 2H), 1.69-1.52 (m, 2H), 1.39-1.33 (m, 1H), 1.37 (d, *J* = 2.9 Hz, 3H), 0.99 (d, *J* = 6.8 Hz, 3H). **^{13}C NMR** (101 MHz, $CDCl_3$) δ = 208.1, 177.5, 171.3, 74.6, 63.2, 61.0, 52.8, 51.0, 46.5, 35.3, 34.8, 27.4, 24.4, 19.8, 16.1. **HRMS ESI** calc. for $C_{15}H_{22}NaO_6$ $[M-Na]^+$: 321.1309, found: 321.1308.

Iodide (89): Alcohol **87** (26.0 mg, 0.087 mmol, 1.0 eq.) was dissolved in dry benzene (5 mL) under nitrogen atmosphere. Triphenylphosphine (45.7 mg, 0.174 mmol, 2.0 eq.), imidazole (23.7 mg, 0.0349 mmol, 4.0 eq.), and iodine (44.2 mg, 0.174 mmol, 2.0 eq.) were added at r.t. and the resulting mixture was stirred overnight. The crude mixture was filtered, washed with

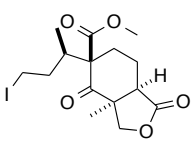

benzene and evaporated under reduced pressure. The crude oil was purified by flash chromatography (pentane/EtOAc 2:1) giving iodide **89** (33.8 mg, 0.083 mmol, 95%) as a white solid.

R_f = 0.44 (pentane/EtOAc 2:1). **Optical rotation**: $[\alpha]_D$ = –9.8 (*c* = 0.58, $CHCl_3$). **FTIR**: ν = 3245, 2971, 2927, 2860, 2171, 1762, 1728, 1700, 1591, 1532, 1489, 1439, 1385, 1368, 1287, 1230, 1207, 1173, 1119, 1069, 1012, 977, 961, 922, 905, 852, 773, 764, 722, 692 cm^{-1}. **^{1}H NMR** (400 MHz, $CDCl_3$) δ = 4.48 (d, *J* = 9.3 Hz, 1H), 3.93 (d, *J* = 9.3 Hz, 1H), 3.71 (s, 3H), 3.33 (ddd, *J* = 9.8, 7.7, 4.3 Hz, 1H), 3.07 (td, *J* = 9.5, 7.1 Hz, 1H), 2.68-2.60 (m, 1H), 2.37-2.14 (m, 3H), 2.05-1.91 (m, 2H), 1.89-1.78 (m, 1H), 1.71-1.60 (m, 1H), 1.37 (s, 3H), 0.97 (d, *J* = 6.8 Hz, 3H). **^{13}C NMR** (101 MHz, $CDCl_3$) δ = 207.7, 177.4, 171.0, 74.6, 63.1, 52.9, 51.0, 46.4, 39.5, 35.6, 27.6, 24.5, 19.7, 15.1, 4.4. **HRMS ESI** calc. for $C_{15}H_{22}IO_5$ $[M-H]^+$: 409.0506, found: 409.0508. **X-ray crystal structure** is given in the appendix.

Samarium(II) iodide: Samarium (151 mg, 1.0 mmol, 1.0 eq.) was activated by hot stirring with a heat gun *in vacuo*. After cooling, 1,2-diiodoethane (prewashed by extraction with saturated aqueous $Na_2S_2O_3$ solution, 141 mg, 0.5 mmol, 1.0 eq.) was added under argon atmosphere. THF (dried over sodium, 2 mL) was added and the mixture was stirred for 5 min at room temperature. After that time, more THF (3 mL) was added and the solution was stirred until it turned dark blue and SmI_2 was obtained as a 0.1 M solution in THF and was used as such. Procedure was and observations are in agreement with literature.

Literature: M. Szostak, M. Spain, D. J. Procter, *J. Org. Chem*. **2012**, *77*, 3049.

Lactone (57): Iodide **89** (118.0 mg, 0.289 mmol, 1.0 eq.) was dissolved in

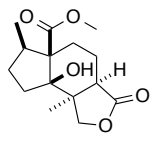

hexamethylphosphoramide (500 µL, 2.890 mmol, 10.0 eq.) under nitrogen atmosphere and cooled down to 0 °C. A freshly prepared SmI_2 solution (0.1 M in THF, 7.22 mL, 0.722 mmol, 2.5 eq.) was added and the resulting mixture was slowly heated up to r.t. and stirred for 1 hour. The reaction

was quenched by addition of a saturated aqueous Rochelle's salt solution and stirred at that temperature for 20 min. Extraction was performed three times with EtOAc. Combined organic layers were dried over Na_2SO_4, filtered and evaporated under reduced pressure. The crude was purified by flash chromatography on silica (pentane/EtOAc 4:1, CAM dip) giving the tricyclic product **57** (61.5 mg, 0.218 mmol, 76%) as the side-product **86** (5.8 mg, 0.026 mmol, 9%) as white solids.

R_f = 0.41 (pentane/EtOAc 4:1). **Optical rotation**: $[\alpha]_D$ = –17.6 (*c* = 0.29, MeOH). **FTIR**: ν = 3495, 2959, 2900, 2877, 1770, 1708, 1454, 1435, 1384, 1354, 1325, 1291, 1270, 1239, 1181, 1148, 1102, 1076, 1058, 1040, 1009, 988, 966, 920, 896, 845, 768, 739, 714, 681 cm^{-1}. **^{1}H NMR** (400 MHz, $CDCl_3$) δ = 5.17 (d, *J* = 2.1 Hz, 1H), 4.44 (d, *J* = 9.5 Hz, 1H), 3.97 (d, *J* = 9.5 Hz, 1H), 3.79 (s, 3H), 2.40-2.32 (m, 1H), 2.24-2.16 (m, 1H), 2.14-2.00 (m, 2H), 1.96-1.86 (m, 2H), 1.82-1.71 (m, 1H), 1.66-1.58 (m, 1H), 1.43 (td, *J* = 13.9, 2.6 Hz, 1H), 1.35-1.29 (m, 1H), 1.23 (s, 3H), 1.00 (d, *J* = 6.9 Hz, 3H). **^{13}C NMR** (126 MHz, $CDCl_3$) δ = 178.8, 178.5, 85.4, 74.6, 58.0, 52.6, 48.1, 46.8, 45.1, 36.9, 33.8, 29.4, 23.1, 22.4, 21.2. **HRMS ESI** calc. for $C_{15}H_{22}NaO_5$ $[M\text{-}Na]^+$: 305.1359, found: 305.1359.

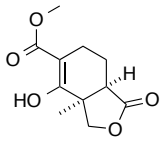

R_f = 0.30 (pentane/EtOAc 4:1). **Optical rotation**: $[\alpha]_D$ = –164.9 (*c* = 0.58, $CHCl_3$). **FTIR**: ν = 2957, 2920, 2852, 2364, 1786, 1656, 1614, 1459, 1440, 1357, 1342, 1285, 1231, 1216, 1147, 1111, 1071, 1037, 1011, 949, 827, 760, 734, 701 cm^{-1}. **^{1}H NMR** (400 MHz, $CDCl_3$) δ = 12.25 (s, 1H), 4.52 (d, *J* = 9.2 Hz, 1H), 3.86 (d, *J* = 9.2 Hz, 1H), 3.66 (s, 3H), 2.49 (t, *J* = 4.5 Hz, 1H), 2.27-2.13 (m, 2H), 2.01 (ddd, *J* = 17.5, 8.5, 4.8 Hz, 1H), 1.65 (dddd, *J* = 14.0, 10.0, 6.9, 4.4 Hz, 1H), 1.34 (s, 3H), 1.19-1.12 (m, 1H). **^{13}C NMR** (126 MHz, $CDCl_3$) δ = 177.3, 172.7, 170.0, 99.5, 75.2, 52.1, 46.2, 43.9, 22.1, 19.4, 18.2. **HRMS ESI** calc. for $C_{11}H_{15}O_5$ $[M\text{-}H]^+$: 227.0914, found: 227.0916.

Chloride (91): Deprotected aldehyde **81** (6.3 mg, 0.019 mmol, 1.0 eq.) was dissolved in $EtOH/CH_2Cl_2$ (1:4, 5 mL) and cooled down to –78 °C. Sodium borohydride (7.4 mg, 0.190 mmol, 10.0 eq.) was added and the reaction was stirred at this temperature for 2.5 h. The reaction was quenched with saturated NH_4Cl solution and extracted three times with EtOAc. Combined organic layers were dried over Na_2SO_4, filtered and evaporated under reduced pressure. The residue was purified by flash chromatography (pentane/EtOAc 2:3) giving chloride **91** (4.6 mg, 0.014 mmol, 73%) as colourless oil.

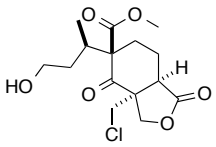

$\mathbf{R_f}$ = 0.27 (pentane/EtOAc 2:3). **^{1}H NMR** (400 MHz, $CDCl_3$) δ = 4.36 (d, *J* = 10.3 Hz, 1H), 4.24 (d, *J* = 11.0 Hz, 1H), 4.03 (d, *J* = 10.3 Hz, 1H), 3.74 (s, 3H), 3.64-3.56 (m, 1H), 3.44 (d, *J* = 11.0 Hz, 1H), 3.23 (dd, *J* = 11.3, 7.2 Hz, 1H), 2.42-2.27 (m, 3H), 2.08-1.96 (m, 1H), 1.88-1.74 (m, 1H), 1.69-1.52 (m, 2H), 1.40-1.29 (m, 2H), 1.02 (d, *J* = 6.8 Hz, 3H).

Iodide (90): Alcohol **91** (13.1 mg, 0.0394 mmol, 1.0 eq.) was dissolved in dry benzene (5 mL) under argon atmosphere. Triphenylphosphine (20.7 mg, 0.0787 mmol, 2.0 eq.), imidazole (10.7 mg, 0.157 mmol, 4.0 eq.) and iodine (20.0 mg, 0.078 mmol, 2 eq.) were added at r.t. and the resulting mixture was stirred for 2 hours at that temperature. The reaction was quenched with a 1:1 mixture of saturated $NaHCO_3$ and $Na_2S_2O_3$ solution and subsequently extracted twice with EtOAc. Combined organic layers were dried over Na_2SO_4, filtered and evaporated under reduced pressure. The crude residue was purified by flash chromatography (pentane/EtOAc 4:1) giving iodide **90** (2.0 mg, 0.0045 mmol, 12%) as colourless oil.

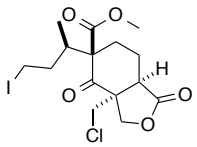

$\mathbf{R_f}$ = 0.20 (pentane/EtOAc 4:1). **^{1}H NMR** (400 MHz, $CDCl_3$) δ = 4.36 (d, *J* = 10.3 Hz, 1H), 4.25 (d, *J* = 11.0 Hz, 1H), 4.02 (d, *J* = 10.3 Hz, 1H), 3.76 (s, 3H), 3.42 (d, *J* = 11.0 Hz, 1H), 3.33 (ddd, *J* = 9.9, 7.2, 4.2 Hz, 1H), 3.22 (dd, *J* = 11.6, 7.3 Hz, 1H), 3.05 (td, *J* = 9.8, 6.5 Hz, 1H), 2.39-2.26 (m, 3H), 1.90-1.73 (m, 2H), 1.68-1.59 (m, 1H), 1.01 (d, *J* = 6.8 Hz, 3H).

Aldehyde (92): In a dry round bottomed flask under argon atmosphere was dissolved

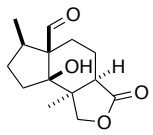

ester **57** (19.7 mg, 0.070 mmol, 1.0 eq.) in dry THF (2 mL) and cooled down to 0°C. Borane-methyl sulfide complex (2 M in THF, 70 µL, 0.140 mmol, 2.0 eq.) was added, the resulting mixture was stirred for 15 min at 0°C and subsequently at 45 °C for 5.5 h. The mixture was allowed to cool down to r.t. for 10 min before ethanol was added until bubbling (exothermic) ceased. The solution was evaporated giving a colourless oil. Purification was performed by flash chromatography (pentane/EtOAc 3:2) giving aldehyde **92** (11.6 mg, 0.0460 mmol, 66%) as a white solid.

R_f = 0.32 (pentane/EtOAc 3:2, CAM dip). **Optical rotation**: $[\alpha]_D$ = –13.7 (*c* = 0.19, MeOH). **^{1}H NMR** (400 MHz, $CDCl_3$) δ = 9.84 (s, 1H), 4.23 (d, *J* = 0.8 Hz, 1H), 3.95 (d, *J* = 9.6 Hz, 1H), 3.51 (s, 1H), 2.29-2.18 (m, 2H), 2.12 (dddd, *J* = 14.4, 10.4, 9.1, 2.2 Hz, 2H), 1.98-1.84 (m, 2H), 1.82-1.72 (m, 1H), 1.72-1.60 (m, 1H), 1.51-1.41 (m, 1H), 1.41-1.32 (m, 1H), 1.22 (d, *J* = 0.8 Hz, 3H), 1.08 (d, *J* = 7.0 Hz, 3H). **^{13}C NMR** (101 MHz, $CDCl_3$) δ = 210.1, 178.9, 86.4, 75.0, 59.8, 47.5, 46.4, 44.6, 37.8, 31.5, 30.5, 22.5, 22.3, 19.8.

Lactone (93): In a dry round bottomed flask under argon atmosphere was dissolved

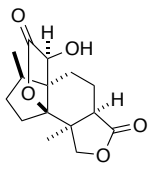

ester **57** (31.8 mg, 0.113 mmol, 1.0 eq.) in dry THF (3 mL) and cooled down to 0°C. Borane-methyl sulfide complex (2 M in THF, 113 µL, 0.225 mmol, 2.0 eq.) was added, the resulting mixture was stirred for 15 min at 0°C and subsequently at 45 °C for 7 h. The mixture was allowed to cool down to r.t. for 10 min before ethanol was added until bubbling (exothermic) ceased. The solution was evaporated giving a colourless oil. Crude aldehyde **92** was dissolved in THF/water (1:1, 4 mL) and potassium cyanide (25.8 mg, 0.396 mmol, 3.5 eq.) was added. The mixture was stirred for 2 d before EtOAc was added and the mixture was stirred for a further day. The phases were separated and the aqueous layer was extraction with EtOAc for a further day. Extractions were performed until no more product was observed in the organic layer. Combined organic layers were dried over Na_2SO_4, filtered and evaporated under reduced pressure. The crude was purified by flash chromatography (EtOAc/pentane

3:2) giving lactone **93** (20.0 mg, 0.0713 mmol, 63%) as a white solid.

$\mathbf{R_f}$ = 0.33 (EtOAc/pentane 1:1). **Optical rotation**: $[\alpha]_D$ = –41.9 (*c* = 0.16, MeOH). **FTIR** ν = 3421, 2965, 2888, 1774, 1758, 1678, 1462, 1379, 1254, 1196, 1159, 1132, 1091, 1026, 974, 944, 876, 820, 753, 716 cm^{-1}. **^{1}H NMR** (400 MHz, $CDCl_3$) δ = 4.40 (d, *J* = 9.6 Hz, 1H), 4.35 (d, *J* = 2.8 Hz, 1H), 3.92 (d, *J* = 9.6 Hz, 1H), 2.69 (d, *J* = 2.9 Hz, 1H), 2.47 (dt, *J* = 8.3, 4.2 Hz, 1H), 2.29-2.19 (m, 1H), 2.12-2.00 (m, 3H), 1.90-1.78 (m, 2H), 1.75-1.65 (m, 1H), 1.35 (s, 3H), 1.08 (d, *J* = 6.7 Hz, 3H). **^{13}C NMR** (101 MHz, $CDCl_3$) δ = 179.7, 176.8, 98.1, 75.7, 68.7, 53.5, 44.7, 44.3, 43.0, 34.5, 30.2, 25.3, 22.3, 20.2, 14.5. **HRMS ESI** calc. for $C_{15}H_{21}O_5$ $[M-H]^+$: 281.1384, found: 281.1380.

Ketone (94): Alcohol **93** (3.7 mg, 0.0128 mmol, 1.0 eq.) was dissolved in dry CH_2Cl_2 (2 mL) under nitrogen atmosphere. Dess-Martin periodinane (10.9 mg, 0.0257 mmol, 2.0 eq.) was added and the mixture was stirred for 2 h at r.t. The reaction was quenched by addition of saturated $NaHCO_3$ solution and extracted three times with EtOAc. Combined organic layers were dried over Na_2SO_4, filtered and evaporated under reduced pressure. The crude product was purified by flash chromatography (pentane/EtOAc 1:1) giving ketone **94** (3.6 mg, 0.0128 mmol, quant.) as a white solid.

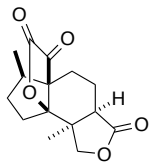

$\mathbf{R_f}$ = 0.37 (pentane/EtOAc 1:1). **^{1}H NMR** (400 MHz, $CDCl_3$) δ = 3.97 (d, *J* = 9.9 Hz, 1H), 3.51 (dd, *J* = 9.9, 0.6 Hz, 1H), 2.48-2.44 (m, 1H), 2.40 (dd, *J* = 14.1, 5.7 Hz, 1H), 2.33-2.19 (m, 1H), 2.11-2.00 (m, 2H), 2.00-1.86 (m, 2H), 1.76 (td, *J* = 13.7, 6.4 Hz, 1H), 1.61 (dd, *J* = 14.7, 2.7 Hz, 1H), 1.46 (d, *J* = 0.6 Hz, 3H), 1.35 (ddd, *J* = 26.5, 13.3, 5.8 Hz, 1H), 1.00 (d, *J* = 7.1 Hz, 3H). **^{13}C NMR** (101 MHz, $CDCl_3$) δ = 198.2, 178.9, 159.8, 97.2, 75.9, 56.6, 46.8, 46.2, 43.9, 37.0, 31.3, 27.4, 24.2, 21.5, 15.0.

Lactone (95): Lactone **38** (23.0 mg, 0.087 mmol, 1.0 eq.) and a catalytic amount of Rh/C (5%, 17.9 mg, 0.009 mmol, 10 mol%) were dissolved in dry EtOH (4 mL). The mixture was hydrogenated with 60 bar H_2 atmosphere overnight and subsequently filtered through silica and celite and washed with EtOAc. The solvent was removed under reduced pressure. The crude material was purified by flash chromatography (EtOAc/cyclohexane 1:1) giving the reduced product **95** (23.2 mg, 0.087 mmol, quant.) as colourless crystals.

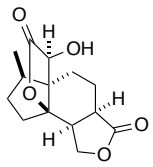

$\mathbf{R_f}$ = 0.20 (EtOAc/cyclohexane 1:1, CAM dip). **Optical rotation**: $[\alpha]_D$ = –50.7 (*c* = 0.31, MeOH). **FTIR** ν = 3467, 2961, 2891, 1775, 1747, 1454, 1384, 1234, 1189, 1150, 1106, 1081, 989, 949, 886, 818, 755, 725 cm^{-1}. **^{1}H NMR** (400 MHz, $CDCl_3$) δ = 4.52 (dd, *J* = 9.7, 1.6 Hz, 1H), 4.45 (dd, *J* = 9.7, 7.3 Hz, 1H), 4.31 (s, 1H), 2.90 (dd, *J* = 19.7, 9.9 Hz, 1H), 2.60-2.53 (m, 1H), 2.45 (ddd, *J* = 13.9, 4.2, 2.8 Hz, 1H), 2.21-2.10 (m, 2H), 1.89-1.79 (m, 3H), 1.57-1.50 (m, 1H), 1.36-1.27 (m, 2H), 1.09 (d, *J* = 6.4 Hz, 3H). **^{13}C NMR** (101 MHz, $CDCl_3$) δ = 178.4, 177.0, 93.9, 67.8, 67.6, 54.7, 43.9, 42.0, 36.8, 36.8, 30.6, 24.7, 18.7, 14.0. **HRMS ESI** calc. for $C_{14}H_{19}O_5$ $[M-H]^+$: 267.1227, found: 267.1225. **X-ray crystal structure** is given in the appendices section.

Ketone (96): Alcohol **95** (4.7 mg, 0.0176 mmol, 1.0 eq.) was dissolved in dry CH_2Cl_2 (2 mL) under nitrogen atmosphere. Dess-Martin periodinane (8.3 mg, 0.0194 mmol, 1.1 eq.) was added and the mixture was stirred for 2 h at r.t. The reaction was quenched by addition of saturated $NaHCO_3$ solution and extracted three times with EtOAc. Combined organic layers were dried over Na_2SO_4, filtered and evaporated under reduced pressure. The crude was purified by flash chromatography **(**EtOAc/pentane 1:1) giving ketone **96** (4.7 mg, 0.0176 mmol, quant.) as a white solid.

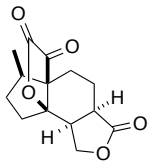

$\mathbf{R_f}$ = 0.11 (pentane/EtOAc 1:1). **Optical rotation**: $[\alpha]_D$ = –43.1 (*c* = 0.29, $CHCl_3$). **FTIR** ν = 2968, 2928, 2873, 2361, 1775, 1756, 1478, 1382, 1337, 1277, 1257, 1210, 1190, 1164, 1147, 1064, 1030, 984, 966, 935, 897, 870, 831, 802, 731 cm^{-1}. **^{1}H NMR**

(400 MHz, $CDCl_3$) δ = 4.49 (dd, *J* = 10.0, 8.4 Hz, 1H), 4.04 (dd, *J* = 10.0, 6.3 Hz, 1H), 3.16 (ddd, *J* = 10.1, 8.4, 6.3 Hz, 1H), 2.98-2.87 (m, 1H), 2.41 (dd, *J* = 13.9, 6.3 Hz, 1H), 2.20-2.09 (m, 1H), 2.01-1.84 (m, 3H), 1.74-1.53 (m, 3H), 1.37-1.28 (m, 1H), 1.06 (d, *J* = 7.0 Hz, 3H). **^{13}C NMR** (101 MHz, $CDCl_3$) δ = 199.1, 178.1, 159.2, 93.6, 68.1, 56.3, 47.2, 40.7, 39.4, 36.9, 31.5, 28.6, 19.9, 14.4. **HRMS ESI** calc. for $C_{14}H_{17}O_5$ $[M-H]^+$: 265.1071, found: 265.1069.

TES ether (97): Lactone **41** (10.0 mg, 0.0264 mmol, 1.0 eq.) and a catalytic amount of $Pd(OH)_2/C$ (20%, 1.85 mg, 0.00264 mmol, 0.1 eq.) were dissolved in dry EtOH (1 mL) and hydrogenated under 70 bar H_2 pressure overnight. The reaction mixture was filtered through silica and celite and washed with EtOAc. The solvent was evaporated under reduced pressure to give the reduced product **97** (10.0 mg, 0.0264 mmol, quant.) as a white solid.

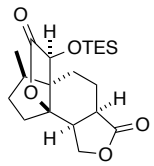

R_f = 0.21 (EtOAc/pentane 1:4). **Optical rotation**: $[\alpha]_D$ = –32.6 (*c* = 0.40, MeOH). **FTIR** ν = 2954, 2922, 2875, 1777, 1758, 1457, 1381, 1236, 1193, 1162, 1147, 1088, 1062, 1038, 1003, 968, 945, 891, 835, 807, 741, 719 cm^{-1}. **^{1}H NMR** (400 MHz, $CDCl_3$) δ = 4.49 (dd, *J* = 9.6, 2.3 Hz, 1H), 4.42 (dd, *J* = 9.6, 7.6 Hz, 1H), 4.33 (s, 1H), 2.87 (dd, *J* = 19.0, 10.0 Hz, 1H), 2.59 (ddd, *J* = 10.0, 7.6, 2.3 Hz, 1H), 2.41 (ddd, *J* = 13.7, 5.2, 2.7 Hz, 1H), 2.17-2.05 (m, 2H), 1.89-1.70 (m, 3H), 1.52-1.31 (m, 2H), 1.25 (dt, *J* = 7.0, 6.6 Hz, 1H), 1.04 (d, *J* = 6.5 Hz, 3H), 1.00-0.92 (m, 9H), 0.82-0.61 (m, 6H). **^{13}C NMR** (101 MHz, $CDCl_3$) δ = 178.7, 175.4, 92.7, 69.0, 67.8, 54.3, 44.0, 41.8, 37.3, 37.0, 25.3, 18.8, 14.2, 7.0, 5.4. **HRMS ESI** calc. for $C_{20}H_{26}NO_5Si$ $[M-NH_4]^+$: 398.2357, found: 398.2352.

Alcohol (98): To a solution of the protected lactone **97** (7.0 mg, 0.0184 mmol, 1 eq.) in dry THF (3 mL) at –78 °C was added LiHMDS (1 M in THF, 28 µL, 0.0276 mmol, 1.5 eq.) drop wise. After stirring for 30 min triphenyl phosphite (8.8 mg, 0.0276 mmol, 1.5 eq.) was added. Oxygen was then passed through the reaction until TLC showed near disappearance of

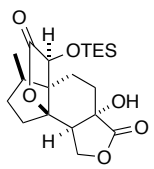

starting material. The reaction was then quenched by the addition of 1 M HCl solution at –78 °C. The resulting mixture was slowly heated up to r.t. overnight and extracted three times with EtOAc. Combined organic layers were washed with brine, dried over Na_2SO_4, filtered and evaporated under reduced pressure. The crude residue was purified by flash chromatography (pentane/EtOAc 2:1) to yield the hydroxylated product **98** (3.4 mg, 0.0184 mmol, 47%) as a white solid.

R_f = 0.29 (pentane/EtOAc 2:1). **^{1}H NMR** (400 MHz, $CDCl_3$) δ = 4.53 (dd, *J* = 9.5, 8.8 Hz, 1H), 4.40 (dd, *J* = 9.6, 5.7 Hz, 1H), 4.33 (s, 1H), 2.75 (dd, *J* = 8.7, 5.7 Hz, 1H), 2.55 (dd, *J* = 14.3, 7.2 Hz, 1H), 2.22 (ddd, *J* = 14.2, 8.0, 3.3 Hz, 1H), 2.14-1.99 (m, 2H), 1.94-1.76 (m, 4H), 1.42-1.29 (m, 2H), 1.06 (d, *J* = 6.9 Hz, 3H), 1.00-0.92 (m, 9H), 0.80-0.62 (m, 6H). **^{13}C NMR** (101 MHz, $CDCl_3$) δ = 178.8, 175.2, 93.5, 73.9, 70.0, 67.3, 53.3, 48.5, 46.2, 43.6, 38.1, 30.9, 29.5, 23.0, 14.7, 6.9, 5.1.

Lactone (99): Alcohol **93** (2.5 mg, 0.0089 mmol, 1.0 eq.) was dissolved in dry THF (1 mL) under nitrogen atmosphere and cooled down to –78 °C. LDA (0.28 M in THF, 96 µL, 0.0268 mmol, 3.0 eq.) was added at –78 °C and the mixture was stirred for 1 h. Phenylselenyl bromide (4.2 mg, 0.0178 mmol, 2.0 eq.) was dissolved in THF (0.15 mL) and added at –78 °C. The resulting mixture was stirred for 1 h at that temperature and subsequently heated up to 0 °C and stirred for further 30 min. The reaction mixture was diluted with a saturated NH_4Cl solution and EtOAc. The layers were separated and the aqueous layer was extracted two times with EtOAc. Combined organic layers were dried over Na_2SO_4, filtered and evaporated under reduced pressure. The residue was dissolved in THF (1 mL) and cooled down to 0 °C. One drop of AcOH and H_2O_2 (35% in H_2O) were added and the mixture was stirred for 2 h before a saturated $NaHCO_3$ solution was added and stirred 1 h at r.t. Extraction with performed three times with EtOAc. Combined organic layers were dried over Na_2SO_4, filtered and evaporated under reduced pressure. Purification was performed by flash chromatography to yield the desired product **99** (1.2 mg, 0.00431 mmol, 48%) as a crystalline solid.

R_f = 0.21 (pentane/EtOAc 1:4). **Optical rotation**: $[\alpha]_D$ = –68.4 (*c* = 0.29, MeOH). **FTIR**: ν = 3357, 2923, 2853, 1762, 1662, 1467, 1378, 1263, 1208, 1159, 1095, 1022, 962, 930, 902, 795, 748 cm^{-1}. **^{1}H NMR** (400 MHz, d_4-MeOD) δ = 4.75 (t, *J* = 5.7 Hz, 1H), 4.65 (d, *J* = 9.3 Hz, 1H), 4.01 (s, 1H), 3.87 (d, *J* = 9.3 Hz, 1H), 3.07 (d, *J* = 5.2 Hz, 1H), 2.31-2.21 (m, 2H), 2.09-1.94 (m, 4H), 1.36 (s, 3H), 1.27-1.15 (m, 1H), 1.08 (d, *J* = 7.0 Hz, 3H). **^{13}C NMR** (101 MHz, d_4-MeOD) δ = 177.7, 174.9, 101.9, 78.7, 75.6, 75.5, 60.4, 55.4, 44.7, 39.0, 35.4, 34.0, 32.8, 27.3, 15.8. **HRMS ESI** calc. for $C_{15}H_{19}O_5$ $[M-H]^+$: 279.1227, found: 279.1223. **X-ray crystal structure** is given in the appendix.

Silyl ether (100): Lactone **99** (1.1 mg, 0.004 mmol, 1.0 eq.) was dissolved in dry THF (1 mL) under argon atmosphere and cooled down to –78 °C and 1 drop of lithium *bis*(trimethylsilyl)amide (1 M in THF) was added and the mixture was stirred for 1 h at that temperature. After that time, 1 drop of trimethylchlorosilane was added and the mixture was stirred 30 min at –78 °C. The mixture was heated up to 0 °C and stirred for 30 min before it was quenched by addition a saturated $NaHCO_3$ solution. The mixture was diluted with EtOAc, dried over Na_2SO_4 and filtered over a pad of silica. The organic layer was evaporated under reduced pressure. The crude ^{1}H-NMR showed already quite pure product. Yield was not determined due to the low amount used for the reaction.

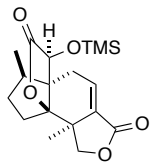

^{1}H NMR (400 MHz, d_4-MeOD) δ = 7.02 (dd, *J* = 7.9, 3.1 Hz, 1H), 4.65 (d, *J* = 9.1 Hz, 1H), 4.46 (s, 1H), 4.16 (d, *J* = 9.1 Hz, 1H), 3.19 (dd, *J* = 16.7, 7.9 Hz, 1H), 2.27 (ddd, *J* = 15.0, 10.9, 8.5 Hz, 1H), 2.14-2.00 (m, 1H), 2.05 (dd, *J* = 16.7, 3.1 Hz, 2H), 1.95 (ddd, *J* = 20.2, 13.6, 8.0 Hz, 2H), 1.76-1.63 (m, 1H), 1.33 (s, 3H), 1.07 (d, *J* = 6.7 Hz, 3H), 0.22 (s, 9H).

Silyl ether (101): Lactone **99** (1.1 mg, 0.004 mmol, 1.0 eq.) was dissolved in dry THF (1 mL) under argon atmosphere and cooled down to –78 °C and 1 drop of lithium *bis*(trimethylsilyl)amide (1 M in THF) was added and the mixture was stirred for 1 h at that temperature. After that time, 1 drop of trimethylchlorosilane was added and the mixture was stirred 30 min at –78 °C. The mixture was heated up to 0 °C and stirred for 30 min before it was quenched by addition a saturated $NaHCO_3$ solution. The mixture was diluted with EtOAc, dried over Na_2SO_4 and filtered over a pad of silica. The organic layer was evaporated under reduced pressure. Purification was performed by flash chromatography (pentane/EtOAc 1:1) to yield the desired product **101** along with some remaining reagents. Yield was not determined due to low amount used for the reaction.

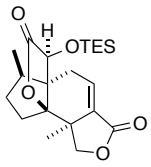

R_f = 0.66 (pentane/EtOAc 1:1). **^{1}H NMR** (400 MHz, d_4-MeOD) δ = 7.02 (dd, *J* = 7.9, 3.2, 1H), 4.66 (d, *J* = 9.2, 1H), 4.44 (s, 1H), 4.16 (d, *J* = 9.1, 1H), 3.22 (dd, *J* = 16.6, 7.9, 1H), 2.27 (ddd, *J* = 15.0, 11.2, 8.5, 1H), 2.15-2.03 (m, 2H), 2.00-1.88 (m, 2H), 1.72-1.59 (m, 1H), 1.34 (s, 3H), 1.09 (d, *J* = 6.7, 3H), 1.03-0.98 (m, 9H), 0.84-0.65 (m, 6H).

10-Deoxy-jiadifenolide (102): TMS-protected alcohol **100** (1.4 mg, 0.0039 mmol) was dissolved in a MeOH/THF mixture (4 mL, 3:1) and cooled down to 0 °C. One drop of hydrogen peroxide (35% in water) and one drop of an aqueous 1 M NaOH solution were added and the resulting mixture was stirred for 1 h at 0 °C and subsequently for 15 h at r.t. EtOAc was added and the mixture was dried over Na_2SO_4 and filtered over a pad with silica. The filtrate was evaporated under reduced pressure. Purification was performed by flash chromatography (EtOAc/pentane 4:1) and the desired product was obtained as a white solid. Yield was not determined due to low amount used for the reaction.

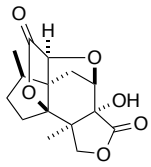

R_f = 0.25 (CH_2Cl_2/MeoH 20:1). **^{1}H NMR** (500 MHz, d_4-MeOD) δ = 4.63 (d, *J* = 9.4 Hz, 1H), 4.39 (d, *J* = 5.8 Hz, 1H), 3.97 (s, 1H), 3.82 (d, *J* = 9.4 Hz, 1H), 2.30-2.18 (m, 3H), 2.12 (d, *J* = 13.0 Hz, 1H), 2.09-2.05 (m, 2H), 1.99 (dtd, *J* = 8.4, 4.7, 1.9 Hz, 1H), 1.22 (s, 3H), 1.07 (d, *J* = 7.0 Hz, 3H). **^{13}C NMR** (126 MHz,

d_4-MeOD) δ = 177.9, 174.6, 100.5, 81.2, 78.4, 78.3, 74.5, 60.4, 47.6, 38.6, 34.3, 33.0, 32.5, 19.3, 15.3. **HRMS ESI** calc. for $C_{15}H_{18}NaO_6$ $[M\text{-}Na]^+$: 317.0996, found: 317.0994.

Olefin (103): Lactone **99** (1.3 mg, 0.005 mmol, 1.0 eq.) was dissolved in dry THF (1 mL) under argon atmosphere and cooled down to -78 °C and 1 drop of lithium *bis*(trimethylsilyl)amide (1 M in THF) was added and the mixture was stirred for 1 h at that temperature. Dess-Martin periodinane (5.9 mg, 0.014 mmol, 3.0 eq.) was added and the resulting mixture was stirred 30 min at the same temperature and subsequently heated up to r.t. for 1 h. Reaction was quenched by addition a saturated $NaHCO_3$ solution. The mixture was diluted with EtOAc, dried over Na_2SO_4, filtered over a pad of silica and washed with EtOAc. The filtrate was evaporated under reduced pressure. The crude product was used for further reactions without additional purification. Yield was not determined due to low amount used for the reaction.

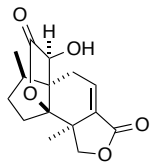

^{1}H NMR (400 MHz, d_4-MeOD) δ = 7.04 (dd, *J* = 7.9, 3.1, 1H), 4.65 (dd, *J* = 9.1, 0.5, 1H), 4.38 (s, 1H), 4.16 (d, *J* = 9.1, 1H), 3.22 (dd, *J* = 16.9, 7.9, 1H), 2.29 (ddd, *J* = 15.1, 10.9, 8.7, 1H), 2.14-2.00 (m, 2H), 2.00-1.88 (m, 2H), 1.76-1.63 (m, 1H), 1.33 (s, 3H), 1.09 (d, *J* = 6.7, 3H).

Keto lactone (104): Alcohol **103** (0.5 mg, 0.0018 mmol, 1.0 eq.) was dissolved in dry CH_2Cl_2 (2 mL) and Dess-Martin periodinane (1.5 mg, 0.0036 mmol, 2.0 eq.) was added. The resulting mixture was stirred overnight at room temperature. The reaction was quenched by addition of an aqueous saturated $NaHCO_3$ solution. Extraction was performed three times with EtOAc and combined organic layers were dried over Na_2SO_4, filtered and evaporated under reduced pressure. Product **104** was obtained along with some traces of the starting material and was used for further reactions without additional purification. Yield was not determined due to low amount used for the reaction.

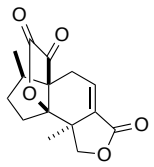

^{1}H NMR (400 MHz, d_4-MeOD) δ = 6.95 (dd, *J* = 7.7, 3.2, 1H), 4.26 (d, *J* = 9.4, 1H), 3.04 (dd, *J* = 16.6, 7.7, 1H), 2.54 (dd, *J* = 16.6, 3.2, 1H), 2.45 (ddd, *J* = 14.6, 12.8, 6.7, 1H), 2.28-2.18 (m, 1H), 2.14 (dd, *J* = 14.5, 6.1, 1H), 2.09-1.98 (m, 2H), 1.40 (d, *J* = 0.6, 3H), 1.08 (d, *J* = 6.9, 3H). One of the C-13 protons is hidden under the water peak between 4.89 and 4.85 ppm.

Mesylate (105): Lactone **99** (2.9 mg, 0.0104 mmol, 1.0 eq.) was dissolved in dry THF (1.5 mL) under argon atmosphere and cooled down to –78 °C. One drop of lithium *bis*(trimethylsilyl)amide (1 M in THF) was added and the mixture was stirred for 40 min at that temperature before one drop of methanesulfonyl chloride was added. The resulting mixture was stirred for 1.5 h at –78 °C, heated up to 0 °C and stirred for a further hour. Finally, the solution was warmed up to room temperature and quenched with an aqueous saturated $NHCl_4$ solution after 20 min. The mixture was diluted with EtOAc, dried over Na_2SO_4 and filtered over a pad of silica. The organic layer was evaporated under reduced pressure. The crude product was used for further reactions without additional purification. Yield was not determined due to low amount used for the reaction and impurities present in the crude product.

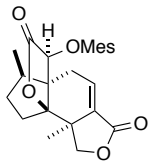

^{1}H NMR (400 MHz, d_4-MeOD) δ = 7.07 (dd, *J* = 7.8, 3.3, 1H), 5.45 (s, 1H), 4.66 (dd, *J* = 9.3, 0.4, 1H), 4.19 (d, *J* = 9.3, 1H), 3.35 (s, 3H), 3.08 (dd, *J* = 17.7, 7.1, 1H), 2.36-2.23 (m, 2H), 2.20-2.09 (m, 1H), 2.06-1.94 (m, 2H), 1.82-1.69 (m, 1H), 1.36 (s, 3H), 1.17 (d, *J* = 6.8, 3H).

Alcohol (106): Crude mesylate **105** was dissolved in a water/ethanol mixture (0.9 mL, 1:2) and some drops of an aqueous 1 M NaOH solution were added. The resulting mixture was stirred for 1 h at room temperature. Solution was diluted with EtOAc, dried over Na_2SO_4, filtered over a pad of silica and dried *in vacuo*. The crude product was used for further reactions without additional purification. Yield was not determined due to low amount used for the reaction and impurities present in the crude product.

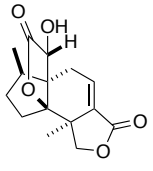

^{1}H NMR (500 MHz, d_4-MeOD) δ = 6.92 (dd, *J* = 7.8, 2.7, 1H), 4.73 (s, 1H), 4.57 (dd, *J* = 8.5, 0.5, 1H), 4.05 (d, *J* = 8.5, 1H), 2.89 (dd, J=17.3, 7.8, 1H), 2.14-2.08 (m, 1H), 2.09 (dd, *J* = 17.4, 2.8, 1H), 2.02-1.95 (m, 2H), 1.95-1.86 (m, 1H), 1.76 (d, *J* = 7.7, 1H), 1.10 (s, 3H), 1.09 (d, *J* = 7.1, 3H). **^{13}C NMR** (125 MHz, $CDCl_3$) δ = 174.3, 171.1, 138.9, 135.53, 98.1, 75.8, 74.0, 58.5, 46.9, 43.4, 33.7, 32.4, 28.6, 21.7, 12.3.

Lactone (108): Ester **57** (4.5 mg, 0.0159 mmol, 1.0 eq.) was dissolved in dry THF (1 mL) under nitrogen atmosphere and cooled down to –78 °C. LDA (0.28 M in THF, 171 µL, 0.0478 mmol, 3.0 eq.) was added at –78 °C and the mixture was stirred for 1 h. Phenylselenyl bromide (7.5 mg, 0.0319 mmol, 2.0 eq.) was dissolved in THF (0.25 mL) and added at –78 °C. The resulting mixture was stirred for 1 h at that temperature and subsequently heated up to 0 °C and stirred for further 30 min. The reaction mixture was diluted with a saturated NH_4Cl solution and EtOAc. The layers were separated and the aqueous layer was extracted two times with EtOAc. Combined organic layers were dried over Na_2SO_4, filtered and evaporated under reduced pressure. The residue was dissolved in THF (1 mL) and cooled down to 0 °C. One drop of AcOH and H_2O_2 (35% in H_2O) were added and the mixture was stirred for 2 h before a saturated $NaHCO_3$ solution was added and stirred 1 h at r.t. Extraction with performed three times with EtOAc. Combined organic layers were dried over Na_2SO_4, filtered and evaporated under reduced pressure. Purification was performed by flash chromatography (pentane/EtOAc 4:1 to 3:1) to yield the desired product **108** (2.4 mg, 0.0086 mmol, 54%) as a white solid and unreacted starting material (1.5 mg, 0.0053 mmol, 81% *brsm*).

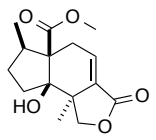

R_f = 0.23 (pentane/EtOAc 3:1). **Optical rotation**: $[\alpha]_D$ = +11.4 (*c* = 0.48, $CHCl_3$). **FTIR**: ν = 3478, 2944, 2921, 2891, 1729, 1683, 1467, 1374, 1343, 1327, 1270, 1250, 1236, 1193, 1168, 1132, 1109, 1080, 1043, 1027, 997, 975, 897, 851, 791, 763, 749 cm^{-1}. **^{1}H NMR** (400 MHz, $CDCl_3$) δ = 6.80 (dd, *J* = 7.5, 2.9 Hz, 1H), 4.54 (d, *J* = 1.5 Hz, 1H), 4.51 (dd, *J* = 8.5, 0.8 Hz, 1H), 4.00 (d, *J* = 8.5 Hz, 1H), 3.70 (s, 3H), 3.04 (dd, *J* = 17.1, 7.6 Hz, 1H), 2.23-2.13 (m, 2H), 2.12-1.94 (m, 4H), 1.79 (ddt, *J* = 12.0, 6.8, 3.4 Hz, 1H), 1.29 (d, *J* = 0.8 Hz, 3H), 1.02 (d, *J* = 7.0 Hz, 3H).

^{13}C NMR (101 MHz, $CDCl_3$) δ = 176.1, 169.3, 138.6, 132.7, 87.3, 76.0, 61.3, 52.4, 48.1, 43.8, 35.8, 34.3, 30.7, 22.4, 19.5. **HRMS ESI** calc. for $C_{15}H_{21}O_5$ $[M-H]^+$: 281.1384, found: 281.1383.

8 APPENDICES

8.1 Crystal Structures

Table 14: Crystal data for **25**.

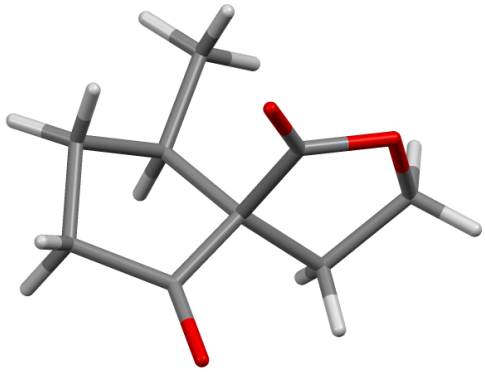

Formula	$C_9H_{12}O_3$
Formula weight	168.19 g · Mol^{-1}
Z, calculated density	4, 1.341 Mg · m^{-3}
F(000)	360
Description and size of crystal	colourless, 0.060 · 0.140 · 0.270 mm^3
Absorption coefficient	0.100 mm^{-1}
Min/max transmission	0.99 / 0.99
Temperature	123K
Radiation (wavelength)	Mo K_α (λ = 0.71073 Å)
Crystal system, space group	orthorhombic, $P\ 2_1\ 2_1\ 2_1$
a	6.0219(6) Å
b	10.7615(11) Å
c	12.8590(12) Å
α	90°
β	90°
γ	90°
V	833.32(14) $Å^3$
Min/max Θ	2.468° / 33.721°
Number of collected reflections	21946
Number of independent reflections	1926 (merging r = 0.041)
Number of observed reflections	1606 (I>2.0σ(I))
Number of refined parameters	109
r	0.0286
rW	0.0408
Goodness of fit	1.0898

Table 15: Crystal data for **33**.

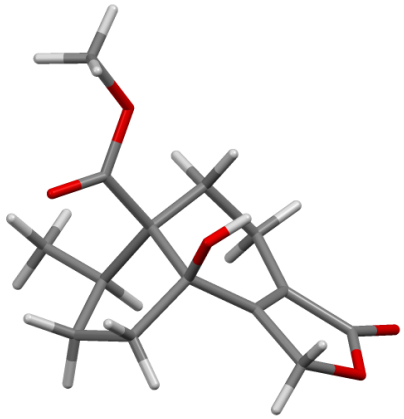

Formula	$C_{14}H_{18}O_5$
Formula weight	266.29 g · Mol^{-1}
Z, calculated density	2, 1.372 Mg · m^{-3}
F(000)	284
Description and size of crystal	colourless, 0.020 · 0.070 · 0.340 mm^3
Absorption coefficient	0.104 mm^{-1}
Min/max transmission	0.99 / 1.00
Temperature	123K
Radiation (wavelength)	Mo K_α (λ = 0.71073 Å)
Crystal system, space group	monoclinic, $P\,2_1$
a	8.2257(4) Å
b	8.6177(4) Å
c	9.4412(4) Å
α	90°
β	105.591(3)°
γ	90°
V	644.63(5) $Å^3$
Min/max Θ	2.240° / 33.031°
Number of collected reflections	15153
Number of independent reflections	2573 (merging r = 0.046)
Number of observed reflections	2011 (I>2.0σ(I))
Number of refined parameters	172
r	0.0360
rW	0.0476
Goodness of fit	1.1258

Table 16: Crystal data for **35**.

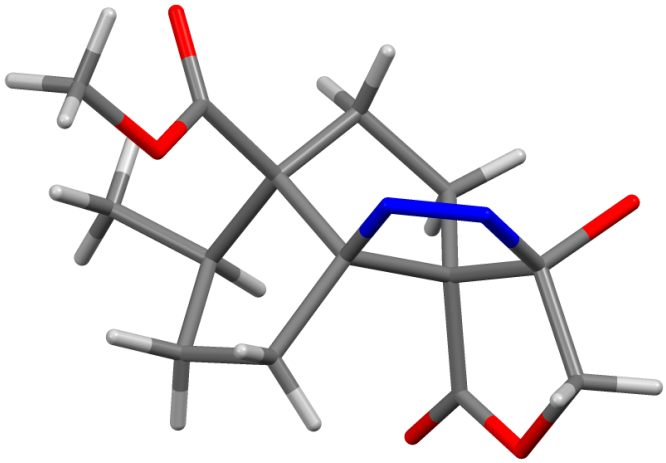

Formula	$C_{14}H_{19}N_2O_5$
Formula weight	294.31 g · Mol^{-1}
Z, calculated density	4, 1.277 Mg · m-3
F(000)	572
Description and size of crystal	colourless, ? · ? · ? mm^3
Absorption coefficient	0.072 mm^{-1}
Min/max transmission	1.0000 / 1.0000
Temperature	293K
Radiation (wavelength)	Mo K_α (λ = 0.71073 Å)
Crystal system, space group	orthorhombic, $P\ 2_1\ 2_1\ 2_1$
a	34.202(14) Å
b	6.366(3) Å
c	6.432(2) Å
α	90°
β	90°
γ	90°
V	1400.5(10) $Å^3$
Min/max Θ	2.382° / 26.425°
Number of collected reflections	8620
Number of independent reflections	1702 (merging r = 0.180)
Number of observed reflections	865 (I>2.0σ(I))
Number of refined parameters	68
r	0.2266
rW	0.3259
Goodness of fit	0.8879

Table 17: Crystal data for **38**.

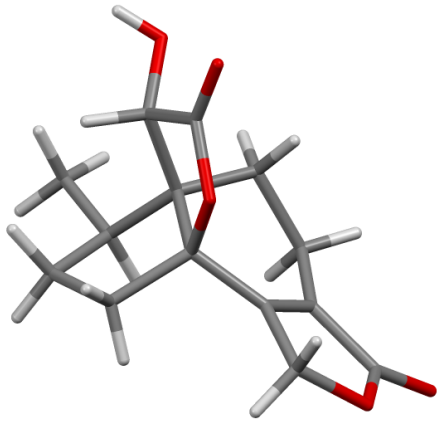

Formula	$C_{14}H_{16}O_5$
Formula weight	264.28 g · Mol^{-1}
Z, calculated density	4, 1.403 Mg · m^{-3}
F(000)	560
Description and size of crystal	colourless, 0.030 · 0.150 · 0.330 mm^3
Absorption coefficient	0.107 mm-1
Min/max transmission	0.98 / 1.00
Temperature	173K
Radiation (wavelength)	Mo K_α (λ = 0.71073 Å)
Crystal system, space group	orthorhombic, $P\,2_1\,2_1\,2_1$
a	7.7488(2) Å
b	11.5545(3) Å
c	13.9686(4) Å
α	90°
β	90°
γ	90°
V	1250.66(6) $Å^3$
Min/max Θ	2.287° / 35.631°
Number of collected reflections	40767
Number of independent reflections	3247 (merging r = 0.033)
Number of observed reflections	2704 (I>2.0σ(I))
Number of refined parameters	172
r	0.0308
rW	0.0469
Goodness of fit	1.0627

Table 18: Crystal data for **39**.

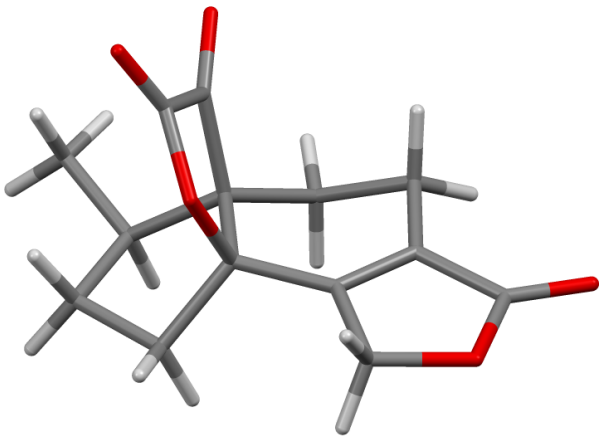

Formula	$C_{14}H_{14}O_5$
Formula weight	262.26 g · Mol^{-1}
Z, calculated density	8, 1.418 Mg · m^{-3}
F(000)	1104
Description and size of crystal	colourless, 0.030 · 0.090 · 0.230 mm^3
Absorption coefficient	0.108 mm^{-1}
Min/max transmission	0.99 / 1.00
Temperature	173K
Radiation (wavelength)	Mo K_α (λ = 0.71073 Å)
Crystal system, space group	orthorhombic, $P\ 2_1\ 2_1\ 2_1$
a	7.1075(2) Å
b	13.8782(4) Å
c	24.9039(7) Å
α	90°
β	90°
γ	90°
V	2456.50(12) $Å^3$
Min/max Θ	1.635° / 32.583°
Number of collected reflections	61046
Number of independent reflections	5007 (merging r = 0.048)
Number of observed reflections	3825 (I>2.0σ(I))
Number of refined parameters	343
r	0.0437
rW	0.0731
Goodness of fit	1.0932

Table 19: Crystal data for **45**.

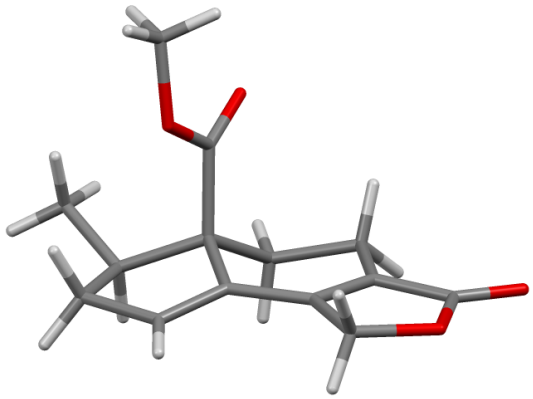

Formula	$C_{14}H_{16}O_4$
Formula weight	248.28 g · Mol^{-1}
Z, calculated density	2, 1.355 Mg · m^{-3}
F(000)	264
Description and size of crystal	colourless, 0.020 · 0.160 · 0.210 mm^3
Absorption coefficient	0.099 mm^{-1}
Min/max transmission	0.98 / 1.00
Temperature	123K
Radiation (wavelength)	Mo K_α (λ = 0.71073 Å)
Crystal system, space group	monoclinic, $P\,2_1$
a	6.4095(17) Å
b	13.267(3) Å
c	7.6203(19) Å
α	90°
β	110.130(12)°
γ	90°
V	608.4(3) $Å^3$
Min/max Θ	2.847° / 31.582°
Number of collected reflections	12794
Number of independent reflections	2109 (merging r = 0.068)
Number of observed reflections	1737 (I>2.0σ(I))
Number of refined parameters	163
r	0.0537
rW	0.0751
Goodness of fit	1.1043

Table 20: Crystal data for **51**.

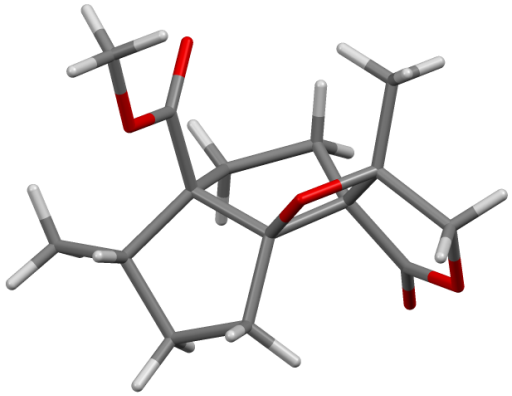

Formula	$C_{15}H_{20}O_5$
Formula weight	280.32 g · Mol^{-1}
Z, calculated density	4, 1.314 Mg · m^{-3}
F(000)	600
Description and size of crystal	colourless, 0.030 · 0.080 · 0.310 mm^3
Absorption coefficient	0.098 mm^{-1}
Min/max transmission	0.99 / 1.00
Temperature	123K
Radiation (wavelength)	Mo K_α (λ = 0.71073 Å)
Crystal system, space group	monoclinic, $P\,2_1$
a	12.9173(5) Å
b	7.3710(3) Å
c	15.3483(6) Å
α	90°
β	104.086(2)°
γ	90°
V	1417.42(10) $Å^3$
Min/max Θ	1.852° / 30.032°
Number of collected reflections	18394
Number of independent reflections	4442 (merging r = 0.034)
Number of observed reflections	3663 (I>2.0σ(I))
Number of refined parameters	361
r	0.0339
rW	0.0466
Goodness of fit	1.1259

Table 21: Crystal data for **60**.

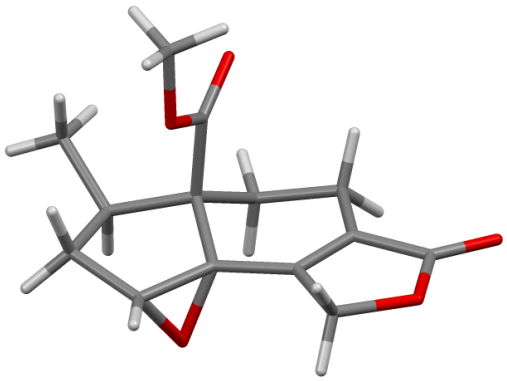

Formula	$C_{14}H_{16}O_5$
Formula weight	264.28 g · Mol^{-1}
Z, calculated density	4, 1.377 Mg · m^{-3}
F(000)	560
Description and size of crystal	colourless, 0.040 · 0.170 · 0.230 mm^3
Absorption coefficient	0.105 mm^{-1}
Min/max transmission	0.98 / 1.00
Temperature	123K
Radiation (wavelength)	Mo K_α (λ = 0.71073 Å)
Crystal system, space group	monoclinic, $P\,2_1$
a	9.9581(4) Å
b	9.1172(4) Å
c	14.0670(6) Å
α	90°
β	93.587(2)°
γ	90°
V	1274.64(9) $Å^3$
Min/max Θ	2.584° / 32.580°
Number of collected reflections	35267
Number of independent reflections	4892 (merging r = 0.029)
Number of observed reflections	4161 (I>2.0σ(I))
Number of refined parameters	343
r	0.0302
rW	0.0435
Goodness of fit	1.1028

Table 22: Crystal data for **63**.

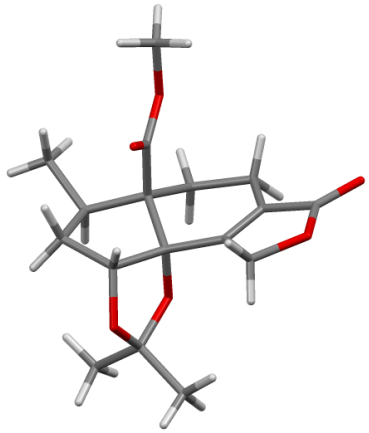

Formula	$C_{17}H_{22}O_6$
Formula weight	322.36 g · Mol^{-1}
Z, calculated density	2, 1.314 Mg · m^{-3}
F(000)	344
Description and size of crystal	colourless, 0.010 · 0.070 · 0.220 mm^3
Absorption coefficient	0.099 mm^{-1}
Min/max transmission	0.99 / 1.00
Temperature	173K
Radiation (wavelength)	Mo K_α (λ = 0.71073 Å)
Crystal system, space group	monoclinic, $P\,2_1$
a	9.3651(9) Å
b	10.4682(10) Å
c	9.3907(10) Å
α	90°
β	117.748(4)°
γ	90°
V	814.76(14) $Å^3$
Min/max Θ	2.451° / 25.030°
Number of collected reflections	7520
Number of independent reflections	1523 (merging r = 0.126)
Number of observed reflections	1219 (I>2.0σ(I))
Number of refined parameters	208
r	0.0599
rW	0.1075
Goodness of fit	1.0557

Table 23: Crystal data for **75**.

Formula	$C_{14}H_{20}O_6$
Formula weight	284.31 g · Mol^{-1}
Z, calculated density	4, 1.391 Mg · m^{-3}
F(000)	608
Description and size of crystal	colourless, 0.020 · 0.110 · 0.280 mm^3
Absorption coefficient	0.109 mm^{-1}
Min/max transmission	0.99 / 1.00
Temperature	123K
Radiation (wavelength)	Mo K_α (λ = 0.71073 Å)
Crystal system, space group	orthorhombic, $P\,2_1\,2_1\,2_1$
a	8.7432(5) Å
b	12.2122(7) Å
c	12.7131(8) Å
α	90°
β	90°
γ	90°
V	1357.42(14) $Å^3$
Min/max Θ	3.283° / 39.394°
Number of collected reflections	48036
Number of independent reflections	4479 (merging r = 0.037)
Number of observed reflections	3516 (I>2.0σ(I))
Number of refined parameters	181
r	0.0314
rW	0.0524
Goodness of fit	1.0609

Table 24: Crystal data for **84**.

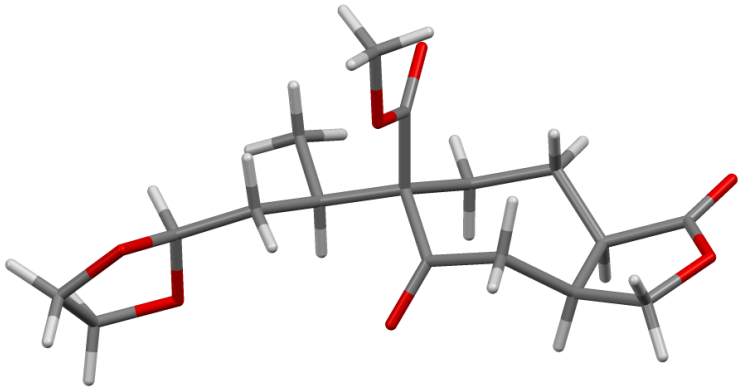

Formula	$C_{17}H_{24}O_7$
Formula weight	340.37 g · Mol^{-1}
Z, calculated density	2, 1.382 Mg · m^{-3}
F(000)	364
Description and size of crystal	colourless, 0.020 · 0.170 · 0.190 mm^3
Absorption coefficient	0.898 mm^{-1}
Min/max transmission	0.86 / 0.98
Temperature	123K
Radiation (wavelength)	Cu K_α (λ = 1.54178 Å)
Crystal system, space group	monoclinic, $P\,2_1$
a	10.7060(13) Å
b	6.2176(8) Å
c	12.2984(19) Å
α	90°
β	92.267(10)°
γ	90°
V	818.01(19) $Å^3$
Min/max Θ	3.597° / 68.402°
Number of collected reflections	5437
Number of independent reflections	2714 (merging r = 0.059)
Number of observed reflections	2270 (I>2.0σ(I))
Number of refined parameters	219
r	0.0953
rW	0.1148
Goodness of fit	1.0534

Table 25: Crystal data for **89**.

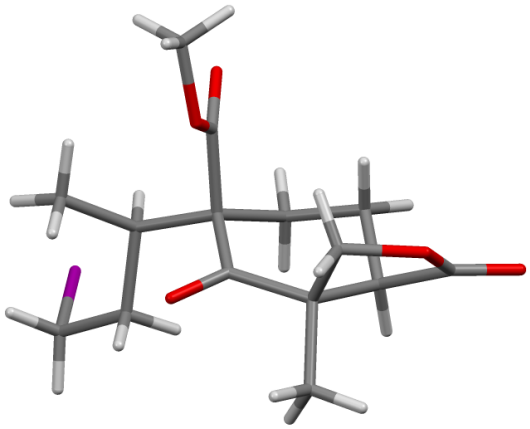

Formula	$C_{15}H_{21}I_1O_5$
Formula weight	408.23 g · Mol^{-1}
Z, calculated density	4, 1.711 Mg · m^{-3}
F(000)	816
Description and size of crystal	colourless, 0.010 · 0.020 · 0.230 mm^3
Absorption coefficient	2.039 mm^{-1}
Min/max transmission	0.96 / 0.98
Temperature	123K
Radiation (wavelength)	Mo K_α (λ = 0.71073 Å)
Crystal system, space group	orthorhombic, $P\,2_1\,2_1\,2_1$
a	6.2741(8) Å
b	13.1986(16) Å
c	19.138(2) Å
α	90°
β	90°
γ	90°
V	1584.8(3) $Å^3$
Min/max Θ	1.874° / 27.480°
Number of collected reflections	17159
Number of independent reflections	3612 (merging r = 0.117)
Number of observed reflections	2203 (I>2.0σ(I))
Number of refined parameters	191
r	0.0603
rW	0.0628
Goodness of fit	1.0854

Table 26: Crystal data for **95**.

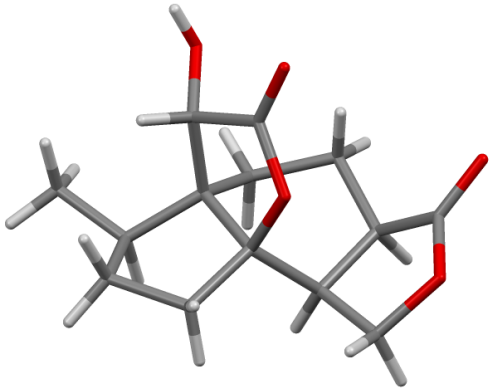

Formula	$C_{14}H_{18}O_5$
Formula weight	266.29 g · Mol^{-1}
Z, calculated density	4, 1.401 Mg · m^{-3}
F(000)	568
Description and size of crystal	colourless, 0.050 · 0.120 · 0.210 mm^3
Absorption coefficient	0.106 mm^{-1}
Min/max transmission	0.99 / 0.99
Temperature	123K
Radiation (wavelength)	Mo K_α (λ = 0.71073 Å)
Crystal system, space group	orthorhombic, $P\ 2_1\ 2_1\ 2_1$
a	8.3912(4) Å
b	10.4988(5) Å
c	14.3311(7) Å
α	90°
β	90°
γ	90°
V	1262.53(11) $Å^3$
Min/max Θ	2.405° / 39.412°
Number of collected reflections	49860
Number of independent reflections	4197 (merging r = 0.038)
Number of observed reflections	3448 (I>2.0σ(I))
Number of refined parameters	172
r	0.0290
rW	0.0428
Goodness of fit	1.0609

Table 27: Crystal data for **99**.

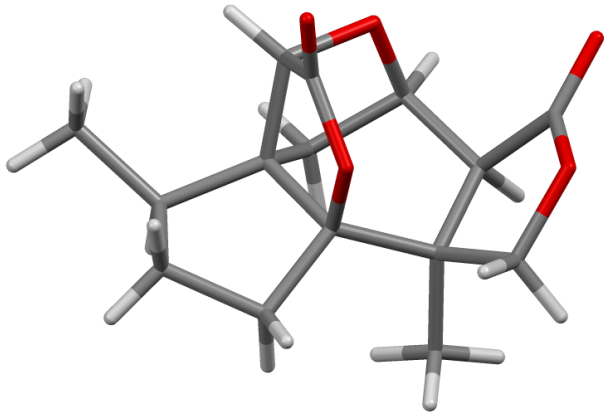

Formula	$C_{15}H_{18}O_5$
Formula weight	278.30 g · Mol^{-1}
Z, calculated density	2, 1.347 Mg · m^{-3}
F(000)	296
Description and size of crystal	colourless, 0.060 · 0.130 · 0.210 mm^3
Absorption coefficient	0.840 mm^{-1}
Min/max transmission	0.90 / 0.95
Temperature	293K
Radiation (wavelength)	Cu K_α (λ = 1.54178 Å)
Crystal system, space group	monoclinic, $P\ 2_1$
a	7.3214(4) Å
b	9.0142(6) Å
c	10.4450(6) Å
α	90°
β	95.474(3)°
γ	90°
V	686.19(7) $Å^3$
Min/max Θ	6.072° / 67.672°
Number of collected reflections	6473
Number of independent reflections	2329 (merging r = 0.034)
Number of observed reflections	2232 (I>2.0σ(I))
Number of refined parameters	182
r	0.0341
rW	0.0375
Goodness of fit	1.1221

8.2 ^{1}H and ^{13}C NMR Spectra

^{1}H and ^{13}C NMR Spectra for the all characterized compounds can be found on the enclosed CD to this PhD thesis.

Acknowledgements

At first, I would like to express my deepest gratitude to my supervisor, Prof. Dr. *Karl Gademann*, for the opportunity to be a member of his research group, his steady guidance, his scientific mentoring and for providing me with challenging research projects. I am outmost thankful for his trust in my decisions and this constant support.

I would like to thank Prof. Dr. *Karl-Heinz Altmann* for accepting the co-examination of my thesis.

I am thankful to Prof. Dr. *Dennis Gillingham* not only for chairing my defense, but also for helpful discussions and good advice in the last years.

A special thank goes to my four highly skilled Master students *Elias Kaufmann*, *Natalie Huber*, *Christophe Daeppen* and *Annakaisa Heikinheimo*. This thesis would not have been possible without their hard work and motivation.

I am very grateful to Prof. Dr. *Leo Eberl* and *Alexander Grunau* from the University of Zurich for the fruitful collaboration we had and their great knowledge and advice concerning microbiological questions.

A further thanks goes to Dr. *Adrien K. Lawrence* for providing the fundament for the quorum sensing projects.

Dr. *Johannes Hoecker* and Dr. "Oberassistent" *Christof Sparr* are acknowledged for critically proofreading and thereby substantially improving this manuscript.

I would like to thank the senior members of Gademann research group: Dr. *Johannes Hoecker* for sharing my passion for organic chemistry and for his friendship, Dr. *Patrick Burch* for his contagious optimistic nature and for trying to make our lab a safer place, and Dr. *Samuel Bader*, our wise team member, for sharing his worldly wisdom with all of us.

I thank all current and former members of the Gademann group for the great time we had and for sharing numerous apéros in the institute: Dr. *Chandan K. Jana*, Dr. *Henning J. Jessen*, Dr. *Jean-Yves Wach*, *Christophe Thommen*, Dr. *Elamparuthi Elangovan*, Dr. *Erika Crane*, Dr. *Malika Makhlouf*, *Manuel Scherer*, *Isabel Kerschgens*, *Fabian Schmid*, *Robin Wehlauch*, *Verena Grundler*, Dr. *Hideki Miyatake Ondozabal*, Dr. *Suman de Sarkar* and *Simon Sieber*.

Additionally, I would like to thank *Florian Bächle*, *Marc-André Müller*, Dr. *Adnan Ganic*, Dr. *Jürgen Rotzler* and Dr. *Michael Parmentier* for fruitful chemical discussions, for the weekly football battles and for the great time we spent together.

I thank Dr. *Markus Neuburger*, Dr. *Daniel Häusinger* and Dr. *Heinz Nadig* for their excellent work and analytical measurements.

I am thankful to *Marina Mambelli Johnson* for being the best secretary ever, for her organization skills and for her friendly nature.

I would like to thank the technical staff of the organic chemistry department for their excellent work and support.

A special thank goes to the Zermatter gang for the awesome time we spent together and for providing me the best chemistry-free time possible.

I am more than thankful to *Marina Bär* for her love and for showing me the real important things in life.

Finalmente, agradeço a minha família pelo apoio e pela confiança que me deram ao longo dos meus estudos. Nada disto teria sido possível sem eles. Muito obrigado por tudo.

Curriculum Vitae

José Rui Paixão Gomes, born January 23th 1985 in Torres Novas, Portugal

Education and Professional Experience

03. 2010 – 03. 2014	Ph. D. studies at the **University of Basel** Research group of **Prof. Dr. Karl Gademann** "*Synthesis of Majucin-Type Sesquiterpenes and Immobilization and Visualization of Quorum Sensing Signaling Molecules*"
09. 2008 – 02. 2010	Master studies at the **University of Berne** with the major „Chemical Biology and Organic Synthesis" Research group of **Prof. Dr. Philippe Renaud** „*Towards an Asymmetric Carboazidation of Methylene-cyclohexane Derivatives Using Dimethylphenylsilane as a Removable Directing Group*"
06. 2008 – 09. 2008	Internship at **Lonza AG**, Visp Supervised by **Dr. Viktor Dick** „*Selektive Chlorierung von Nikotinsäure*"
10. 2005 – 06. 2008	Bachelor in studies at the University of Berne in „Chemie und molekulare Wissenschaften" Research group of **Prof. Dr. Philippe Renaud** „*Radical Bis-Allylation Strategy Towards the Synthesis of Enantiomerically Pure Spiroketals*"
08. 2000 – 06. 2005	Matura, Kollegium Spiritus Sanctus **Brig** with the major in mathematics and physics
07. 1992 – 06. 2000	Elementary- und high school in Zermatt

Awards

2012	Best Poster Presentation SCS Fall Meeting, ETH Zürich
2012	SCNAT/SCS Chemistry Travel Award
2011	Best Poster Prize, Summer School Villars
2011	Faculty Prize for Best Master Thesis, University of Berne

List of Publications

J. Gomes, A. Grunau, A. K. Lawrence, L. Eberl, and K. Gademann
Bioinspired, Releasable Quorum Sensing Modulators
Chem. Commun. **2013**, *49*, 155.

J. Gomes, A. Grunau, A. K. Lawrence, L. Eberl, and K. Gademann
Bioinspired Surfaces Against Bacterial Infections
CHIMIA, **2013**, *67*, 275.

J. Gomes, N. Huber, A. Grunau, L. Eberl, and K. Gademann
Fluorescent Labeling Agents for Quorum Sensing Receptors (FLAQS) in Live Cells
Chem. Eur. J. **2013**, *19*, 9766.

Poster Presentations

06. 2013	"Progress Towards the Total Synthesis of Jiadifenolide" J. Gomes, E. Kaufmann, C. Daeppen, A. Heikinheimo, K. Gademann, Komppa Symposium, Espoo, Finland
09. 2012	"*A Unified Approach Towards the Total Synthesis of Majucin-Type seco-Prezizaanes*" J. Gomes, E. Kaufmann, C. Daeppen, K. Gademann, SCS Fall Meeting, ETH Zürich, Switzerland
06. 2012	"*A Unified Approach Towards the Total Synthesis of Majucin-Type seco-Prezizaanes*" J. Gomes, E. Kaufmann, C. Daeppen, K. Gademann, BOSS XIII, Leuven, Belgium
09. 2011	"*Polyfunctional Quorum Sensing Modulators: An Application Oriented Approach*" J. Gomes, A. Grunau, A. K. Lawrence, N. Huber, S. Glauser, L. Eberl, K. Gademann, SCS Fall Meeting, Lausanne, Switzerland
08. 2011	"*Synthetic Studies on Majucin-Type seco-Prezizaanes*" J. Gomes, E. Kaufmann, K. Gademann, CUSO Summer School, Villars, Switzerland
03. 2011	"*TiO2 Particles Functionalized with Natural Product Hybrids as Powerful Quorum Sensing Modulators"* J. Gomes, A. Grunau, A.K, Lawrence, L. Eberl, K. Gademann, Frontiers in Medicinal Chemistry, Saarbrücken, Germany
01. 2011	"*TiO2 Particles Functionalized with Natural Product Hybrids as Powerful Quorum Sensing Modulators"* J. Gomes, A. Grunau, A.K, Lawrence, L. Eberl, K. Gademann, Rigi Workshop, Rigi, Switzerland

Teaching Experience

2010 – 2013	Supervision of four Master students and five semester students
2011 and 2012	Teaching Assistant *Organische Chemie 1*, University of Basel
2011 and 2012	Lab Course Assistant for "*Advanced Organic Chemistry"*, Bachelor Degree, University of Basel
2010	Lab Course Assistant for "*Organic Chemistry"*, Bachelor Degree, University of Basel

Languages

Portuguese (mother tongue) / German (second mother tongue) / English (fluent) / French (fluent) / Italian / (good knowledge) / Spanish (good knowledge)

Basel, March 2014